



Thomas, Elizabeth Baby (2015) *Analysis of protein kinases regulating the Trypanosoma brucei cell cycle*. PhD thesis.

<https://theses.gla.ac.uk/6229/>

Copyright and moral rights for this work are retained by the author

A copy can be downloaded for personal non-commercial research or study, without prior permission or charge

This work cannot be reproduced or quoted extensively from without first obtaining permission in writing from the author

The content must not be changed in any way or sold commercially in any format or medium without the formal permission of the author

When referring to this work, full bibliographic details including the author, title, awarding institution and date of the thesis must be given

Enlighten: Theses

<https://theses.gla.ac.uk/>
research-enlighten@glasgow.ac.uk

Analysis of Protein Kinases Regulating the *Trypanosoma brucei* Cell Cycle

Elizabeth Baby Thomas

BSc (Hons), MSc

**Thesis submitted in fulfilment of the requirements for the degree of Doctor
of Philosophy**

Institute of Infection, Immunity and Inflammation

University of Glasgow

March 2015

Table of Contents

Table of Contents.....	ii
List of Tables	v
List of Figures	vi
List of Accompanying Material	viii
Acknowledgments	ix
Author's Declaration	x
Abbreviations.....	xi
Abstract	xvi
1 Introduction.....	1
1.1 The African Trypanosomiases.....	1
1.1.1 Natural resistance against <i>T. brucei</i>	4
1.1.2 Current therapies against HAT	6
1.1.3 Drug development and new treatment prospects	9
1.2 <i>Trypanosoma brucei</i> life cycle, cellular structure and biology.....	12
1.2.1 <i>T. brucei</i> life cycle and differentiation	12
1.2.1.1 Bloodstream stages.....	12
1.2.1.2 Insect stages.....	15
1.2.2 Structure of <i>T. brucei</i> cell	17
1.3 The cell cycle and its regulation	22
1.3.1 General eukaryotic cell cycle events.....	22
1.3.2 <i>T. brucei</i> cell cycle events and co-ordination.....	23
1.3.3 Eukaryotic cell cycle regulation	26
1.3.4 <i>T. brucei</i> cell cycle regulation	28
1.3.4.1 G ₁ /S transition	28
1.3.4.2 G ₂ /M transition.....	29
1.3.4.3 Spindle assembly and chromosome segregation	30
1.3.4.4 Mitotic exit and cytokinesis	32
1.4 Research Aims	33
2 Materials and Methods	35
2.1 Cell Culture	35
2.1.1 Bacterial cell culture	35
2.1.1.1 Bacterial strains.....	35
2.1.1.2 Bacterial culture and media	35
2.1.1.3 Storage of bacterial strains	36
2.1.2 <i>T. brucei</i> cell culture	36
2.1.2.1 <i>T. brucei</i> strains	36
2.1.2.2 <i>T. brucei</i> culture and media	37
2.1.2.3 Storage of <i>T. brucei</i> strains	39
2.1.2.4 Mouse infections	39
2.2 Genetic manipulation.....	40
2.2.1 Transformation of bacterial cells	40
2.2.1.1 Generating competent <i>E. coli</i> cells	40
2.2.1.2 Transformation of competent <i>E. coli</i> cells.....	40
2.2.2 Transfection of <i>T. brucei</i> cells	41
2.3 Molecular Biology - DNA preparation and manipulation	42

2.3.1	DNA Preparation	42
2.3.1.1	Extraction of plasmid DNA from <i>E. coli</i>	42
2.3.1.2	Extraction of genomic DNA from <i>T. brucei</i>	43
2.3.1.3	Determination of DNA concentration	44
2.3.2	DNA manipulation	44
2.3.2.1	Agarose gel electrophoresis	44
2.3.2.2	Polymerase chain reaction (PCR).....	45
2.3.2.3	Site-directed mutagenesis.....	47
2.3.2.4	Restriction endonuclease digests.....	49
2.3.2.5	DNA extraction from agarose gels.....	50
2.3.2.6	Cloning of amplified genes/fragments into generic cloning vectors	50
2.3.2.7	Subcloning	51
2.3.2.8	Addition of multiple cloning sites	55
2.3.2.9	DNA sequencing	56
2.3.2.10	Purification of linearised DNA for transfection into <i>T. brucei</i> .	57
2.4	Protein analysis, purification and biochemistry	57
2.4.1	Polyacrylamide gel electrophoresis (PAGE) and Western Blotting .	58
2.4.1.1	Sodium dodecyl sulphate (SDS)-PAGE.....	58
2.4.1.2	Coomassie staining	59
2.4.1.3	Western blotting.....	60
2.4.2	Bacterial recombinant protein production.....	61
2.4.2.1	Protein expression.....	61
2.4.2.2	His-tagged protein purification	62
2.4.2.3	GST-tagged protein purification.....	62
2.4.2.4	Determination of protein concentration and storage of purified proteins	63
2.4.3	Kinase assays	63
2.5	Microscopy.....	64
2.6	Flow cytometry	64
3	Regulation of <i>T. brucei</i> Polo-like kinase in procyclic form parasites.....	66
3.1	Discovery of Polo and Polo-like kinases	66
3.2	Cell cycle functions of PLK1	67
3.3	PLK1 structure and regulation.....	71
3.3.1	PLK1 structure	72
3.3.2	Control of expression	79
3.3.3	Activation of kinase activity	81
3.3.4	Repression of kinase activity	81
3.3.5	PLK1 localisation	82
3.4	<i>T. brucei</i> PLK.....	84
3.4.1	TbPLK functions.....	84
3.4.2	TbPLK regulation	86
3.5	Project aims.....	88
3.6	Results	89
3.6.1	The expression assay.....	89
3.6.2	The importance of T-loop residues T198 and T202 for TbPLK kinase activity in vitro and in vivo.	96
3.6.3	The role of the polo-box domain.....	104
3.6.4	Domains important for TbPLK expression.....	110
3.7	Discussion.....	115
4	Regulation of <i>T. brucei</i> Polo-like kinase in bloodstream form parasites	121

4.1	TbPLK in <i>T. brucei</i> BSF parasites.....	121
4.2	Project aims.....	121
4.3	Results	121
4.3.1	TbPLK expression	121
4.3.2	TbPLK RNAi complementation	124
4.3.2.1	<i>TbPLK</i> knockdown via RNAi targeting its 3' UTR	124
4.3.2.2	The RNAi complementation assay	125
4.3.2.3	Role of the KD and PBD	128
4.3.2.4	Role of T198	130
4.4	Discussion.....	131
5	RNAi-based Screening for Protein Kinases Involved in the <i>T. brucei</i> Cell Cycle.....	134
5.1	RNAi - discovery and mechanism.....	134
5.2	RNAi-based cell cycle screens in other model organisms.....	136
5.3	RNA interference in <i>T. brucei</i>	139
5.3.1	Development of inducible RNAi systems in <i>T. brucei</i>	140
5.3.2	RNAi based screens in <i>T. brucei</i>	142
5.4	<i>T. brucei</i> kinome-wide RNAi library	145
5.5	Project aim.....	148
5.6	Results	149
5.6.1	Screening of RNAi cell lines for PKs involved in the <i>T. brucei</i> cell cycle.....	149
5.6.1.1	Cell lines showing no growth defects and no cell cycle defects following RNAi induction	154
5.6.1.2	Cell lines showing growth defects but no notable cell cycle defects following RNAi induction.....	157
5.6.1.3	Cell lines showing G ₁ /S defects following RNAi induction	163
5.6.1.4	Cell lines showing mitosis defects following RNAi induction ..	164
5.6.1.5	Cell lines showing cytokinesis defects following RNAi induction	167
5.6.1.6	Cell lines showing kinetoplast duplication defects following RNAi induction	170
5.6.1.7	Cell lines showing mitosis and cytokinesis defects following RNAi induction	172
5.6.1.8	Cell lines showing kinetoplast duplication and cytokinesis defects following RNAi induction.....	176
5.6.1.9	Cell lines showing growth defects and/or cell cycle defects that were unclassified following RNAi induction.....	180
5.7	Discussion.....	181
6	General Discussion.....	186
6.1	<i>T. brucei</i> PLK.....	187
6.1.1	Procyclic stage	188
6.1.2	Bloodstream form	189
6.2	<i>T. brucei</i> cell cycle regulation by protein kinases	190
	References	192

List of Tables

Table 1-1	Drugs registered for treatment against HAT.....	6
Table 2-1	<i>E. coli</i> strains used in this study.....	35
Table 2-2	Antibiotics used when culturing bacterial strains.	36
Table 2-3	<i>T. brucei</i> strains used in this study.	37
Table 2-4	Drugs used when culturing <i>T. brucei</i> strains.	38
Table 2-5	Plasmids used in this study.....	43
Table 2-6	Amounts of components added to make up one PCR reaction.....	45
Table 2-7	PCR primers used in this study for gene cloning.	47
Table 2-8	Primers used for site-directed mutagenesis.	48
Table 2-9	Details of mutations introduced into <i>TbPLK</i> genes including parent plasmids and primers used, and the resulting plasmids that were generated.....	49
Table 2-10	<i>TbPLK</i> gene fragments amplified with details of templates and primers used.	51
Table 2-11	Details of plasmids generated in this study following subcloning and modification.....	55
Table 2-12	Primers used to generate linker sequences for adding multiple cloning sites into pHG341 and pHG342.	56
Table 2-13	Primers used for sequencing.	57
Table 2-14	12 % Separating gel recipe..	58
Table 2-15	4 % Stacking gel recipe.	59
Table 2-16	Primary antibodies used for Western blotting.....	61
Table 2-17	Secondary antibodies used for Western blotting.....	61
Table 3-1	PLK family of kinases in selected organisms across various taxons.	67
Table 5-1	Summary of the characteristics of investigated RNAi cell lines..	151

List of Figures

Figure 1-1	Schematic representing morphological changes during a <i>T. brucei</i> life cycle.	17
Figure 1-2	Overview of the <i>T. brucei</i> flagellum.....	19
Figure 1-3	Schematic representation of trypanosome cell architecture depicting the location of the major structural features of the trypanosome cell.	21
Figure 1-4	Morphogenesis of the bloodstream and procyclic forms of <i>T. brucei</i> through the cell division cycle.....	26
Figure 3-1	Schematic representation of domains in PLK1.	72
Figure 3-2	Schematic diagram of human Plk1 kinase domain structure.	74
Figure 3-3	Schematic diagram of human Plk1 PBD-phosphopeptide complex.	75
Figure 3-4	Model suggesting multi-level regulation of zebrafish Plk1.	79
Figure 3-5	Expression of ty-tagged TbPLK in PCF cells.....	90
Figure 3-6	Plasmid map of pHG366.	91
Figure 3-7	TbPLK variants that were analysed in this study.	91
Figure 3-8	Expression of YFP-tagged TbPLK and TbPLK N169A in PCF cells....	93
Figure 3-9	Localisation of YFP-tagged TbPLK proteins in PCF parasites.....	95
Figure 3-10	Expression of YFP-tagged TbPLK T198A and T198D in PCF cells.	97
Figure 3-11	Expression of YFP-tagged TbPLK T198 and T202 mutants in PCF <i>T. brucei</i> cells.	99
Figure 3-12	Cell cycle analysis of PCF <i>T. brucei</i> cells expressing YFP-tagged TbPLK T198 and T202 mutants.	100
Figure 3-13	Localisation of YFP-tagged TbPLK T198 T202 mutants in PCF cells 102	102
Figure 3-14	Expression of YFP-tagged TbPLK T202E in PCF <i>T. brucei</i> cells....	103
Figure 3-15	<i>In vitro</i> kinase activity of recombinant 6His-tagged (N-terminus) TbPLK proteins.....	104
Figure 3-16	Expression of YFP-tagged TbPLK H704A K706A in PCF cells.....	105
Figure 3-17	The PBD does not inhibit TbPLK kinase activity but acts as a substrate <i>in vitro</i>	107
Figure 3-18	Expression of YFP-tagged TbPLK truncations in PCF cells.	109
Figure 3-19	Localisation of YFP-tagged TbPLK truncations in PCF cells.	110
Figure 3-20	Expression of YFP-tagged TbPLK truncations in PCF cells.	112
Figure 3-21	Localisation of YFP-tagged TbPLK truncations in PCF cells..	113
Figure 3-22	Western blots of all YFP:TbPLK fusion proteins.....	115
Figure 4-1	Plasmid map of pHG399.	122
Figure 4-2	Expression of YFP-tagged TbPLK and TbPLK N169A in BSF cells. ...	123
Figure 4-3	Western blot analysis of TbPLK knockdown via RNAi of its 3' UTR.	125
Figure 4-4	Controls for the RNAi complementation assay in BSF cells.....	127
Figure 4-5	Analysis of the roles of the kinase domain and the PBD of TbPLK in BSF cells using an RNAi complementation assay.	130
Figure 4-6	Analysis of the role of the TbPLK T198 residue in BSF cells using an RNAi complementation assay.	131
Figure 5-1	Schematic representing RNAi mechanism.....	135
Figure 5-2	Schematic illustrating the cell division cycle of <i>T. brucei</i>	148
Figure 5-3	<i>In vitro</i> growth and cell cycle analysis of RNAi cell lines simultaneously knocking down two protein kinases.	153

Figure 5-4	<i>In vitro</i> growth and cell cycle analysis for cell lines showing no growth or cell cycle defects following RNAi induction.....	157
Figure 5-5	<i>In vitro</i> growth and cell cycle analysis for cell lines showing growth defects but no notable cell cycle defects following RNAi induction.	163
Figure 5-6	<i>In vitro</i> growth and cell cycle analysis for cell lines showing G ₁ /S defects following RNAi induction.....	164
Figure 5-7	<i>In vitro</i> growth and cell cycle analysis for cell lines showing mitosis defects following RNAi induction.....	167
Figure 5-8	<i>In vitro</i> growth and cell cycle analysis for cell lines showing cytokinesis defects following RNAi induction.	170
Figure 5-9	<i>In vitro</i> growth and cell cycle analysis for cell lines showing kinetoplast duplication defects following RNAi induction.	171
Figure 5-10	<i>In vitro</i> growth and cell cycle analysis for cell lines showing mitosis and cytokinesis defects following RNAi induction..	176
Figure 5-11	<i>In vitro</i> growth and cell cycle analysis for cell lines showing kinetoplast duplication and cytokinesis defects following RNAi induction.....	180
Figure 5-12	<i>In vitro</i> growth and cell cycle analysis for cell lines showing growth and/or cell cycle defects that were unclassified following RNAi induction.....	181
Figure 5-13	Schematic representation of BSF <i>T. brucei</i> cell cycle and protein kinases implicated in the regulation of indicated stages of the cell cycle.....	185

List of Accompanying Material

Supplemental memory stick containing:

Table S1 Details of abnormal cells that were generated following RNAi induction as observed by DAPI staining. The numbers of nuclei (N) and kinetoplasts (K) in each cell ($n \geq 200$) following DAPI staining of samples were recorded at the indicated time points post addition of tetracycline to the induced samples. Analyses of non-induced cells (tet-) are also shown as controls. Actual numbers and percentages of each cell type are shown. Separate tabs for each cell line are provided and are colour coded according to the growth/cell cycle phenotype generated following RNAi induction (as assigned in Chapter 5) - purple: no growth defects and no cell cycle defects; yellow: growth defects but no notable cell cycle defects; red: G₁/S defects; green: mitosis defects; black: cytokinesis defects; aqua: kinetoplast duplication defects; pink: mitosis and kinetoplast duplication defects; dark blue: kinetoplast duplication and cytokinesis defects; orange: unclassified

Acknowledgments

Not to us, O Lord, not to us, but to your name give glory,
for the sake of your steadfast love and your faithfulness! Psalm 115:1 (ESV)

Firstly, I would like to thank God for leading me here in Glasgow and for His love and faithfulness which kept me going during my time here.

A huge thank you to my supervisor, Tansy Hammarton, for the support and guidance she has given me these past 4 years with an honest, fair and conscientious approach which I have really valued and appreciated. I am grateful to the past members of the Hammarton lab - Corinna Benz, Cristina Costa, Fiona McMonagle and Glynn Forsythe; also Elaine Brown and Jim Scott for their advice, technical help and encouragement at the bench. I would also like to thank Jeremy Mottram for temporarily supervising me whilst Tansy was away on maternity leave. Thank you to my assessors Sylke Müller and Mike Barrett for their feedback and help. Thanks also to MRC and BBSRC for their financial support.

I have loved being part of the research community here in Glasgow (and further afield) and learning so much from them. I have really appreciated the stimulating, positive and helpful environment, prevalent in III and WTCMP, which has been priceless in helping me progress through my PhD work. Thanks to all my friends here in the lab (and others) for making my time here amazing! - Amy, Andrea, Antonio, Ben, Becky, Brenda, Cat, Corinna, Craig, Cris, Dan, Dave, Elaine, Ellie, Elmarie, Fede, Fernanda, Fernando, Isabella, Julie, Larissa, Laurence, Manu, Manuel, Marko, Mel, Nath, Sam, Saskia, Sonal, Susan, Tamsin, Tania, Tiago, Tom, Vivi, Will, and anyone else I have accidentally missed here.

Huge thank you to the past and present members of South Glasgow Baptist Church who have been like a family to me. Thank you so much for your love, care and encouragement. Thanks to those who put me up in their homes in Glasgow when I needed it - Robert, Christine, Amy, Ruth, Claire, Claire and Jean. Finally, thank you to my family for supporting me and being there for me.

Author's Declaration

The results stated in this thesis are my own work, except where otherwise stated, and has not been submitted for any other degree.

Elizabeth Baby Thomas

Abbreviations

μ	micro
3-MB-PP1	1-(<i>tert</i> -Butyl)-3-(3-methylbenzyl)-1H-pyrazolo[3,3-d]pyrimidin-4-amine
aa	amino acid
AAT	Animal African trypanosomiasis
AAT6	amino acid transporter 6
AGO	argonaute
AMP	adenosine monophosphate
Amp	ampicillin
APC	anaphase promoting complex
ApoA1	apolipoprotein-A1
ApoL1	apolipoprotein L-1
ATP	adenosine triphosphate
BARP	brucei alanine-rich protein
BBB	blood-brain barrier
Bleo	bleomycin
bp	base pair
BSD	blasticidin
BSF	bloodstream form
Cam	chloramphenicol
cAMP	cyclic AMP
CDE	cell cycle-dependent element
Cdk	cyclin-dependent kinase
CHR	cell cycle genes homology region
CNS	central nervous system
CPC	chromosomal passenger complex
CRK	cdc2-related kinase
CYC	cyclin
DALYS	disability adjusted life years
DAPI	4,6-diamidino-2-phenylindole
DARPin	designed selective ankyrin-repeat protein
DFMO	D,L-a- difluoromethylornithine

dH ₂ O	distilled H ₂ O
DIC	differential interference contrast
DNA	deoxyribonucleic acid
DND <i>i</i>	Drugs for Neglected Diseases initiative
ds	double-stranded
DTT	dithiothreitol
ECL	enhanced chemiluminescence
EDTA	ethylene diamine tetraacetic acid
EF-1 α	elongation factor 1 a
EGTA	ethylene glycol tetraacetic acid
EMI1	early mitotic inhibitor 1
ER	endoplasmic reticulum
ES	expression site
esiRNA	endoribonuclease-prepared siRNA
FAZ	flagellar attachment zone
FPC	flagellar pocket collar
GEF	guanine nucleotide-exchange factor
GFP	green fluorescent protein
GPI	glycosylphosphatidylinositol
GST	glutathione-S-transferase
GTP	guanosine triphosphate
h	hour
HA	hemagglutinin
HAPT1	high-affinity transporter 1
HAT	Human African Trypanosomiasis
Hb	haemoglobin
HDL	high density lipoprotein
His	histidine
HMI	Hirumi's modified Iscove's medium
Hp	haptoglobin
Hpr	haptoglobin-related protein
HRP	horseradish peroxidase
Hyg	hygromycin B
IDL	inter-domain linker
Ig	immunoglobulin

IPTG	isopropyl β-D-thio-galactopyranoside
k	kilo
K	kinetoplast
KAB	kinase assay buffer
Kan	kanamycin
kDa	kilo Dalton
kDNA	kinetoplast DNA
L/l	litre
LAPT1	low-affinity pentamidine transporter 1
LB	Luria-Bertani
m	milli/metre
M	molar
MAP	microtubule-associated protein
MBq	megabecquerel
MCAK	mitotic centromere-associated kinesin
MCS	multiple cloning site
MEN	mitotic exit network
MeOH	methanol
MOB1	mps one binder 1
MOPS	3-(N-morpholino) propanesulfonic acid
mRNA	messenger RNA
MTOC	microtubule organising centre
MtQ	microtubule quartet
mVSG	metacyclic VSG
n	nano
N	nucleus
NDR	nuclear DBF1-related
NECT	eflornithine:nifurtimox combination therapy
Neo	neomycin
NLP	Ninein-like protein
NLS	nuclear localisation signal
OD	optical density
ORF	open reading frame
PAGE	polyacrylamide gel electrophoresis
PARP	procyclic acidic repetitive protein

PB	polo-box
PBD	polo-box domain
PBS	phosphate buffered saline
PC	polo-box cap
PCF	procyclic form
PCR	polymerase chain reaction
PFR	paraflagellar rod
Phleo	phleomycin
PI	propidium iodide
PK	protein kinase
PLK	polo-like kinase
pSer	phosphoserine
pThr	phosphothreonine
PTRE	post-treatment reactive encephalopathy
Puro	puromycin
PVDF	polyvinylidene fluoride
qPCR	quantitative PCR
RdRp	RNA-dependent RNA polymerase
RISC	RNA-induced silencing complex
RIT-seq	RNAi target sequencing
RNA	ribonucleic acid
RNAi	RNA interference
RRM	RNA recognition motif
rRNA	ribosomal RNA
s	second
SAC	spindle attachment checkpoint
SDM	semi defined medium
SDS	sodium dodecyl sulphate
si	short interfering
SIF	stumpy induction factor
SIN	septation initiation network
SPB	spindle pole bodies
spp	species
SRA	serum resistance associated
ss	single-stranded

SUMO	small ubiquitin-like modifier
<i>T. b.</i>	<i>Trypanosoma brucei</i>
TAC	tri-partite attachment complex
TBE	tris-borate-EDTA
TDB	trypanosome dilution buffer
T _e	elongation temperature
TE	tris-EDTA
TEMED	tetramethylethylenediamine
tet	tetracycline
TetO	tet operator
TetR	tet repressor
TLF	trypanosome lysis factor
TLK	tousled-like kinase
T _m	melting temperature
U	units
UTR	untranslated region
UV	ultraviolet
V	volts
v/v	volume to volume
VSG	variant surface glycoprotein
w/v	weight to volume
WHO	World Health Organisation
WT	wild-type
WTCMP	Wellcome Trust Centre for Molecular Parasitology
YFP	yellow fluorescent protein
Zeo	zeocin

Abstract

Trypanosoma brucei spp. are protozoan parasites that cause Human African Trypanosomiasis in humans, and Nagana in cattle. These diseases are mostly fatal if left untreated and there is an urgent need for safe, effective drugs that can be easily administered. *T. brucei* has a complex cell cycle, the regulation of which appears to be divergent compared to other model eukaryotes. This implies that the regulators of the *T. brucei* cell cycle could be exploited as a source of novel drug targets. One such cell cycle regulator of interest is *T. brucei* polo-like kinase (TbPLK), a serine/threonine protein kinase thought to diverge from its canonical functions in eukaryotic mitosis and be mainly involved in the duplication of the parasite's cytoskeletal structures. This study sought to investigate how the activity and localisation of TbPLK is regulated in procyclic form (PCF) and bloodstream form (BSF) parasites. More specifically, the importance of two threonine residues (T198 and T202) within the activating T-loop of the N-terminal kinase domain and the C-terminal polo-box domain (PBD), which in other organisms plays a key role in PLK localisation and activity, was investigated.

An ectopic TbPLK expression assay was employed in PCF cells, whereby expression of wild-type (WT) TbPLK resulted in cell cycle defects, whilst expression of a kinase dead variant did not. A number of TbPLK mutants/truncations were expressed, and the resulting growth and cell cycle phenotypes were compared with those of WT and kinase dead TbPLK, to assess if they demonstrated kinase activity *in vivo*. The expressed proteins were also N-terminally tagged with YFP to track their localisation. Results showed that T198, and possibly T202, phosphorylation is essential for TbPLK kinase activity, in agreement with published data (Yu *et al*, 2012). *In vitro* studies did not identify any auto-inhibitory role for the PBD on TbPLK activity which is in contrast to what is known in other organisms. On the other hand, the PBD was found to be required for TbPLK localisation similar to its homologues in other organisms. However, a putative His-Lys pincer in the PBD was found to not be required for TbPLK activity and localisation. All the full-length TbPLK variants localised in a dynamic manner in agreement with previous studies (Ikeda & de Graffenried, 2012). Truncation studies also revealed that TbPLK possesses a functional

nuclear localisation signal (NLS) motif and a destruction box, the biological importances of which are yet to be determined.

Efforts were also made to translate these studies on TbPLK regulation to the mammalian stages of the parasite. In the absence of notable TbPLK expression phenotypes in BSF cells, attempts were made to establish an RNAi complementation assay. The 3' UTR of endogenous *TbPLK* was targeted via RNAi so that TbPLK variants could be ectopically expressed unhindered, and assessed for their ability to complement *TbPLK* RNAi. T198 was found to be important for TbPLK kinase activity similar to what was found in PCF parasites. Evidences of differential regulation of TbPLK between the two life cycle stages were also seen. It seems that the putative His-Lys pincer is required for TbPLK activity in BSF cells, which is in contrast to what is seen in PCF parasites. Altogether, despite TbPLK's divergent functions, some of the ways by which it is regulated appear to be conserved.

A second aim of this study was to identify novel protein kinases (PKs) which regulate the *T. brucei* cell cycle by screening part of a kinome-wide RNA interference (RNAi) library of BSF cell lines, that has recently been established (Jones et al. 2014). The cell lines had already been assessed for proliferation defects upon RNAi induction by using an Alamar blue viability assay. In this study, the cell lines which displayed proliferation defects were further screened for cell cycle defects using growth curves and DAPI staining, to identify as yet uncharacterised protein kinases required for *T. brucei* cell cycle regulation. 50 PKs had been shown to be required for viability *in vitro* and were screened for potential cell cycle roles. Of these, 25 were identified as potential cell cycle regulators, 15 of which were detected for the first time. The majority of the hits were deemed to be involved in either just cytokinesis, or cytokinesis in combination with kinetoplast duplication or mitosis, with surprisingly few in G₁/S. Knockdown of a number of these putative cell cycle PKs induced cell death signifying their potential as drug targets. Indeed, one of the hits, CLK1, was genetically validated as a potential drug target in a mouse model. The identification of these putative cell cycle kinases has also provided valuable starting points by which the signalling pathways that regulate the cell division cycle of these parasitic organisms can be elucidated.

1 Introduction

1.1 The African Trypanosomiases

Trypanosoma brucei spp. are the causative agents of the African trypanosomiases known to affect humans, livestock and wild animals. African trypanosomes are vector-borne parasites and are exclusively transmitted by the tsetse fly (*Glossina* species). These parasitic protozoa belong to the order Kinetoplastida, which also includes *Trypanosoma cruzi*, the causative agent of Chagas disease in South America, and *Leishmania* spp. which is responsible for the Leishmaniases in much of the tropical and subtropical world. The two morphologically indistinct *Trypanosoma brucei* sub-species, *T. b. rhodesiense* (found in East and Southern Africa) and *T. b. gambiense* (West and Central Africa) cause sleeping sickness in humans (also known as human African trypanosomiasis, or HAT). *T. b. rhodesiense* is considered as a host-range variant of the non-human infective sub-species, *T. b. brucei*, which causes Nagana in livestock (Sternberg & Maclean 2010); it expresses the serum-associated resistance (SRA) gene which confers its human infectivity (see section 1.1.1). *T. b. gambiense* can be divided further into at least two groups which differ in population genetic structure, virulence in experimental rodents and similarity to *T. b. brucei* (Sternberg & Maclean 2010). *T. congolense*, *T. vivax*, *T. evansi* and *T. equiperdum* are other important etiological agents of animal African trypanosomiasis (AAT). HAT and AAT affect people and livestock living in 36 sub-Saharan countries, which correspond to an area of more than 9 million km², equivalent to a third of Africa's total land area (WHO/TDR 2012).

The two human-infective *T. brucei* sub-species cause diseases that follow distinct clinical courses. Rhodesian sleeping sickness is a more acute form of the disease with rapid onset of the late stages. This is in contrast to the more common Gambian sleeping sickness (over 98% of reported cases overall according to the WHO), which is more chronic in nature, with the disease lasting for months to years. A bite from an infected tsetse fly (sometimes causing a primary lesion or a chancre to develop at the bite site which lasts for up to 5-15 days) leads to the development of the first of the two stages of the diseases - the

early, or the haemolymphatic stage, where the parasites proliferate in the bloodstream and the lymphatic tissues. During this period, patients present with febrile illness lasting 1-7 days, together with enlarged lymph nodes and several other nonspecific symptoms such as malaise, headache, arthralgia, generalized weakness, and weight loss (Kennedy 2004). The parasites can then go on to invade multiple organs including the spleen, liver, skin, cardiovascular system, endocrine system, eyes and eventually the central nervous system (CNS) (Kennedy 2004).

CNS invasion marks the onset of the late meningo-encephalitic stage of sleeping sickness. Symptoms of neurological involvement include mental disturbances such as irritability, lassitude, apparent changes in personality, sometimes including violence, hallucinations, suicidal tendencies, and mania; evidence of motor system involvement such as seizures, muscle fasciculation and sometimes paralysis; disorders of the sensory system and the characteristic sleep pattern disturbances. If left untreated, the disease progresses to its final stage which is characterised by coma, systemic organ failure and eventually death (Kennedy 2004). In the acute Rhodesian form of the disease, CNS involvement occurs within weeks following the infective bite, while in the Gambian form, CNS involvement does not occur for months or years after the initial infection. At this point, it is important to note that disease progression does not always occur with such predictable outcomes. Variability in clinical manifestations of trypanosome infections, with regards to clinical symptoms, disease severity and duration of illness, involving both forms of the sub-species, has been reported. It is now known that both host and parasite genetics and mixed infections of different parasite clones can influence the clinical outcomes of the infection, with reports of trypanotolerance in both humans and livestock (Murray et al. 1982; Naessens et al. 2003). This can mean that sleeping sickness is not always fatal when left untreated as had been previously believed (for reviews, see Sternberg & Maclean 2010; Morrison 2011; La Greca & Magez 2011).

T. b. gambiense and *T. b. rhodesiense* possess varying transmission cycles. Though *T. b. gambiense* parasites have been isolated from domestic and wild animals, humans are still considered as their main reservoir host (Maudlin 2006). On the other hand, *T. b. rhodesiense* is zoonotic with antelopes, hyenas, lions, sheep and cattle found to act as reservoir hosts, thus maintaining prevalence of

the disease (Maudlin 2006). The distribution of HAT incidence is focal, as it depends on the distribution of the tsetse fly, and that of suitable mammalian hosts, occurring within the range of the vector. Incidences tend to occur in localised breakouts, generally following certain types of human activity such as mass migration or man-made developments, resulting in the establishment of favourable breeding grounds for flies (Steverding 2008) or, as is the case for *T. b. rhodesiense*, trading of infected livestock (Fèvre et al. 2001). Following the huge epidemics in the late 19th century, the colonial regimes implemented rigorous control programs, bringing down the incidence of HAT to almost zero by the 1960s. However, political unrest during the post-independence period saw a steep rise in incidences through the next thirty years, leading up to devastating epidemics in the 1980s and 1990s. In 2008, an estimated 1.78 million disability adjusted life years (DALYS) were lost across Africa due to sleeping sickness (Fèvre et al. 2008). In 2009, the World Health Organization (WHO) reported 9878 new cases of HAT, representing a steady decline compared to more than 17600 in 2004 and almost 38000 in 1998. The real number of cases is, however, likely to be at least three times higher than those reported, as outbreaks tend to occur among the rural poor and during civil strife rendering surveillance and diagnosis difficult to achieve in its entirety (Odiit et al. 2005; Simarro et al. 2011). Nevertheless, the decline in disease incidences below the significant 10,000 cases per year has allowed renewed hope for achieving eradication of the disease. In 2012, the WHO set a roadmap aiming for HAT elimination by 2020 - to bring down the incidence of the disease to fewer than 1 case per 10,000 of the population in at least 90% of the areas where cases exist (Maurice 2013). This inspired the London Declaration on Neglected Tropical Diseases where donors, the World Bank, pharmaceutical companies, government agencies and the WHO jointly committed to aiding WHO's roadmap through initiating a collaborative disease eradication programme. The challenge then remains to ensure sustained surveillance, vector control and drug availability with eradication and not just elimination as the end-point, elimination being the point in time when vertical intervention approaches are no longer cost-effective (Simarro et al. 2011).

1.1.1 Natural resistance against *T. brucei*

The sera from humans and other primates was first noted for their trypanolytic properties in 1902 (Laveran 1902). Normal human serum was found to be able to kill *T. b. brucei* whilst not harming the human infective *T. b. rhodesiense* and *T. b. gambiense*. This remarkable human innate response involves trypanocidal factors which associate with serum complexes in normal human sera and are termed trypanosome lytic factors (TLFs). Two TLFs, TLF1 and TLF2, have now been defined as multi-subunit complexes with separate modes of uptake (Barth 1989; Hajduk et al. 1989; Raper et al. 1996). Nevertheless, they share their modes of trypanosome lysis which is mediated by one of their subunits - the pore-forming toxin, apolipoprotein L-1 (ApoL1; Vanhamme et al. 2003). Following uptake of TLF1 or TLF2 into the trypanosome, ApoL1 enters the endocytic pathway where it is progressively acidified, causing it to dissociate from the original TLF1/TLF2 complex and to insert into endosomal membranes (Pérez-Morga et al. 2005). The bacterial colicin-like pore-forming domain of ApoL1 then triggers an influx of chloride ions from the cytoplasm causing osmotic-swelling of the lysosome and activating compensatory entry of chloride ions from the extracellular medium. The swollen lysosome eventually occupies the whole cell body ultimately compromising the outer plasma membrane and killing the parasite. This model along with other proposed mechanisms have been discussed in detail by Pays et al. 2006.

TLF1 is a lipid-rich subtype of serum-derived high-density lipoprotein (HDL) - HDL₃ and is composed of apolipoprotein-A1 (ApoA1; Tomlinson et al. 1997), a serine-protease-like protein, haptoglobin-related protein (Hpr; Smith et al. 1995; Tomlinson et al. 1997), and ApoL1. Uptake of the TLF1 complex is mediated via Hpr. Hpr binds to haemoglobin (Hb) to form the Hpr-Hb complex which is then recognised by the *T. b. brucei* sub-species receptor, TbHpHbR (Widener et al. 2007; Vanhollebeke et al. 2008). TbHpHbR, a GPI-anchored glycoprotein thought to supply the bloodstream form (BSF; mammalian life cycle stage; see section 1.2.1) *T. brucei* parasites with haem for growth, is unable to distinguish between host-derived haptoglobin (Hp)-Hb and TLF1-Hpr-Hb complexes, enabling TLF1 uptake by the parasites (Vanhollebeke & Pays 2010).

The TLF2 complex is composed of IgM, ApoA1, Hpr and ApoL1 (Tomlinson et al. 1997; Raper et al. 1999) but, unlike TLF1, is mainly internalized in a manner independent of TbgHpHbR. It has been suggested that TLF2 is the dominant lytic factor in normal human sera and its entry is mediated via low-affinity/high capacity interactions with VSGs (variant surface glycoproteins) whose rapid turnover and recycling through the endocytic system may explain the efficiency of TLF2-mediated killing (Vanhollebeke & Pays 2010).

Whilst *T. b. brucei* is susceptible to the innate trypanocidal activity of ApoL1, *T. b. rhodesiense* and *T. b. gambiense* have developed ways to evade it. *T. b. rhodesiense* expresses SRA, a member of the VSG family shown to localise within the endocytic system (De Greef et al. 1989; Vanhamme et al. 2003). Through coiled-coiled interactions mediated via its N-terminal domain, SRA binds to ApoL1 thus sequestering it and enabling its degradation via proteolytic cleavage (Vanhamme et al. 2003; Stephens & Hajduk 2011; Alsford et al. 2013). Hosts which express variant forms of ApoL1 are able to circumvent SRA-mediated *T. b. rhodesiense* resistance to human serum; this has been found to be the case with people of West African descent, although at the cost of a higher susceptibility to developing kidney disease (Genovese et al. 2010). *T. b. gambiense*, which does not express SRA, has developed multiple strategies to avoid ApoL1-mediated killing. Group 1 *T. b. gambiense* parasites feature reduced uptake of TLF1-bound ApoL1 via downregulated expression of (Kieft et al. 2010), and, single amino-acid substitutions to (Symula et al. 2012; Higgins et al. 2013) its HpHb receptor (TbgHpHbR). The comparative importance of these two strategies, i.e. the neutralisation of ApoL1 and reduced uptake of TLF1, and how this group avoids TLF2-mediated lysis are questions that are yet to be addressed. Group 2 parasites, which display variable resistance against normal human serum, are unimpeded in their ability to internalise TLF1, yet are still resistant to ApoL1. This suggests that Group 2 parasites employ alternative means by which they are able to neutralise ApoL1 toxic activity (Capewell et al. 2011).

The natural host resistance mechanisms against *T. b. brucei* highlight the opportunities which receptor-mediated endocytosis provide in delivering toxins to human-infective trypanosomes. The high-rate of uptake and the essentiality of endocytosis could be exploited to design novel therapeutics which could be

engineered to specifically enter parasites through this route (Alsford et al. 2013; Stijlemans et al. 2011).

1.1.2 Current therapies against HAT

Currently, there are no vaccines available for prophylactic immunisation, thus rendering chemotherapy as the only means available for combating HAT. Unless complete eradication is achieved, the issue of the lack of effective, safe and easy-to-administer drugs will still remain. To date only five drugs have been registered for treatment against HAT which have been summarised in Table 1-1 (for recent review see Babokhov et al. 2013).

	Stage 1	Stage 2
<i>T. b. rhodesiense</i>	Suramin	Melarsoprol
<i>T. b. gambiense</i>	Pentamidine	Melarsoprol Eflornithine NECT

Table 1-1 Drugs registered for treatment against HAT.

Suramin, the oldest trypanocidal drug that has been in use since the early 1920s, is a naphthylamine-benzamide urea derivative, similar to trypan blue, that is used to treat early stage Rhodesian sleeping sickness (Barrett et al. 2007; Steverding 2010). Some degree of kidney damage is common following administration and adverse effects include cutaneous lesions, anaphylactic shock, renal failure and neurotoxicity (Kaur et al. 2002; Bitton et al. 1995). In the case of the Gambian form of the disease, the diamine, pentamidine, is the preferred drug of choice. This drug, in comparison, is better tolerated but can cause side effects such as hypo- or hyperglycemia and hypotension, nephrotoxicity, leucopenia and liver enzyme abnormalities (Sands et al. 1985; Doua & Yapo 1993). Suramin and pentamidine are both unable to cross the blood-brain barrier (BBB) efficiently and, therefore, cannot be used to treat CNS-stage disease. Until recently, melarsoprol has been the mainstay drug for treatment against late-stage HAT. This drug is an organo-arsenic compound and is, therefore, highly toxic. Side effects following administration are very common. 5-10% of treated patients develop post-treatment reactive encephalopathy (PTRE) which is a severe condition with fatality rates close to

50% among those affected (Barrett et al. 2007; Burri 2010). Melarsoprol is dissolved in propylene glycol which, in itself causes irritation at the site of injection, and needs to be administered over a 10-day period (Kuepfer et al. 2012). Intensive use of this drug has led to a growing problem of resistance with several foci reporting treatment failures of up to 30% of those treated. Yet, melarsoprol is the only available option for effective treatment of late stage Rhodesian HAT. In contrast, further treatment options are now available against *T. b. gambiense*. These include eflornithine and the recently developed nifurtimox-eflornithine combination therapy (NECT). Adverse reactions to eflornithine are similar to those of other cytotoxic drugs that are used to treat cancer, the severity of which depends on the length of treatment and the general condition of patient. Reports of eflornithine treatment failures (Burri 2010; Balasegaram et al. 2009) have led to the development of combination therapies with the view of maintaining the efficacy of this drug. The result of this is NECT, with proven higher efficacy compared to monotherapies. Nifurtimox, an orally administered drug used to treat Chagas' disease, had previously been used for compassionate treatment of relapsed HAT. Following successful trials where the two drugs were used in combination to treat HAT (Priotto et al. 2006; Priotto et al. 2007), nifurtimox and eflornithine have now been added to WHO's Essential List of Medicines for the treatment of HAT. The trypanocidal mechanisms of action of these drugs, apart from eflornithine, are yet to be fully elucidated. A recent RNA interference target sequencing (RIT-seq) study employing high-throughput sequencing of a drug-selected RNA interference (RNAi) library, has helped unearth new players responsible for the mode of action of these drugs while, at the same time, corroborating previous studies (Alsford et al. 2012).

As a highly charged molecule, it had been speculated that suramin would have high-affinity to serum proteins allowing its uptake via receptor-mediated endocytosis and intralysosomal accumulation (Vansterkenburg et al. 1993). Consequently, a variety of targets had been proposed for suramin (McGeary et al., 2008; Stein, 1993). The RIT-seq study identified the invariant surface glycoprotein, ISG75, as a key protein contributing to suramin efficacy in addition to proteins which affect ISG75 copy number and members of the endocytic apparatus (Alsford et al. 2012; Alsford et al. 2013). Altogether, this

study supports the importance of receptor-mediated endocytosis of suramin and its targeted accumulation in lysosomes in its efficacy in a BSF stage-specific manner (Natesan et al. 2007; Alsford et al. 2012). However, no receptor for suramin has been found beyond ISG75 and, consequently, the final target of this drug still remains elusive.

Pentamidine, an aromatic diamidine, one of the most successful classes of drugs with anti-protozoal activity, has been in use since the 1930s. Other members of this class are diminazene aceturate, a first-line treatment against AAT, and DB75, the active compound of the new drug candidate, pafuramidine (DB289). Pafuramidine was meant to be a new line of treatment targeting early-stage HAT and, unlike already available treatments, was to be administered orally. However, toxicity issues meant that phase III clinical trials had to be discontinued (Paine et al. 2010). Pentamidine is a nucleic acid binding compound and is transported into the parasite via the P2 adenosine/adenine transporter encoded by the *TbAT1* gene in addition to high-affinity pentamidine transporter (HAPT1) and low-affinity pentamidine transporter (LAPT1) (de Koning & Jarvis 2001; de Koning 2001). Recent research identified HAPT1 to be the aquaglyceroporin, TbAQP2 (Baker et al. 2013; Munday et al. 2014). Once transported, pentamidine has been shown to localise to the mitochondrion where it is thought to mediate its trypanocidal activity via disruption of kinetoplast DNA and/or mitochondrion membrane potential (Alsford et al. 2012; Baker et al. 2013). Resistance against pentamidine is a well-documented phenomenon and strongly coincides with cross-resistance to melarsoprol, highlighting the shared pathway by which diamidines and arsenicals are taken up by the parasite (Baker et al. 2013).

Melarsoprol is a melaminophenyl arsenical drug thought to act by forming a stable adduct with trypanothione known as Mel-T. The RIT-seq screen identified a cohort of proteins which directly or indirectly regulate the levels of trypanothione suggesting that Mel-T itself is toxic to the parasite (Alsford et al. 2012). Separate studies have also linked melarsoprol's mode of action to energy metabolism (Denise & Barrett 2001). It is highly likely that, similar to pentamidine, melarsoprol targets a number of essential intracellular processes; this is supported by the fact that resistance against these compounds mainly focuses on blocking uptake of the drugs (Baker et al. 2013). Similar to

pentamidine, melarsoprol uptake is dependent on the *TbAT1* encoding P2 aminopurine transporter and *TbAQP2* (HAPT1) (Munday et al. 2014).

Eflornithine or D,L-a-difluoromethylornithine (DFMO), originally developed as an anti-neoplastic, is the only drug for which a defined mode of action is known (Barrett et al., 2007). Developed in 1981, this drug is an analogue of the amino acid, ornithine, which acts as an inhibitor of the enzyme ornithine decarboxylase - an enzyme required for polyamine biosynthesis. Lack of polyamine availability causes a trypanostatic effect and requires immunological action for complete elimination of the parasites (Barrett et al., 2007). Eflornithine therapy is, therefore, unsuitable for patients with suppressed immune systems. Eflornithine activity has been found to be limited in *T. b. rhodesiense* and the more rapid turnover of ornithine decarboxylase in this sub-species has been thought to be the reason for it (Iten et al. 1995; Iten et al. 1997).

Administration of these drugs is not straight-forward. All of them need to be administered intravenously, which requires technically trained staff and multiple visits to a health centre. For melarsoprol and eflornithine, hospitalization is mandatory due to the possibility of adverse reactions. In areas where HAT is endemic, access to health facilities is often difficult sometimes preventing timely access to the appropriate drugs. With no vaccines available, there is a pressing need for the development of safe and easy-to-administer novel drugs, especially in the treatment of CNS-stage HAT - an area of research that has failed to successfully advance in recent years, as evidenced by the fact that the latest novel drug was developed some 50 years ago.

1.1.3 Drug development and new treatment prospects

Reports of trypanotolerance in cattle, mice and humans gives hope that vaccination against trypanosomes is possible as it demonstrates the ability of hosts to successfully mount immune responses against these parasites (Courtin et al. 2008). The same reports also indicate the importance vaccines will play in eradicating HAT and AAT as trypanotolerant mammals will continue to act as reservoirs of the parasite. As mentioned earlier, there are no current vaccines against HAT, and attempts to develop a clinically effective one is a long way-off

(La Greca & Magez 2011). This is mainly attributed to the remarkable immune evasion strategy of antigenic variation which trypanosomes have adopted (see section 1.2.1) where regular switching of trypanosomes' outer surface protein, VSG, prevents mammalian hosts from mounting an effective response. It has been argued that the use of in-bred murine models could give rise to artefacts, thus becoming a hindrance in vaccine development and that alternatives might need to be considered (La Greca & Magez 2011). With the development of an efficient vaccine out of reach, the only viable means through which the available anti-HAT therapeutics can be improved upon are by countering the limitations of current drugs or by developing new ones.

One of the disadvantages of treating late-stage HAT with melarsoprol is that it is highly toxic and that it is poorly soluble in water, requiring its solubilisation in propylene glycol, thereby restricting its administration through the intravenous route. In an attempt to counter these issues, melarsoprol was complexed with cyclodextrin molecules which was shown to increase its oral bioavailability and reduce its toxic effects (Rodgers et al. 2011). Plans to test this complex in a phase II is currently underway (Rodgers et al. 2011).

Fexinadazole, the most promising drug candidate against HAT to have entered clinical trials, is a member of the nitroimidazole class of drugs. Nitroimidazoles have long been used to treat infectious diseases with notable examples such as nifurtimox, metrinidazole (anti-bacterial) and benzidazole (Chagas disease). Fexinadazole was identified by Drugs for Neglected Diseases initiative (DNDi) in their extensive compound mining efforts to identify further nitroimidazoles with anti-trypanosomal activity, and was shown to treat the early and late stages of both acute and chronic forms of the disease (Torreele et al. 2010). Genotoxicity, which was the leading concern against a related nitroimidazole, megalol, was found to not be an issue with fexinadazole (Torreele et al. 2010; Tweats et al. 2012). The drug, which is orally administered, was well tolerated by healthy individuals in the first in-human studies that were conducted (Tarral et al. 2014) and is currently undergoing a pivotal phase II/III comparative study assessing its efficacy against late stage HAT. If successful, fexinadazole will be the first orally administered drug against HAT, the use of which, due to its potential efficacy against all forms and stages, has the added advantage of removing the requirement for staging the disease in the clinic.

The boron-containing oxaborole carboxamides, are another class of compounds providing promising new drug candidates against HAT. Also orally bioavailable, two lead compounds were able to kill *T. b. gambiense* and *T. rhodesiense in vitro*, cross the BBB and also recover acutely and chronically infected mice, suggesting that these compounds could be used to treat both stages and forms of HAT (Nare et al. 2010). Further optimisation studies, which focussed on improving the pharmacokinetic properties of the lead series, with particular emphasis on improving the extent and duration of brain exposure, yielded the compound SCYX-7158, which entered phase I clinical trials in 2012 (Jacobs et al. 2011).

Another preclinical candidate of note is DB829 which came to light as a result of continued screening of novel diamidines and prodrugs to improve on the toxicity observed during phase I clinical trials testing pafuramidine (DB289). DB829 was able to cure mice with late stage *T. b. brucei* infections and was also active against *T. b. rhodesiense in vitro* and *T. b. gambiense in vivo* (Wenzler et al. 2009; Wenzler et al. 2013) thus making it, along with its prodrug, DB868, ready for phase I clinical trials.

Other compounds of promise have also been identified and have been reviewed briefly recently (Babokhov et al. 2013). The challenges of developing novel drugs lie with the difficulty of generating small-molecules that specifically target genetically validated biomolecules, are pharmacologically sound and are able to convey therapeutic effects. This has caused some to challenge the presently accepted drug development pipeline which disconnects pharmacology from the early stages of target identification and validation (Moellering & Cravatt 2012). A chemoproteomics approach has been suggested where the vast libraries of small molecules with drug-like properties can be taken advantage of and exploited to accelerate drug discovery in the post-genomic era. In this approach, proven inhibitors of specific protein classes can be used to mine a proteome for identification and validation of new targets (Beroza et al. 2002). This was the basis of a recent study, which identified and validated a previously uncharacterised protein kinase, TbCLK1, as a potent drug-target using hypothemycin, a fungal product known to target protein kinases with a CDXG motif. Hypothemycin itself, due to dangers of non-specific binding to host kinases, cannot be developed as a new drug against HAT but provides a start

point for TbCLK1-specific drug development (Nishino et al. 2013). Such chemoproteomic approaches could be promising in enabling future drug development against HAT.

Novel developments are also being made in improving the current models that are used to test the efficacy of new compounds against the second stage of the disease. The current established model is plagued by long screening periods and hinders the process of defining structure activity relationships which often require iterative rounds of chemical synthesis. By capitalising on recent expansions in applying *in vivo* imaging to a broad range of biological studies, Myburgh and colleagues developed a serial, non-invasive bioluminescent imaging system to monitor parasitaemia, thereby reducing the drug screening time by two-thirds of the time taken by previous late-stage drug screening models (Myburgh et al. 2013; McLatchie et al. 2013). The development of such models greatly contributes towards drug evaluation programmes.

1.2 *Trypanosoma brucei* life cycle, cellular structure and biology

1.2.1 *T. brucei* life cycle and differentiation

1.2.1.1 Bloodstream stages

The life cycle of *T. brucei* involves the parasite progressing through a number of different developmental stages within their vector and mammalian hosts (Vickerman 1985) entailing morphological restructuring and biochemical adaptation (Figure 1-1). As an infected tsetse fly takes a blood meal from a mammalian host, it injects non-dividing metacyclic trypomastigotes into the underlying connective tissue. The parasites then quickly enter the bloodstream and the lymphatic tissue, following which they undergo morphological changes and differentiate into rapidly proliferative long slender trypomastigotes. At peak parasitaemia, some BSF long slender trypomastigotes differentiate into non-dividing short stumpy form parasites pre-adapting them for survival in the insect vector.

At these BSF stages the parasites exhibit cyclical antigenic variation, a host survival strategy which is common among bacterial, viral and eukaryotic pathogens. Trypanosomes possess the most comprehensive system of antigenic variation so far described. The trypanosome cell surface is thickly coated with densely packed, homodimeric VSGs. This protective coat shields other, more vulnerable, invariant cell surface membrane epitopes from targeted host immune response. Successive waves of VSG-specific immune response only succeed in eliminating part of the parasite population as new cells expressing switched VSGs emerge, thus prolonging an infection for months to even years in a host, thereby favouring transmission (for recent reviews, see Taylor & Rudenko 2006; Stockdale et al. 2008; Morrison et al. 2009). Only one, of about 15 exclusive VSG expressions sites (ES), is active at a time and only a single VSG, assembled from an archive of >1600 silent VSG genes and pseudogenes (Marcello & Barry 2007), is expressed at a time. VSG switching occurs at a rate of 10^{-2} per cell cycle, spontaneously and stochastically, independent of the host immune response (Lythgoe et al. 2007). VSG mosaicism, where the expressed VSG is a product of segmental gene conversions from two or more VSG donors, adds another layer of variation that can be achieved from a limited archive of VSG genes (Marcello & Barry 2007; Hall et al. 2013).

BSF parasites solely rely on glycolysis of host glucose for carbon supply and subsequent ATP production. Reflecting this, BSF parasites feature a tubular mitochondrion which lacks cristae and is unable to undergo oxidative phosphorylation, thus limiting metabolic options available to the parasite (Coley et al. 2011). However, the availability of abundant nutrients from the bloodstream of the host enables BSF parasites to multiply extensively via binary fission.

Differentiation is the key feature of any parasitic organism which invades multiple hosts during its life cycle; it is characterised by substantial transcriptome alterations, bringing about morphological and biochemical changes thus adapting the parasite to survive the subsequent destination host environment. Stumpy form BSF parasites are metabolically pre-adapted to survive in the tsetse fly vector where glucose is scarce and alternative carbon sources, such as amino acids, have to suffice. Therefore, they are equipped with mitochondria featuring well developed cristae and functional Krebs cycle,

respiratory chain and oxidative phosphorylation enzymes. These metabolic changes, in addition to variations in other cellular features such as cell structure, protein transport, proteolysis and translation, are reflected in the differential gene expression found between slender and stumpy BSF parasites described by recent comparative transcriptome analyses (reviewed in Rico et al. 2013).

A fine balance needs to be struck between immune evasion via antigenic variation and differentiation to quiescent transmissible forms to achieve both infection chronicity and transmissibility (MacGregor et al. 2012). This balancing act includes density-dependent differentiation induction as one of its key players. Similar to bacterial quorum sensing mechanism, differentiation in the mammalian bloodstream from slender to stumpy trypomastigotes has been shown to involve density-sensing, induced by an unidentified parasite-derived molecule termed Stumpy Induction Factor (SIF) (Vassella et al. 1997). Upon reaching the ideal density within the bloodstream, the slender to stumpy differentiation pathway is induced. The downstream pathways following differentiation induction are only just being unravelled. Some negative regulators have been identified, namely, ZFK (Vassella et al. 2001), MAPK5 (Domenicali-Pfister et al. 2006), TOR4 (Barquilla et al. 2012), RDK1 and RDK2 (Jones et al. 2014). Also, *in vitro*-adapted *T. brucei* monomorphic cell-lines have been shown to differentiate to a stumpy-like form in response to hydrolysable cell-permeable cAMP analogues (Vassella et al. 1997; Laxman et al. 2006; Barquilla et al. 2012) suggesting the importance of the cAMP signalling pathway in regulating the slender to stumpy differentiation pathway of trypanosomes in mammalian bloodstreams. Indeed, a recent genome-wide RNAi study identified a host of proteins linked to cAMP analogue processing, signal transduction and regulatory effector molecules to be involved in the differentiation-inducing cAMP analogue response pathway. Further *in vivo* analyses using pleomorphic cell lines confirmed the physiological relevance of some of these factors (involving kinases, phosphatases and effectors) in promoting density-dependent differentiation of slender trypomastigotes to stumpy form bloodstream parasites (Mony et al. 2014).

1.2.1.2 Insect stages

The *T. brucei* life cycle continues when a tsetse fly takes a blood meal from an infected mammal. Entry into the insect midgut brings about a dramatic change in the environment for the parasite with a drop in temperature and an alteration in the chemical environment inducing their differentiation (Engstler & Boshart 2004; MacGregor & Matthews 2010). Within the insect posterior midgut, ingested stumpy-form trypomastigotes, which have been shown to express PAD1, a citrate transporter required to transduce a citrate and/or cis-aconitate signal, then differentiate to procyclic form (BSF) trypomastigotes, while ingested BSF slender trypomastigotes either first transform into stumpy forms in the anterior midgut or die (Vickerman et al. 1988). This differentiation from stumpy form to PCF has been shown to be regulated by a phosphatase cascade (Szöör et al. 2006; Szöör et al. 2010). PCF trypomastigotes are able to replicate via binary fission and progressively lose their VSG coat (Bülow et al. 1989; Overath et al. 1983) which is then replaced by an equally dense coat of two classes of procyclins - EP (dipeptide repeats; EP1, EP2 and EP3) and GPEET (protease-resistant pentapeptide) (Roditi et al. 1987; Roditi & Clayton 1999). GPEET expression is transient and is down-regulated when PCF trypomastigotes mature (Knüsel & Roditi 2013). PCF trypomastigotes are characterised by increased cell length, kinetoplast repositioning, extensive mitochondrial branching, further increase in Krebs cycle associated enzymes and respiratory chain proteins and reduced endocytosis. When mature, PCF trypomastigotes invade the ectoperitrophic space, via active penetration of the peritrophic membrane, from where they migrate, via a marathon journey through the oesophagus, mouthparts and salivary ducts, to the salivary glands (Vickerman et al. 1988). Throughout this journey, they undergo a number of differentiation events thereby progressing through up to 11 further developmental stages (Figure 1-1; Rotureau & Van Den Abbeele 2013).

Once in the peritrophic matrix, PCF trypomastigotes elongate to form non-proliferative long mesocyclic trypomastigotes which then migrate to the anterior part of the insect's midgut. The parasites then migrate to the proventriculus where the mesocyclic cells become thinner and take on the epimastigote morphological form (the kinetoplast is positioned between the nucleus and the anterior end of the cell unlike trypomastigotes where the kinetoplast is

positioned on the opposite side of the nucleus). These long dividing epimastigotes then begin to undergo asymmetric division, each producing a long and a short epimastigote, whilst migrating upstream from the proventriculus to the salivary glands of the insect via the foregut and the proboscis (Van Den Abbeele et al. 1999). This migratory stage from the midgut to the salivary glands acts as a pronounced bottleneck as only between 0-5 parasites succeed in accomplishing it which results in the amplification of rare variants that are subsequently disseminated into the mammalian host population (Oberle et al. 2010). Once in the salivary glands, the short epimastigotes remain attached to the epithelium (attached epimastigote), via dendritic outgrowths of the flagellum termed 'flagellopodia' and hemidesmosome-like junctional complexes, and elongate (Vickerman 1985; Tetley & Vickerman 1985; Vickerman et al. 1988). Epimastigotes in the salivary glands are also characterised by a switch in their surface coats from procyclins to brucei alanine-rich proteins (BARP; Urwyler et al. 2007). At this stage the attached epimastigotes proliferate via two distinct cycles simultaneously whilst remaining attached to the salivary gland epithelium - 1) producing two equivalent cells which occurs at the early phase of the infections ensuring rapid colonisation; 2) asymmetric division producing a daughter cell which matures into a non-dividing infective metacyclic trypomastigote (Rotureau et al. 2012) featuring a metacyclic VSG (mVSG) surface coat that is expressed in ways distinct from BSF VSG coats (Tetley et al. 1987; Ginger et al. 2002). These infective metacyclics are subsequently released into the saliva, ready for transmission into mammalian hosts. MKK1 and the RNA-binding proteins, RBP6, ALBA 3 and ALBA4, remain the sole identified putative regulators/ effectors of trypanosome differentiation in the insect stages (Subota et al. 2011; Morand et al. 2012; Kolev et al. 2012).

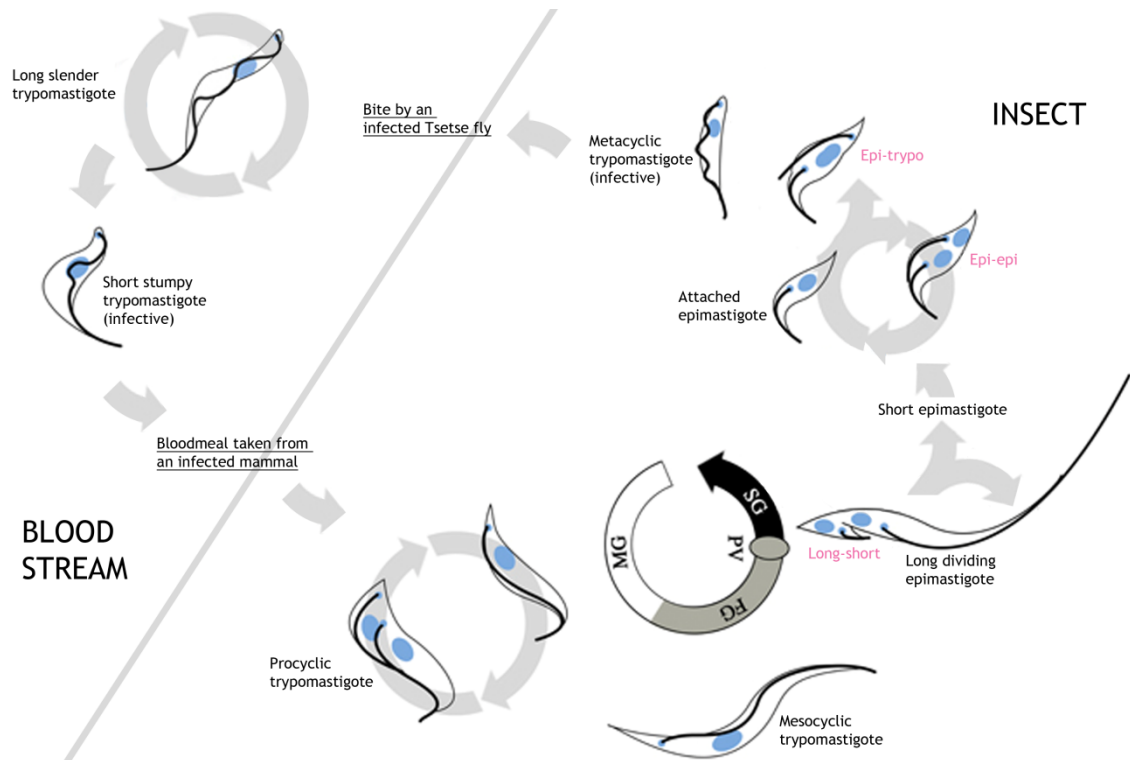


Figure 1-1 Schematic representing morphological changes during a *T. brucei* life cycle. MG - midgut; FG - foregut; PV - proventriculus; SG - salivary glands (SG); long-short - asymmetrical division of long dividing epimastigotes generating short and long epimastigotes; epi-epi - cell division generating two equal attached epimastigotes; epi-trypo - asymmetrical division of attached epimastigotes generating attached epimastigotes and metacyclic trypomastigotes. Adapted from Ooi & Bastin 2013.

1.2.2 Structure of *T. brucei* cell

The *T. brucei* cell body is vermiform in shape, 19-25 μm long, with defined anterior and posterior ends along a long axis. Its cell surface is characterised by the plasma membrane, the associated glycocalyx (defined by the several integral and peripheral proteins, glycoproteins, including GPI-anchored glycoproteins, such as the VSGs in BSF parasites, and glycolipids) and the underlying subpellicular corset of microtubules. The subpellicular corset is an array of microtubules which nucleate at randomly distributed sites, are regularly spaced, are arranged helically along the long axis of the cell and have the same polarity with their positive ends facing the posterior end of the cell (Sherwin & Gull 1989; Robinson et al. 1995; Gull 1999). The corset is extremely stable which can be attributed to the microtubules being linked to each other and the plasma membrane by cross-bridges featuring microtubule-associated proteins (MAPs)

(Sherwin & Gull 1989). The corset accommodates two specialised regions, which are definitive trypanosome cytoskeletal features.

At one point, along the length of the microtubule array, a gap exists which accommodates the bead-like filament part of the flagellum attachment zone (FAZ; Figure 1-2). The FAZ is responsible for the attachment of the single flagellum to the main cell body via a series of punctate transmembrane junctions (Bastin et al. 2000), thus forming an undulating membrane between the cell body and flagellum. To the left of this filament (when the cell is viewed from the posterior end of the cell) is an extremely stable set of four microtubules (the microtubule quartet; MtQ; Figure 1-2) which remains associated with the cell endoplasmic reticulum (ER) throughout the length of the cell (Sherwin & Gull 1989) and is also considered as part of the FAZ. The microtubules of the MtQ, which nucleate between the basal and pro-basal bodies (described later) at the posterior end of the cell, have opposite polarity to the rest of the subpellicular microtubules (Lacomble et al. 2009). Following nucleation, the MtQ wraps around the other specialised region found in the corset, the flagellar pocket, before traversing the length of the cell.

The flagellar pocket is a small invagination within the pellicular membrane from which the flagellum exits the cytoplasm (Figure 1-2). It is a vase-like structure which covers only 5% of the cell surface, is the most posterior structure on the outside of the cell and is the sole site of endo/exocytosis including vital processes such as VSG recycling (Engstler et al. 2004). In line with its specific roles in membrane traffic interchange, the flagellar pocket membrane is characterised by a distinct proteome (Field & Carrington 2009). The lumen of the flagellar pocket asymmetrically surrounds the flagellum as it just emerges following nucleation from the mature basal body (Figure 1-2; Lacomble et al. 2010). As the flagellum exits the flagellar pocket, its membrane along with those of the flagellar pocket and cell surface are constricted together by the flagellar pocket collar (Figure 1-2; FPC). Once the flagellum exits the cytoplasm, it is surrounded by its own membrane which is functionally distinct to the plasma membrane and the flagellar pocket membrane (Oberholzer et al. 2011).

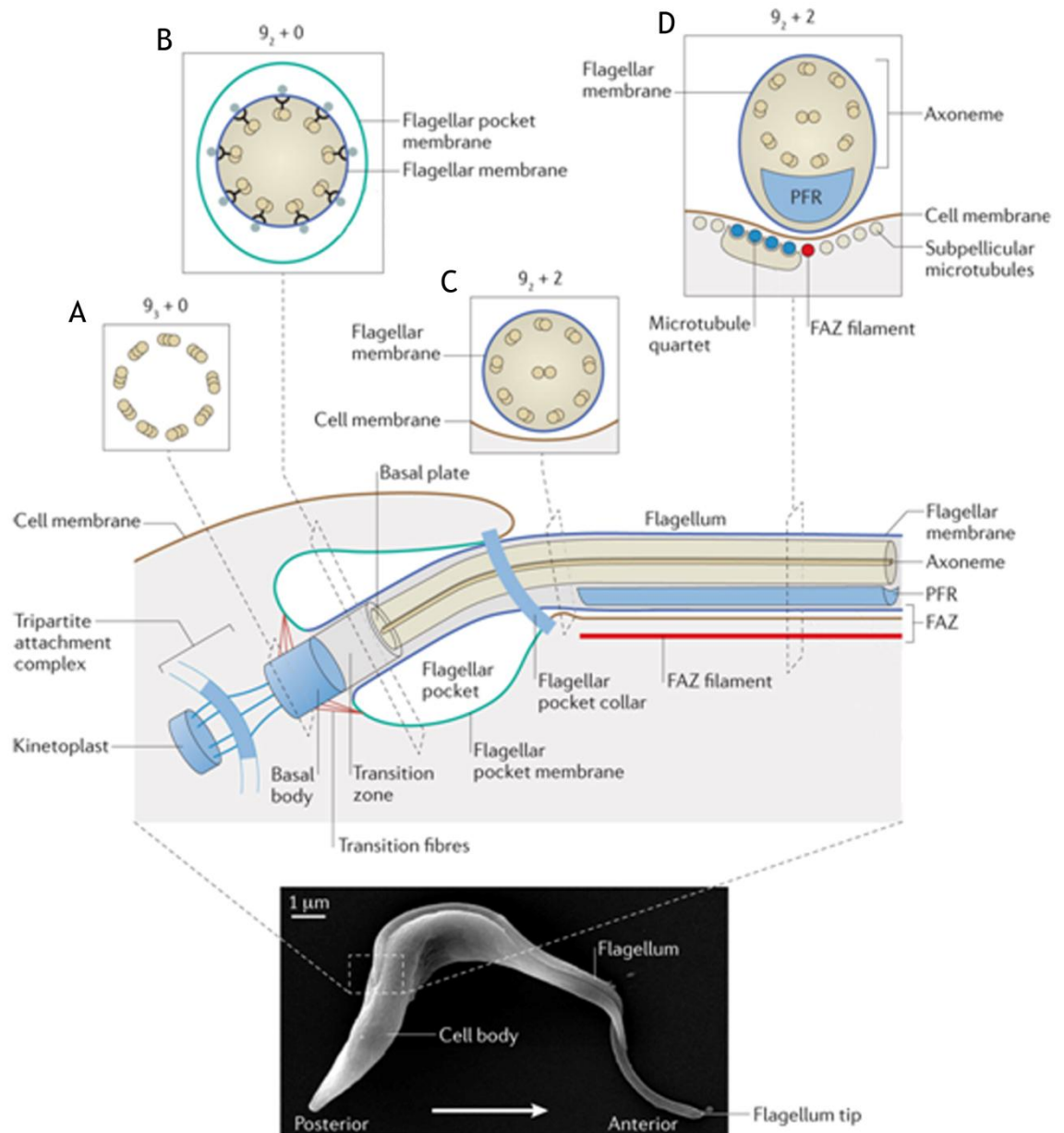


Figure 1-2 Overview of the *T. brucei* flagellum. Lower panel - Scanning electron micrograph of a *T. brucei* PCF cell with the direction of cell propulsion shown (arrow). Top panel - Diagram depicting flagellum emergence from the flagellar pocket at the posterior end of the cell (boxed region in lower panel). Cross sections of the basal body (A), transition zone (B) and two points of the emerging flagellum (C and D) depicting microtubule patterns are shown. Adapted from Langousis & Hill 2014.

The mature basal body and its tightly associated pro-basal body are the only recognisable microtubule organising centres (MTOC) found in a trypanosome cell and are located immediately under the flagellar pocket membrane. It is from the mature basal body that the microtubular core of the flagellum, the axoneme, nucleates (Figure 1-2). At the distal end, the mature basal body is characterised by nine peripheral triplet microtubules with no central pair (Figure 1-2A). As the

proximal end of the mature basal body, which marks the origin of the axoneme, invades the flagellar pocket, the peripheral microtubules become doublets thus forming the transition zone (Figure 1-2B). At the basal plate, where the transition zone ends, the two central pair microtubules nucleate and the canonical 9+2 (nine doublet microtubules that are symmetrically arranged around a central pair of singlet microtubules) axoneme begins which is then continued all the way along the flagellum (Figure 1-2C and D; Lacomble et al. 2009). Trypanosome axonemes possess components such as the inner and outer dynein arms, the radial spokes which connect the peripheral doublets to the central pair, the nexin links which are associated with peripheral doublets and the projections of, and connections between, the central pair of microtubules, all of which are well conserved axonemal features found in other eukaryotic organisms (Bastin et al. 2000). ATP-dependent dynein motors that are attached to one of the tubules of a doublet walk along the adjacent doublet generating sliding forces responsible for the movements of the flagellum.

The flagellum also features an extra axonemal accessory in the form of a paracrystalline structure called the paraflagellar rod (PFR; Figure 1-2) which is attached directly to both the axoneme (via outer arm dyneins to the peripheral doublets 4-7 when numbered according to convention; Hughes et al. 2012) and the FAZ. The PFR, along with the axoneme, is essential for flagellar motility (Hughes et al. 2012). The lattice-like structure of the PFR can be divided into three distinct zones: proximal, intermediate and distal. The proximal domain mediates PFR linking to the FAZ via distinct filaments (Portman & Gull 2010). A few studies have now been performed characterising the proteome of the PFR and interactions between its components (Pullen et al. 2004; Portman et al. 2009). Protein components of the PFR can be classified as those that are vital for structural viability, those involved in adenine nucleotide signalling and metabolism, those involved in calcium signalling and those with as yet unknown function altogether suggesting a role for the PFR in acting as a regulatory and metabolic platform for the sensory and motility functions of the flagellum (Portman & Gull 2010).

The flagellar basal bodies are anchored to a differentiated region of the mitochondrial membrane, and subsequently the kinetoplast, through a series of filaments known as the tri-partite attachment complex (TAC; Figure 1-2;

Ogbadoyi et al. 2003). The *T. brucei* kinetoplast - the definitive feature of the Kinetoplastida order - is an intricately structured nucleoid in which the genome of the single mitochondrion is condensed into a 100 nm thick, 650 nm wide disc (Klingbeil & Englund 2004). These continuous links between the kinetoplast, basal bodies and the flagellum act as guide ropes enabling connection of kinetoplast segregation to the replication and segregation of the rest of the cytoskeletal elements.

Closely associated to the exit point of the flagellum from where the FAZ is seen to begin and adjacent to the Golgi apparatus, is a hook-shaped structure termed the bilobe (Figure 1-3). The bilobe, which appears to be unique to trypanosomes, was serendipitously discovered (He et al. 2005) and has only been linked to Golgi biogenesis so far (de Graffenried et al. 2008). The cytoplasmic region between the flagellar pocket and the centrally positioned nucleus is home to single copy organelles such as the Golgi apparatus and the lysosome where protein degradation occurs (Figure 1-3).

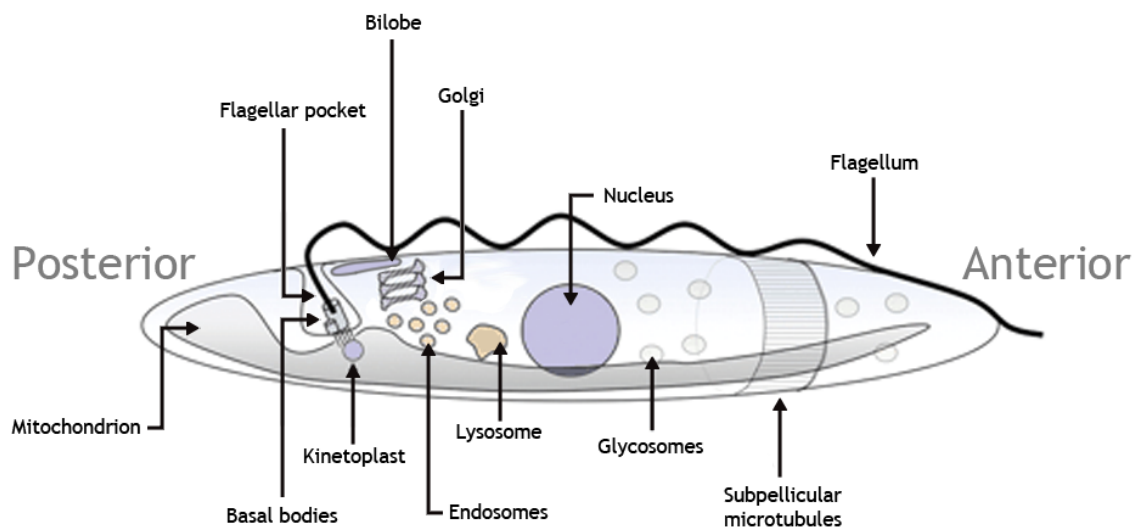


Figure 1-3 Schematic representation of trypanosome cell architecture depicting the location of the major structural features of the trypanosome cell. Adapted from Matthews 2005.

The precise positioning of these single copy organelles points to the importance of strict regulation of organellar and cytoskeletal replication and duplication in trypanosomes. This study has focussed on cell cycle regulation in *T. brucei*. Before gaining a background in *T. brucei* cell cycle events and regulation, what

is already known about this subject in other better studied eukaryotic models, shall be briefly looked into first.

1.3 The cell cycle and its regulation

1.3.1 General eukaryotic cell cycle events

A typical eukaryotic cell cycle can be subdivided into four phases -G₁, S, G₂ and M phases. During G₁ phase, the cell, in response to environmental conditions, decides whether to proliferate, quiesce, or differentiate. Under favourable conditions, determined by the ready availability of nutrients and an appropriate cell size, the cell proceeds to S phase when DNA replication occurs. This is followed by another gap phase, G₂ phase, when the cell grows even further and is primed for mitotic cell division. During M phase, or mitosis, replicated DNA and organelles segregate and cells divide to produce viable daughter cells which then re-enter G₁ phase. When conditions are not favourable to enter S phase, progression through the cell cycle is arrested and G₁ cells enter the quiescent G₀ phase, where they remain metabolically active but no longer proliferate without external stimuli. For some cell types, this quiescent stage is irreversible.

The major events of M phase in eukaryotes are broadly categorized into four stages. Mitosis begins with prophase during which chromosomes condense to form sister chromatids and spindle assembly is initiated following localisation of the duplicated centrosomes at opposite sides of the nucleus (see Hirano 2000 for review of chromosome cohesion, condensation and separation during the cell cycle). This is followed by an intermediate pro-metaphase, during which the chromosomes bind to the mitotic spindle. This process of attachment and alignment of the chromatids to the centre of the metaphase plane is mediated through the kinetochore - a complex of proteins bound to the centromeres of the chromatids. The cell is now said to have reached metaphase. Anaphase commences with the disruption of the link between the chromatids. Active remodelling of the spindle structure moves the chromatids towards the opposite ends of the pole. By this point, cytoplasmic division, or cytokinesis, would already have begun (Pollard 2010). Meanwhile, mitosis progresses through to telophase when nuclear DNA decondenses to form two separate nuclei.

Cytokinesis can, in general, be described to occur in three stages - initiation, furrow ingression and abscission. In animal cells, cytokinesis is initiated via signalling events leading to the formation of a contractile actin-myosin ring which promotes division of the cells along the cleavage plane (Barr & Gruneberg 2007). This is followed by abscission which causes an irreversible fission of the plasma membrane between the dividing cells producing two daughter cells (Guizetti & Gerlich 2010).

Progression through the various stages in the right order is essential for the viability of progeny. Although the *T. brucei* cell cycle events broadly follows the scheme described for general eukaryotes, the parasite cell replication displays many unique features and is characterised by strict regulation of its organelle positioning. This is to enable faithful replication, segregation and localisation of its nuclear/kinetoplast genome and that of its single copy major organelles, some of which feature only in trypanosomatids.

1.3.2 *T. brucei* cell cycle events and co-ordination

Sherwin and Gull first described the order of *T. brucei* cell cycle events in PCF parasites through the use of immuno-fluorescence and electron microscopy (Sherwin & Gull 1989) and this work still informs much of our current knowledge of this subject today. In BSF parasites, the order of events have been found to be largely similar with variations in the kinetics and the length of the cell cycle (about 6 hours for BSF compared to 8.5 hours for PCF parasites; Hammarton et al. 2007). Variations in morphology also occur which shall be pointed out as the cell cycle events are described and have been summarised in Figure 1-4.

The earliest microscopically detectable cell cycle events begin with the maturation of the pro-basal body at the G₁/S transition where it elongates to form the transition zone and basal plate (Sherwin & Gull 1989; Lacomble et al. 2010). A new flagellum begins to extend from the newly mature basal body which is now associated with a duplicated pro-basal body positioned anterior to the new flagellum/basal body complex (Lacomble et al. 2010). Once the new flagellum exits the existing flagellar pocket, the extension of the paraflagellar rod is initiated. The tip of the new flagellum goes on to physically connect with

the old flagellum via a transmembrane mobile junction termed the 'flagellar connector' (Briggs et al. 2004; Vaughan & Gull 2008), an association which is crucial for the spatial organisation of the new cellular structures. In BSF cells, this tethering of the new flagellum is achieved by the distal tip of the new flagellum being embedded in an indentation of the cell body called the groove, but does not last as long as it does in PCF parasites (Hughes et al. 2013). Following penetration into the flagellar pocket and the association with the flagellar connector by the new flagellum, the new basal body complex subtending the new flagellum, is repositioned via a rotational movement around its old counterpart in an anti-clockwise direction (Lacomble et al. 2010). This movement causes the new basal body and associated flagellum to take on a more posterior position in the cell. One of the consequences of this rotational movement is the formation of the new flagellar pocket which is formed by the partitioning of the existing flagellar pocket (Farr & Gull 2012). The force required for the rotational movement of the new basal body/flagellum complex has been linked to the nucleation of the new microtubule quartet, which precedes pro-basal body extension or new pro-basal body formation, as it extends in a helical pattern around the basal body/flagellum complex before inserting into the subpellicular microtubule corset (Lacomble et al. 2010).

Basal body replication, in addition to replication of the TAC and remodelling of the kDNA/TAC (Ogbadoyi et al. 2003), *de novo* synthesis of a new Golgi body (He et al. 2004; He et al. 2005; Selvapandiyan et al. 2007), duplication of the bilobe (He et al. 2005) and growth and duplication of the FPC (Bonhivers et al. 2008), all coincide with kinetoplast DNA (kDNA) S phase (Sherwin & Gull 1989). Nuclear and kinetoplast replication are two independent events with the kDNA S phase seeming to occur just before the initiation of nuclear S phase. The kinetoplast replication and division cycle, which has been shown to occur in five distinct morphological stages (Gluenz et al. 2011), is shorter compared to nuclear replication, and ends before the initiation of nuclear mitosis (Woodward & Gull 1990). Segregation of replicated kDNA is coupled with basal body segregation (Robinson & Gull 1991) mediated via the interlinking TAC complex. Inhibition of basal body segregation in turn inhibits kinetoplast segregation. Kinetoplast segregation coincides with the branching of the mitochondrion which does not completely detach until after the end of mitosis (Tyler et al. 2001).

Initiation of nuclear mitosis follows kinetoplast segregation and occurs without chromosome condensation or nuclear envelope breakdown (Galanti et al. 1998; Ogbadoyi et al. 2000). Bipolar spindle generation does not involve MTOCs, such as centrioles, but instead is co-ordinated via chromatin dependent pathways. As the nucleus elongates, it repositions towards the anterior of the basal bodies and straddles the axis of the mature flagellum and the growing new flagellum next to it. As a result, once the two nuclei separate they take on a linear 'KNKN' configuration relative to the positions of the kinetoplasts (when taken from the posterior to the anterior) (Robinson et al. 1995). Each daughter nucleus is thus localised next to a flagellum/basal body which is essential for accurate segregation during cytokinesis. At this point too, differences emerge between PCF and BSF cell division. In BSF cells, the kinetoplast is maintained at the posterior end of the cell throughout the cell cycle and such nuclear repositioning events are not seen (Tyler et al. 2001). The resulting organelle configuration is 'KKNN' which is in contrast to that found in PCF parasites.

Unlike mammalian cells, cytokinesis in *T. brucei* occurs via ingression of a cleavage furrow which occurs longitudinally and continues unidirectionally (from anterior to posterior), along the helical axis of the cell (reviewed in Hammarton et al. 2007). Also, cytokinesis in *T. brucei* can be divided into four distinct stages - division fold generation (or initiation), division furrow ingression, pre-abscission and abscission (Wheeler et al. 2013). Initiation of cytokinesis occurs at a point near to the distal end of the new flagellum. An invagination of the cell body is generated between the two flagella which continues to deepen. Both the posterior and the anterior ends of the cell remain attached via the flagellar connector until the pre-abscission stage (Briggs et al. 2004; Wheeler et al. 2013). However, in BSF parasites only the posterior ends of the nascent daughter cells remain attached as the new flagellum seems to disconnect from the cell body soon after division fold generation (Hughes et al. 2013; Wheeler et al. 2013). Furrow ingression continues dividing replicated organelles equally. Disconnection of the two flagella from the flagellar connector releases the anterior ends of the daughter cells in PCF parasites. In the pre-abscission stage, the posterior ends of the nascent daughter cells of BSF and PCF stages remain connected to each other via a thin membrane linking the two, termed the 'cytoplasmic bridge' (Wheeler et al. 2013). The cytoplasmic bridge differs

morphologically between PCF and BSF cells, i.e., in breadth and in volume (Wheeler et al. 2013). Final re-modelling and resolution of the new posterior end then facilitates final abscission (Farr & Gull 2012; Wheeler et al. 2013).

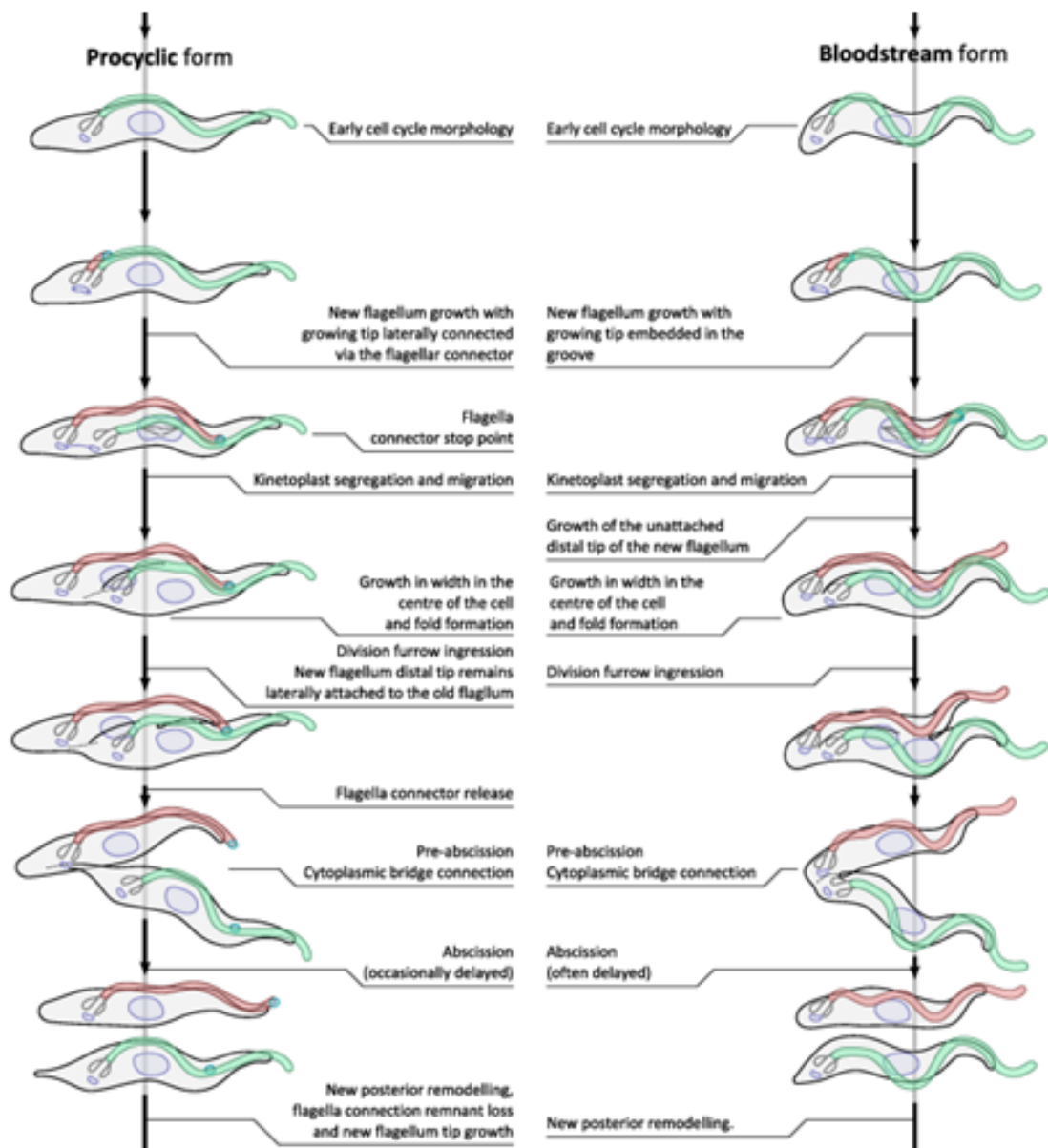


Figure 1-4 Morphogenesis of the bloodstream and procyclic forms of *T. brucei* through the cell division cycle. Major morphogenetic cell cycle events are shown alongside cartoon representations of the associated cell morphologies. Adapted from Wheeler et al. 2013.

1.3.3 Eukaryotic cell cycle regulation

It is crucial that cell cycle events occur in their correct sequence and are well-timed to ensure the production of viable progeny. Therefore, progression through the cell cycle, i.e. entry and exit from one phase to another, is strictly

regulated. There are checkpoints where control mechanisms verify whether the previous phase of the cell cycle has been accurately completed before entry into the next phase. These checkpoints ensure vital processes such as genomic DNA replication, at the S/M transition, or chromosome segregation, at the M/cytokinesis transition, have been completed faithfully and accurately. Events which drive the cell cycle forward involve the sequential activation and inactivation of cyclin-dependent kinases (Cdks). Cyclins bind Cdks and activate them. Activation of checkpoints, which stall the cell cycle, requires modulation of Cdk activities. Cdks are serine/threonine protein kinases featuring conserved catalytic cores which include an ATP-binding pocket, a PSTAIRE-like cyclin-binding domain and an activation loop (also known as the T-loop) motif, whilst cyclins, which have been classified into many different types, are more diverse and are mainly characterised by their cyclin box which mediates binding to Cdks (Lim & Kaldis 2013).

Yeasts possess only one major Cdk (CDC28 in *Saccharomyces cerevisiae* and Cdc2 in *Schizosaccharomyces pombe*; collectively CDK1; Beach et al. 1982). Yeast CDK1 is able to regulate the diverse cell-cycle transitions (G_1/S , S and G_2/M phases) by associating with different cell-cycle stage-specific cyclins. In higher organisms, specialised multiple homologues of yeast Cdk1 perform the multiple functions of yeast Cdk1 (Malumbres & Barbacid 2005; Malumbres & Barbacid 2009). Approximately 20 Cdk-related proteins have now been discovered which regulate cell-cycle events in higher eukaryotes via complex combinations with different cyclins (Satyanarayana & Kaldis 2009). Cyclins are synthesised and degraded at specific-points during the cell-cycle while different types of cyclins pair with specific Cdks. Cyclins confer substrate specificity and regulation (such as activation, inactivation, localisation and binding of subunits) to Cdk-cyclin complexes. However, further analyses on these complexes have shown that wide-spread redundancies do occur (Satyanarayana & Kaldis 2009).

Many Cdk-cyclin complexes, along with their roles in driving the cell cycle, have been well characterised in mammalian cells and yeast (for reviews see Malumbres and Barbacid, 2005; Malumbres and Barbacid, 2009). In mammalian cells, a subset of Cdk-cyclin complexes remains at the front-line of cell cycle control by directly regulating cytoskeletal events which promote progression through the cell cycle. The Cdks and cyclins that are directly involved in

mammalian cell cycle include three interphase CDKs (Cdk2, Cdk4 and Cdk6), a mitotic CDK (Cdk1) and ten cyclins that belong to four different classes (the A-, B-, D- and E-type cyclins) (Malumbres & Barbacid 2009). It is important to note that some of these Cdk-cyclin pairs only act within specific cellular contexts (Malumbres & Barbacid 2009). Additional layers of control factors orchestrate the cytoskeletal events required for the replication and segregation of all cellular components and cytokinesis. Detailed summaries outlining cell cycle regulation in model organisms and *T. brucei*, within the various stages, can be found in the next section and its sub-sections

1.3.4 *T. brucei* cell cycle regulation

T. brucei possesses eleven homologues of Cdks, termed cdc2-related kinases (CRKs): CRK1-4 and CRK6-12 (Parsons et al., 2005; Hammarton, 2007). Ten different *T. brucei* cyclins (CYCs; CYC2-11) have also been identified (Hammarton, 2007). Six of these (CYC2, CYC4, CYC5, CYC7, CYC10 and CYC11) resemble the budding yeast PHO80 cyclin, which is involved in signalling phosphate starvation, and three cyclins (CYC3, CYC6 and CYC8) are homologous to the mitotic B-type cyclins found in mammals (Hammarton 2007). The last, CYC9, resembles cyclin C transcriptional cyclins (Hammarton, Monnerat, et al. 2007). The publication of the 'TriTryp' (*T. brucei*, *T. cruzi* and *Leishmania major* - Berriman et al., 2005; El Sayed et al., 2005; Ivens et al., 2005) genome has enabled the extensive use of RNAi in investigating how the *T. brucei* cell-cycle is regulated via the various CRK:CYC interactions in addition to the roles played by *T. brucei* homologues of many other major cell-cycle regulators.

1.3.4.1 G₁/S transition

During G₁ phase, cells follow environmental cues to decide whether to proliferate, differentiate, quiesce or undergo apoptosis. Following favourable stimuli, once sufficient nutrients and growth factors are available, the decision is made to commit to the cell cycle and the cells transition from G₁ phase to S phase. In mammalian cells, binding of D-type cyclins to Cdk4 and/or Cdk6 activates the kinases, initiating the phosphorylation of the retinoblastoma protein, which leads to the release of the E2F transcription factors and

subsequent expression of E2F responsive genes (Dyson 1998; Weinberg 1995; Sherr & Roberts 1999; Sherr & Roberts 2004). These include E- and A-type cyclins (Sherr & Roberts 1999). Activation of Cdk2 by cyclin E further activates E2F mediated transcription which drives the G₁/S transition. Cdk2 activation by A-type cyclins triggers DNA replication and entry into S phase (Coverley et al. 2000; Petersen et al. 1999). Deregulation of G₁/S transition is a hallmark of cancer in metazoans (Massagué 2004).

In *T. brucei*, not much is understood regarding the molecular pathways which drive cells into the S-phase. A number of putative regulators have been identified. RNAi of *CYC2* (also called cyclin E1) and *CYC4* has revealed that they play a major and minor role in the G₁/S transition, respectively (Hammarton et al. 2004; Li & Wang 2003). RNAi of *CRK1* alone, and in combination with *CRK2*, *CRK4* and *CRK6*, indicated a primary role of *CRK1* and accessory roles of *CRK2*, *CRK4* and *CRK6* for progression into S phase (Tu & Wang 2004; Tu & Wang 2005). *CRK1* has been shown to interact with *CYC2* forming, what is thought to be, the primary CRK-cyclin pair for promoting the G₁/S transition (Gourguechon et al. 2007). RNAi of *CYC2* (in PCF cells and not in BSF cells) also displayed a ‘nozzle’ phenotype characterised by elongation of the posterior end of the cells thereby linking G₁/S transition to morphogenesis (Hammarton et al. 2004). The joint knockdown of *CRK1* and *CRK2* generated a similar morphological phenotype indicating that *CRK1*, *CYC2* and *CRK2* are involved in the same pathway modulating PCF cell morphogenesis. Using yeast-two hybrid screens, *CRK1* was also shown to interact with *CYC4*, *CYC5* and *CYC7*, in addition to *CYC2* (Liu et al. 2013). Similar to *CRK1*, *CYC2* and *CYC4*, RNAi of *CYC5* and *CYC7* also led to cells being blocked from transitioning into S phase, indicating a more complicated regulatory scheme for G₁/S transition in *T. brucei* cells (Liu et al. 2013). In addition, the yeast-two hybrid experiments also revealed that *CYC2* can interact with six other CRKs (*CRK2*, *CRK3*, *CRK6*, *CRK8*, *CRK10* and *CRK12*) in addition to *CRK1* (Liu et al. 2013). However, the physiological relevance of these interactions in *T. brucei* is yet to be determined.

1.3.4.2 G₂/M transition

During G₂ phase, the cell assesses the state of chromosome replication and prepares to undergo mitosis and cytokinesis. B-type cyclins are key for

progression through the G₂/M boundary. In mammals, activation of Cdk1 by cyclin B, the protein kinase that sets the mitotic state (for example, by promoting chromosome condensation and nuclear envelope breakdown), leads to entry and progression through mitosis. To prevent early entry into mitosis, Cdk1 is maintained in an inactive state via the phosphorylation activities of Wee1 and Myt1 (Dunphy 1994). Dephosphorylation of Cdk1 via Cdc25 during G₂ phase activates it, thus promoting mitotic entry (Kumagai & Dunphy 1991). Cdc25 is activated by Polo-like kinase (PLK) which also promotes degradation of the Cdk1 inhibitor Wee1 (Archambault & Glover 2009). Human PLK1 is activated by Aurora A kinase in G₂ phase, which ultimately constitutes the pivotal event driving G₂/M transition.

RNAi of the Cdk1 homologue in *T. brucei*, CRK3, established its role in regulating mitotic entry, possibly through binding with CYC6 (also termed CYCB2; demonstrated in PCF and BSF cells; (Hammarton et al. 2003; Tu & Wang 2004; Li & Wang 2003). CRK3 has also been shown to form a complex with CYC2 (demonstrated in PCF cells; Van Hellemond et al. 2000), however, whether this complex directly regulates mitotic entry is yet to be shown. In addition, CRK9 and CYC8 have also been shown to be required for the G₂/M transition (Li & Wang 2003; Gourguechon & Wang 2009). *T. brucei* does possess homologues of Wee1 and PLK. Recently, Wee1 was shown to be essential for PCF cell proliferation and to be able to rescue Wee1 deficient yeast mutants suggesting that *T. brucei* does possess a functional homologue of Wee1 (Boynak et al. 2013). Depletion of *Wee1* via RNAi in PCF cells generated zoids suggesting defects in mitosis. Studies characterising TbPLK have found no evidence for its localisation in the nucleus and role in mitosis (Chapter 3). In all, the pathways by which these factors collectively promote the G₂/M transition are yet to be fully understood.

1.3.4.3 Spindle assembly and chromosome segregation

Chromosome segregation requires the setting of the bipolar mitotic spindle which is made of microtubule bundles. In mammalian cells, the mitotic spindle nucleates either from MTOCs or via chromatin-mediated pathways (Walczak & Heald 2008; Meunier & Vernos 2012). In yeast, spindle pole bodies (SPB) act as the nucleation site for spindle fibres (McIntosh & O'Toole 1999). Maintenance of

these spindle fibres requires the joint activities of microtubule motors, such as kinesin-5, kinesin-14 and the kinesin-13 microtubule depolymeriser, mitotic centromere-associated kinesin (MCAK), in addition to the phosphorylation activities of Aurora kinases on these motor proteins (Carmena et al. 2012; Waitzman & Rice 2014; Moore & Wordeman 2004). The spindle assembly checkpoint (SAC) ensures timely activity of the APC ligase until proper attachment of the mitotic spindle to kinetochores before progression into anaphase (Kops & Shah 2012). APC ligase activation promotes cleavage of sister chromatids and degradation of B-type cyclins (in turn inactivating Cdk1 and promoting mitotic exit).

Trypanosomes are acentrosomal. The bipolar spindle is therefore likely to be mediated via chromatin-dependent pathways (Ogbadoyi et al. 2000; Li 2012). Aurora B kinase (AUK1) and MCAK homologues in trypanosomes have been found to be essential for spindle assembly and/or spindle microtubule dynamics in (Tu et al. 2006; Li & Wang 2006). In addition, AUK1 forms a unique chromosomal passenger complex (CPC) with two novel proteins, CPC1 and CPC2 (Li, Lee, et al. 2008; Li, Umeyama, et al. 2008). The CPC has been shown to display dynamic localisation during mitosis and cytokinesis (Earnshaw & Cooke 1991; Cooke et al. 1987). In other organisms, the CPC targets Aurora B to its substrates (Carmena et al. 2012). Whether the CPC in *T. brucei* plays a similar role is yet to be ascertained. *T. brucei* also possesses homologues of tousel-like kinase (TLK; TbTLK1 and TbTLK2) which in other eukaryotes are essential for activating Aurora B activity (Yeh et al. 2010; Silljé et al. 1999). TbTLKs have been found to be required for spindle assembly and chromosome segregation and although a substrate for AUK1, do not appear to be an activator of it (Li, Umeyama, et al. 2008; Li et al. 2007). *T. brucei* possesses orphan kinesins (TbKINA and TbKINB) which also appear to regulate spindle assembly (Li, Lee, et al. 2008). TbKif13-2, a member of the kinesin-13 family was found to possess microtubule depolymerase activity (Chan & Ersfeld 2010). Additionally, several other proteins have also been reported to be involved in mitosis and chromosome segregation, such as TbNOP86 (Boucher et al. 2007), TbAGO1 (Durand-Dubief & Bastin 2003), and the small ubiquitin-like modifier (SUMO; Liao et al. 2010). Trypanosomes express all the components of the APC/C, of which, only two APC/C subunits, APC1 and Cdc27, are essential for trypanosome mitosis (Kumar & Wang 2005). In

addition, homologues of separase and the components of the cohesin complex of which SMC3, SCC1, and separase were all shown to be essential for chromosome segregation (Bessat & Ersfeld 2009; Gluenz et al. 2008).

1.3.4.4 Mitotic exit and cytokinesis

Mitotic exit requires the inactivation of the Cdk1-cyclin B complex which is achieved via its degradation by the anaphase promoting complex (APC) ligase. Activation of the APC is achieved by PLK (Archambault & Glover 2009). In yeasts, the SIN (septation initiation network) or MEN (mitotic exit network) pathways replace the role played by the mammalian APC ligase in promoting mitotic exit and are initiated by PLK. These SIN/MEN pathways involve a number of proteins which are also conserved in mammals and *T. brucei* such as PLK, Mps One Binder 1 (MOB1) and nuclear DBF1-related (NDR) kinases.

Cytokinesis involves a number of cytoskeletal events involving components of the cytoskeleton and the cell membrane. The core regulatory pathways are well conserved amongst eukaryotes. In mammalian cells, cytokinesis requires the definition of the cleavage plane by the central spindle. The phosphorylating activities of Aurora kinase and PLK are required at the central spindle and midbody (Archambault & Glover 2009). They regulate the centralspindlin complex recruitment of the guanine nucleotide exchange factor, Ect2, to the midbody. Ect2 then goes on to activate the small GTPase, RhoA, which leads to formation of the actinomyosin contractile ring.

In *T. brucei* the cleavage furrow for cytokinesis is likely to be defined by the new FAZ and flagellum (Kohl et al. 2003; Wheeler et al. 2013). Mechanistic division of the cell is mediated via the ingression of this cleavage furrow which involves major remodelling of cytoskeletal components such as the subpellicular corset (Wheeler et al. 2013). CRK9 has been suggested to play a role in cytokinesis in PCF parasites. Depletion of CRK9 in BSF cells, on the other hand, did not seem to have any effect on their growth (Gourguechon and Wang, 2009). Other factors that have been shown to be involved in *T. brucei* cytokinesis such as the SIN/MEN homologues TbPLK, MOB1 and NDR kinases (Hammarton, Kramer, et al. 2007; Hammarton et al. 2005; Ma et al. 2010), the RHO kinase, TRACK

(Rothberg et al. 2006), components of the trypanosome CPC - AUK1, CPC1 and CPC2 (Li, Lee, et al. 2008; Li & Wang 2006; Tu et al. 2006), the MAP, AIR9 (May et al. 2012), to name a few (see Li 2012 for an extended list); it is however, quite likely that not all of these proteins are direct regulators of cytokinesis. Initiation of cytokinesis is usually associated with the mitotic exit checkpoint in order to ensure accurate inheritance of the replicated nuclei by daughter cells. In *T. brucei* PCF cells this checkpoint is missing making the generation of “zooids” (ON1K cells) possible as a result of unregulated cell division. This dissociation between mitotic exit and cytokinesis initiation has not been found to be the case in BSF parasites (Hammarton et al. 2003; Tu & Wang 2005).

1.4 Research Aims

Much is yet to be understood about how the cell cycle is regulated in *T. brucei*. Studies characterising various aspects of the cell cycle have identified divergence in *T. brucei* compared to other organisms. PLK is one such example. The only PLK homologue found in *T. brucei*, TbPLK, has been found to possess no mitotic role yet and features a dynamic localisation instead of a nuclear one. Detailed studies have now already provided clues to TbPLK function in *T. brucei* cytokinesis, and replication and segregation of cytoskeletal elements, in BSF and PCF parasites, respectively. One of the aims of this project was to characterise how TbPLK is regulated. The main thrust of the studies was to ascertain if the key regulatory features, as understood in other eukaryotes, have been conserved for TbPLK. Investigations were made in PCF (Chapter 3) and BSF cells (Chapter 4).

Since cell cycle progression is essential for *T. brucei* survival and has been shown to diverge from what has been demonstrated in mammalian cells, cell cycle regulators of *T. brucei* make attractive drug targets. It was hypothesised that due to the divergence in *T. brucei* cell cycle regulation there are novel cell cycle regulatory protein kinases that are yet to be discovered. Uncovering such novel kinases has been the second aim of this project. The establishment of a kinome-wide RNAi library (Jones et al. 2014) has enabled a simple screen where kinases which affect *T. brucei* growth following their knockdown via RNAi, were

investigated for potential cell cycle roles, via microscopic analysis of DAPI stained cells (Chapter 5).

2 Materials and Methods

2.1 Cell Culture

2.1.1 Bacterial cell culture

2.1.1.1 Bacterial strains

Escherichia coli (*E. coli*) strains were used for the purposes of cloning and protein expression in this study (Table 2-1).

Strain	Genotype	Comments
XL1-Blue	<i>recA1 endA1 gyrA96 thi-1 hsdR17 supE44 relA1 lac</i> [F' <i>proAB lacI^qZΔM15 Tn10</i> Tetracycline (Tet) ^r]	Host strain used for plasmid storage (via glycerol stocks), propagation and purifications.
BL21 DE3 pLysS	F- <i>ompT hsdS_B</i> (<i>r_B⁻, m_B⁻</i>) <i>dcm gal λ(DE3) pLysS</i> Chloramphenicol (Cam) ^r	Used for isopropyl β-D-thio-galactopyranoside (IPTG) inducible expression of a target gene driven by the T7 promoter. Contains pLysS plasmid encoding T7 lysozyme which inhibits T7 polymerase, preventing basal expression from the T7 promoter, without interfering with the level of expression achieved following IPTG induction.

Table 2-1 *E. coli* strains used in this study.

2.1.1.2 Bacterial culture and media

Bacterial strains were routinely cultured in Luria-Bertani broth (LB-broth; 86 mM NaCl, 10 gL⁻¹ tryptone and 5 gL⁻¹ yeast extract, adjusted to pH 7 and autoclaved), with shaking at 180-220 rpm or on LB-agar plates (LB-broth supplemented with 15 gL⁻¹ agar and autoclaved) at 37°C. 12-16 hours of incubation were typically required to obtain stationary phase liquid cultures or single colonies on plates. As required, media were supplemented with antibiotics, which were stored as 1000 X stock concentrations at -20°C (Table 2-2).

Antibiotic	Final concentration	Dissolved in
Ampicillin (Amp)	100 $\mu\text{g ml}^{-1}$	70 % ethanol
Kanamycin (Kan)	25 $\mu\text{g ml}^{-1}$	dH ₂ O
Chloramphenicol (Cam)	25 $\mu\text{g ml}^{-1}$	50 % ethanol

Table 2-2 Antibiotics used when culturing bacterial strains.

In order to determine the cell density of a liquid bacterial culture, 1 ml was pipetted into a cuvette and the OD_{600 nm} was measured using a spectrophotometer (Shimadzu Biospec-mini DNA/RNA/protein analyser).

2.1.1.3 Storage of bacterial strains

For long term storage of bacterial strains, pellets from 10 ml overnight liquid cultures were obtained via centrifugation (3000 g, 10 minutes at 4°C) and subsequently resuspended in 1 ml LB containing 2 % peptone and 40 % glycerol before storing them at -80°C. Frozen strains were revived by streaking a small amount of glycerol stock onto LB-agar plates and incubating at 37°C overnight so that single colonies were obtained.

2.1.2 *T. brucei* cell culture

2.1.2.1 *T. brucei* strains

427 Lister *T. b. brucei* parasites, adapted for *in vitro* culturing, and their derivatives were used in this study as described in Table 2-3.

Life-cycle stage	Genotype	Comments
PCF	Lister 427	Wild-type
BSF	Lister 427	Wild-type
PCF	Lister 427 pHD449	Zeo ^r . Features constitutive expression of the tet repressor (TetR). Allows tet-inducible expression of genes of interest (Wirtz & Clayton 1995; Biebinger et al. 1997).
BSF	Lister 427 pLew13 pLew90	Hyg ^r . Neo ^r . Features constitutive expression of T7 RNA polymerase and T7 promoter driven TetR. Allows tet-inducible expression of

		genes of interest and constitutive expression of proteins (including selectable markers) that are under the control of T7 promoter (Wirtz et al. 1999).
BSF	2T1	Single <i>ribosomal RNA (rRNA)</i> spacer targeted for homologous recombination via the introduction of an incomplete hygromycin-resistance marker. Enables consistent robust regulated expression of constructs introduced (Alsford & Horn 2008).

Table 2-3 *T. brucei* strains used in this study.

2.1.2.2 *T. brucei* culture and media

T. brucei PCF strains were cultured in the presence of 5 % CO₂ at 27°C in complete semi-defined media (SDM)-79 medium (Brun et al. 1979). Cells were routinely diluted to maintain mid-log phase growth (1×10^6 - 1×10^7 cells ml⁻¹).

SDM-79 was prepared by dissolving one pot of SDM-79 powder (Invitrogen; makes 5 L) and 10 g Na(CO₃)₂ in 4.5 L dH₂O before adjusting its pH to 7.3 with NaOH. This incomplete medium was then filter-sterilised and stored as 450 ml aliquots in sterile bottles at 4°C. The incomplete SDM-79 was routinely supplemented with heat-inactivated tetracycline-free fetal bovine serum (Gibco) to a final concentration of 10 % (v/v) and 500 Uml⁻¹ penicillin and 50 µg ml⁻¹ streptomycin and pre-warmed to 27°C before use.

T. brucei BSF strains were cultured in the presence of 5 % CO₂ at 37°C in Hirumi's modified Iscove's medium (HMI)-9 (Hirumi & Hirumi 1989) or, for 2T1 cells which were used to generate the kinome-wide RNAi library described in Chapter 5, in HMI-11 (Jones et al. 2014). Cells were routinely diluted to maintain mid-log phase growth (1×10^5 - 1×10^6 cells ml⁻¹).

HMI-9 was prepared by dissolving one pot of HMI-9 powder (Invitrogen; makes 5 L) in 3.8 L dH₂O following which 71.5 µl β-mercaptoethanol and 200 ml 75 gL⁻¹ Na(CO₃)₂ solution was mixed in before adjusting its pH to 7.4 with NaOH. This

incomplete medium was then filter-sterilised and stored as 400 ml aliquots in sterile bottles at 4°C. The incomplete HMI-9 was routinely supplemented with heat-inactivated tetracycline-free fetal bovine serum (Gibco) to a final concentration of 20 % (v/v) and 500 Uml⁻¹ penicillin and 50 µg ml⁻¹ streptomycin and pre-warmed to 37°C before use. In the case of HMI-11, 10 % (v/v) heat-inactivated tetracycline-free fetal bovine serum was used to supplement incomplete HMI-9 instead.

As needed, drugs were added to maintain selection for cells with successfully integrated constructs or, in the case for tetracycline, to induce expression of RNAi or a target protein. Different concentrations were used for drugs when supplementing HMI-11 to culture cell lines belonging to the kinome-wide RNAi library. Table 2-4 summarises details of the drugs used.

Drug	Final concentration in medium (µg ml ⁻¹)			Company
	PCF (SDM-79)	BSF (HMI-9)	BSF (HMI-11)	
Hygromycin (Hyg)	50	5	2.5	Invitrogen
Neomycin (Neo)	10	2.5	-	Calbiochem
Blasticidin (BSD)	20	10	10	InvivoGen
Phleomycin (Phleo)	-	2.5	0.5	InvivoGen
Zeocin (Zeo)	10	-	-	Calbiochem
Puromycin (Puro)	-	-	0.2	InvivoGen
Tetracycline (tet)	1	1	1	Sigma

Table 2-4 Drugs used when culturing *T. brucei* strains.

In order to determine the cell density of a culture, 10 µl of cell suspension was loaded onto a Neubauer Improved haemocytometer. In order to ensure accuracy (limited to between 1 x 10⁵ to 1 x 10⁶ cells ml⁻¹), at times, the cell suspension was first diluted before loading onto the haemocytometer. Cells in the four outer quadrants of the haemocytometer, each representing 1 mm², were counted using phase contrast microscopy and the original cell density of the culture was determined by using the following calculation:

$$\text{cells ml}^{-1} = \text{average number of cells/mm}^2 \times \text{dilution factor} \times 10^4.$$

For downstream applications, trypanosomes were harvested via centrifugation (PCF parasites - 600 X g; BSF parasites - 1500 X g) for 10 minutes. When needed, harvested cells were also washed before use. BSF parasites were washed in

sterile trypanosome dilution buffer (TDB; 20 mM Na₂HPO₄, 2 mM NaH₂PO₄·2H₂O, 80 mM NaCl, 5 mM KCl, 1 mM MgSO₄·7H₂O, 20 mM glucose and adjusted to pH 7.4), whilst PCF parasites were washed sterile in phosphate-buffered saline (PBS; 137 mM NaCl, 2.7 mM KCl, 8 mM Na₂HPO₄, 1.8 mM KH₂PO₄ and adjusted to pH 7.4).

2.1.2.3 Storage of *T. brucei* strains

For the purposes of long-term storage, glycerol stock stabilates of cultures were made. Cells from, typically, 10 ml (to make 4 stabilates) of mid-log phase cultures, were harvested (PCF parasites - 600 g, 10 minutes; BSF parasites 1500 g, 10 minutes) to obtain pellets. The pellets were then resuspended in 4 ml fresh culture medium (without selective drugs) supplemented with 10 % (v/v) sterile glycerol (filter-sterilised after adding glycerol and stored at 4°C) and placed as 1 ml aliquots into cryotubes. The stabilates were first allowed to freeze overnight in an insulated container at -80°C before being transferred to liquid nitrogen.

When needed, stabilates removed from liquid nitrogen were allowed to thaw gently at room temperature before the contents were transferred into 10 ml of the appropriate pre-warmed culture media. The cells were allowed to recover without selective drugs for a day before such drugs were added. Cells were typically subpassaged 3-4 times before their use in experiments.

2.1.2.4 Mouse infections

ICR mice were inoculated with appropriate *T. brucei* cell numbers (as determined by the severity of infection expected). The inoculum volume was adjusted to 500 µl in trypanosome dilution buffer (TDB; 20 mM Na₂HPO₄, 2 mM NaH₂PO₄·2H₂O, 80 mM NaCl, 5 mM KCl, 1 mM MgSO₄·7H₂O, 20 mM glucose and adjusted to pH 7.4). RNAi was induced by offering doxycycline-hyclate (Sigma Aldrich D9891 - 5 g) laced sugar water (0.2 g/L doxycycline-hyclate plus 50 g/L sucrose). Mice with parasitaemia above 1 x 10⁸ cells/ml were humanely culled. All animal work was conducted in accordance with Home Office regulations by licensed animal handlers.

2.2 Genetic manipulation

2.2.1 Transformation of bacterial cells

2.2.1.1 Generating competent *E. coli* cells

Competent bacterial cells were generated in the lab. In order to do this, cells from an appropriate overnight culture were diluted 1/500 into 50 ml fresh LB-broth supplemented with the appropriate antibiotics and incubated at 37°C with shaking at 200 rpm until the cell density reached OD_{600 nm} 0.6. The culture was then cooled on ice for 10 minutes before harvesting the cells via centrifugation (957 g, 15 minutes at 4°C). The resulting pellet was then, via gentle vortexing, resuspended in 16 ml ice-cold sterile RF1 buffer (100 nM RbCl, 50 mM MnCl₂·4H₂O, 30 mM CH₃COOK, 10 mM CaCl₂·2H₂O and 15 % (v/v) glycerol adjusted to pH 5.8 with acetic acid). The suspension was then incubated on ice for 15 minutes before harvesting the cells (775 g, 15 minutes at 4°C). The resulting pellet was resuspended in 4 ml cold RF2 buffer (10 mM 3-(N-morpholino) propanesulfonic acid (MOPS), 10 mM RbCl, 75 mM CaCl₂·4H₂O and 15 % (v/v) glycerol, adjusted to pH 6.8 with NaOH) and incubated on ice for 1 hour. 200 µl aliquots were frozen rapidly in a dry ice/ethanol slurry before being transferred to -80°C for long term storage.

2.2.1.2 Transformation of competent *E. coli* cells

Competent *E. coli* cells were transformed with plasmid DNA or ligation products as part of cloning and protein expression protocols. 100 µl aliquots of competent cells were thawed on ice before incubating the required amount (25 - 50 µl cells per construct) with β-mercaptoethanol (0.85 µl per 100 µl cell suspension) on ice for 5 minutes. To these cells, DNA (5 µl ligation product or 10-50 ng plasmid DNA) was added and incubated on ice for a further 20 minutes. The cells were then heat-shocked (42°C for 42 s) and allowed to recover by adding LB-broth (pre-warmed to 42°C; 900 µl per 100 µl competent cells) and incubating the cells with shaking (200 rpm) at 37°C for 30-90 minutes. 100 µl of the cell suspension were then plated aseptically onto an LB-agar plate supplemented with appropriate drugs which was then incubated overnight at 37°C to obtain single

colonies. As controls, an aliquot of cells incubated with dH₂O (instead of DNA), and another aliquot of cells which were plated untransformed onto antibiotic free LB-agar plates, were also included in transformation experiments.

2.2.2 Transfection of *T. brucei* cells

Transfections of *T. brucei* cells were performed using the Amaxa™ Nucleofector™ Technology (Lonza). Cells (5 x 10⁶ PCF cells/3 x 10⁷ BSF cells per construct/control) from parental cultures at mid-log phase were harvested (section 2.1.2.2). The supernatant was then decanted ensuring no residual medium was left before resuspending the cell pellet with 100 µl Amaxa Human T-cell Nucleofector solution (supplemented as per the manufacturer's instruction). The resulting cell suspension was then mixed by slow pipetting with 5-10 µg linearised and purified DNA (section 2.3.2.10; or 5-10 µl dH₂O to set up a mock transfection as a negative control) and transferred to a cuvette supplied with the kit. The cuvette was then placed into the Nucleofector™ cuvette holder and the X-001 program was applied. The transfected cells were then immediately transferred into pre-warmed media (10 ml complete SDM-79 supplemented with 15 % instead of 10 % (v/v) fetal bovine serum for transfected PCF parasites or 30 ml complete HMI-9 for BSF parasites) containing drugs selective for the parental strain. After this step, the protocol varied between the two life cycle stages.

The 10 ml cell suspension of transfected PCF cells was immediately split into 3 x 3.3 ml cultures and allowed to recover for 16 hours (27°C, 5 % CO₂). To each flask, the drugs selective for the transfected constructs were then added. 1/10 and 1/100 dilutions of each flask were then plated as 100 µl aliquots per well into 96-well plates. The plates were incubated for 10 days before the culture volumes from a set of usually six selected positive wells were gradually increased to allow analysis of cell lines (when possible) and the generation of stabilates (section 2.1.2.3). Wells were selected for further culturing only when less than 20 % of the wells contained viable parasites after the selection period.

In the case of BSF parasites, immediately after the transfection, 1 ml aliquots per well of neat, 1/10 and 1/100 dilutions of the 30 ml cell suspension were

plated into 24-well plates and the cells were allowed to recover for 6-12 hours (37°C, 5 % CO₂). 1 ml complete HMI9/HMI11 medium containing 1 X concentration of drugs selective for the parental cell line and 2 X concentration of drugs selective for the transfected constructs was pipetted into each well. The plates were then incubated for 7 days before volumes from usually six selected positive wells were gradually increased to allow analysis of cell lines (when possible) and the generation of stabilates (section 2.1.2.3). Wells were selected for further culturing only when less than 25 % of the wells contained viable parasites after the selection period.

2.3 Molecular Biology – DNA preparation and manipulation

2.3.1 DNA Preparation

2.3.1.1 Extraction of plasmid DNA from *E. coli*

Plasmid DNA from 5 ml overnight liquid cultures of *E. coli* strains was purified using the QIAprep Spin Miniprep kit (Qiagen) in accordance with the manufacturer's protocol. Plasmid DNA was always eluted using 30-50 µl dH₂O. Table 2-5 outlines plasmids that were previously generated/obtained and used in this study.

Plasmid	Details	Source
pGL202	Hyg ^r . Also known as pHD675. <i>T. brucei</i> expression vector featuring PARP-promoter modified to include tet operators (TetO) which drives the expression of a gene of interest in a tet-inducible manner. Linearised with NotI allowing integration into the rRNA gene array.	(Biebinger et al. 1997)
pGL605	Bleo ^r . Also known as p2T7 _{ti} :GFP. <i>T. brucei</i> RNAi vector featuring opposing promoters allowing the generation of dsRNA in a tet-inducible manner. NotI site mutated, therefore, requires linearisation with EcoRV instead prior to transfection into <i>T. brucei</i> parasites to allow integration into the rRNA gene	(LaCount et al. 2000)

	array.	
pHG314/315/316	BSD ^r /Bleo ^r /Hyg ^r , respectively. <i>T. brucei</i> dual promoter expression vector featuring T7 promoters and terminators associated with the resistance gene and Tet-inducible, RNA polymerase promoter driven-expression of gene of interest. Linearised with NotI to allow integration into the rRNA gene array.	Cross lab (http://tryps.rockefeller.edu/trypsru2_plasmids.html).
pET28a+	Kan ^r . Bacterial 6His-tagged protein expression vector.	Novagen
pGEX-5X1	Amp ^r . Bacterial GST-tagged protein expression vector.	GE Lifesciences
pGL1278	Amp ^r . Hyg ^r . Inducible ty-tagged <i>TbPLK</i> expression vector; pGL202 backbone.	(Hammarton et al. 2007)
pGL1279	Amp ^r . Hyg ^r . Inducible ty-tagged <i>TbPLK N169A</i> expression vector; pGL202 backbone.	(Hammarton et al. 2007)
pHG3	Kan ^r . Inducible 6His-tagged <i>TbPLK</i> expression vector; pET28a(+) backbone.	(May 2010)
pHG4	Kan ^r . Inducible 6His-tagged <i>TbPLK N169A</i> expression vector; pET28a(+) backbone.	(May 2010)
pHG123	Kan ^r . Inducible 6His-tagged <i>TbPLK T198V</i> expression vector; pET28a(+) backbone.	(May 2010)
pHG153	Kan ^r . Inducible 6His-tagged <i>PBD⁴³¹ (431-763 aa)</i> expression vector; pET28a(+) backbone.	(May 2010)
pHG152	Kan ^r . <i>TbPLK H704A H706A</i> cloned into pSC-A.	(May 2010)
pHG157	Kan ^r . Inducible 6His-tagged <i>TbPLK T198A</i> expression vector; pET28a(+) backbone.	(May 2010)
pHG329	Bleo ^r . Inducible YFP-tagged <i>PBD (468-763 aa)</i> expression vector; pLew100 backbone.	de Graffenried lab.

Table 2-5 Plasmids used in this study.

2.3.1.2 Extraction of genomic DNA from *T. brucei*

Genomic DNA from *T. brucei* was either extracted using the DNeasy blood and tissue kit (Qiagen) following the manufacturer's instructions or a simple 'mini-prep' procedure using LiCl (Medina-Acosta & Cross 1993). For genomic extraction using the DNeasy kit, 5×10^6 cells were harvested and washed once (section 2.1.2.2) before applying the protocol. For genomic extraction using the 'mini-prep' procedure, 1×10^7 - 1×10^8 cells were harvested and washed once before applying the protocol. Briefly, cell pellets were resuspended in 150 μ l TELT

buffer (50 mM TrisCl at pH 8; 62.5 mM EDTA at pH 9; 2.4 M LiCl and 4 % (v/v) Triton X-100) and incubated for 5 minutes at room temperature before adding 150 μ l of phenol:dH₂O (1:1) and separating the phases via centrifugation (13,000 g for 5 minutes). The aqueous phase was then transferred to separate tube to which 300 μ l of 100 % ethanol was added. The mixture was mixed gently before being incubated for 5 minutes at room temperature. The precipitated DNA was pelleted via centrifugation (13,000 g for 10 minutes) and then washed with 1 ml 100 % ethanol. The DNA was then allowed to air-dry before being resuspended in 100 μ l TE buffer (10 mM TrisCl at pH 8 and 1 mM EDTA at pH 8) with 2 ng μ l⁻¹ pancreatic ribonuclease and incubating it at 37°C for 30 minutes.

2.3.1.3 Determination of DNA concentration

The concentration of prepared DNA samples was measured using a NanoDrop 1000 Spectrophotometer (Thermo Scientific) by measuring absorbance at OD₂₆₀ nm.

2.3.2 DNA manipulation

2.3.2.1 Agarose gel electrophoresis

In order to prepare an agarose gel, 0.7-1 % (w/v) agarose was added to 0.5 % Tris-borate-EDTA (TBE) buffer (44.6 mM Tris-base, 44.5 mM boric acid and 1 mM EDTA) and the mixture then heated in a microwave until all agarose dissolved. The solution was allowed to cool before adding SYBR® Safe DNA Gel Stain (Invitrogen, 1/30,000 dilution). The solution was then poured into a prepared gel cast following which a suitable gel-comb was set in place to make wells. The gel was then allowed to set at room temperature. Once set and the comb removed, the gel was immersed into an appropriate gel tank filled with 0.5 % TBE. DNA samples were prepared by adding DNA loading buffer (6 X stock solution: 0.25 % (w/v) xylene cyanol, 0.25 % (w/v) bromophenol blue and 15 % Ficoll) to a final concentration of 1 X. The DNA samples were then loaded into the wells of the agarose gel. 10 μ l of 1 kb Plus DNA Ladder (Invitrogen; 0.052 μ g ml⁻¹ in 1 X DNA loading buffer) were added to one lane in order to allow size estimation of sample DNA bands. The gels were typically electrophoresed for 30-45 minutes at

100 V before bands were visualised using the GelDoc (BioRad) system and the associated Quantity One Software (BioRad).

2.3.2.2 Polymerase chain reaction (PCR)

PCR was used to amplify genes or parts of a gene from purified plasmid/genomic DNA (section 2.3.1) or from *E. coli* colonies harbouring plasmids (colony PCR; sections 2.3.2.6 and 2.3.2.7). The PCR was also used to introduce mutations into genes on plasmids (site-directed mutagenesis; section 2.3.2.3).

In this study, two different polymerases, *Taq* DNA Polymerase (NEB) and the proof reading polymerase, Phusion™ High-Fidelity DNA Polymerase (Finnzymes), were used. *Taq* polymerase was used to test primer pairs (Table 2-7) for their ability to successfully amplify the required product and for colony PCR. Phusion polymerase was used to amplify genes or gene fragments with high-fidelity for subsequent cloning. Table 2-6 shows the composition of reaction mixes for each enzyme.

Reagents	Polymerase	
	Taq	Phusion®
Buffer	1 X <i>Taq</i> PCR mix*	1 X Phusion PCR mix**
dNTPs	included in <i>Taq</i> PCR mix	0.2 mM
Forward primer	20 ng	20 ng
Reverse primer	20 ng	20 ng
DNA***	5-10 ng	5-10 ng
Enzyme	1 U	0.4 U
Final volume	20 µl	20 µl

Table 2-6 Amounts of components added to make up one PCR reaction.

*Composed of: 113 µg ml⁻¹ BSA, 45 mM Tris (pH 8.8), 11 mM (NH₄)₂SO₄, 4.5 mM MgCl₂, 0.047 % (v/v) β-mercaptoethanol, 4.4 µM EDTA (pH 8) and 1 mM dNTPs (Invitrogen).

**Provided with the enzyme as a 5 X stock solution

***Prepared plasmid/genomic DNA or a small portion of an *E. coli* colony.

For *Taq* polymerase reactions, the PCR programme was set as follows:

- 1 cycle of 95°C for 30 s (for amplification from DNA) or 1 cycle of 95°C for 5 minutes (for colony PCR to ensure cell lysis)
- 30 cycles of 95°C for 50 s; T_m for 50 s; 72°C for 1 minute, where T_m was adjusted depending on the primers used.
- 1 cycle of 72°C for 5 minutes

For Phusion polymerase reactions, the PCR programme was set as follows:

- 1 cycle of 98°C for 30 s
- 35 cycles of 98°C for 10 s; T_m for 30 s; 72°C (T_e) for 15 s, where T_m was adjusted depending on the primers used and T_e was calculated by allowing 15-30 s per 1 kb of amplified product.
- 1 cycle of 72°C for 10 minutes

Primer	5' → 3' sequence and restriction site	Details
OL2138	NheI CCAAGCTAGCATGCACGCAACCGCTGAGAC	Sense primer to amplify <i>TbPLK</i> (from base 4).
OL2139	XhoI GGTTCTCGAGCTAAATATCACGGTTTTGTATG	Antisense primer to amplify <i>TbPLK</i> (up to the final base).
OL2142	BamHI CCAAGGATCCACGCAACCGCTGAGACGTG	Sense primer to amplify <i>TbPLK</i> (from base 4). Designed specifically for cloning into pGEX-5X1.
PR318	NheI GTGACTCGAGCTAGTAGAAGAGTGTGGTAGG	Antisense primer to amplify <i>TbPLK</i> (up to base 936)
PR368	BamHI ACAAGGATCCACGCAACCGCTGAGACGTG	Sense primer to amplify <i>TbPLK</i> (from base 4).
PR369	BamHI ACTGGGATCCGCGGTGAGCATCCCGTCACC	Sense primer to amplify <i>TbPLK</i> (from base 1291).
PR385	BamHI CGACGGATCCAAGGAAAAGAAATG	Sense primer to amplify 3'UTR of <i>TbPLK</i> (from the base which is 1 base upstream of the stop codon).
PR386	HindIII CGTCAAGCTTCCTTCGCCCTTCTC	Antisense primer to amplify 3' UTR of

		<i>TbPLK</i> (up to the base which is 549 bases upstream of the stop codon).
PR403	XhoI GATACTCGAGCTAAGCACTGTTAATGGGG	Antisense primer to amplify <i>TbPLK</i> (up to base 1290).
PR404	BamHI GTTAGGATCCAGTTCACGCCGCGTCAG	Sense primer to amplify <i>TbPLK</i> (from base 937).

Table 2-7 PCR primers used in this study for gene cloning.

1 µl samples, made up to 10 µl volume with dH₂O, of all PCR reactions were electrophoresed via agarose gel electrophoresis to verify appropriate amplification.

2.3.2.3 Site-directed mutagenesis

Site-directed mutagenesis was performed using the Quikchange II Site-directed Mutagenesis kit (Agilent) and mutagenised plasmid mixes were transformed into XL1-Blue supercompetent cells according to the manufacturer's instructions. The primers used to introduce mutations are given in Table 2-8. Plasmid DNA was prepared (section 2.3.1.1) from selected colonies obtained, tested via small-scale restriction digests (section 2.3.2.4) and analysed via DNA sequencing to verify the introduction of the desired mutation and the absence of any unwanted mutations in the sequence of the gene of interest (section 2.3.2.9). Table 2-9 describes plasmids that were successfully mutated via site-directed mutagenesis in this study.

Primer	5' → 3' sequence	Details
PR387	CGCGCCATTTGTGGCGCCCCCAATTATATCGCACC G	Sense primer to introduce T202A mutation into <i>TbPLK</i> T198A.
PR388	CGGTGCGATATAATTGGGGGCGCCACAAATGGCG CG	Antisense primer to introduce T202A mutation into <i>TbPLK</i> T198A.
PR389	CGCGACATTTGTGGCGACCCCCAATTATATCGCACC GG	Sense primer to introduce T202D mutation into <i>TbPLK</i> T198D.

PR390	CCGGT G CGATATAATTGGGG T CGCCACAAATGTC GCG	Antisense primer to introduce T202D mutation into <i>TbPLK T198D</i> .
PR391	CGCGCCATTTGTGGCG A CCCCAATTATATCGCACC G	Sense primer to introduce T202D mutation into <i>TbPLK T198A</i> .
PR392	CGGTGCGATATAATTGGGG T CGCCACAAATGGCG CG	Antisense primer to introduce T202D mutation into <i>TbPLK T198A</i> .
PR393	CGCGACATTTGTGGCG C CCCCAATTATATCGCACC G	Sense primer to introduce T202A mutation into <i>TbPLK T198D</i> .
PR394	CGGTGCGATATAATTGGGG G CGCCACAAATGTCG CG	Antisense primer to introduce T202A mutation into <i>TbPLK T198D</i> .
PR395	CGCACTATTTGTGGCG C CCCCAATTATATCGCACC G	Sense primer to introduce T202A mutation into <i>TbPLK</i> .
PR396	CGGTGCGATATAATTGGGG G CGCCACAAATAGTG CG	Antisense primer to introduce T202A mutation into <i>TbPLK</i> .
PR397	CGCACTATTTGTGGCG A CCCCAATTATATCGCACC GGAG	Sense primer to introduce T202D mutation into <i>TbPLK</i> .
PR398	CTCCGGT G CGATATAATTGGGG T CGCCACAAATA GTGCG	Antisense primer to introduce T202D mutation into <i>TbPLK</i> .
PR409	CGCACTATTTGTGGCG A GCCCAATTATATCGCACC GGAG	Sense primer to introduce T202E mutation into <i>TbPLK</i> .
PR410	CTCCGGT G CGATATAATTGGG C CGCCACAAATAG TGCG	Antisense primer to introduce T202E mutation into <i>TbPLK</i> .

Table 2-8 Primers used for site-directed mutagenesis. Bases shown in bold highlight mutations that are to be introduced.

Original gene	Parent plasmid*	Primers used**		Mutation introduced	Resulting plasmid
		Sense	Anti-sense		
<i>TbPLK T198A</i>	pHG393	PR387	PR388	T202A	pHG438
<i>TbPLK T198D</i>	pHG395	PR389	PR390	T202D	pHG439
<i>TbPLK T198A</i>	pHG393	PR391	PR392	T202D	pHG440
<i>TbPLK T198D</i>	pHG396	PR393	PR394	T202A	pHG441

<i>TbPLK</i>	pHG389	PR395	PR396	T202A	pHG442
<i>TbPLK</i>	pHG389	PR397	PR398	T202D	pHG443
<i>TbPLK</i>	pHG389	PR409	PR410	T202E	pHG460

*For details of plasmids used, see Table 2-11.

**For details of primers used, see Table 2-8.

Table 2-9 Details of mutations introduced into *TbPLK* genes including parent plasmids and primers used, and the resulting plasmids that were generated.

2.3.2.4 Restriction endonuclease digests

To verify plasmid identity and for cloning experiments, DNA samples were digested with selected restriction endonucleases (NEB).

Plasmid DNA was routinely checked and verified via small-scale digests before further work. To 1 μl (typically 0.2-0.5 μg) of the Mini-prep product (section 2.3.1.1), 10 U of the selected restriction endonuclease(s), 1 $\mu\text{g } \mu\text{l}^{-1}$ bovine-serum albumin and 1 μl of the appropriate buffer were added as prescribed by the manufacturer's protocol. This reaction mixture was then made up to 10 μl with dH_2O before incubating it for 30-60 minutes at the appropriate temperature in accordance with the manufacturer's guidelines.

For cloning and for plasmid linearisation (prior to transfection into *T. brucei*), plasmid DNA was subjected to large scale restriction endonuclease digestion. For cloning, typically 20 μl (4-8 μg) of the Mini-prep product (section 2.3.1.1), 20 U of the selected restriction endonuclease(s), 1 $\mu\text{g } \mu\text{l}^{-1}$ bovine-serum albumin and 10 μl of the appropriate buffer was added. For linearisation, 10 μg of the Mini-prep product (section 2.3.1.1), 20-60 U of the selected restriction endonuclease, 1 $\mu\text{g } \mu\text{l}^{-1}$ bovine-serum albumin and 10 μl of the appropriate buffer were added. These reaction mixtures were then made up to 100 μl with dH_2O before incubating them for 16 hours at the appropriate temperature.

All digest products were analysed via agarose gel electrophoresis (section 2.3.2.1) before being used for downstream applications. In the case of small-scale digests, all 10 μl of the digest products were analysed whilst in the case of large-scale digests, 0.5-1 μl samples that were made up to 10 μl volume with dH_2O , were analysed.

2.3.2.5 DNA extraction from agarose gels

For the purpose of cloning, the required DNA fragments were visualised under blue light following electrophoresis (section 2.3.2.1) and were excised from the gel using clean scalpels. The gel slices were then solubilised and DNA was extracted from them using the QIAquick Gel Extraction kit (Qiagen) in accordance with manufacturer's guidelines. DNA was eluted in 30 µl dH₂O.

2.3.2.6 Cloning of amplified genes/fragments into generic cloning vectors

Phusion polymerase-amplified products (section 2.3.2.2) were always first cloned into the pSC-B-Amp/Kan blunt cloning vector (Stratgene) following the manufacturer's instructions before they were sub-cloned into the appropriate final destination vector (section 2.3.2.7). A set of colonies were then screened for the presence of the gene/fragment of interest within pSC-B-Amp/Kan (section 2.3.2.2). At least two of the colonies confirmed to have an insert were then analysed via small-scale restriction digests (section 2.3.2.4) and subsequently by DNA sequencing to confirm the presence of the desired gene/fragment (section 2.3.2.9). Table 2-10 describes the genes/fragments that were amplified in this project along with the resulting plasmids that were generated following the cloning of these amplified products into pSC-B-Amp/Kan.

Sequence amplified	Template DNA	Primers used***		pSC-B-Amp/Kan plasmid
		Sense	Anti-sense	
<i>KD</i>	pGL1278*	OL2142	PR318	pHG304
<i>KD N169A</i>	pGL1279*	OL2142	PR318	pHG376
<i>TbPLK</i>	pGL1278*	PR368	OL2139	pHG379
<i>TbPLK N169A</i>	pGL1279*	PR368	OL2139	pHG380
<i>KD</i>	pGL1278*	PR368	PR318	pHG381
<i>KD N169A</i>	pGL1279*	PR368	PR318	pHG382
<i>TbPLK T198A</i>	pHG157*	PR368	OL2139	pHG383
<i>TbPLK T198V</i>	pHG123*	PR368	OL2139	pHG384
<i>TbPLK T198D</i>	pHG163*	PR368	OL2139	pHG385
<i>TbPLK H704A H706A</i>	pHG152*	PR368	OL2139	pHG386
<i>PBD</i> ⁴³¹	pGL1278*	PR369	OL2139	pHG387

<i>PBD⁴³¹ H704A H706A</i>	pHG152*	PR369	OL2139	pHG388
<i>TbPLK 3'UTR</i>	BSF 427 genomic DNA	PR385	PR386	pHG444
<i>TbPLK ΔPBD⁴³¹</i>	pGL1278*	PR368	PR403	pHG447
<i>TbPLK ΔKD+PBD⁴³¹</i>	pGL1278*	PR404	PR403	pHG448
<i>TbPLK ΔKD</i>	pGL1278*	PR404	OL2139	pHG449
<i>TbPLK T198D T202D</i>	pHG439**	OL2138	OL2139	pHG463
<i>TbPLK T198A T202D</i>	pHG440**	OL2138	OL2139	pHG464
<i>TbPLK T202A</i>	pHG442**	OL2138	OL2139	pHG465
<i>TbPLK T202D</i>	pHG443**	OL2138	OL2139	pHG466
<i>TbPLK T202E</i>	pHG460**	OL2138	OL2139	pHG467

*For details of plasmids used, see Table 2-5.

**For details of plasmids used, see Table 2-9.

***For details of primers used, see Table 2-7.

Table 2-10 *TbPLK* gene fragments amplified with details of templates and primers used. Also included are the names of the resulting plasmids when the amplified fragments were cloned into the generic blunt cloning vector pSC-B-Amp/Kan. KD - kinase domain; PBD - Polo-box domain.

2.3.2.7 Subcloning

DNA ligation was used to insert restriction endonuclease digested fragments into a recipient plasmid.

First, appropriate large-scale restriction digests (section 2.3.2.4) were performed to cut the desired fragment out of the donor plasmid (insert) and to cut the destination vector backbone (vector). Digests were electrophoresed on agarose gels to separate the fragments, and the required fragments were excised from the gel under blue light using a clean scalpel blade. DNA was then purified from the gel slices obtained (section 2.3.2.5) and the concentrations of the purified products were ascertained (section 2.3.1.3).

In order to set up a ligation reaction, the relative amounts of purified insert and vector DNA was then determined using the formula:

$$[(\text{ng vector} \times \text{kb insert}) / (\text{kb vector})] \times \text{molar ratio of insert:vector} = \text{ng insert}$$

where the molar ratio of 3:1 (insert:vector) was routinely used. Volumes used were such that the vector and insert would collectively measure less than 8 μ l.

Also, a vector only reaction was set up as a negative control.

Typically, 10 μ l ligation reactions were set up. 1 X T4 DNA ligase buffer (NEB) and 0.4 U T4 DNA ligase (NEB) were added to the insert and vector DNA and the final volume was then made up to 10 μ l with dH₂O. The reaction mixture was then incubated, either for 1 hour at room temperature or for 16 hours at 4°C, before transforming the resulting products into XL1-Blue cells (sections 2.1.1.1 and 2.2.1.2).

The colonies obtained were then screened via PCR (section 2.3.2.2) to determine whether they likely harboured the desired final plasmid. Plasmid DNA was extracted from PCR-positive colonies and further analysed via small-scale restriction digests (section 2.3.2.4).

Sub-cloning reactions that were carried out in this project have been described in Table 2-11.

Plasmid	Fragment subcloned from	Final destination vector	Restriction sites used	Details
pHG321	pHG304*	pGEX-5XI**	BamHI+XhoI	Amp ^r . <i>KD</i> cloned into pGEX-5XI to generate GST-tagged protein.
pHG341	pHG329**	pGL202**	HindIII+BamHI	Amp ^r . Bleo ^r . <i>YFP</i> cloned into pGL202 (pHD675).
pHG342	pHG329**	pHG316**	HindIII+BamHI	Amp ^r . Hyg ^r . <i>YFP</i> cloned into pHG316 (pLew100v5).
pHG366	fragment generated by annealing complementary primers, PR364 and PR365***	pHG341	BamHI+BclI overhangs in fragment cloned into BamHI site in pHG341	Amp ^r . Bleo ^r . MCS introduced into pHG341 to allow N-terminal YFP-tagged overexpression of target protein in PCF <i>T. brucei</i> parasites.
pHG367	fragment generated by annealing complementary primers,	pHG342	BamHI+BclI overhangs in fragment cloned into BamHI site in	Amp ^r . Hyg ^r . MCS introduced into pHG342 to allow N-terminal YFP-tagged overexpression of target

	PR366 and PR367***		pHG342	protein in BSF <i>T. brucei</i> parasites.
pHG378	pHG376*	pGEX-5XI**	BamHI+XhoI	Amp ^r . <i>KD N169A</i> cloned into pGEX-5X1 to generate GST-tagged protein.
pHG389	pHG379*	pHG366	BamHI+XhoI	Amp ^r . Hyg ^r . <i>TbPLK</i> cloned into pHG366 (see above).
pHG390	pHG380*	pHG366	BamHI+XhoI	Amp ^r . Hyg ^r . <i>TbPLK N169A</i> cloned into pHG366 (see details for pHG366).
pHG391	pHG381*	pHG366	BamHI+XhoI	Amp ^r . Hyg ^r . <i>KD</i> cloned into pHG366 (see details for pHG366).
pHG392	pHG382*	pHG366	BamHI+XhoI	Amp ^r . Hyg ^r . <i>KD N169A</i> cloned into pHG366 (see details for pHG366).
pHG393	pHG383*	pHG366	BamHI+XhoI	Amp ^r . Hyg ^r . <i>TbPLK T198A</i> cloned into pHG366 (see details for pHG366).
pHG394	pHG384*	pHG366	BamHI+XhoI	Amp ^r . Hyg ^r . <i>TbPLK T198V</i> cloned into pHG366 (see details for pHG366).
pHG395	pHG385*	pHG366	BamHI+XhoI	Amp ^r . Hyg ^r . <i>TbPLK T198D</i> cloned into pHG366 (see details for pHG366).
pHG396	pHG386*	pHG366	BamHI+XhoI	Amp ^r . Hyg ^r . <i>TbPLK H704A K706A</i> cloned into pHG366 (see details for pHG366).
pHG397	pHG387*	pHG366	BamHI+XhoI	Amp ^r . Hyg ^r . <i>PBD⁴³¹</i> cloned into pHG366 (see details for pHG366).
pHG398	pHG388*	pHG366	BamHI+XhoI	Amp ^r . Hyg ^r . <i>PBD⁴³¹ H704A K706A</i> cloned into pHG366 (see details for pHG366).
pHG399	pHG315**	pHG367	HindIII+NotI	Amp ^r . Switched resistance cassette of pHG367 from Hyg ^r to Bleo ^r (see details for pHG367).
pHG402	pHG379*	pHG399	BamHI+XhoI	Amp ^r . Bleo ^r . <i>TbPLK</i> cloned into pHG366 (see details for pHG366).

pHG403	pHG380*	pHG399	BamHI+XhoI	Amp ^r . Bleo ^r . <i>TbPLK N169A</i> cloned into pHG366 (see details for pHG366).
pHG404	pHG381*	pHG399	BamHI+XhoI	Amp ^r . Bleo ^r . <i>KD</i> cloned into pHG366 (see details for pHG366).
pHG405	pHG382*	pHG399	BamHI+XhoI	Amp ^r . Bleo ^r . <i>KD N169A</i> cloned into pHG366 (see details for pHG366).
pHG406	pHG383*	pHG399	BamHI+XhoI	Amp ^r . Bleo ^r . <i>TbPLK T198A</i> cloned into pHG366 (see details for pHG366).
pHG407	pHG384*	pHG399	BamHI+XhoI	Amp ^r . Bleo ^r . <i>TbPLK T198V</i> cloned into pHG366 (see details for pHG366).
pHG408	pHG385*	pHG399	BamHI+XhoI	Amp ^r . Bleo ^r . <i>TbPLK T198D</i> cloned into pHG366 (see details for pHG366).
pHG409	pHG386*	pHG399	BamHI+XhoI	Amp ^r . Bleo ^r . <i>TbPLK H704A K706A</i> cloned into pHG366 (see details for pHG366).
pHG410	pHG387*	pHG399	BamHI+XhoI	Amp ^r . Bleo ^r . <i>PBD⁴³¹</i> cloned into pHG366 (see details for pHG366).
pHG411	pHG388*	pHG399	BamHI+XhoI	Amp ^r . Bleo ^r . <i>PBD⁴³¹ H704A K706A</i> cloned into pHG366 (see details for pHG366).
pHG450	pHG447*	pHG366	BamHI+XhoI	Amp ^r . Hyg ^r . <i>ΔPBD⁴³¹</i> cloned into pHG366 (see details for pHG366).
pHG451	pHG448*	pHG366	BamHI+XhoI	Amp ^r . Hyg ^r . <i>ΔKD+PBD⁴³¹</i> cloned into pHG366 (see details for pHG366).
pHG452	pHG449*	pHG366	BamHI+XhoI	Amp ^r . Hyg ^r . <i>ΔKD</i> cloned into pHG366 (see details for pHG366).
pHG456	pHG314**	pGL605**	SnaBI	Amp ^r . Switched resistance cassette from Bleo ^r to BSD ^r (see details of pGL605 in Table 2-5).
pHG457	pHG444*	pHG456	HindIII+BamHI	Amp ^r . BSD ^r . <i>TbPLK 3'UTR</i> cloned into pHG456 to induce RNAi.

pHG468	pHG463*	pET28a+**	NheI+XhoI	Kan ^r . <i>TbPLK T198D T202D</i> cloned into pET28a+ to generate His-tagged protein.
pHG469	pHG464*	pET28a+**	NheI+XhoI	Kan ^r . <i>TbPLK T198A T202D</i> cloned into pET28a+ to generate His-tagged protein.
pHG470	pHG465*	pET28a+**	NheI+XhoI	Kan ^r . <i>TbPLK T202A</i> cloned into pET28a+ to generate His-tagged protein.
pHG471	pHG466*	pET28a+**	NheI+XhoI	Kan ^r . <i>TbPLK T202D</i> cloned into pET28a+ to generate His-tagged protein.
pHG472	pHG467*	pET28a+**	NheI+XhoI	Kan ^r . <i>TbPLK T202E</i> cloned into pET28a+ to generate His-tagged protein.

*For details of plasmids used, see Table 2-10

**For details of plasmids used, see Table 2-5

***For further details, see section 2.3.2.8.

Table 2-11 Details of plasmids generated in this study following subcloning and modification. *KD* comprises of bases 4-936 (2-312 aa) of *TbPLK*; *PBD*⁴³¹ comprises of bases 1292-end (431-763 aa) of *TbPLK*; Δ *PBD*⁴³¹ comprises of bases 4-1291 (1-430 aa) of *TbPLK*; Δ *KD*+*PBD*⁴³¹ comprises of bases 937-1291 (313-430 aa) of *TbPLK*; Δ *KD* comprises of bases 937-end (313-763 aa) of *TbPLK*.

2.3.2.8 Addition of multiple cloning sites

In order to add multiple cloning sites into the plasmids pHG341 and pHG342, linker DNA sequences were generated using primers PR364+PR365 and PR366+PR367, respectively (Table 2-12).

To do this 0.5 μ g each of the sense and antisense primers, diluted with dH₂O to a final volume of 100 μ l, were heated at 95°C for 2 minutes and then allowed to cool at room temperature. These linker sequences (inserts) were then subcloned into pHG341 and pHG342 (vectors) as described in section 2.3.2.7.

Primer	5' → 3' sequence	Details
PR364	BamHI <u>MluI</u> XhoI <u>HpaI</u> BclI	Sense primer to introduce a multiple

	GATCC <u>ACGCGTCTCGAGGTTAACT</u>	cloning site into the BamHI site of pHG341
PR365	BclI HpaI XhoI MluI BamHI GATCAGTTAACCTCGAGACGCGTG	Antisense primer to introduce a multiple cloning site into the BamHI site of pHG341
PR366	BamHI ApaI XhoI HpaI BclI GATCCGGGCCCTCGAGGTTAACT	Sense primer to introduce a multiple cloning site into the BamHI site of pHG342
PR367	BclI HpaI XhoI ApaI BamHI GATCAGTTAACCTCGAGGGGCCCG	Sense primer to introduce a multiple cloning site into the BamHI site of pHG342

Table 2-12 Primers used to generate linker sequences for adding multiple cloning sites into pHG341 and pHG342.

2.3.2.9 DNA sequencing

DNA samples were sequenced by the University of Dundee sequencing service (<http://www.dnaseq.co.uk/home.html>). The primers that were routinely used for sequencing have been listed in Table 2-13.

Primer	5' → 3' sequence	Details
M13 forward	GTAAAACGACGGCCAGT	Sense primer to sequence insert in pSC-B.
M13 reverse	GGAAACAGCTATGACCATG	Antisense primer to sequence insert in pSC-B.
OL87	CTGCAGGCGCACCTCCCTGCTG	Antisense primer to sequence up to the 3' end of the MCS in pGL202 (pHD675).
OL88	TAGGGGTTATCGGGTAGGGATC	Sense primer to sequence from the 5' end of the MCS in pGL202

		(pHD675).
OL2223	CAGTTCACGCCGCGTCAGC	Sense primer to sequence <i>TbPLK</i> (from base 936).
OL2224	GCCACCCGCACACAAACC	Sense primer to sequence <i>TbPLK</i> (from base 1516).
OL3035	GCATGGACGAGCTGTACAAG	Sense primer to sequence <i>GFP/YFP</i>

Table 2-13 Primers used for sequencing.

2.3.2.10 Purification of linearised DNA for transfection into *T. brucei*

To purify linearised DNA (section 2.3.2.4), ½ volume chloroform:isoamyl alcohol (24:1) and ½ volume phenol were added to the digested DNA and the mixture vortexed before centrifugation (17968 g, for 2 minutes at room temperature) to separate the lower organic phase from the upper aqueous layer containing the DNA. The top layer was carefully pipetted into a new tube to which 1 volume of chloroform:isoamyl alcohol was added before the mix was vortexed and centrifuged as described above. This step was repeated once more following which the top layer was decanted, and 1/10 volume 3 M CH₃COONa and 1 volume isopropanol were added. The tube was gently mixed causing the DNA to precipitate. To pellet the DNA, this mixture was centrifuged for 20 minutes, 17968 g at 4°C. The pellet was then washed with 70 % ethanol and centrifuged as above to pellet the DNA. The ethanol was decanted and the DNA pellet was then dried under a sterile hood until no ethanol remained. The DNA pellet was then solubilised in dH₂O to a final concentration of 1 µg µl⁻¹. Protein analysis, purification and biochemistry

2.4 Protein analysis, purification and biochemistry

2.4.1 Polyacrylamide gel electrophoresis (PAGE) and Western Blotting

2.4.1.1 Sodium dodecyl sulphate (SDS)-PAGE

SDS-PAGE was used to size-separate proteins in denaturing conditions as a means of analysing protein preparations and cell lysates. Gels were then Coomassie stained (section 2.4.1.2) to visualise separated proteins or probed further with specific antibodies via Western-blotting (section 2.4.1.3).

Typically, 12 % separating gels were used with a layer of 5 % stacking gel on top to focus samples before separation. In order to prepare the separating gel, all the reagents described in Table 2-14 (except TEMED and ammonium persulphate) were mixed together. TEMED and ammonium persulphate were added at the end, following which the solution was mixed again before being poured into a gel cassette (Invitrogen). A layer of isopropanol was then added on top to remove air bubbles.

Reagent	Volume
30 %/0.8 % (w/v) Acrylamide/Bis acrylamide	6 ml
10 % (w/v) SDS	250 μ l
1 M Tris HCl (pH 8.8)	9.4 ml
dH ₂ O	8.8 ml
5 % (w/v) Ammonium persulphate	625 μ l
TEMED	6.25 μ l

Table 2-14 12 % Separating gel recipe. Final volume enough to make four 1 mm thick mini gels using Invitrogen gel cassettes.

Once set, the isopropanol was decanted before pouring in the stacking gel. The stacking gel was prepared mixing in all the ingredients described in Table 2-15 as described above for the separating gel. Once poured into the cast as an overlay to the already set separating gel, gel combs were set into place to generate wells for loading protein samples. Once set, the combs were removed, and the cassettes were placed in gel tanks and immersed in 1 X Tris-Glycine-SDS Page Buffer (10 X stock; National Diagnostics)

Reagent	Volume
30 %/0.8 % (w/v) Acrylamide/Bis acrylamide	1 ml
10 % (w/v) SDS	125 μ l
0.375 M Tris HCl (pH 6.8)	4.2 ml
dH ₂ O	6.3 ml
5 % (w/v) Ammonium persulphate	1 ml
TEMED	5 μ l

Table 2-15 4 % Stacking gel recipe. Final volume sufficient to make four 1 mm thick mini gels using Invitrogen gel cassettes.

For analysis via Western blotting, protein samples or *T. brucei* cell pellets (prepared by harvesting cells and washing them once (section 2.1.2.2) were prepared by addition of 1 X Laemmli loading dye (final concentration; 25 mM Tris-HCl pH 6.8, 1 % SDS, 0.05 % bromophenol blue, 50 mM dithiothreitol (DTT)) where the final concentration of *T. brucei* cell samples was maintained at 1×10^5 cells μ l⁻¹. All samples were then heated at 95°C for 5-10 minutes before loading.

Samples were loaded into the wells and electrophoresed for 1 hour at 200 V. Standard ladders were also electrophoresed with the samples to allow determination of the molecular weights of protein bands. For Coomassie staining, 10 μ l of BenchMark™ Protein Ladder (Invitrogen; unstained, prepared according to manufacturer's instructions) was used whilst for Western blotting, 10 μ l of Novex® Sharp Pre-stained Protein Standard (Invitrogen) was used.

2.4.1.2 Coomassie staining

Following electrophoresis, SDS-PAGE gels were incubated with Coomassie blue stain (0.25 % (w/v) Coomassie Blue-R250, 10 % (v/v) acetic acid and 45 % (v/v) methanol) for 1 hour, before being destained with 10 % (v/v) acetic acid, 45 % (v/v) methanol. The destain solution was changed once after 30 minutes and destaining was continued until a background staining was reduced to acceptable levels.

The gels were imaged under epi-white illumination using the Gel Doc™ system (Bio-Rad) and dried onto filter-papers using a Model 583 Gel Dryer (Bio-Rad).

2.4.1.3 Western blotting

Once electrophoresed, proteins from an SDS-PAGE gel were transferred onto a blotting membrane such as PVDF or nitrocellulose by electro-transfer. PVDF transfer membrane (Perkin Elmer) or Hybond ECL nitrocellulose membrane were prepared by soaking them in 100 % methanol or transfer buffer (Tris-SDS-Glycine and 10 % (for one gel) or 20 % (for two gels) methanol), respectively. The XCell II™ Blot Module (Invitrogen) was assembled according to the manufacturer's instructions and immersed in transfer buffer. The electrotransfer was carried out for 1.5 hours at 30 V. To visualize transferred proteins, the membrane was stained for 5 minutes with Ponceau reagent and destained to an appropriate level under running tap water.

Following transfer and Ponceau staining, the membrane was blocked in PBS-T (0.5 % (v/v) Tween 20 in PBS) containing 5 % (w/v) Marvel skimmed milk powder (PBS-T milk), shaking, for either 16 hours at 4°C or for 1 hour at room temperature. The membrane was then given a quick rinse with PBS-T before being probed with the primary antibody (diluted in PBS-T milk; Table 2-16), shaking, either for 16 hours at 4°C or for 1 hour at room temperature. The membrane was then washed three times with PBS-T (1 x 15 minutes and then 2 x 5 minutes) before being incubated with the secondary antibody (diluted in PBS-T milk; Table 2-17) for 1 hour, shaking, at room temperature. The membrane was then washed in PBS-T as earlier, before developing it using an enhanced chemiluminescence (ECL) HRP substrate (Super Signal® WestPico/Dura/Femto) to reveal antibody labeling according to manufacturer's instructions. Chemiluminescence was visualized by exposing the developed membrane to an X-ray film and processing the film using an X-Omat automatic developer machine.

Antibody	Company/Gift from	Dilution
α-GFP mouse monoclonal (clone JL-8)	Living Colors®, Clontech	1:400
α -EF1α mouse monoclonal (clone CBP-KK1)	Millipore	1:10,000
α-TY-1 mouse monoclonal IgG1 (clone BB2)	Mathews lab (Bastin et al. 1996)	1:50
α-PLK rabbit polyclonal	de Graffenreid lab (Ikeda & de Graffenreid 2012)	1:300

Table 2-16 Primary antibodies used for Western blotting

Antibody	Company	Dilution
α -mouse IgG-HRP conjugate	Promega	1:10,000
α -rabbit IgG-HRP conjugate	Sigma	1:10,000

Table 2-17 Secondary antibodies used for Western blotting.

2.4.2 Bacterial recombinant protein production

E. coli strains (Table 2-1) expressing recombinant proteins were generated by transforming BL21 DE3 pLysS cells (section 2.2.1) with expression plasmids (pET28a+ or pGEX-5X1 backbones to generate His-tagged or GST-tagged proteins, respectively) (see Table 2-11). Before transformation into the BL21 derived cells, the final pET28a+ or pGEX-5X1 constructed plasmids (section 2.3.2.7 and Table 2-11) were first transformed into XL1-Blue cells (section 2.2.1) to allow stable storage. The plasmids for transformation into BL21 DE3 pLysS cells were prepared from these XL1-Blue colonies and verified via small-scale digest.

2.4.2.1 Protein expression

For large scale protein production, overnight liquid cultures of the appropriate BL21 DE3 pLysS bacterial strain were diluted 1:100 in 400 ml LB-broth and allowed to grow at 37°C, shaking at 200 rpm until the density of the culture reached OD_{600 nm} 0.6-1. If needed, cultures were then cooled to the appropriate temperature (optimised experimentally via small scale expression experiments and analysis of the insoluble and soluble fractions of the resultant cell pellets to ensure adequate expression levels of soluble protein) at which the cells were to be induced for protein production. In this study, expression of the described proteins from the pET28a+ and the pGEX-5X1 plasmids required induction with 1 mM IPTG at 20°C for 18-20 hours.

Cells were harvested via centrifugation (5285 g, 10 minutes at 4°C). The resulting pellets were then resuspended in 10 ml (per 400 ml liquid culture) ice-cold lysis buffer supplemented with EDTA-free protease inhibitor cocktail (Roche). For His-tagged proteins, the buffer used was Buffer A (20 mM NaH₂PO₄ pH 7.5, 0.5 M NaCl, 20 mM imidazole pH 7.5 and 5 mM β -mercaptoethanol). For

GST-tagged proteins, PBS was used. The pellets were then stored at -80°C for at least one hour in order to promote lysis.

The frozen pellets were then thawed to room temperature before lysing the cells via sonication. The 10 ml lysates were sonicated using a Soniprep 150 (MSE), on ice, with 10 blasts of 10 s, with at least 10 s rest in between each blast, at 30 % amplitude. The soluble fraction was then separated from the insoluble fraction via centrifugation (20000 g, 20 minutes at 4°C).

2.4.2.2 His-tagged protein purification

His-tagged proteins were purified using Ni-NTA agarose beads (Qiagen) by following a bench-top protocol. 0.5-1 ml of 50 % slurry (per soluble fraction originating from a 400 ml liquid culture) was prepared by washing the beads in 5 ml buffer A. The beads were then harvested (500 g, 2 minutes) before incubating them with the soluble fraction for 1 hour at 4°C on a rotary mixer.

The beads potentially bound with the target protein were then harvested as described above and washed four times with 10 ml ice-cold buffer A. The washed beads were then resuspended in 4 ml buffer B (as buffer A but with 250 mM imidazole pH 7.5). Disposable polypropylene columns (Pierce) were set up with the provided polyethylene filter discs and prepared for use by washing them first with water, buffer A and finally with buffer B. The beads resuspended in buffer were then transferred into the prepared columns and allowed to settle. The resulting eluate was then allowed to drip through and be collected in a separate tube. A further 1 ml buffer B was added to the beads and the resulting eluate was also collected.

To determine the efficiency of the purification, samples were collected at each stage of expression and purification, and analysed by SDS-PAGE and Coomassie staining.

2.4.2.3 GST-tagged protein purification

GST-tagged proteins were purified using glutathione sepharose beads (GE Healthcare) by following a bench-top protocol. 200 μl of glutathione sepharose

beads slurry (per 5 ml of soluble fraction) were prepared by washing them in 2 ml PBS. The beads were then harvested (500 g, 5 minutes) before incubating them with 5 ml soluble fraction for 1 hour at room temperature on a rotary mixer.

The beads potentially bound with the target protein were then harvested as described above and washed with 1 ml PBS, three times. Bound proteins were then eluted by resuspending the washed beads in 200 μ l of glutathione elution buffer (10 mM glutathione, 50 mM Tris HCl pH 8) and incubating the mixture for 10 minutes at room temperature on a rotary mixer. The beads were harvested as described above and the resulting supernatant collected as an eluate. These elution steps were repeated twice and the resulting eluates were pooled together at the end.

To determine the efficiency of the purification, samples were collected at each stage of expression and purification, and analysed by SDS-PAGE and Coomassie staining.

2.4.2.4 Determination of protein concentration and storage of purified proteins

As soon as possible, buffers of the pooled eluates were exchanged with kinase storage buffer (40 mM Tris-Cl pH 7.6, 50 mM NaCl, 1 mM DTT, 10 % glycerol using Amicon® Ultra-15 Centrifugal Filter Devices (Millipore)). The purified proteins were stored at -80°C .

Following buffer exchange, protein concentrations were determined using a NanoDrop 1000 Spectrophotometer (Thermo Scientific).

2.4.3 Kinase assays

The kinase activities of purified recombinant proteins (section 2.4.2) were analysed using protein kinase assays.

Equimolar amounts of recombinant proteins, made up to a volume of 20 μ l with kinase assay buffer (KAB; 50 mM MOPS pH 7.4, 20 mM MgCl_2 , 2 mM DTT, 10 mM

ethylene glycol tetraacetic acid (EGTA)), were added to 20 μ l of kinase assay mixture (KAB supplemented with 5 μ g of α -casein when needed, 4 μ M ATP, and 0.037 MBq [γ - 32 P] ATP) and incubated for 30 minutes at 30°C. Reactions were stopped by adding Laemmli loading buffer to a final concentration of 1 X and boiling for 5 minutes. Reaction mixtures were then electrophoresed by SDS-PAGE using 12 % gels, which were then Coomassie stained and dried before exposing them to a phosphorimager screen or an X-ray film (later processed using Typhoon Phosphorimaging system/X-Omat automatic developer machine, respectively).

2.5 Microscopy

5×10^5 - 1×10^6 *T. brucei* cells were harvested and washed (section 2.1.2.2), resuspended in the residual supernatant and spread onto glass microscope slides. The slides were then air-dried before placing them in methanol at -20°C for at least 20 minutes to fix the cells. When the slides were ready to be used, they were air-dried and the cells were rehydrated using PBS. The slides were mounted with Vectashield mounting medium (Vector labs) containing DAPI which was sealed with a cover-slip and the application of nail varnish.

The fixed *T. brucei* cells were viewed under oil immersion using a Zeiss Axioscope fluorescent microscope at 1000 X magnification and images were processed using Openlab (Perkin Elmer) version 5.5 software or Volocity 3D Image Analysis Software (Perkin Elmer). For cell-cycle analysis, the slides were viewed at 630 X magnification and the number of nuclei and kinetoplasts per cell were counted (at least 200 cells per sample).

2.6 Flow cytometry

Flow cytometry was used to characterise the DNA content of a particular *T. brucei* cell population. To prepare the cells, 5×10^6 to 1×10^7 cells were harvested (section 2.1.2.2) and washed once with PBS. The cells were then resuspended in the 300 μ l PBS before carefully adding in 700 μ l methanol whilst mixing gently to prevent cells clumping together. The fixed cells were left at 4°C for at least 16 hours (or up to a month) before harvesting the cells via

centrifugation (section 2.1.2.2) and washing them once in PBS. The cells were then resuspended in 1 ml PBS containing $10 \mu\text{g ml}^{-1}$ propidium iodide (PI) and $10 \mu\text{g ml}^{-1}$ RNase A, and incubated at 37°C for 45 minutes in the dark. The cell suspensions were then filtered with the aid of cell strainers (BD Biosciences) before analysing their DNA content using a FACSCalibur™ (BD Biosciences) and the detector FL2-A. Data were analysed using FlowJo software (TreeStar).

3 Regulation of *T. brucei* Polo-like kinase in procyclic form parasites

3.1 Discovery of Polo and Polo-like kinases

Fewer than 30 years ago the *polo* gene was discovered to be essential for mitosis in *Drosophila melanogaster* as its mutants displayed defective spindle pole formation (hence the name) and chromosomal arrangement (Sunkel & Glover 1988). *polo* was soon found to encode a protein kinase which showed cyclical changes in distribution throughout the cell cycle (Llamazares et al. 1991) and to be part of a wider family of Polo-like kinases (PLK) that are highly conserved across the majority of the eukaryotic lineages. No homologues of this protein kinase have yet been identified in bacteria, archaea or plants. The PLK family can be divided into further three subfamilies: PLK1, PLK2 and PLK4, which have distinctive functions and evolutionary histories (Table 3-1; de Cárcer, Escobar, et al. 2011).

The budding yeast, *Saccharomyces cerevisiae*, and the fission yeast, *Schizosaccharomyces pombe*, each possess only one PLK homologue: Cdc5 (Kitada et al. 1993) and plo1 (Ohkura et al. 1995), respectively, both of which, in addition to mammalian Plk1 (Clay et al. 1993; Hamanaka et al. 1994) and *Xenopus laevis* Plx1 (Kumagai & Dunphy 1996), are Polo's closest orthologues and together belong to the PLK1 subfamily. Mammals and *X. laevis* possess further four PLKs, which belong to PLK2 and PLK4 subfamilies (Table 3-1), and that are orthologous between species and paralogous within a species - Plk2/Plx2 (originally Snk; Simmons et al. 1992; Duncan et al. 2001), Plk3/Plx3 (originally Fnk or Prk; Donohue et al. 1995; Li et al. 1996; Duncan et al. 2001), Plk4/Plx4 (originally SAK; Fode et al. 1994; Eckerdt et al. 2011); and the recently described Plk5/as yet uncharacterised putative *Xenopus* Plx5 (de Cárcer, Manning, et al. 2011; de Cárcer, Escobar, et al. 2011; Andrysik et al. 2010). *D. melanogaster* has just one other PLK family member in addition to *polo* - SAK, an orthologue of Plk4 (Bettencourt-Dias et al. 2005), while *Caenorhabditis elegans* possesses four altogether: plc1-3 which belong to the PLK1 subfamily (Ouyang et al. 1999; Dan Chase et al. 2000; D Chase et al. 2000) and the PLK4 member, zyg-

1 (O'Connell et al. 2001; Jana et al. 2012). Table 3.1 summarises the various sub-divisions within the wider PLK family (see de Cárcer, Manning, et al. 2011 for review). PLKs are now understood to be major players in cell cycle regulation. The PLK1 subfamily is especially involved in mitosis and shall be the focus of this mini-review. Paralogues, such as PLK2-4 in mammals, perform specialised yet some overlapping functions in aiding cell proliferation owing to the higher levels of complexity associated with multi-cellular organisms (for reviews see Winkles & Alberts 2005; Archambault & Glover 2009; Zitouni et al. 2014). They have also been found to play non-traditional roles that go beyond the cell cycle (de Cárcer, Escobar, et al. 2011).

Sub-families	Organism					
	<i>D. melanogaster</i>	<i>S. cerevisiae</i>	<i>S. pombe</i>	<i>C. elegans</i>	<i>X. laevis</i>	Mammals
PLK1	polo	Cdc5	plp1	plc1 plc2 plc3	Plx1	Plk1
PLK2					Plx2 Plx3 Plx5	Plk2 Plk3 Plk5
PLK4	SAK			zyg-1	Plx4	Plk4

Table 3-1 PLK family of kinases in selected organisms across various taxons. The names of PLK(s) in each organism are given and are assigned to their subfamily. Members of the PLK2 subfamily are only found in some bilaterian animals whilst those of PLK4 subfamily are found in all animals. Adapted from de Cárcer, Manning, et al. 2011.

3.2 Cell cycle functions of PLK1

Consistent with its mitotic functions, in humans, the mRNA and protein levels of PLK1 remain low throughout G1 phase, start to increase in the S and G2 phases and peak during mitosis before rapidly decreasing at the end of mitosis (Lee et al. 1995; Hamanaka et al. 1995; Uchiumi et al. 1997). Throughout interphase, PLK1 localises to the cytoplasm and the centrosomes, whilst during mitosis and cytokinesis, it concentrates to the kinetochores and the cytokinetic bridge,

respectively. Mammalian Plk1 and its well-studied orthologues, polo and Cdc5, have been found to be essential in mitotic entry, centrosome maturation and spindle assembly, chromatin segregation, mitotic exit and cytokinesis as described below.

One of the major roles played by PLK1s is the promotion of mitotic entry. Entry into M phase requires nuclear translocation and activation of the Cdk1-cyclin B complex - widely regarded as the master regulator of mitosis (Malumbres & Barbacid 2005). The activity of this complex is affected by the phosphorylation state of Cdk1 which is determined by the inhibitory kinases, Wee1 and Myt1, and an antagonising phosphatase, CDC25. Dephosphorylation of Cdk1 at specific sites, achieved by simultaneous inhibition of Wee1 and Myt1 and activation of CDC25, activates the Cdk1/cyclin B complex which then phosphorylates a wide-range of substrates triggering events during both the G₂/M transition and progression through mitosis (Takizawa & Morgan 2000). PLK1s have been shown to bring about Cdk1 activation via their phosphorylation of Wee1, Myt1 and CDC25 (for reviews see Barr et al. 2004; van Vugt & Medema 2005; Petronczki et al. 2008) - a role which is conserved in humans (Booher et al. 1997; Watanabe et al. 2004) yeast (reviewed in Lee et al. 2005) and frogs (Kumagai & Dunphy 1996; Watanabe et al. 2004; Inoue & Sagata 2005).

Defects in spindle formation were some of the phenotypes exhibited by the *D. melanogaster* polo mutants (Sunkel & Glover 1988) and human cells micro-injected with α -Plk antibodies (Lane & Nigg 1996). In both cases, the PLK-depleted cells presented with disorganised, mono- and multipolar spindles indicating the key role of PLK1s in generating functional bipolar spindles during mitosis. MTOCs mastermind the generation of mitotic spindles. Timely separation and maturation of MTOCs are essential for spindle generation, positioning and regulation at the poles of mitotic spindles (Mardin & Schiebel 2012). These processes are characterised by migration of duplicated MTOCs to the poles of the cells and their growth by increased microtubule recruitment. This requires the additional recruitment of multiple MAPs, microtubule nucleators and motor proteins thus setting the stage for increased microtubule nucleation activity. MTOCs differ greatly in their structure and organisation in yeast (SPB) and mammals (centrosomes), yet the bipolar spindle assembly function of PLK1s at the MTOCs is one of their most conserved cellular roles

(Zitouni et al. 2014). In animal cells, PLK1s are key players in the centriole duplication cycle and promote centriolar cohesion in centrosomes during prophase whilst also contributing to centriole disengagement during mitotic exit (for reviews see Mardin & Schiebel 2012; Zitouni et al. 2014). Also, PLK1s are required for the recruitment of γ -tubulin ring complexes to mitotic MTOCs from yeast to metazoans. In budding yeast, cdc5 phosphorylates Spc72 to help anchor γ -tubulin ring complexes to the SPB (Snead et al. 2007; Maekawa et al. 2007). In *Drosophila*, polo regulates the MAP, Asp, which holds γ -tubulin ring complexes at the mitotic centrosome (do Carmo Avides & Glover 1999; Donaldson et al. 2001). In human cells, the phosphorylation of the centrosomal protein, Ninein-like protein (NLP), by Plk1 results in the inhibition of the dynein-dynactin-dependent transport of NLP, thus enabling the recruitment of other centrosomal proteins such as components of the γ -tubulin ring complexes to the centrosomes (Casenghi et al. 2003; Casenghi et al. 2005). In addition, by controlling the centrosomal localization of Aurora A kinase, mammalian Plk1 makes a further contribution towards centrosomal maturation. Phosphorylation of the centrosome-associated protein, Kizuna, by Plk1 was also shown to be essential for formation of functional mitotic centrosomes (Oshimori et al. 2006). PLK1s have also been shown to associate with other MAPs (Petronczki et al. 2008; Archambault & Glover 2009; Zitouni et al. 2014). Phosphorylation and dephosphorylation of microtubule-binding proteins changes their stabilisation activities on microtubules thus indirectly regulating microtubule motility and finally orchestrating spindle-dynamics during anaphase.

Sister chromatids need to be correctly aligned before separation. To achieve this, spindle microtubules are attached to the kinetochores of the chromatids and then the SAC ensures that the onset of anaphase does not occur until the sister chromatids are correctly aligned and that their attachment to the spindle microtubules are under equal tension. PLK1s phosphorylate a number of distinct kinetochore substrates in a dynamic manner to stabilise kinetochore-microtubule attachment in order to satisfy the SAC (Petronczki et al. 2008; Archambault & Glover 2009). These include dynein (Bader et al. 2011), which is required for its recruitment to the kinetochore where it has been implicated in microtubule capture and correcting inappropriate microtubule attachments; CLIP-170 of the +TIP group of MAPs, which is required for its dynein/dynactin-dependent

kinetochore localisation and timely formation of microtubule-kinetochore attachments (Li et al. 2010); the MAP, CLASP2, which increases its recruitment to the kinetochores stabilising kinetochore attachment to microtubules (Maia et al. 2012); and the kinesin-13 family of microtubule depolymerising enzyme members, MCAK (Zhang et al. 2011) and Kif2b (Hood et al. 2012), which are required for the correction of aberrant kinetochore-microtubule attachment. Cleavage and removal of cohesin, the cohesion complex which attaches sister chromatids together, is required for their separation during anaphase ensuring equal distribution of duplicated genomes to daughter cells at the end of mitosis and cytokinesis, and PLK1s have been shown to be required for this. For instance, phosphorylation of SCC1 and SA2 by mammalian Plk1 promotes their own cleavage and removal of cohesin complexes from chromosomal arms and the centromere (Sumara et al. 2002; Hauf et al. 2005; N. Zhang et al. 2011). PLK1s have been shown to also co-ordinate the more complex meiotic chromosome segregation in frogs and flies (reviewed in Archambault & Glover 2009; Zitouni et al. 2014).

Mitotic exit requires the inactivation of the Cdk1-cyclin B complex, which occurs through the inactivation of Cdk1 or universal degradation of mitotic cyclins mediated by the APC, a multi-subunit ubiquitin ligase. In mammalian cells, activation of the APC is mediated through the degradation of its inhibitor, EMI1 (early mitotic inhibitor 1). This is achieved by the phosphorylating activity of mammalian Plk1 which targets EMI1 for ubiquitination and subsequent degradation (Hansen et al. 2004; Moshe et al. 2004). A similar function for Plx1 in *Xenopus* has also been described (Descombes & Nigg 1998). In yeast, though mitotic exit is mediated by completely different complexes (SIN in fission yeast, and MEN and FEAR pathways in budding yeast), PLK1 homologues, Plo1 and Cdc5 in fission yeast and budding yeast, respectively, initiate equivalent kinase cascades promoting exit from mitosis (reviewed Lee et al. 2005).

Cytokinesis is a dynamic process which varies depending on the organism, yet the step-by-step complex processes involved follow the same pattern - selection of the division site, assembly of the contractile apparatus, co-ordination of cytokinesis with the nuclear cycle, constriction of the contractile ring/septation and abscission (for reviews see Balasubramanian et al. 2004; Barr & Gruneberg 2007; Guizetti & Gerlich 2010). Differences in cytokinetic events occur between

yeast and mammalian cells. In yeasts, the cleavage plane, referred to as the bud selection site or the cortical band in budding or fission yeast, respectively, is determined early in the cell cycle which constrains the localisation of the mitotic nucleus; whilst in mammalian cells, the cleavage plane is only determined during the anaphase to metaphase transition as the central spindle is assembled. In yeasts, the process of cytokinesis occurs through septation whilst in mammalian cells it occurs through constriction of the contractile ring. When temperature sensitive yeast Plo1/cdc5 mutants failed to septate and generated a 'chain' phenotype, the direct roles for Plo1 and Cdc5 in yeast cytokinesis were established (Bähler et al. 1998; Ohkura et al. 1995; Park et al. 2003; Tanaka et al. 2001). Localisation of human Plk1 to the anaphase spindle (Golsteyn et al. 1995) pointed towards the key regulatory function of Plk1 in mammalian cytokinesis. Studies involving the use of chemical tools such as small molecule mammalian Plk1 inhibitors and analogue sensitive mutants have allowed previously unfeasible post-mitotic studies of Plk1 function and have together established its regulatory role in cytokinesis (Petronczki et al. 2007; Santamaria et al. 2007; Burkard et al. 2007; Brennan et al. 2007). Post-anaphase inhibition of Plk1 prevented formation of the actomyosin contractile ring thus inhibiting its contraction. Formation of the contractile ring requires the activation of the small GTPase RhoA which is brought about by the Rho guanine nucleotide-exchange factor (GEF) protein Ect2. This is only possible following localisation of Ect2 to the central spindle which has been shown to be mediated by PLK1 (reviewed in Petronczki et al. 2007).

PLK1s orchestrate further cellular functions which also have implications on the cell cycle. Plk1 has been implicated in Golgi inheritance during cell division (Lin et al. 2000). PLK1s have also emerged as important modulators of the DNA damage checkpoint during S and G₂ phases (Takaki et al. 2008; Bahassi 2011; Zitouni et al. 2014).

3.3 PLK1 structure and regulation

Due to their pivotal positions as master regulators of various mitotic and cytokinetic activities, PLK1s are subject to tight regulation to prevent cell cycle defects. The control of their activities occur in terms of both time and space and

is strongly linked with the structure of these kinases which shall be first described.

3.3.1 *PLK1 structure*

All PLKs share a conserved structure featuring an N-terminal serine/threonine kinase domain and C-terminal polo-box domain (PBD; Figure 3-1; Lowery et al. 2005). The two domains are joined together by an inter-domain linker (IDL). The PLK kinase domains are typical of the catalytic domains of any other serine-threonine kinases and mediate the catalytic function of PLKs in their structure, regulation and function as described below. The phosphopeptide-binding PBDs are unique to PLKs. In the majority of the PLK family members, the PBD feature two structurally homologous tandem domains, termed polo-boxes that are separated by linker regions (Lowery et al. 2005). Exceptions are members of the PLK4 subfamily which possess only one canonical polo-box and are unconventional in how they regulate and perform their functions (Lowery et al. 2005).

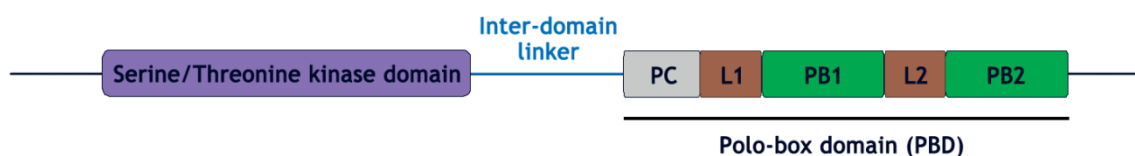


Figure 3-1 Schematic representation of domains in PLK1. PC - polo-box cap; L1 - linker 1; PB1 - polo-box 1; L2 - linker 2; PB2 - polo-box 2.

Efforts to generate a crystal structure of the full length protein have so far proven to be unsuccessful (Lowery et al. 2005; Lee et al. 2005; Johnson et al. 2008). However, separate crystal structures of either the kinase domain or the PBD have been solved (Leung et al. 2002; Cheng et al. 2003; Elia, Rellos, et al. 2003; Kothe et al. 2007; Bandejas et al. 2008; Yun et al. 2009) and have greatly enabled the modelling of PLK activity and regulation.

Kothe et al solved crystal structures of the kinase domain of Plk1 (T210V) (Figure 3-2; inactive kinase; section 3.3.3) complexed with two different non-hydrolysable ATP analogues, both of which produced similar structures (Kothe et al. 2007). The Plk1 kinase domain displayed a typical kinase fold characterised

by a bi-lobed structure: an N-terminal lobe (residues 37-131) composed almost entirely of anti-parallel β -sheets apart from a single α -helix (termed the “C-helix”) and a C-terminal lobe (residues 138-330), which is predominantly α -helical and includes part of the IDL, also known as the C-terminal tail, connecting the kinase domain and PBD (residues 306-330). The two lobes are connected via a hinge region forming a cleft within which the ligands were found to bind, thus highlighting the ATP binding site. The connecting hinge region was also found to make conserved backbone interactions with the bound ligand highlighting the physiological interactions of the adenine ring of ATP with the residues of this hinge region. The C-terminal lobe housed the activation loop (or T-loop) which was book-ended with ¹⁹⁴DFG (Asp-Phe-Gly) and APE²²¹ (Ala-Pro-Glu) motifs characteristic of the T-loops of other kinases. The T-loop includes phosphorylatable residues such as T210 in human Plk1 that mediate conformational changes which, in collaboration with other regulatory events, arrange the kinase at various conformational stages of activity/inactivity as described below.

This work was closely followed by the solved crystal structures of the WT (wild-type) Plk1 kinase domain bound to a designed selective ankyrin-repeat protein (DARPin 3H10) which acted as a surface modifier enabling effective crystal growth (Bandeiras et al. 2008). The structures reported in this paper largely agreed with those generated by Kothe and colleagues. Similar to other kinases, activation of the Plk1 kinase domain was found to include conformational changes in the C-helix of the N-terminal lobe. Rotational movement of this helix forms a salt bridge between one of its own conserved residues, Glu101, and another conserved residue also part of the N-terminal lobe, at the back wall of the ATP binding cleft, Lys82, which allows the lysine to come in contact with the phosphates of bound ATP in a catalytically productive manner (Bandeiras et al. 2008). Both structures were thought to feature T-loops in their active conformation suggesting that the default conformation of this truncated protein is in its active state despite the lack of detectable phosphorylation within the kinase domain, demonstrating additional layers of regulation mediated by the missing PBD.

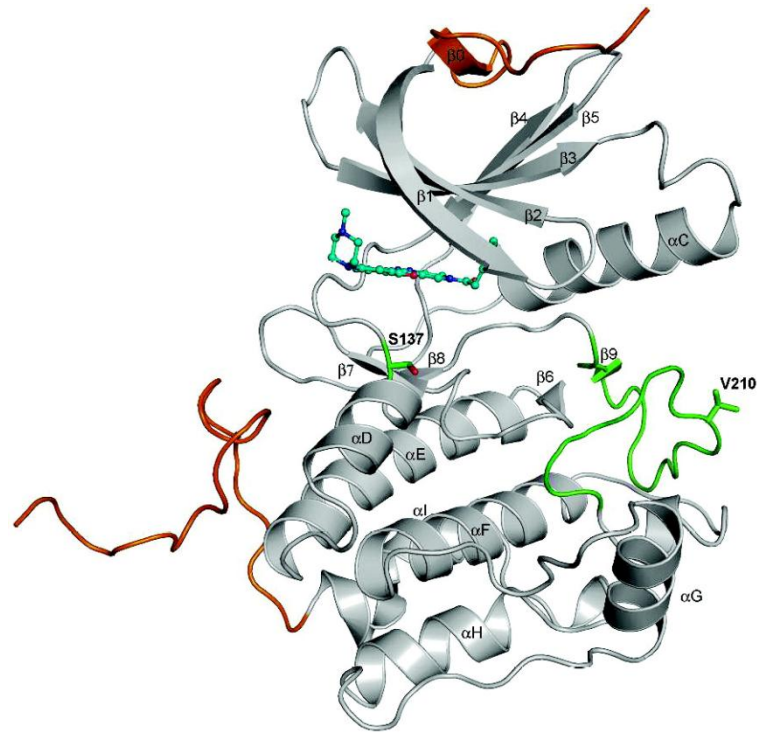


Figure 3-2 Schematic diagram of human Plk1 kinase domain structure. A crystal structure of the kinase domain of human Plk1 T210V in complex with nonhydrolysable ATP was obtained. Plk1 kinase domain core is shown in gray ribbon representation with N- and C-terminal extensions in orange. The T-loop is shown in green. Residues V210 in the T-loop (primary phosphorylation site T210 in WT Plk1) and S137 (secondary phosphorylation site) are shown as green sticks. Adapted from Kothe et al. 2007.

The structure of the PBD was first published by Cheng et al (Cheng et al. 2003) where, following the identification and characterisation of its optimal phosphopeptide substrates (Elia, Cantley, et al. 2003), the crystals of human Plk1 PBD with and without bound phosphopeptides were obtained and solved. The solved structure of human Plk1 PBD revealed a typical fold comprising two ~80 aa long repeats termed polo-boxes - PB1 (residues 411-492) and PB2 (residues 511-592) with an N-terminal extension, which links to the kinase domain, later termed the polo-box cap (PC; residues 372-410) (Elia, Rellos, et al. 2003). Although the two Polo-boxes displayed just 12% sequence identity, they shared the same structural folds - a continuous six-stranded antiparallel β -sheet shielded by one α -helix. The PC, extending from the N-terminus of PB1 was found to wrap around PB2, packing it against PB1. There was no conformational change detected between the bound and unbound PBDs (Cheng et al. 2003). Elia and colleagues had also published a structure of human Plk1 PBD-phosphopeptide complex in the same year (Figure 3-3; Elia, Rellos, et al.

2003) and the two were found to largely agree. The two polo-boxes were found to pack together to form a 12-stranded β sandwich flanked by three α -helical segments - two belonging to PB1 and one belonging to PB2. The PC was found to consist of one helical segment followed by a loop and then a short helix which connected to the first β -strand of PB1 via one of the two linkers within the PBD - L1. PB1 and PB2 were connected via L2, the 2nd short linker chain within the PBD. L1 and L2 ran in anti-parallel directions in between the β -strand sandwich away from the phosphopeptide-binding cleft. The bound phosphopeptide interacted mainly with one β -sheet from PB1, two β -sheets from PB2 and the N-terminal end of L2 (Elia, Rellos, et al. 2003).

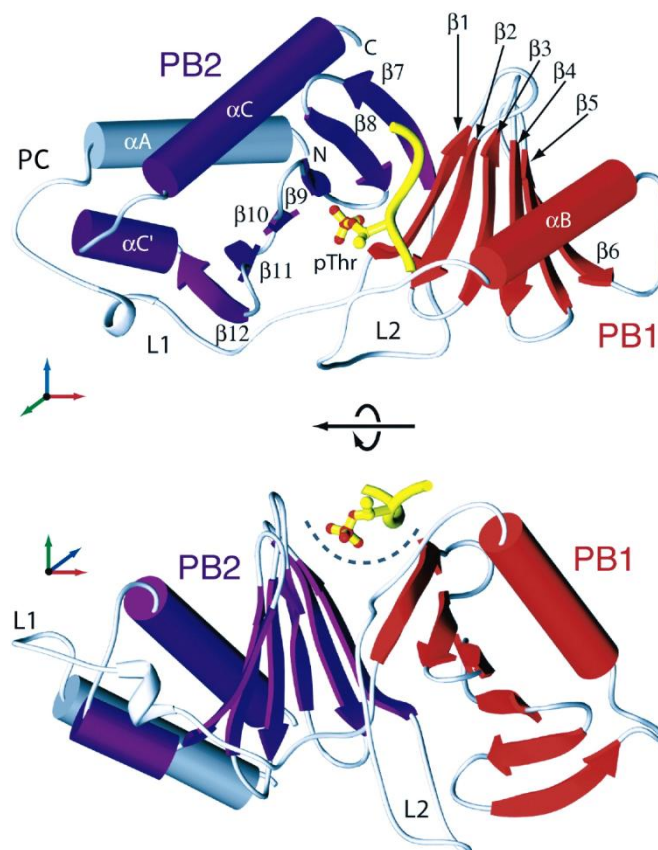


Figure 3-3 Schematic diagram of human Plk1 PBD-phosphopeptide complex. A crystal structure of human Plk1 PBD in complex with a pThr-containing peptide (shown as a ball and stick representation in yellow) was obtained. Polo-box 1 (PB1) is shown in red whilst polo-box 2 (PB2) is shown in purple. The linker regions (L1 and L2) and the polo-box cap (PC) are shown in grey. The phosphopeptide binds at one end of a pocket formed between PB1 and PB2. Adapted from Elia, Rellos, et al. 2003.

This structure is unlike that assumed by the PBD of the divergent PLK4 family. Structural analysis of the single polo-box of murine Plk4/SAK, revealed that the

domain crystallised as an intermolecular dimer featuring a clam-like fold made up of two α -helices and two six-stranded β -sheets contributed by the two monomers (Leung et al. 2002; Lowery et al. 2005). Although the structure assumed by the SAK polo-box dimers broadly resembled the structure formed by the two interacting polo-boxes in Plk1, the residues most closely involved in phosphopeptide binding by Plk1 are not conserved in SAK (Lowery et al. 2005; van de Weerd et al. 2008). Actual ligands that bind to the SAK polo-box dimers remain to be identified.

As mentioned earlier, the PBD is a phosphoserine (pSer)/phosphothreonine (pThr) binding motif. This was determined by the use of a proteomic screen, where an immobilised library of partially degenerate phosphopeptides featuring pSer and pThr motifs (which resembled the phosphorylating action of Cdks and mitogen-activated protein kinases) were used to isolate phospho-binding domains that specifically recognised pSer/pThr containing motifs (Elia, Cantley, et al. 2003). Through this study the consensus sequence of PBD ligands was determined as [Pro/Phe]-[φ /Pro]-[ϕ]-[Thr/Gln/His/Met]-Ser-[pThr/pSer]-[Pro/X] where φ represents hydrophobic amino acids and X is any residue. This consensus sequence testifies to the key interactions required for PBD binding to its substrate. Among other interactions, a His-Lys pincer in PB2 (H538 and K540) was found to be vital for mediating binding of peptide substrates via direct electrostatic contacts with the negatively charged phosphate group of the phosphorylated serine and threonine residues while W414 in PB1 was found to be crucial for hydrogen bonding with the serine at the pThr-1 position of the phosphopeptide (Elia, Rellos, et al. 2003). In 2009, Yun et al. determined the minimal phosphopeptide sequence required to bind Plk1 PBD and to bind Plk1 specifically instead of PLKs from the other subfamilies. This study revealed that having prolines at the pThr-4 and -3 positions are essential for this specificity and affinity together with the crucial contribution histidine at the -2 position for binding. This study proved that Plk1 localisation and activity can be specifically regulated compared to other PLKs via Plk1 PBD substrates featuring the described optimal phosphopeptide sequence (Yun et al. 2009).

The PBD has crucial regulatory roles. By serving as a phosphopeptide binding module, it is responsible for the proper subcellular localisation of the whole kinase. In addition, it also inhibits PLK kinase activities via its intramolecular

interaction with the kinase domain (section 3.3.4). A priming phosphorylation is usually required to relieve this auto-inhibition. However, *Drosophila* Map205 has previously been shown to bind strongly with PBD of *Drosophila* polo or human Plk1 in a phospho-independent manner (Archambault et al. 2008). Taking advantage of this, Xu et al. have recently co-crystallised individually isolated kinase domain and PBD of zebrafish Plk1 in complex with the PBD binding domain of *Drosophila* Map205 (Map205^{PBM}; Xu et al. 2013). This has significantly cemented the current model of PLK structure and regulation by providing a greater understanding of how the two domains interact with each other.

Here, the structure of the kinase domain and the PBD were found to be identical to those already described earlier, apart from a few key differences accounting for the regulatory effects of the kinase domain and PBD being in the same complex as had already been hinted at experimentally (see section 3.3.4). The interacting surface between the kinase domain and the PBD is contributed by the C-terminal tail (linker connecting kinase domain and PBD), helix α D from the C-terminal lobe together with the hinge region and β 1 strand of the N-terminal lobe on the side of the kinase domain, and the two linkers, L1 and L2 and the tips of β -strands polo-boxes on the side of the PBD. This interface is opposite to the phosphopeptide binding groove lending credibility to observations made by Elia et al that phosphopeptide binding to the PBD has minimal effect on kinase domain-PBD binding (Elia, Rellos, et al. 2003). This paper also provided structural evidence for a phenomenon that had already been established previously, that kinase domain-PBD binding is auto-inhibitory to PLK kinase activity (section 3.3.4). Mutations of crucial residues required for this interaction were found to increase the activity of full length zebrafish Plk1. In contrast, mutation of residues that have nothing to do with the kinase domain-PBD interface had no effect on full length zebrafish Plk1 activity. The L1 of the PBD was found to impact on the flexibility of the kinase domain's hinge region and interlobe cleft which is known to be required for kinase activity as discussed later on. In addition, the IDL was found to also have an inhibitory effect potentially by sequestration of the phosphorylatable threonine in the T-loop. When the phosphopeptide-bound human PBD (also similar to the apo form; Elia, Rellos, et al. 2003) was super-imposed with the kinase domain-bound zebrafish Plk1 PBD, a large conformational change in L2 was apparent, indicating its role

as the key switch between the on and off states of Plk1. When the PBD inhibits the catalytic activity of the kinase domain by staying bound to it, L2 remains in an open state. When a phosphopeptide binds to the PBD, the conformational change that is brought about in the L2 brings it into its closed state, causing a steric hindrance between the L2 and the C-terminal tail of the kinase domain, thus releasing it to perform its kinase activity.

The bound Map205^{PBM} was found to pack against the PBD in a torsion spring-like conformation occupying both the classical phosphopeptide-binding site and the newly identified binding channel even though a Ser-(pThr/pSer) motif cannot be found in Map205^{PBM}. This is in keeping with its role as a sequestering factor for Plk1s, targeting them and stabilising their auto-inhibition, until a mitotic kinase such as Cdk1 is able to release Plk1 via phosphorylation of the protein (Archambault et al. 2008).

The crystal structure of the kinase domain-PBD- Map205^{PBM} heterotrimeric complex has provided a structural framework for understanding how PLK1 is regulated and the authors were then able to propose a model for how various active/inactive states of PLK1 are brought about (see Figure 3-4; Xu et al. 2013). The PBD and IDL inhibit the kinase domain by reducing the flexibility of the hinge region or sequestering the activation loop. Phosphorylating T196 (T210 in human Plk1) of the activation loop prevents such a sequestration, thus partially activating PLK1. Phosphorylation of the conserved serine residue at the end of the hinge region S123 (Ser137 in hPLK1) during late mitosis, leads to the intramolecular interaction between the kinase domain and PBD being disrupted, thus further activating PLK1. This intramolecular interaction can be further disrupted when the PBD binds to its phosphorylated target, which further relieves the auto-inhibition and also adds the spatial layer of Plk1 regulation. These multiple layers of PLK1 regulation allow for multi-level regulation of PLK1, which is important to satisfy its multiple functions throughout the whole cell cycle.

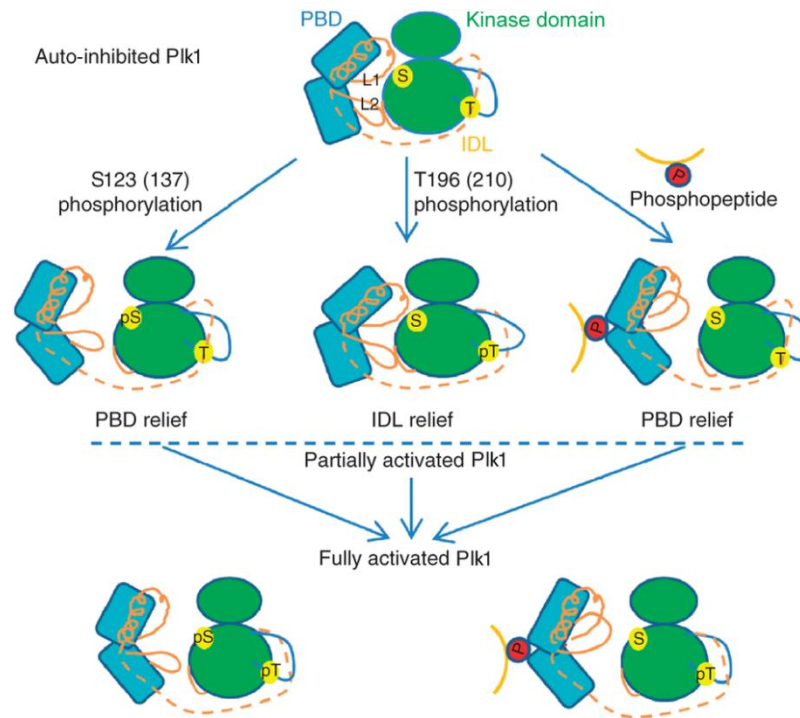


Figure 3-4 Model suggesting multi-level regulation of zebrafish Plk1. Auto-inhibited zebrafish Plk1 (top) can be partially or fully activated through phosphorylation of T196 (center; T210 in human Plk1) and S123 (center left; S137 in human Plk1), and phosphopeptide binding (center right). These events can occur independently or sequentially at different stages of the cell cycle and at different subcellular localisations. Dashed orange lines indicate the possible packing mode of the IDL. pT - phosphothreonine; pS - phosphoserine. Adapted from Xu et al. 2013.

Regulation of PLK ensures a) its expression at the right time-points during the cell cycle - this is achieved through transcriptional control, phosphorylation and proteolysis; and b) its accurate localisation and targeting to downstream substrates - this is achieved via its PBD mediated protein-protein interactions. Deregulation of the activity of PLK1s is lethal. High expression levels of mammalian Plk1 have been directly linked with malignancy of tumours. Therefore, Plk1 is widely considered as a potential anti-cancer therapeutic target (Strebhardt & Ullrich 2006).

3.3.2 Control of expression

The concordant changes in transcript and protein levels of PLK1s suggest that their expressions are primarily controlled transcriptionally in the various phases of the cell cycle. Evidence of transcription level control of PLK1 expression was shown in human cells where Plk1 promoter activation was demonstrated to peak

around G₂/M phase (Uchiumi et al. 1997). The promoter of mammalian *Plk1* has been found to feature many regulatory elements which are conserved among many mammalian mitotic kinases. One of these is the bipartite element CDE/CHR (cell cycle dependent element/cell cycle genes homology region) which needs to remain unbound for the promoter to be active. Other activating elements such as a GC stretch, CCAAT motif and FKH-TF binding sites, amongst others, have been linked with the stimulation of mammalian *Plk1* expression (Bräuninger et al. 1995; Uchiumi et al. 1997; Alvarez et al. 2001; for review see Martin & Strebhardt 2006). However, FKH-TFs are the only transcription factors that have been directly demonstrated to activate *PLK1* promoters to date in yeast and mammals (Alvarez et al. 2001; Murakami et al. 2010). The initial stimuli by which the increase of PLK1 level is achieved, and other factors that are downstream of such stimuli, are yet to be elucidated. Most of what is known about *PLK1* transcription regulation pertains to repression of *PLK1* levels rather than the upregulation of them.

Downregulation of PLK1s is an important feature of the G₂/M checkpoint which is induced upon the detection of DNA damage following replication during S-phase. As mentioned earlier, the CDE/CHR element is key for the downregulation of mammalian *Plk1* expression. Mutations within this element significantly diminished cell cycle dependent regulation of human *Plk1* expression (Uchiumi et al. 1997). The dynamic interactions of the tumor suppressor protein, p53, the cyclin-dependent kinase inhibitor, p21, the transcription factor, NF- κ B, and Rb proteins with promoter elements such as the CCAAT box, p53RE1/2, EF2 binding box and CDE/CHR element, and with each other, have been shown to orchestrate downregulation of mammalian *Plk1* expression following DNA damage (Uchiumi et al. 1997; Zhu et al. 2002; Ando et al. 2004; Jackson et al. 2005; Lin et al. 2014). The DNA damage kinases ATM and ATR (van Vugt et al. 2001) are also crucial to these pathways. These *Plk1* transcriptional control pathways promise to be intricate and complex and remain important means by which *Plk1* transcript levels are upregulated upon entry into G₂ and downregulated to prevent mitotic entry upon DNA damage. Transcriptional regulation of *PLK2-4* appears to be different and has been discussed in detail by van de Weerd & Medema 2006.

3.3.3 Activation of kinase activity

Activation of PLKs by auto-phosphorylation and phosphorylation via upstream kinases are crucial ways by which their activities are regulated. Mitotic mammalian Plk1 was found to migrate slower upon gel electrophoresis and this phenomenon was found to be abrogated upon phosphatase treatment (Hamanaka et al. 1995; Mundt et al. 1997). Phosphopeptide mapping suggested Thr210 and Ser137 as important phosphorylation sites in human Plk1. The phosphorylation of such highly conserved threonine and serine residues in the T-loops (also known as the activation loops; see section 3.3.1) of their kinase domains is a conserved phenomenon by which the phosphorylating activities of protein kinases are regulated. In Plk1, when one such T-loop threonine residue, T210, was mutated to prevent phosphorylation (T210V), Plk1 kinase activity was abrogated while mutating the same residue to mimic phosphorylation (T210D) increased its kinase activity and invoked premature mitotic entry and delayed mitotic exit (Jang, Ma, et al. 2002; Jang, Lin, et al. 2002). Ser137 was also investigated as another potential regulatory residue. However, this residue was not detected as a phosphorylation site *in vivo* and therefore was thought to be an unlikely target for upstream kinases (Jang, Ma, et al. 2002). Several protein kinases capable of activating Plk1 have been identified. These include the members of the Ste 20-like kinase family (Johnson et al. 2008), BORA and Aurora kinase A (Macurek et al. 2008; Seki et al. 2008; Bruinsma et al. 2014) which phosphorylate mammalian Plk1 at T210.

3.3.4 Repression of kinase activity

The ubiquitin-proteasome pathway is a major mechanism through which cellular proteins that are no longer needed are targeted and destroyed. PLK activity is also regulated through this mechanism as non-degradable Plk1 was shown to frequently interfere with exit from mitosis (Lindon & Pines 2004). The dramatic fall in human Plk1 activity following mitosis has been attributed to the ubiquitin-proteasome pathway (Ferris et al. 1998), shown to be mediated by a conserved destruction box in Plk1 and linked to the activity of APC ubiquitin-ligase (Lindon & Pines 2004; Archambault & Glover 2009).

A further Plk1 regulatory mechanism that has been unearthed involves auto-inhibition through the interaction of the N-terminal kinase domain and the C-terminal PBD. The PBD of Plk1 was found to interact with the kinase domain involving residues that seemed unique to this interaction and was not a consequence of dimerisation (Jang, Lin, et al. 2002). The association of the PBD with Plk1 inhibited its activity against α -casein, an effect which was not repeated when T210 was substituted with aspartic acid. Also, activity of truncated Plk1 featuring just the kinase domain was found to be greater compared to the full length protein. Since the PBD was shown not to be a substrate for Plk1 and, therefore, cannot act as a competitive inhibitor for casein, this study was able to conclude that the PBD imposes an inhibitory effect on Plk1 kinase activity via intramolecular interactions, and that phosphorylation of T210 relieves this auto-inhibitory binding of PBD with the kinase domain of Plk1. This inhibition can also be relieved by the PBD binding to an optimal phosphopeptide (Elia, Rellos, et al. 2003). The generation of such primed PBD-substrates thus remain an important point of regulation of PLK activity (section 3.3.5). In prometaphase and metaphase, Cdk1 acts as the primary priming kinase of PBD substrates (Elia, Rellos, et al. 2003; Elia, Cantley, et al. 2003; Barr et al. 2004; Lowery et al. 2005) whilst other factors such as PRC1 and MKlp2 do the same during anaphase and cytokinesis (Neef et al. 2007). Thus the phosphorylation of T210 and the binding of the PBD with a primed substrate act as intermediate switches which additively activate Plk1 kinase activity. Structural studies of human and zebrafish Plk1 constructs have shed light on how these switches mechanistically activate Plk1 kinase activity (section 3.3.1).

3.3.5 PLK1 localisation

The PBD is essential for targeting PLKs to their substrates. Mutating the PBD of mammalian Plk1 disrupted its localisation to the spindle poles and cytokinetic neck filaments (Lee et al. 1998) and the importance of the PBD in localising PLK1s (to centrosomes, centromeres, the central spindle and the midbody ring) was also found to be the case in other organisms (Lee et al. 1999; Song et al. 2000; Reynolds & Ohkura 2003; Liu et al. 2004). The PBD was also found to mediate the different functional specificities of the same protein (Hanisch et al.

2006) in addition to the target specificities of PLKs belonging to different subfamilies (van de Weerd et al. 2008).

The frequent requirement for phospho-priming of PLK1 substrates is one of the ways in which its subcellular localisation is regulated (Lee et al. 1998; Elia, Cantley, et al. 2003; Lowery et al. 2005). Two modes by which PLK activity mediates mitotic progression, via PBD-mediated interactions, have been described by Lowery et al. 2005. One of them is referred to as the ‘processive phosphorylation’ model where the PBD directly binds to one site of the target substrate of PLK, that has already been phosphorylated for this purpose by a priming mitotic kinase, and the PLK kinase domain then phosphorylates the same substrate on another site. In this case, the kinase activity of PLK is limited to the time when its substrate has been primed by another mitotic kinase and has not yet been dephosphorylated by phosphatases. Therefore, in this model, the PBD functions as the temporal ‘integrator’ of PLK mitotic function in time. Priming phosphorylation of Bub1 by Cdk1 which enhances Plk1 interaction with Bub1 mediating its recruitment to the kinetochores during mitosis, is one such example of the processive phosphorylation model (Qi et al. 2006; Elowe et al. 2007). Claspin binding of the PBD of Plx1 in a phospho-dependent manner leading to its subsequent phosphorylation by Plx1 is another such example (Kumagai & Dunphy 1996). The second model is referred to as the ‘distributive phosphorylation’ model where the PBD binds to a ligand that is separate from the target substrate of PLK. In this case, PLKs bind to a scaffold or docking protein that is in the vicinity of the substrate to be phosphorylated and, therefore, their kinase activities are limited by their proximity to primed docking sites. Thus, in this model, the PBD functions as the spatial ‘integrator’ of PLK mitotic function in space. The self-regulated recruitment of Plk1 to interphase and mitotic kinetochores, where it generates its own docking sites by priming PBIP1 to function as a scaffold in order to localise itself in proximity of its substrates, is an example of the distributive phosphorylation model of PBD-mediated PLK regulation (Kang et al. 2006). In reality, it is likely that both models work in conjunction with each other. Also, phospho-priming is not always required for PBD binding to a substrate (García-Alvarez et al. 2007; Archambault et al. 2008) which indicates that the two models do not cover the whole story.

3.4 *T. brucei* PLK

Graham et al, first characterised PLK in *T. brucei* (TbPLK). *T. brucei* features a single copy *TbPLK* gene which is located on chromosome 7 (GeneDB accession no. Tb927.7.6310) and encodes a 797 aa long protein sized 86.8 kDa. Amino acid sequence alignment of *TbPLK* with mouse *Plk1* and yeast *cdc5* revealed amino acid homology of 34.4% and 29.6%, respectively, and 50.4% and 54.1%, respectively, within the kinase domain (Graham et al. 1998). Sequence identity between human *Plk1* and TbPLK was found to be 25% for the full length protein and 47.5% for the kinase domain (Kumar & Wang 2006). The protein has a typical N-terminal kinase domain (residues 43-297) and C-terminal PBD comprising two polo-boxes (residues 564-642). *TbPLK* was also found to feature a poly-asparagine sequence between the kinase domain and the PBD, which displayed length polymorphisms depending on the isolate which could be attributed to unequal crossing-over events or polymerase slippage (Graham et al. 1998). The TbPLK protein studied in this project has been derived from the Lister 427 MiTat1.2 strain and is 763 aa long.

3.4.1 *TbPLK* functions

Studies looking into the role of TbPLK in PCF parasites have confirmed its importance in the *T. brucei* cell cycle but not in mitosis. Instead, it has been found to be essential for the division of organelles that are intimately associated with the flagellum and cytokinesis.

Among the first studies, those conducted by Kumar and Wang found that depletion of TbPLK in PCF cells resulted in enlarged cells and aberrant cell types (specifically 2N1K cells). Although the cells were able to progress through the cell cycle, progression was seen to be arrested at early cytokinesis. When an epitope-tagged version of TbPLK, TbPLK-3HA, was over-expressed, an increase in the presence of zoids was observed suggesting premature progression through to cytokinesis before the completion of mitosis (Kumar & Wang 2006). For TbPLK to carry out this function in initiating cytokinesis, the expression of TbAUK1 was supposed to be an essential pre-requisite (Tu et al. 2006). TbPLK did not seem to be involved in mitotic entry or exit suggesting the divergence of TbPLK functions

from those mediated by its homologues in yeast and metazoans. The, somehow, contrasting fact that TbPLK was able to rescue *cdc5* knockout temperature sensitive yeast mutants (Kumar & Wang 2006) confirms it as a true functional and structural homologue of *cdc5*. The lack of a mitotic role for TbPLK in *T. brucei* could be explained by the differences between the biological contexts of *T. brucei* and other relevant eukaryotic organisms. TbPLK appears to be able to bind and phosphorylate the target substrates of *cdc5* and this ability could be due to substrate availability as mediated by the yeast-specific priming activity of upstream kinases.

Further studies showed that TbPLK is not required for cytokinesis *per se*, but is involved in upstream events that eventually impact on cytokinesis initiation. A deeper look into PCF parasites depleted of TbPLK via RNAi showed defective basal body duplication which inhibited kinetoplast segregation thus subsequently preventing cytokinesis (Hammarton et al. 2007). This link between TbPLK and bilobe biogenesis in PCF cells provided further hints at the roles of TbPLK involving duplication and segregation of cytoskeletal structures (de Graffenried et al., 2008). A microscopy based study conducted by the de Graffenried lab confirmed this idea (Ikeda & de Graffenried 2012). TbPLK was shown to dynamically localise within the cells through the cell cycle. α -TbPLK antibody was found to stain cytoskeletal structures as they were replicating, starting with the basal bodies, the FPC, the bilobe and then the anterior end of the new FAZ (possibly the flagellar connector). Ultimately, these events were found to manage the proper inheritance and positioning of the single flagellum. The signal was lost just before the commencement of furrow ingression and cytokinesis. The protein appeared to employ the new MtQ as its track for migrating through the length of the cell body. This study also suggested that the defect in basal body replication did not lie in its duplication (Hammarton et al. 2007) but in its proper segregation. This discrepancy could be explained by differences in the penetrance of RNAi systems used. In all, de Graffenried's study suggests that TbPLK plays a role in basal body segregation, FPC duplication, and FAZ elongation. Defects in FAZ formation could also explain the cytokinesis defects as FAZ defects could block the determination of cleavage points for furrow ingression.

A further study employing chemical genetics allowed in-depth dissection of TbPLK roles (Lozano-Núñez et al. 2013). PCF cells were modified to exclusively express analogue sensitive TbPLK (TbPLK^{as}) from the endogenous locus which could then be specifically inhibited by the bulky ATP analogue, 3MB-PP1. Rapid inhibition of TbPLK^{as} kinase activity in synchronised PCF cells showed, in agreement to the previous study, that TbPLK is directly involved in basal body segregation, bilobe duplication and FAZ initiation and elongation. In addition, the defect in basal body segregation was found to be caused by the failure of the repositioning of the new basal body to the posterior of the cell (see section 1.3.2). In terms of the precise pathways in which TbPLK is involved to bring about the replication of these cytoskeletal structures, there is a lot yet to be discovered. TbCentrin2, a component of *T. brucei* bilobe and flagellum is the only recorded *in vitro* and *in vivo* substrate of TbPLK (de Graffenried et al. 2008; de Graffenried et al. 2013). TbPLK was shown to phosphorylate multiple sites in TbCentrin2. Imaging analysis with anti-TbCentrin2 phospho-specific (pS54) and anti-TbPLK antibodies showed that S54 is phosphorylated at specific points of the cell cycle, especially when TbPLK co-localises with the bilobe. Mutation of this residue to alanine failed to complement conditional TbCentrin2 knockout PCF cells and generated defects in bilobe duplication and FAZ elongation, reminiscent of the defects produced by TbPLK-depleted cells (de Graffenried et al. 2013) thus confirming TbCentrin2 as one of the, presumably, many substrates of TbPLK in PCF cells.

3.4.2 TbPLK regulation

The fact that TbPLK is expressed at specific times of the *T. brucei* cell cycle and is localised sequentially at particular cytoskeletal structures gives the strongest indication possible for its strict regulation in time and space, just like its homologues. As described earlier, the TbPLK structure features a conserved N-terminal kinase domain and C-terminal PBD. This hints at the possibility that some regulatory features described for other PLKs (section 3.3) are conserved in TbPLK.

Initial structure-function relationship studies on TbPLK revealed that truncating distinct domains of TbPLK could alter its localisation. The PBD as a whole was

found to be essential for TbPLK localisation in PCF cells (Sun & Wang 2011). This study also identified a putative bi-partite nuclear localisation signal (NLS) which can be found just after the kinase domain: ³¹⁵RRRQHSDDPRGHAQGGLPLRRQK³³⁷; a puzzling find considering that no nuclear role has yet been identified for TbPLK. This NLS, in the absence of the PBD, was apparently found to localise the truncated TbPLK to the nucleus. A recent study with higher quality images lent credence to this hypothesis (Yu et al. 2012). Over-expressed HA-tagged kinase domain without the NLS showed a cytoplasmic localisation while the addition of the NLS localised it to the nucleus. Addition of the PBD (and linker) to this kinase domain+NLS construct resulted in a cytoplasmic localisation, suggesting that the presence of the PBD prevents nuclear localisation of TbPLK despite the presence of the NLS sequence. These experiments implied the importance of the whole PBD in TbPLK localisation. However, the PBD on its own did not appear to localise like the full length WT protein but again seemed to be cytoplasmic. Altogether, these experiments signalled that the kinase domain and PBD are jointly required for accurate TbPLK localisation.

The obvious question that arises when studying TbPLK regulation is whether what is known of PLK1 regulation is conserved in TbPLK. Some of these questions were asked in a comprehensive study performed by Li's group (Yu et al. 2012). Endogenous TbPLK was successfully knocked down via RNAi against its 3'UTR instead of its coding sequence. This then allowed them to ectopically express TbPLK variants which would not be affected by the RNAi system. Expression of WT TbPLK was able to complement the RNAi phenotype. Using this coupled system, mutants were used to study regulatory features of TbPLK. The conserved threonine residue of the T-loop, T198, was found to be important for TbPLK activity because mutating T198 to alanine (non-phosphorylatable) failed to rescue the RNAi phenotype while mutating it to aspartic acid (phospho-mimetic) did. Using the same mutation strategy, phosphorylation of another conserved threonine residue, T202 was also found to be equally important for kinase activity. Some residues, identified in other PLK1 proteins to be important for PLK1 localisation by making direct contact with its bound phospho-peptide (Trp414, Leu490, His538 and Lys540 in human Plk1) were not found to be entirely conserved. A putative His-Lys pincer (H710 and K712) was identified and along with two other residues, Phe561 (aligns with Trp414 in human Plk1) and

Trp557 (adjacent residue) were individually mutated to alanine and subjected to the same RNAi complementation assay. They were found to play no role in TbPLK function or localisation.

The same study also identified a second *in vitro* substrate, termed p110, for TbPLK, although its identity was not revealed. *In vitro* kinase assays using pulled down kinase domain and PBD indicated that the kinase domain was sufficient for *in vitro* TbPLK binding with p110 and TbCentrin2. Using GST pull-down assays, the kinase domain and PBD were found to interact with each other in a manner which inhibits the activity of the kinase domain. Altogether, TbPLK regulation seems to be conserved (in relation to the regulatory T-loop of its kinase domain and the auto-inhibitory activity of the PBD) and divergent (in relation to the role of PBD as mediator of TbPLK substrate binding) at the same time.

3.5 Project aims

The aims of this study were to characterise how TbPLK activities were regulated in PCF cells. The roles the following domains played in regulating TbPLK activity were investigated:

- the residues T198 and T202 in the T-loop
- the Polo-box domain
- the destruction box

At the time of the beginning of this project in 2010, a lot was yet to be understood about the structure-function relationship of TbPLK in PCF cells. While the project was underway, Yu and colleagues published their study which asked many of the same questions that were to be asked in this project (Yu et al. 2012). Nevertheless, the decision was made to carry on with the project as there were differences in the approach and constructs to be used. This could provide new insights and also shed further light into TbPLK regulation, in addition to allowing the verification of conclusions drawn by Yu et al. Studies were also conducted to understand TbPLK regulation in BSF cells; these have been described separately in Chapter 4.

3.6 Results

3.6.1 The expression assay

To investigate the importance of the putative regulatory domains/residues of TbPLK for its kinase activity *in vivo*, the phenotypic observations made by Hammarton and colleagues (Hammarton et al. 2007) were used as the basis for the *in vivo* assay employed in this work. As described earlier, ectopic expression of WT TbPLK (Figure 3-5A and B) in PCF cells, but not the kinase dead TbPLK N169A protein (Figure 3-5A and B), resulted in a decrease in growth and a rise in aberrant cell types (Figure 3-5C, D and E; Hammarton et al. 2007). Upon expression of WT TbPLK, an initial rise in 2N1K cells was observed which was followed by the appearance of >2N1K cells at later time points (Figure 3-5D and E).

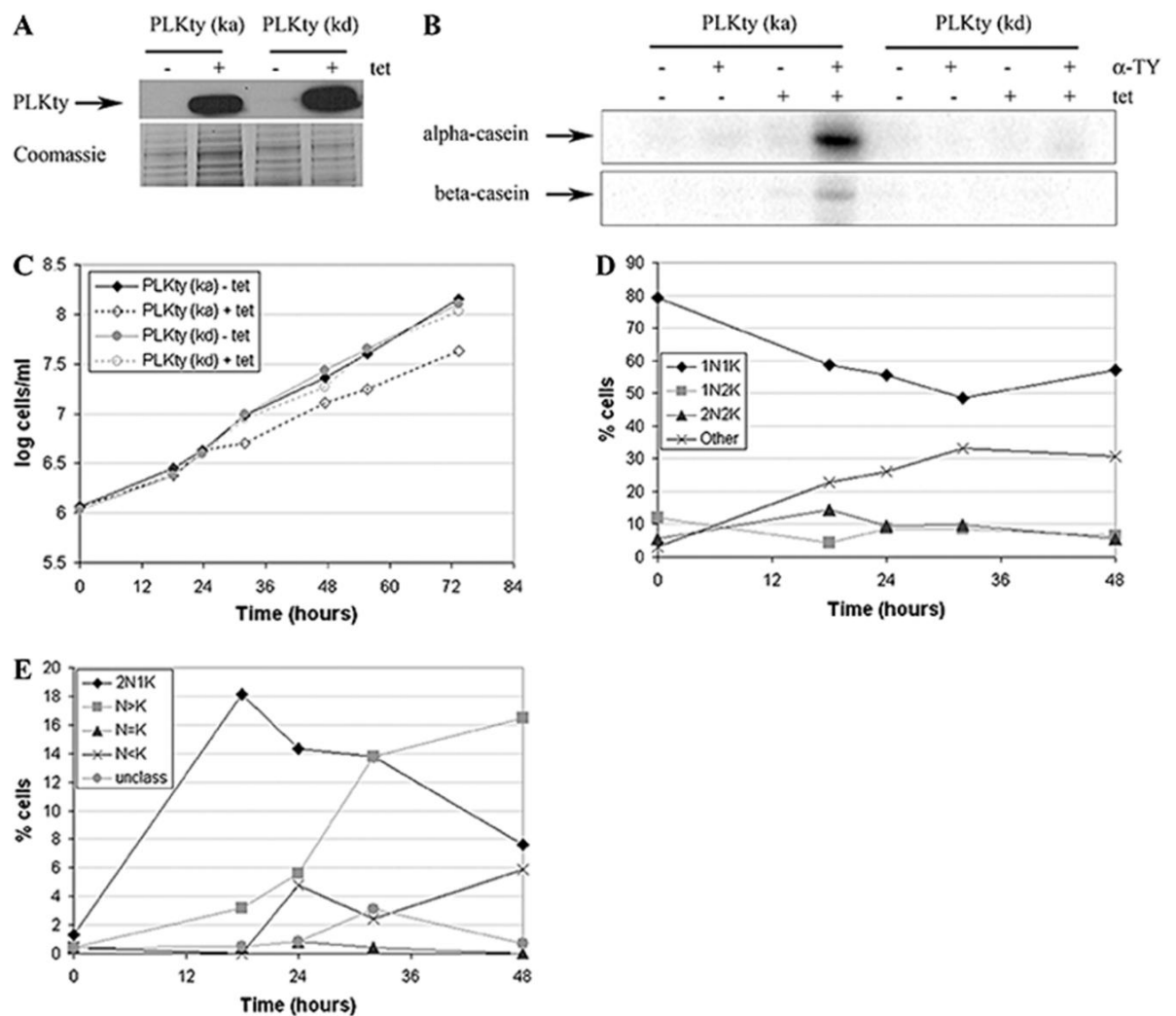


Figure 3-5 Expression of ty-tagged TbPLK in PCF cells. N-terminally TY-1 tagged TbPLK (ka=WT, kd=N169A) were expressed in PCF *T. brucei* with the addition of 1 $\mu\text{g ml}^{-1}$ tetracycline (+tet) in a WT background. Analyses of non-induced cells (-tet) have also been shown as controls (A) Western blots were performed on whole cell extracts (1×10^6 cells/sample) taken at 37 h post addition of tetracycline to detect expression of TbPLK (PLKty (ka))/ TbPLK N169A (PLKty (kd)) using an α -TY antibody. Equal loading was confirmed by Coomassie blue staining of a replica gel (bottom). (B) The expressed proteins were immuno-precipitated with anti-TY antibody and used in a radioactive kinase assay with alpha- and beta-casein as substrates. WT TbPLK was active against alpha-casein and beta-casein while TbPLK N169A did not show any activity. (C) Cumulative growth curves were generated. Expression of the WT protein (PLKty (ka)), and not the N169A kinase dead version (PLKty (kd)), generates growth defects. (D) The numbers of nuclei (N) and kinetoplasts (K) in each PLKty expressing cell ($n \geq 200$) following DAPI staining of samples were recorded at the indicated time points post addition of tetracycline. (E) Detailed analysis of aberrant cells observed when PLKty is expressed. Figure adapted from Hammarton et al. 2007.

These phenotypes were exploited in this study to test whether ectopically expressed TbPLK mutants are active or not *in vivo*. The TbPLK mutants were tagged to allow their localisation to be tracked. This was achieved by modifying pHD675 (Biebinger et al. 1997) to facilitate tagging of TbPLK proteins at their N-terminus with a YFP tag. First, *YFP* was sub-cloned (section 2.3.2.7) from pHG329 (gift from Chris de Graffenried) as a HindIII-BamHI fragment into pGL202 (originally pHD675; see Table 2-5 for details; Biebinger et al. 1997) generating pHG342. Then a multiple cloning site was added at the 3' end of *YFP* to include MluI, XhoI and HpaI restriction sites generating pHG366 (sections 2.3.2.7 and 2.3.2.8; Figure 3-6). *TbPLK* variants (Figure 3-7) were then cloned as BamHI-XhoI fragments into pHG366 (section 2.3.2.7).

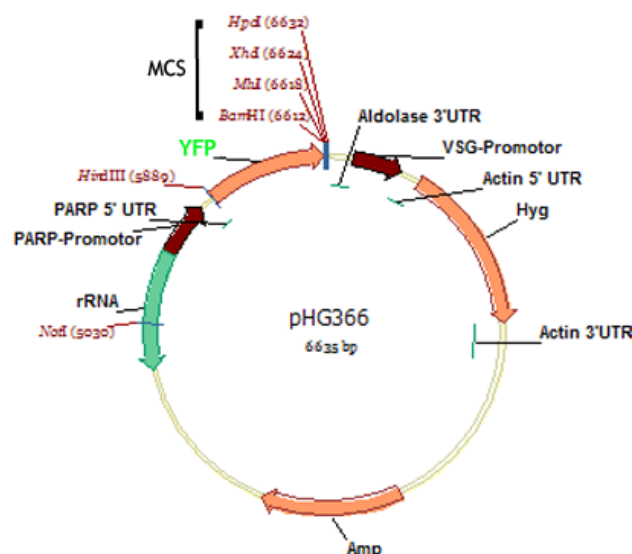


Figure 3-6 Plasmid map of pHG366. pGL202 (originally pHD675, see Table 2-5 for details; Biebinger et al. 1997) was modified to allow expression of N-terminal YFP-tagged proteins and to introduce a multiple cloning site (MCS) featuring the restriction sites MluI, XhoI and HpaI. Amp - Ampicillin resistance cassette. rRNA - ribosomal RNA spacer. Hyg - Hygromycin resistance cassette. For transfection, the constructs were linearised by digestion with with NotI (section 2.3.2.4).

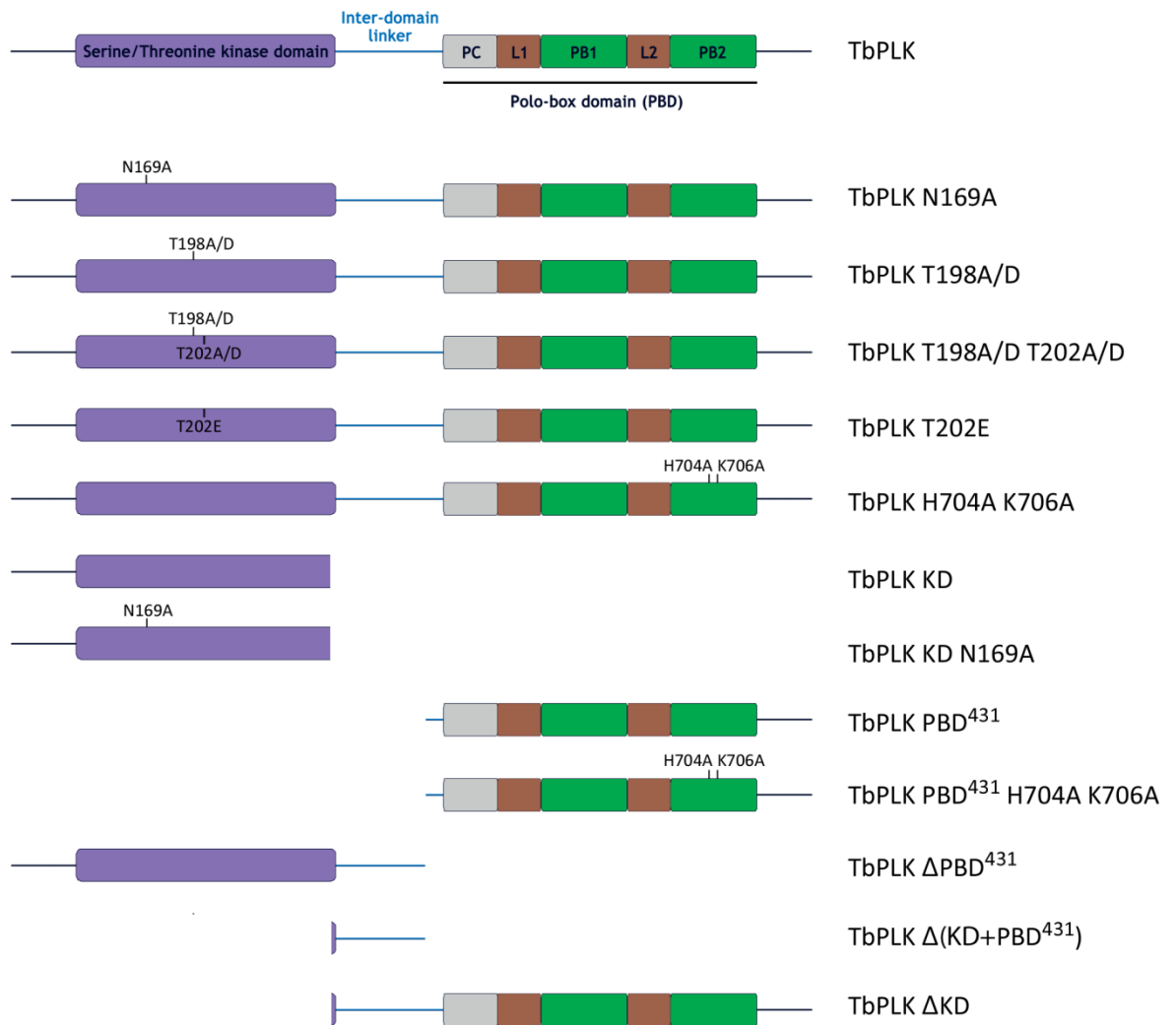


Figure 3-7 TbPLK variants that were analysed in this study.

The effect of expressing full length TbPLK proteins, featuring an N-terminal YFP tag (YFP:TbPLK and YFP:TbPLK N169A), was then analysed via growth curves and cell cycle analysis to determine if they would behave as their ty-tagged counterparts described in Hammarton et al. 2007. Indeed, expression of YFP-tagged TbPLK and TbPLK N169A in a WT background, generated results that were comparable to those of the N-terminal ty-tagged versions (Figures 3-5 and 3-8). Cells expressing WT TbPLK (YFP:TbPLK) displayed impaired growth (Figure 3-8A, top panel) whilst those expressing the kinase dead version (YFP:TbPLK N169A)

did not (Figure 3-8B, top panel). Samples of cells taken at various intervals following tetracycline induction were analysed via DAPI staining (section 2.5) to classify cells according to the number of nuclei (N) and kinetoplasts (K) present in each cell. YFP:TbPLK expression generated an increase in 2N1K cells at 18 h, and multinucleate cells at 24 h (Figure 3-8A, middle panel) whilst expression of YFP:TbPLK N169A had no effect on the cell cycle (Figure 3-8B, middle panel). These observations are consistent with the results obtained by Hammarton et al. The appearance of a growth defect upon TbPLK expression can be explained by delayed kinetoplast segregation causing an initial rise in 2N1K cells, resulting in delays in cytokinesis, leading to subsequent generation of >2N1K cells at later time-points (Hammarton et al. 2007).

Western blotting (section 2.4.1.3) (bottom panels of Figure 3-8) confirmed that the proteins were expressed at detectable amounts as early as 10 h post-induction. For the loading control, a cross-reacting band which appeared at about 35 kDa was used instead of the one representing EF-1 α at about 50 kDa. This was because the size of EF-1 α was mistakenly thought to be 35 kDa during initial experiments. After transfer during western blotting, the blotting membranes were often cut to allow separate incubation with different antibodies. In this experiment, the membrane was cut in such a way that proteins above 45 kDa in size, including EF-1 α , were excluded for incubation with EF-1 α primary antibody. Therefore, it was not possible to employ the EF-1 α as loading control here. This has been also the case for experiments described in Figures 3-10, 3-16 and 3-18, and will all need to be rectified in future repeat experiments.

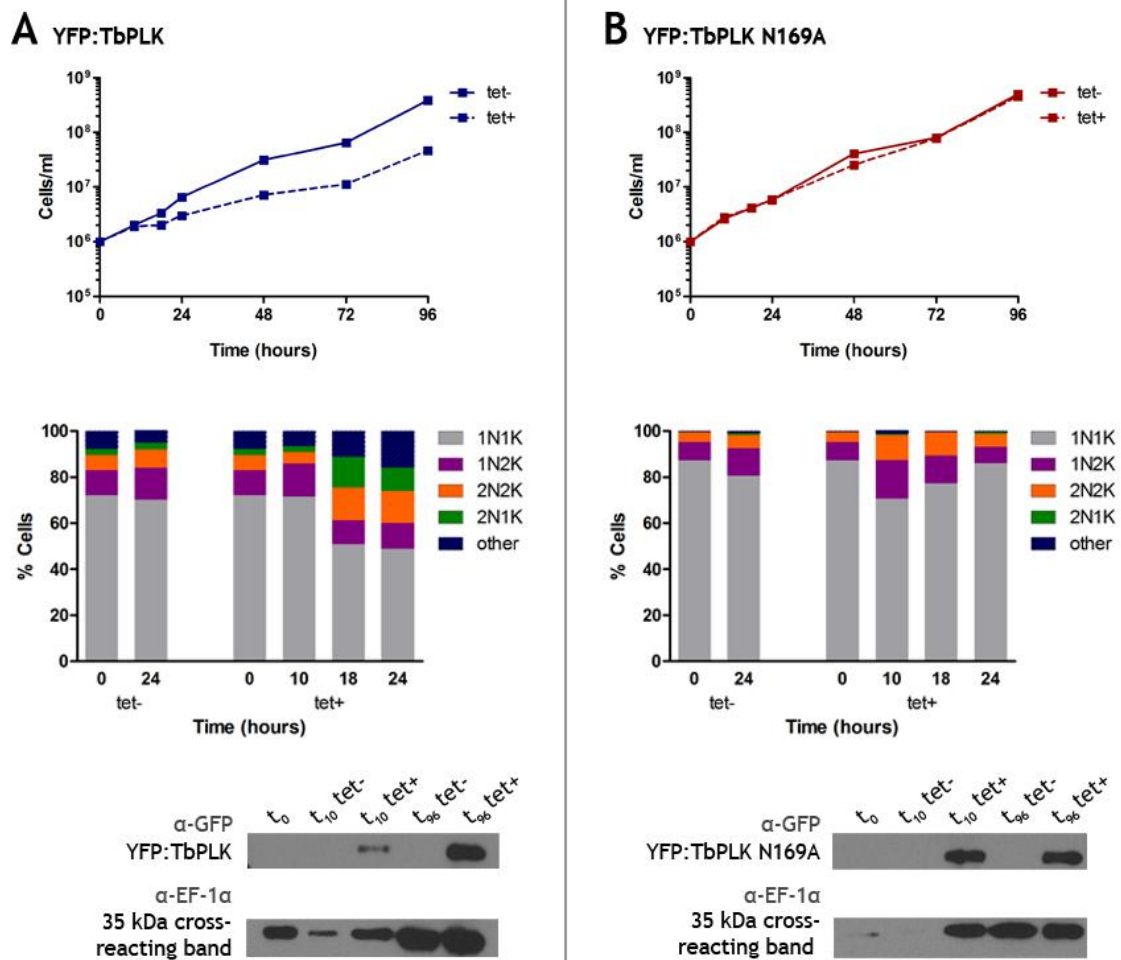


Figure 3-8 Expression of YFP-tagged TbPLK and TbPLK N169A in PCF cells. N-terminally YFP-tagged TbPLK (A) and TbPLK N169A (B) were expressed in PCF *T. brucei* cells with the addition of $1 \mu\text{g ml}^{-1}$ tetracycline (*tet*⁺). Analyses of non-induced cells (*tet*⁻) have also been shown as controls. Cumulative growth curves were generated (top panels of both sections) and the numbers of nuclei (N) and kinetoplasts (K) in each cell ($n \geq 200$) following DAPI staining of samples were recorded at the indicated time points post addition of tetracycline (middle panels of both sections). Western blots (bottom panels of both sections) were performed on whole cell extracts (1×10^6 cells/sample) taken at 0, 10 and 96 h post addition of tetracycline (t_0 , t_{10} and t_{96} , respectively) to detect expression of YFP:TbPLK/YFP:TbPLK N169A using an α -GFP antibody. Western blots were also probed with α -EF-1 α which generated a cross-reacting band at 35 kDa that has been used as the loading control.

Because the cells at t_{10} appeared to be healthy morphologically with NK configurations comparable to those found at t_0 , the decision was made to image cells at this time-point (in this and future experiments with PCF parasites) to localise the expressed proteins via fluorescence microscopy (section 2.5). The cells were fixed on glass slides for at least 20 minutes in MeOH at -20°C before they were rehydrated with PBS, mounted with Vectashield containing DAPI and viewed under the FITC channel. YFP:TbPLK displayed varied localisations

consistent with previous observations of dynamic localisation. It was mainly found to concentrate in an area next to the kinetoplast consistent with it localising in the bilobe area, and possibly along the length and at the tip of the flagellum (Figure 3-9, top panels). TbPLK N169A showed a similar pattern of localisation albeit more diffuse and brighter appearance (Figure 3-9, middle panels). PCF cells featuring integrated YFP:TbPLK constructs, prior to induction of expression with tetracycline, did not express the protein (Figure 3-9, bottom panels).

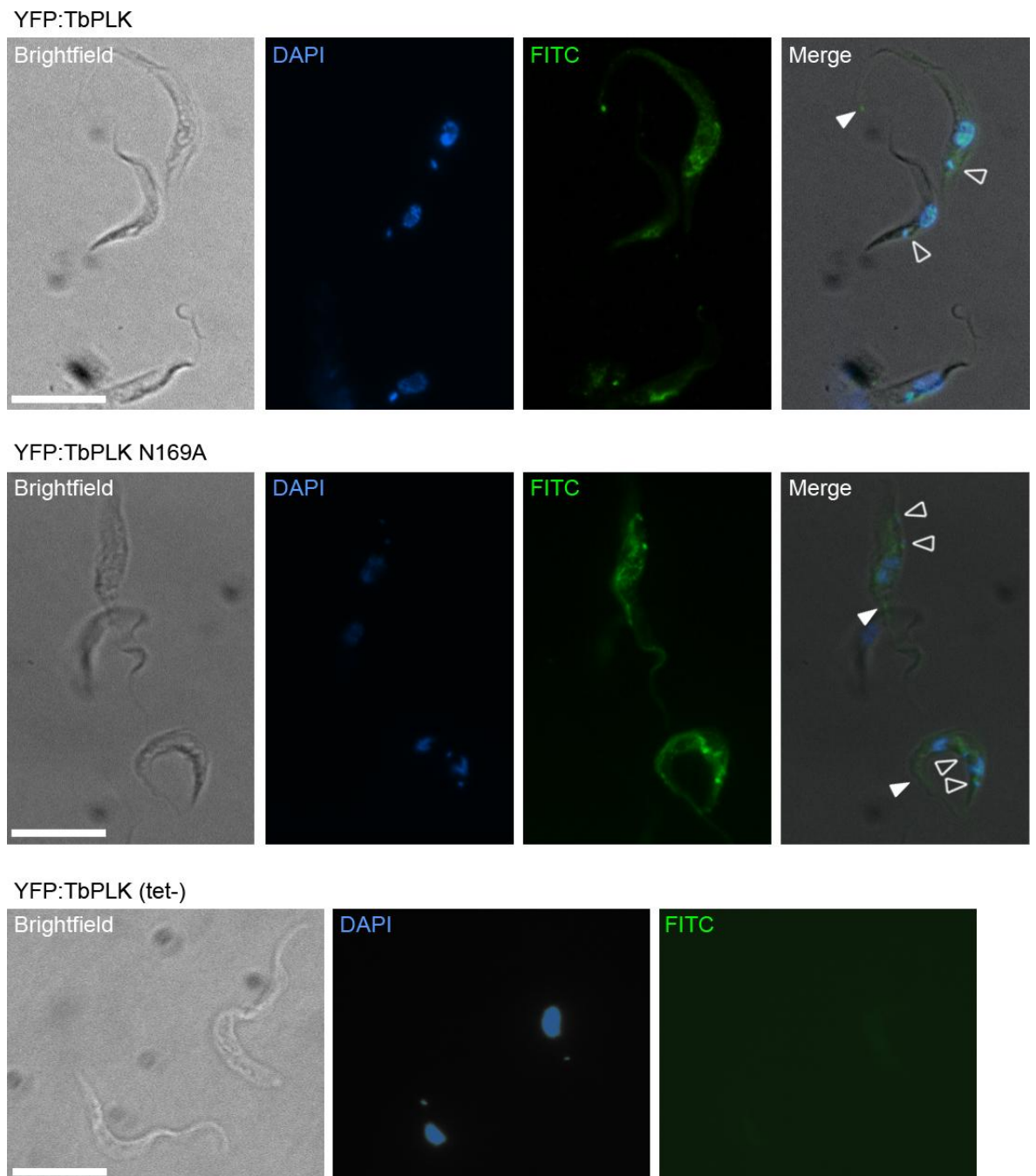


Figure 3-9 Localisation of YFP-tagged TbPLK proteins in PCF parasites. Images show direct fluorescence of YFP-tagged TbPLK (top panels) and TbPLK N169A (middle panels) following 10 h induction with $1 \mu\text{g ml}^{-1}$ of tetracycline. Bottom panels - PCF cells transfected with YFP:TbPLK expression construct, prior to induction. Arrows indicate localisation of fusion proteins in the bilobe (open arrowheads) and flagellar area (closed arrowheads). Brightfield, DAPI and FITC channels are shown (from left to right). Scale bar - $10 \mu\text{m}$.

Previous studies localising TbPLK generally showed the kinase to localise at a dorsal mid-point and the anterior tip of the growing FAZ (Umeyama & Wang 2008; Sun & Wang 2011; Yu et al. 2012). However, a more comprehensive study conducted by de Graffenried's lab has shown TbPLK to dynamically localise at the basal bodies, flagellar pocket collar, bilobe, the old FAZ and the anterior tip of the new FAZ during the cell cycle possibly using the emerging microtubule quartet as a track for movement (Ikeda & de Graffenried 2012). This could explain the variation in localisation that was found in YFP-tagged expressed TbPLK in this experiment. The more diffuse localisation of the kinase dead version is not in agreement with the findings of Yu et al. (Yu et al. 2012) where no such change in localisation was observed, but could be due to the higher level of expression relative to the wildtype TbPLK as detected by the Western blot at 10 h post-induction when the cells were imaged (Figure 3-8).

Now that the ty-tagged TbPLK expression phenotypes described by Hammarton et al. were replicated with the use of YFP-tagged TbPLK proteins, the expression assay was deemed established. Different YFP:TbPLK mutants were then ectopically expressed in order to understand the roles of:

- the residues T198 and T202 in the T-loop (section 3.6.2)
- the Polo-box domain (section 3.6.3)
- the destruction box (section 3.6.4)

in the kinase activity and localisation of TbPLK.

3.6.2 The importance of T-loop residues T198 and T202 for TbPLK kinase activity in vitro and in vivo.

In order to determine if phosphorylation of T198, a conserved residue in the T-loop of TbPLK, is essential for TbPLK kinase activity, YFP:TbPLK T198 mutants were ectopically expressed in PCF parasites in a WT background (for cloning details, see sections 2.3.2.6 and 2.3.2.7). Expression of YFP:TbPLK, with its T198 mutated to the phospho-mimetic aspartic acid (YFP:TbPLK T198D), generated growth and cell cycle defects similar to what is seen when the WT protein is expressed suggesting that YFP:TbPLK T198D is behaving like the kinase active protein (Figures 3-8A and 3-10B). Expression of YFP:TbPLK, with its T198 mutated to the non-phosphorylatable alanine (YFP:TbPLK T198A) did not have any effect on the parasite growth or cell cycle progression which is similar to what was seen when the kinase dead YFP:TbPLK N169A was expressed (Figures 3-8B and 3-10A). This, therefore, suggests that YFP:TbPLK T198A is behaving like the kinase dead TbPLK. This means that phosphorylation of T198 is apparently important for TbPLK kinase activity. The localisations of both T198 mutants were comparable to that of WT YFP:TbPLK (Figures 3-9 and 3-10A and B, bottom right panels). The importance of T198 phosphorylation found in this study is in agreement with recently published work (Yu et al. 2012).

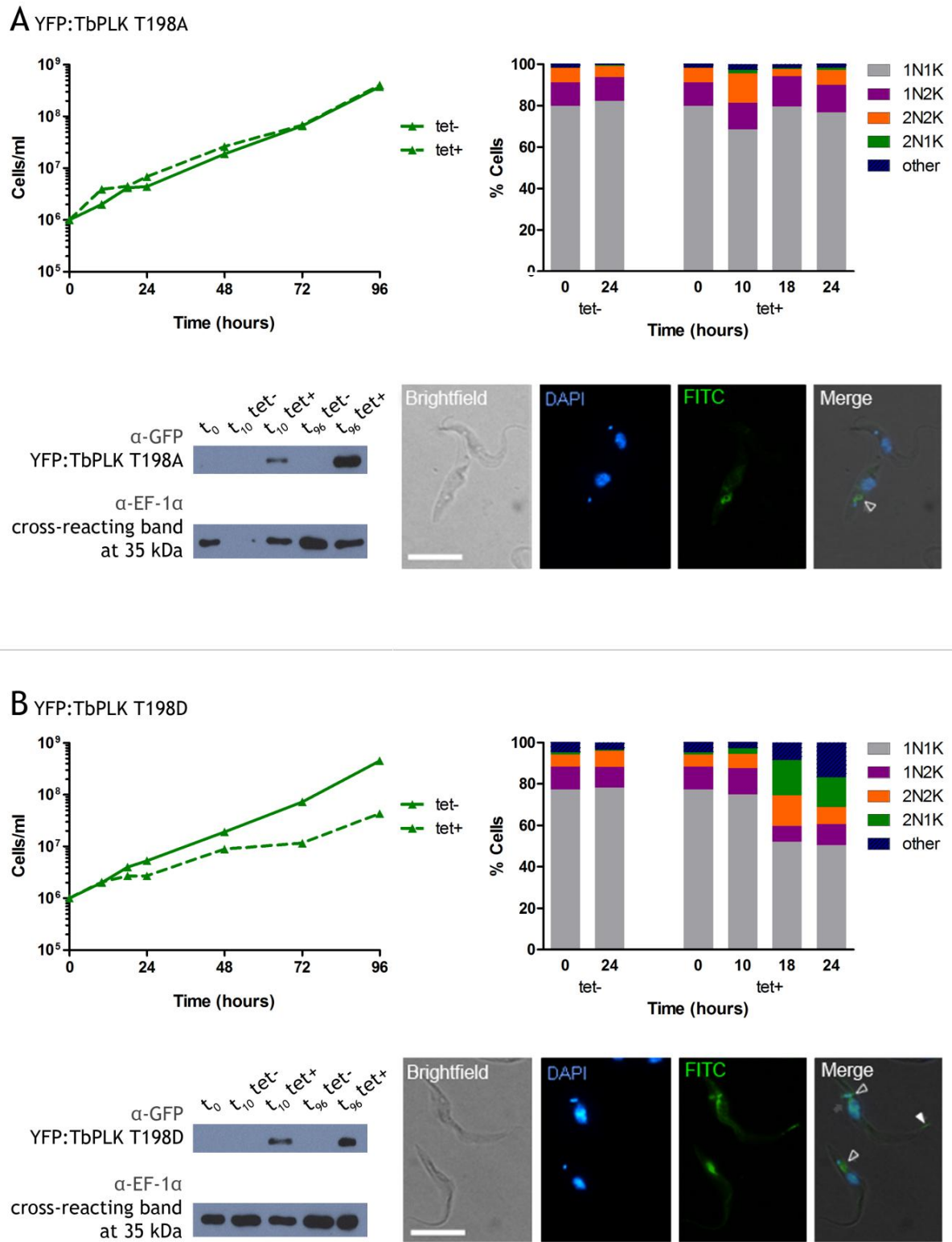


Figure 3-10 Expression of YFP-tagged TbPLK T198A and T198D in PCF cells. N-terminally YFP-tagged TbPLK T198A (A) and TbPLK T198D (B) were expressed in PCF *T. brucei* cells via the addition of $1 \mu\text{g ml}^{-1}$ tetracycline (tet^+). Analyses of non-induced cells (tet^-) have also been shown as controls. Cumulative growth curves were generated (top left of both sections) and the numbers of nuclei (N) and kinetoplasts (K) in each cell ($n \geq 200$) following DAPI staining of samples were recorded at the indicated time points post addition of tetracycline (top right panels of both sections). Western blots were performed on whole cell extracts (1×10^6

cells/sample) taken at 0, 10 and 96 h post addition of tetracycline (t_0 , t_{10} and t_{96} , respectively) to detect expression of YFP:TbPLK T198A/YFP:TbPLK T198D using an α -GFP antibody (bottom left panels of both sections). Western blots were also probed with α -EF-1 α which generated a cross-reacting band at 35 kDa that has been used as the loading control. Also shown are images representing direct fluorescence of YFP-tagged TbPLK T198A and TbPLK T198D following 10 h induction (bottom right panels of both sections; from left to right, Brightfield, DAPI and FITC channels). Arrows indicate localisation of fusion proteins in the bilobe (open arrowheads) and flagellar area (closed arrowheads). Scale bar - 10 μ m.

Yu et al. 2012 also identified a neighbouring threonine residue, T202, to be essential for TbPLK kinase activity. This residue has not been identified as a phosphosite in the only phospho-proteomic study done in PCF parasites so far (Urbaniak et al. 2013) whilst T198 was. However, the same site has been found to be phosphorylated in PLK1 proteins from other organisms (Wind et al. 2002; Kelm et al. 2002; Dulla et al. 2010). Therefore, the relationship between these two residues in mediating TbPLK activity was also investigated.

In order to do this various YFP:TbPLK T198 and/or T202 mutants in a WT background were ectopically expressed in PCF parasites (for cloning details, see sections 2.3.2.3 and 3.6.1) and the growth and cell cycle phenotypes were determined. Note that the clones analysed for growth and localisation phenotypes (Figure 3-11 and 3-13) are not the same as those analysed for cell cycle progression (Figure 3-12).

Expression of YFP:TbPLK T202A did not generate any growth or cell cycle defects indicating a kinase dead phenotype (Figures 3-11A and 3-12A). Mutating T198 to aspartic acid (YFP:TbPLK T198D T202A) was not able to alter this phenotype to resemble a kinase active one (Figures 3-11A and 3-12A). Unsurprisingly, expression of the double mutant YFP:TbPLK T198A T202A also demonstrated a kinase dead phenotype (Figures 3-11A and 3-12A). Mutating T202 to aspartic acid failed to generate a kinase active phenotype, either on its own (YFP:T202D) or in addition to T198A (YFP:T198A T202D) (Figures 3-11B and 3-12B). This phenotype did not change even with the mutation of T198 to aspartic acid (YFP:T198D T202D; Figures 3-11B and 3-12B), which is remarkable as it suggests that TbPLK kinase inactivation by T202D cannot even be rescued by the kinase activating T198D mutation (see above).

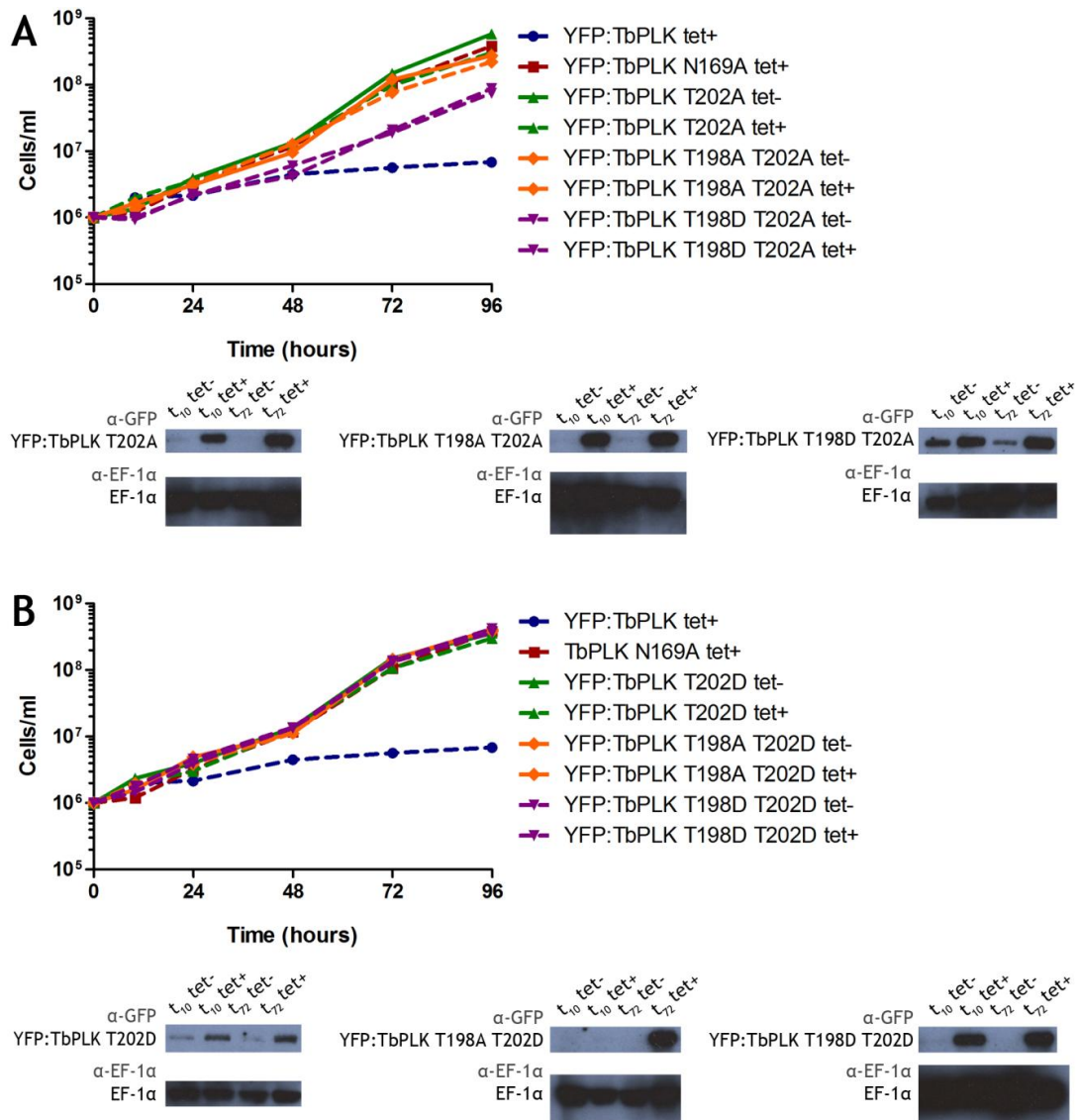


Figure 3-11 Expression of YFP-tagged TbPLK T198 and T202 mutants in PCF *T. brucei* cells. N-terminally YFP-tagged TbPLK T202A, TbPLK T198A T202A and TbPLK T198D T202A (A); as well as TbPLK T202D, TbPLK T198A T202D and T198D T202D (B) were expressed in PCF *T. brucei* cells along with YFP:TbPLK and YFP:TbPLK N169A via the addition of 1 $\mu\text{g ml}^{-1}$ tetracycline (tet+). Analyses of non-induced cells (tet-) have also been shown as controls. Cumulative growth curves were generated (top panels of both sections). Western blots were performed on whole cell extracts (1×10^6 cells/sample) prepared at 10 and 72 h post addition of tetracycline (t_{10} and t_{72} , respectively) to detect expression of each YFP:TbPLK T198 T202 mutant using an α -GFP antibody (bottom panels of both sections). Western blots were also probed with α -EF-1 α as a loading control.

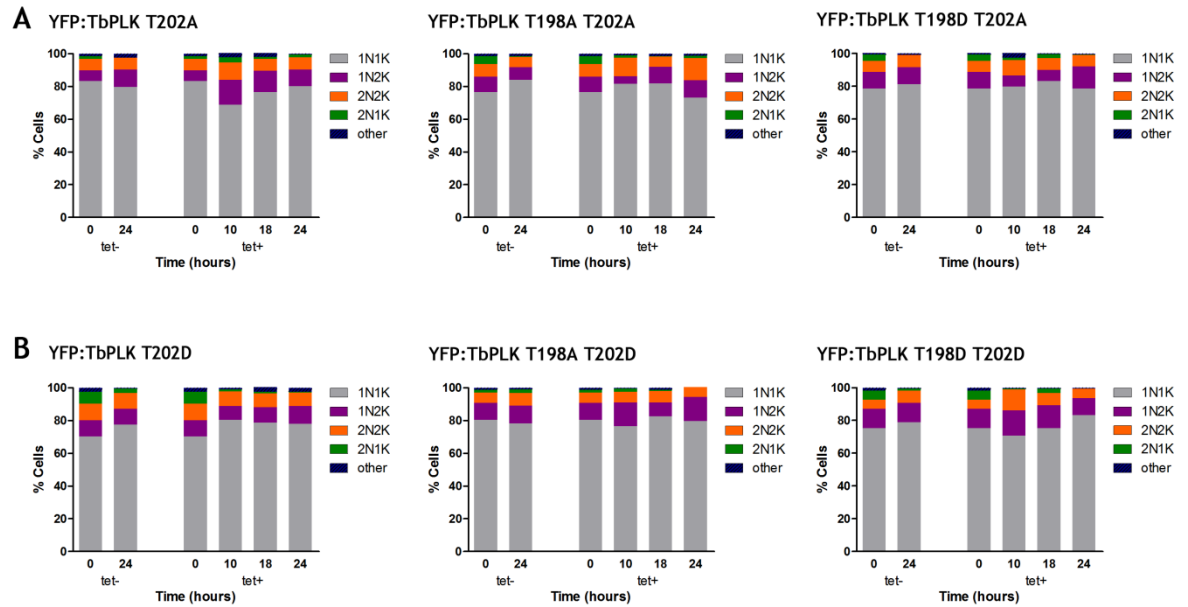
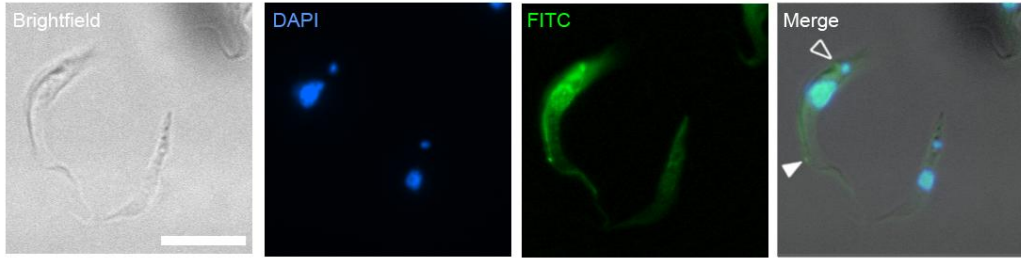


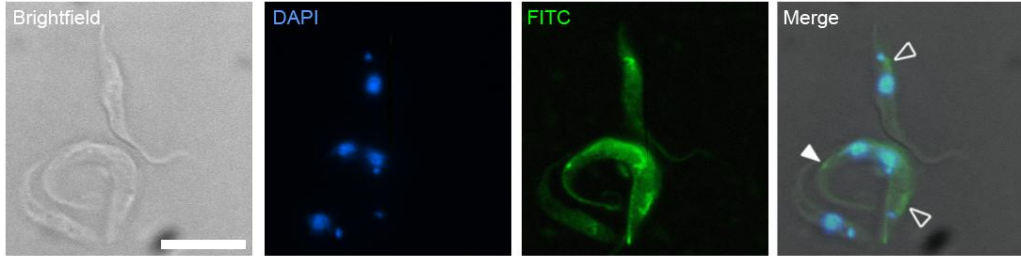
Figure 3-12 Cell cycle analysis of PCF *T. brucei* cells expressing YFP-tagged TbPLK T198 and T202 mutants. Here, a second set of clones were analysed compared to those depicted in Figures 3-11 and 3-13. N-terminally YFP-tagged TbPLK T202A, TbPLK T198A T202A and TbPLK T198D T202A (A); as well as TbPLK T202D, TbPLK T198A T202D and T198D T202D (B) were expressed in PCF *T. brucei* cells with the addition of $1 \mu\text{g ml}^{-1}$ tetracycline (tet+). Analyses of non-induced cells (tet-) have also been shown as controls. Numbers of nuclei (N) and kinetoplasts (K) in each cell ($n \geq 200$) following DAPI staining of samples were recorded at the indicated time points post addition of tetracycline.

All of these proteins seemed to show the same varied localisations (Figure 3-13) as found with YFP:TbPLK (Figure 3-9) albeit that the localisation was a bit more diffuse, which could be explained by their higher levels of expression at the same time-point (Figure 3-22) compared to the WT counterpart.

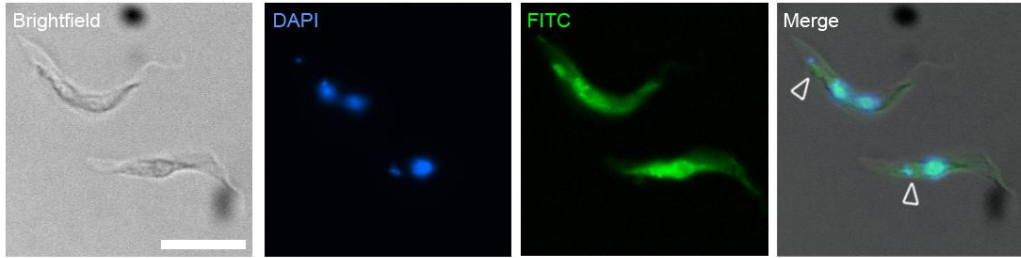
A YFP:TbPLK T202A



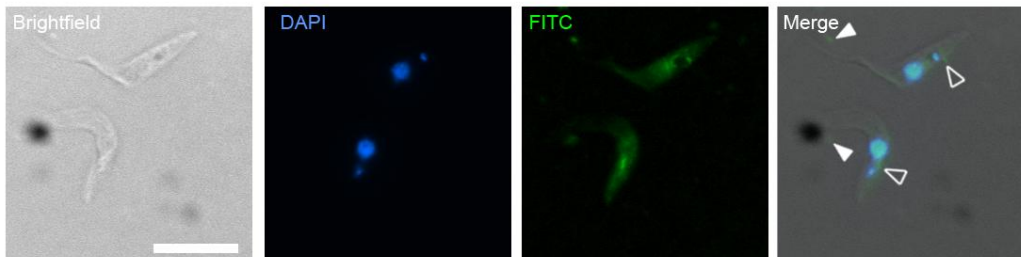
YFP:TbPLK T198A T202A



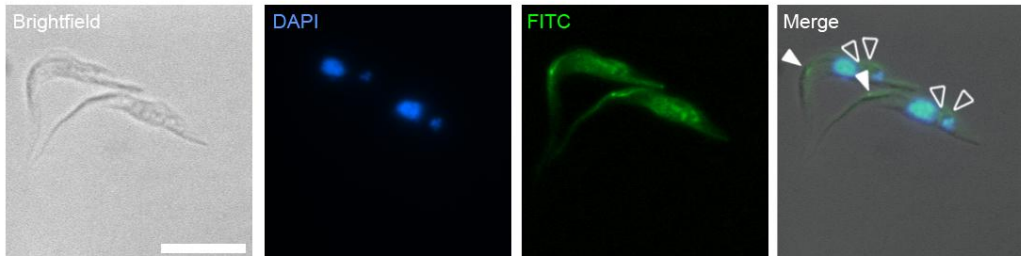
YFP:TbPLK T198D T202A



B YFP:TbPLK T202D



YFP:TbPLK T198A T202D



YFP:TbPLK T198D T202D

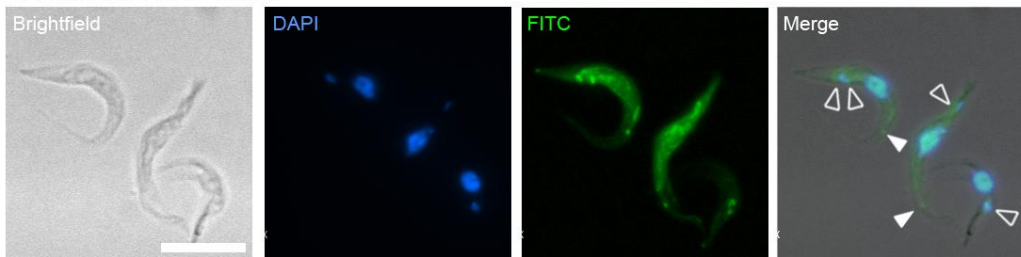


Figure 3-13 Localisation of YFP-tagged TbPLK T198 T202 mutants in PCF cells. Images show direct fluorescence of YFP-tagged TbPLK T202A, TbPLK T198A T202A and TbPLK T198D T202A (A); and TbPLK T202D, TbPLK T198A T202D and T198D T202D (B) following 10 h induction with $1 \mu\text{g ml}^{-1}$ tetracycline (from left to right, Brightfield, DAPI and FITC channels) in PCF *T. brucei* parasites. Arrows indicate localisation of fusion proteins in the bilobe (open arrowheads) and flagellar area (closed arrowheads). Scale bar - $10 \mu\text{m}$.

Overall, it appears that mutating T202 has a detrimental effect on the activity of TbPLK *in vivo*. This led onto the question of whether the T202D mutation was unable to effectively mimic phosphorylation and if another residue also known to mimic phosphorylation, such as glutamic acid (Maciejewski et al. 1995; Barrientes et al. 2000), could be used instead. Additional cell lines were, therefore, made to express a YFP:TbPLK T202E mutant (for cloning details, see sections 2.3.2.3 and 3.6.1). However, this mutant too failed to generate growth and cell cycle defects (Figure 3-14) suggesting that this TbPLK variant is also inactive *in vivo*.

YFP:TbPLK T202E

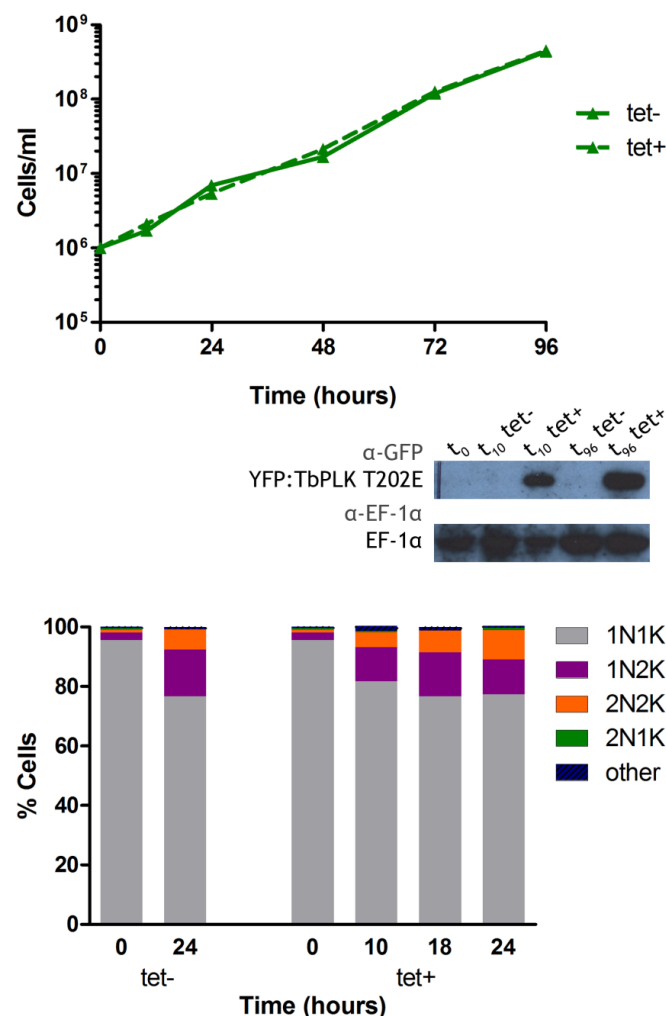


Figure 3-14 Expression of YFP-tagged TbPLK T202E in PCF *T. brucei* cells. N-terminally YFP-tagged TbPLK T202E was expressed in PCF *T. brucei* cells with the addition of $1 \mu\text{g ml}^{-1}$ tetracycline (tet+). Analyses of non-induced cells (tet-) have also been shown as controls. Cumulative growth curves were generated (top panel). Western blotting was performed on whole cell extracts (1×10^6 cells/sample) taken at 0, 10 and 96 h post addition of tetracycline (t_0 , t_{10} and t_{96} , respectively) to detect expression of YFP:TbPLK T202E using an α -GFP antibody (middle panel). The western blot was also probed with α -EF-1 α as a loading control. Numbers of nuclei (N) and kinetoplasts (K) in each cell ($n \geq 200$) following DAPI staining of samples were recorded at the indicated time points post addition of tetracycline (bottom panel).

In order to test if what was observed *in vivo* could be replicated *in vitro*, recombinant 6His-tagged TbPLK variants (for cloning details, see sections 2.3.2.6 and 2.3.2.7; for recombinant protein expression details, see section 2.4.2) were purified and subjected to a kinase assay where $4 \mu\text{g}$ of each recombinant protein were incubated with radio-labelled (^{32}P) γ -ATP (section 2.4.3) in the presence or absence of TbPLK's favoured *in vitro* substrate, α -casein (Hammarton et al. 2007; Figure 3-15). It was found that 6His:TbPLK was highly auto-phosphorylated, which has been observed previously (May 2010) and that it phosphorylates α -casein. This was also accompanied by a change in electrophoretic mobility, which could be attributed to the additional phosphate groups bound to the protein. 6His:TbPLK T198D was also observed to feature a similar change in electrophoretic mobility and was able to phosphorylate α -casein albeit at a lower scale (Figure 3-15). This suggests that this mutation, although to some extent able to mimic phosphorylated T198, is not able to fully activate TbPLK and that other factors may also contribute towards TbPLK activity *in vitro*. 6His:TbPLK T198D T202D appears to show slight ability in phosphorylating itself and α -casein, albeit at a much lower scale compared to 6His:TbPLK and even 6His:TbPLK T198D. However, no detectable change in electrophoretic mobility is seen. Altogether, these observations suggest that the kinase activity of 6His:TbPLK T198D T202D is highly impaired due to the additional mutation of the T202 residue lending credence to what was seen of this mutant *in vivo* (see above). All of the rest of the 6His:TbPLK variants did not seem to be kinase active *in vitro* which is in keeping with what was seen when their counterparts were expressed *in vivo* (see above).

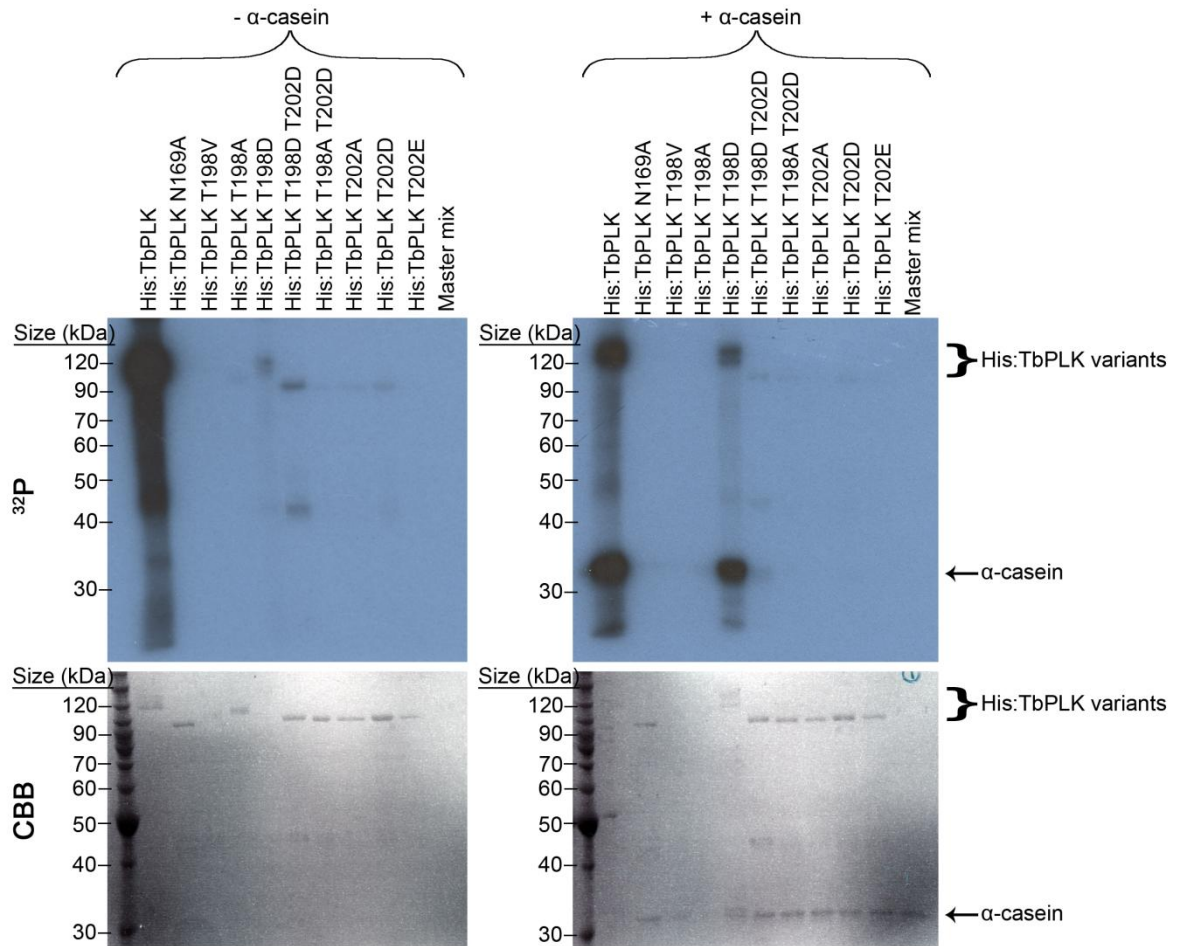


Figure 3-15 *In vitro* kinase activity of recombinant 6His-tagged (N-terminus) TbPLK proteins. Recombinant 6His-tagged TbPLK proteins were subjected to a kinase assay in the presence or absence of the generic substrate, α -casein. The different reaction mixtures were loaded as indicated. The master mix containing no kinase was used as a negative control. Predicted protein sizes - His:TbPLK proteins - 87 kDa; α -casein - 30 kDa. Note - WT and T198D versions of TbPLK migrate more slowly compared to the other proteins due to auto-phosphorylation. Top panels - autoradiograph (^{32}P). Bottom panels - gel stained with Coomassie blue (CBB).

3.6.3 The role of the polo-box domain

As described in sections 3.3.4 and 3.3.5, a His-Lys pincer is important for interaction between the PBD of the PLK and its substrates. An alignment of PLK1 proteins from various organisms with TbPLK showed a putative His-Lys pincer in TbPLK close to those found in the other PLK1 proteins. To test the importance of these residues for TbPLK activity *in vivo*, they were mutated to alanine (YFP:TbPLK H704A K706A; for cloning details, see section 2.3.2.6 and 2.3.2.7) and ectopically expressed in PCF cells (section 3.6.1). As seen in Figure 3-16, these mutations did not make any difference in the phenotypes obtained when

the WT protein (YFP:TbPLK) is expressed. The same growth and cell cycle defects were observed (Figures 3-8A, top and middle panels, and 3-16, top panels) and the fusion protein showed the same varied localisations as YFP:TbPLK (Figures 3-9, top panels, and 3-16, bottom right panel) suggesting that these mutations did not affect the functions of the expressed TbPLK *in vivo*.

YFP:TbPLK H704A K706A

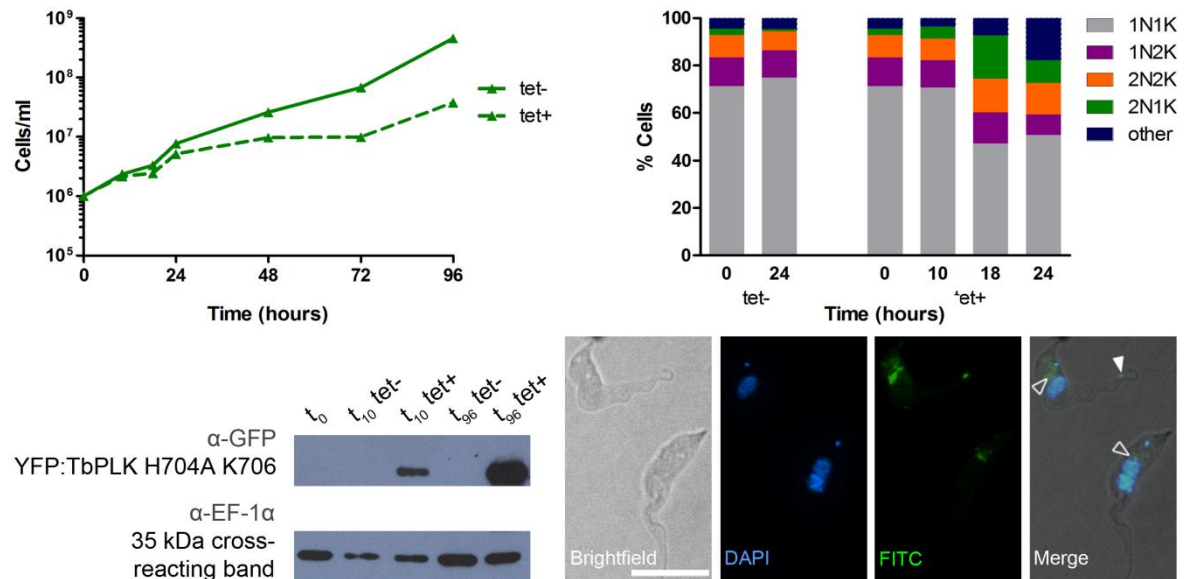


Figure 3-16 Expression of YFP-tagged TbPLK H704A K706A in PCF cells. N-terminally YFP-tagged TbPLK H704A K706A was expressed in PCF *T. brucei* cells with the addition of $1 \mu\text{g ml}^{-1}$ tetracycline (tet+). Analyses of non-induced cells (tet-) have also been shown as controls. Cumulative growth curves were generated (top left panel) and the numbers of nuclei (N) and kinetoplasts (K) in each cell ($n \geq 200$) following DAPI staining of samples were recorded at the indicated time points post addition of tetracycline (top right panel). Western blot analysis was performed on whole cell extracts (1×10^6 cells/sample) taken at 0, 10 and 96 h post addition of tetracycline (t_0 , t_{10} and t_{96} , respectively) to detect expression of YFP:TbPLK H704A K706A using an α -GFP antibody (bottom left panel). Western blots were also probed with α -EF-1 α which generated a cross-reacting band at 35 kDa that has been used as the loading control. Also shown are images representing direct fluorescence of YFP-tagged TbPLK H704A K706A following 10 h induction (bottom right panel; from left to right, Brightfield, DAPI and FITC channels). Arrows indicate localisation of TbPLK H704A K706A in the bilobe (open arrowheads) and flagellar area (closed arrowheads). Scale bar - 10 μm .

Next, the importance of PBD in mediating the kinase activity of the whole protein was investigated. As discussed earlier (section 3.3.5), it is known that the PBD acts as an important mediator between the kinase domain and the *in vivo* substrates of PLK. In addition, the PBD is known to impose auto-inhibition

on the activity of the PLK kinase domain (section 3.3.4). It was investigated whether PBD played the same roles in *T. brucei*. In order to do this TbPLK was truncated to feature just the kinase domain (1-312; KD) and its GST-tagged recombinant version was expressed and purified (for cloning details, see sections 2.3.2.6 and 2.3.2.7; for recombinant protein expression details, see section 2.4.2). Similarly, a TbPLK truncation featuring just the PBD (431-763 aa; PBD⁴³¹) was also expressed and purified as a 6His-tagged fusion protein. The kinase activity of GST:KD was first verified via a kinase assay (section 2.4.3) in the presence and absence of α -casein (Figure 3-17). GST:KD was shown to be highly auto-phosphorylated and to be active against α -casein. Introduction of the N169A mutation into GST:KD (GST:KD N169A) abolished its auto- and trans-phosphorylating activity. Finally, 6His:PBD⁴³¹ was added into the same reaction mixtures to determine if it imposes any auto-inhibitory activity on full length 6His:TbPLK or the GST:KD. No evidence of such auto-inhibition was found *in vitro*. On the contrary, 6His:PBD⁴³¹ itself was found to be a substrate of 6His:TbPLK and GST:KD.

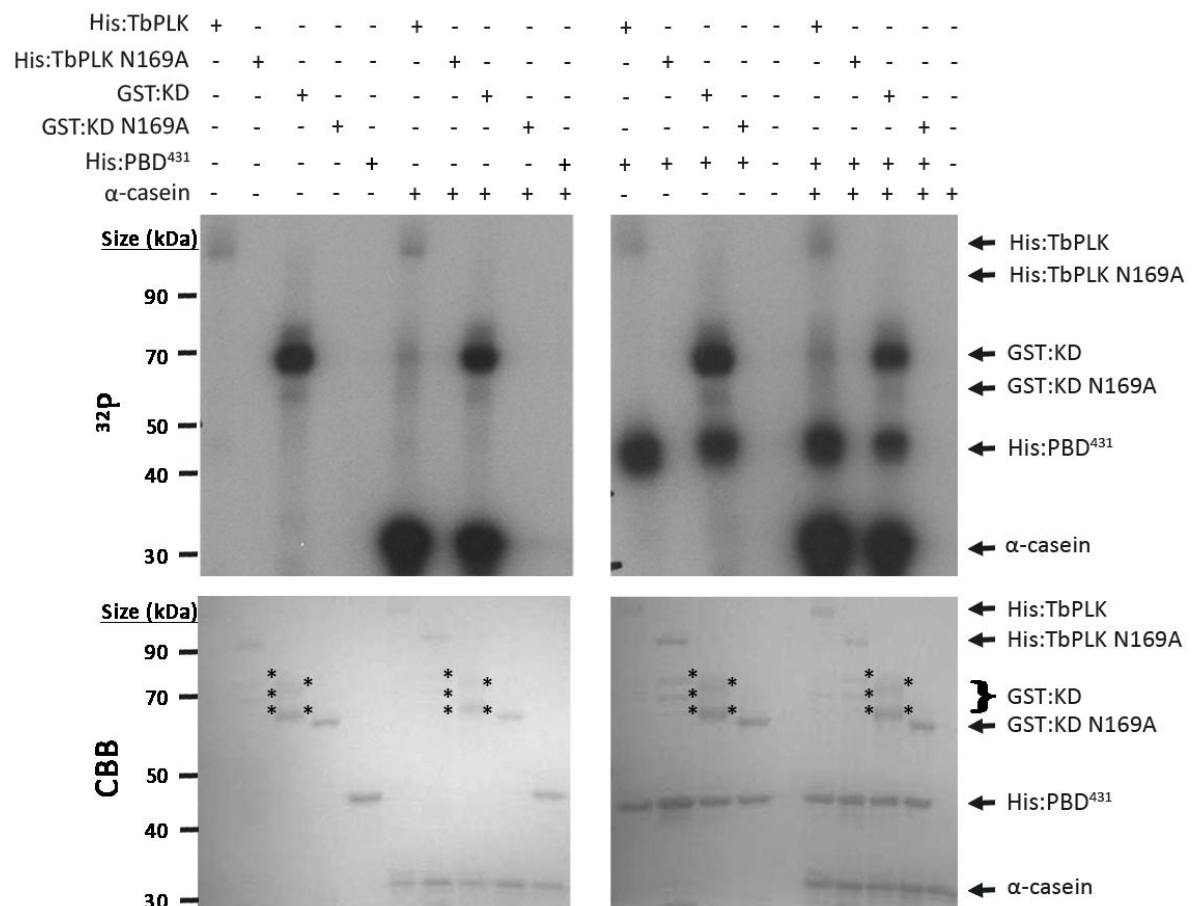


Figure 3-17 The PBD does not inhibit TbPLK kinase activity but acts as a substrate *in vitro*. Recombinant 6His:/GST:TbPLK proteins were subjected to a kinase assay in the presence or absence of 6His:PBD⁴³¹ and the generic substrate, α -casein. The different reaction mixtures were loaded as indicated. Predicted protein sizes - His:TbPLK proteins - 87 kDA; GST:KD proteins - 63 kDA; His:PBD⁴³¹ - 38 kDA; α -casein - 30 kDA. Note - WT versions of TbPLK and KD fusion proteins migrate more slowly compared to their kinase dead counterparts due to auto-phosphorylation. Top panels - autoradiograph (³²P). Bottom panels- SDS-PAGE gel stained with Coomassie blue (CBB). Asterisks on the right of a band indicate degradation products or contaminants found in the protein samples.

On being satisfied that the KD truncation generated is active *in vitro*, the question of whether the lack of a PBD would prevent this protein from localising like the WT TbPLK *in vivo* was investigated. In addition, only the PBD was expressed to see if it would generate a dominant negative phenotype indicating whether it is able to prevent the endogenous TbPLK from carrying out its *in vivo* activities. N-terminally YFP-tagged KD, KD N169A, PBD⁴³¹ and PBD⁴³¹ H704 K706A were, therefore, ectopically expressed (for cloning details, see sections 2.3.2.6, 2.3.2.7 and 3.6.1) and analysed using methods as described earlier for the other TbPLK mutants.

Expression of YFP:KD generated growth and cell cycle defects similar to those of YFP:TbPLK (Figures 3-8A and 3-18A) and the protein appears to have localised uniformly throughout the cell (Figure 3-19A). This suggests that the YFP:KD is unable to localise like the full length protein in the absence of the PBD. Despite this mis-localisation, the YFP:KD is yet able to perform its kinase activity and targets the same substrates as the YFP:TbPLK evidenced by the similarity in the cell cycle and growth phenotypes generated by expressing the two proteins. Expression of its kinase dead version, YFP:KD N169A, did not generate any growth and cell cycle defects (Figure 3-18B) despite displaying the same localisation as the kinase active YFP:KD (Figure 3-19B). It can, therefore, be confirmed that it is the phosphorylating activity of YFP:KD and not just the presence of the protein, that is generating these phenotypes. Expressing YFP:PBD⁴³¹ and YFP:PBD⁴³¹ H704A K706A did not have any effect on the growth or cell cycle progression of the parasites (Figure 3-18C and D, respectively). This, along with observations made earlier regarding expression of the YFP:KD variants, confirmed that the PBD is not responsible for the expression phenotypes seen with the full length WT TbPLK (section 3.6.1).

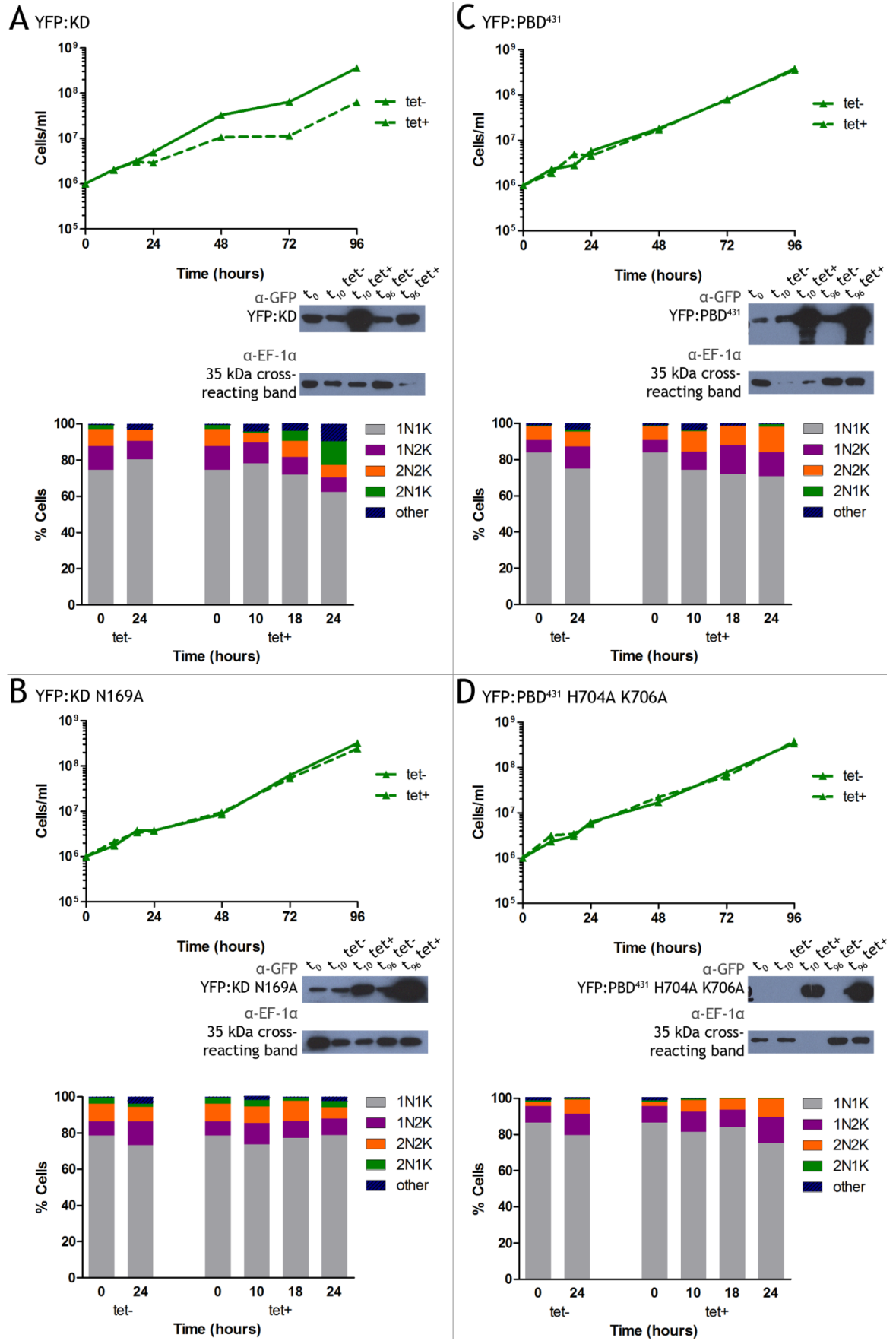


Figure 3-18 Expression of YFP-tagged TbPLK truncations in PCF cells. N-terminally YFP-tagged KD (A), KD N169A (B), PBD⁴³¹ (C) and PBD⁴³¹ H704A K706A (D) were expressed in PCF *T. brucei* cells with the addition of 1 µg ml⁻¹ tetracycline (tet+). Analyses of non-induced cells (tet-) have also been shown as controls. Cumulative growth curves were generated (top panel of each section) and the numbers of nuclei (N) and kinetoplasts (K) in each cell ($n \geq 200$) following DAPI staining of samples were recorded at the indicated time points post addition of tetracycline (bottom panel of each section). Western blots were performed on whole cell extracts (1 x 10⁶ cells/sample) taken at 0, 10 and 96 h post addition of tetracycline (t₀, t₁₀ and t₉₆, respectively) to detect expression of YFP:TbPLK KD N169A/PBD⁴³¹/PBD⁴³¹ H704A K706A using an α-GFP antibody (middle panel of each section). Western blots were also probed with α-EF-1α which generated a cross-reacting band at 35 kDa that has been used as the loading control.

If the PBD is indeed important for localising TbPLK, it can be expected that the expressed YFP:PBD⁴³¹ would localise like the full length version. This does appear to be the case, although the protein seems to have stained the whole length of the flagellum and to have diffused further into the cytoplasm (Figure 3-19C). This localisation did not change with its H704 and K706 residues being mutated to alanine (YFP:PBD⁴³¹ H704A K706A; Figure 3-19D), again suggesting that these residues are not important for PBD (and TbPLK) localisation. The diffuse staining could be explained by the much higher expression of YFP:PBD⁴³¹ and YFP:PBD⁴³¹ H704A K706A (Figure 3-22). TbPLK is known to localise to specific cellular structures as the cell cycle progresses (Ikeda & de Graffenried 2012). It can be assumed that it binds specific substrates which are local to these structures, e.g. TbCentrin2 in the bilobe (de Graffenried et al. 2013). Therefore, it could be possible that the high expression levels of YFP:PBD⁴³¹ and YFP:PBD⁴³¹ H704A K706A might have caused the proteins to bind to all the available substrates within the bilobe area and the FAZ - interactions which are probably under spatial and temporal control when the full length protein is involved. It is important to note that expression of YFP:PBD⁴³¹ and YFP:PBD⁴³¹ H704A K706A did not generate growth or cell cycle defects within the cells. If YFP:PBD⁴³¹ and YFP:PBD⁴³¹ H704A K706A did bind all its available TbPLK substrates and docking proteins (assuming TbPLK adopts the processive and distributive models of PBD-mediated phosphorylation of substrates by PLK1 proteins as described earlier), then the endogenous WT TbPLK would not have been able to access these same binding sites in order to mediate its own cellular functions. However, as expressing the PBD⁴³¹ (and TbPLK N169A) did not generate growth or cell cycle defects, it can be assumed that endogenous TbPLK was not inhibited from

performing its functions. This could be because the phosphorylating activity of the expressed TbPLK by itself (found in kinase active WT TbPLK and KD but not the kinase dead versions) is required for such substrate/docking protein binding *in vivo*. Here, in the absence of the kinase activity of the KD, the binding of the PBD to the available binding sites alone is ineffective in preventing the endogenous TbPLK from accessing the substrates and carrying out its kinase activities.

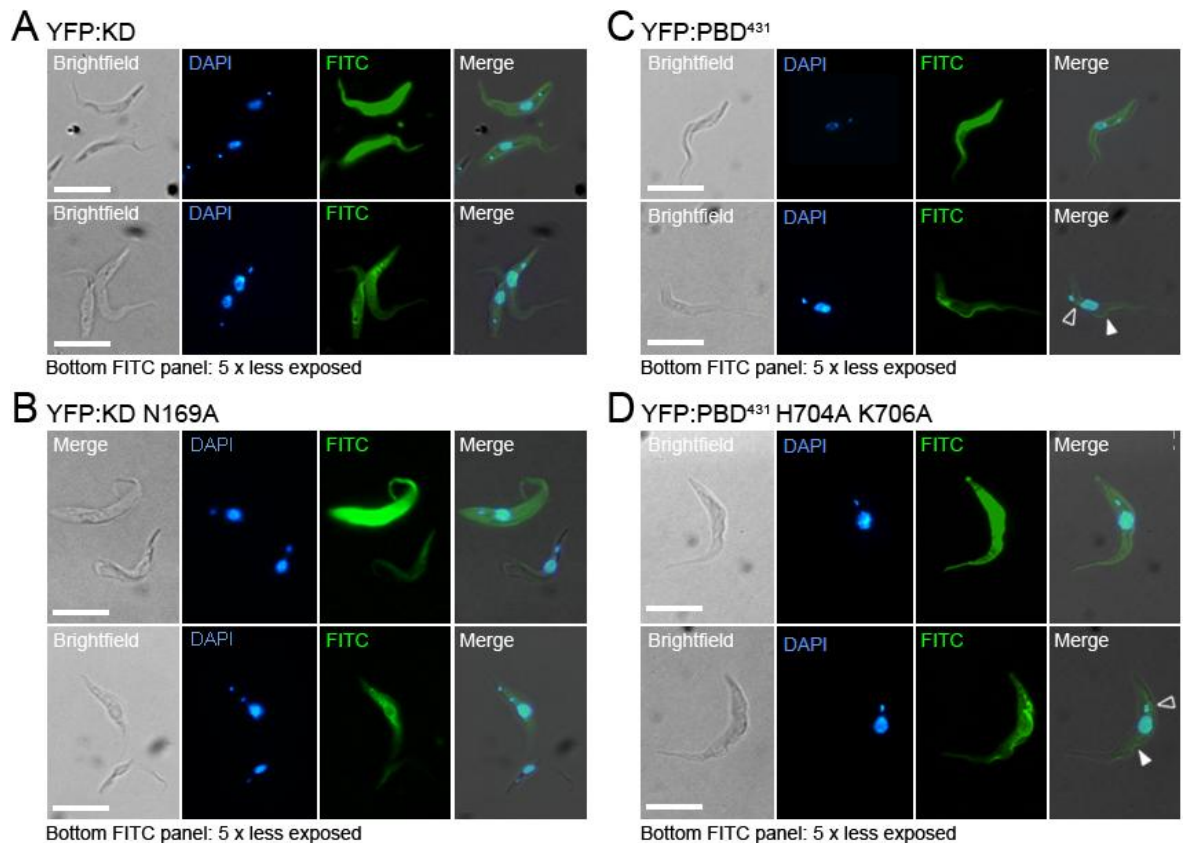


Figure 3-19 Localisation of YFP-tagged TbPLK truncations in PCF cells. Images show direct fluorescence of YFP:KD (A), YFP:KD N169A (B), YFP:PBD⁴³¹ (C) and YFP:PBD⁴³¹ H704A and K706A (D) following 10 h induction with 1 $\mu\text{g ml}^{-1}$ tetracycline (from left to right, Brightfield, DAPI and FITC channels) PCF *T. brucei* parasites. Arrows indicate localisation of fusion proteins in the bilobe (open arrowheads) and flagellar (closed arrowheads) area. Less exposed versions of images taken from the FITC channel are also shown to allow clearer localisation of the fusion proteins (bottom panels). Scale bar - 10 μm .

3.6.4 Domains important for TbPLK expression

Another observation that has been made from the experiments described in the section above is that, following tetracycline induction, truncated TbPLK fusion

proteins (YFP:KD, YFP:KD N169A, YFP:PBD⁴³¹ and YFP:PBD⁴³¹ H704A K706A) were expressed at much higher levels compared to the full length variants (Figure 3-22), despite the same induction and Western blot protocols being used for all cell lines. This can also be seen in the fluorescence images of each cell line, where the exposure time needed to be reduced for all cell lines expressing YFP:TbPLK truncations described above to be able to visualise their localisations clearly (Figures 3-19).

It is known that PLKs feature a destruction box which is important for ubiquitin-mediated degradation of PLKs (Lindon & Pines 2004; Archambault & Glover 2009). Common to both the KD and PBD⁴³¹ fusion proteins, was the lack of the IDL region lying between these two domains in the full length protein, and it was hypothesised that this region might be important for regulating the expression levels of TbPLK *in vivo*. Following a literature search and alignment of various PLK1 proteins, a putative destruction box can be identified within this region - ³⁷⁵REVLQPISTNLPK³⁸⁷ which appears to be diverged in sequence (³³⁷RKPLTVLNK³⁴⁵ - Plk1; ³²⁸RKPLTAINK³³⁶ - Plx1; ³²⁴RKPLSSLNK³³² - zPlk1) preventing its detection via BLAST searches. The minimal consensus sequence for destruction boxes is known to be RXXL (where x is any amino acid; Liu et al. 2012). In order to test the hypothesis that this IDL region is important for regulating TbPLK expression levels, further truncations of TbPLK were generated. By adding the IDL region (which includes the putative destruction box) to the KD or PBD⁴³¹, it was hoped that the expression levels of these mutants would be lower to that of KD and PBD⁴³¹ alone. The following additional truncated TbPLK proteins were expressed:

- ΔPBD⁴³¹ (1-429 aa; up to the beginning of the PBD⁴³¹)
- ΔKD+PBD⁴³¹ (312-429 aa; just the IDL, i.e., from the end of the KD to the beginning of the PBD⁴³¹)
- ΔKD (313-763 aa; from the end of the KD up to the end of PBD⁴³¹)

Two clones of each cell line were analysed and identical results were obtained. Therefore, data from just one clone each have been described. N-terminally YFP-tagged versions of these truncations were ectopically expressed in PCF cells in a WT TbPLK background. Expression of all three constructs failed to generate growth or cell cycle defects (Figure 3-20) suggesting that none of them were able to perform their kinase activities *in vivo*. This was expected for

YFP: Δ KD+PBD and YFP: Δ KD as they did not contain the kinase domain; however, the kinase dead-like phenotype obtained upon expression of Δ PBD was surprising as it still featured the active KD region within the construct. This could be explained by the unusual localisation demonstrated by this protein (Figure 3-20A). This protein can be seen to have exclusively localised within the nucleus (Figure 3-21A). Given that this protein was unable to localise to the bilobe and flagellar area like WT TbPLK, can explain why no kinase active like phenotypes were observed upon its expression in a WT background.

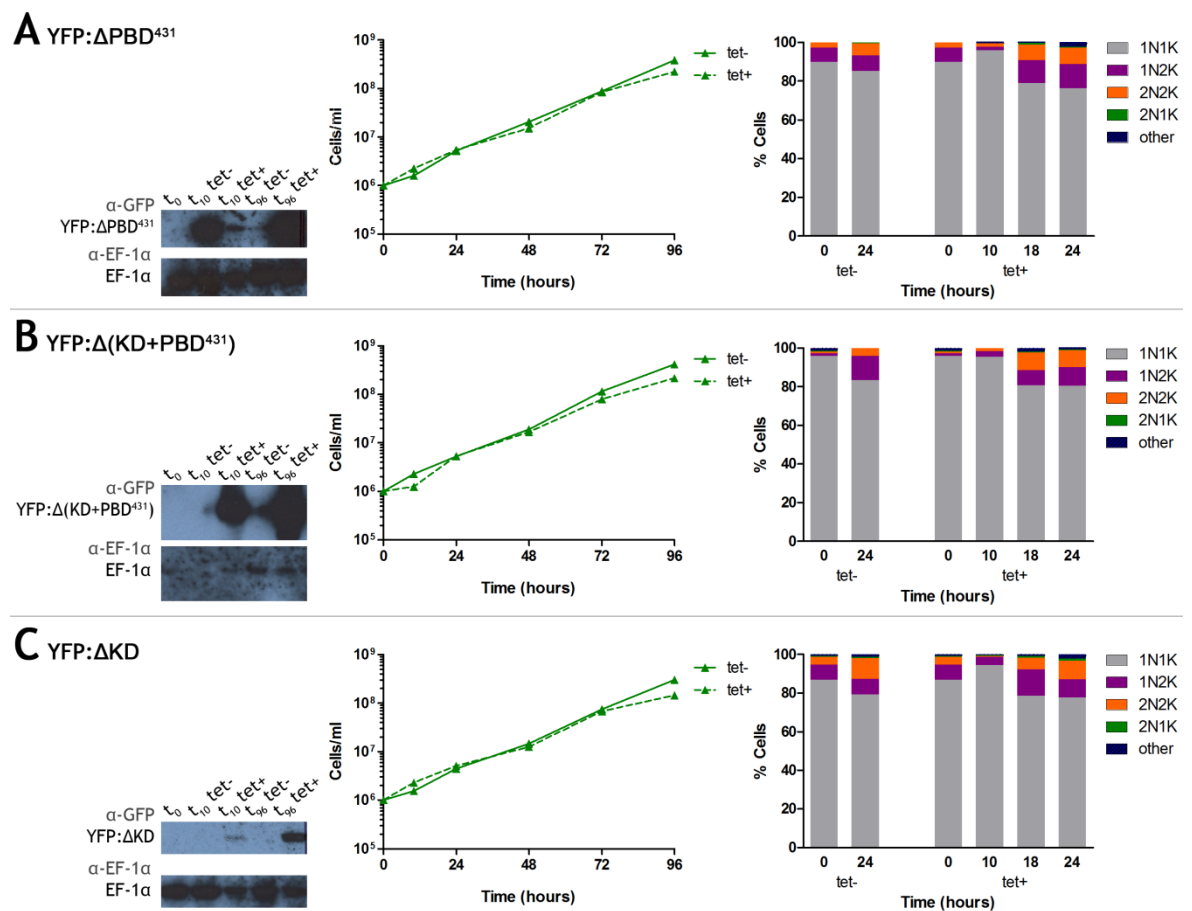


Figure 3-20 Expression of YFP-tagged TbPLK truncations in PCF cells. N-terminally YFP-tagged Δ PBD (A), Δ KD+PBD (B) and Δ KD (C) were expressed in PCF *T. brucei* cells with the addition of $1 \mu\text{g ml}^{-1}$ tetracycline (tet+). Analyses of non-induced cells (tet-) have also been shown as controls. Cumulative growth curves were generated (middle panel of each section) and the numbers of nuclei (N) and kinetoplasts (K) in each cell ($n \geq 200$) following DAPI staining of samples were recorded at the indicated time points post addition of tetracycline (right panel of each section). Western blots were performed on whole cell extracts (1×10^6 cells/sample) taken at 0, 10 and 96 h post addition of tetracycline (t₀, t₁₀ and t₉₆, respectively) to detect expression of YFP:TbPLK Δ PBD/ Δ KD+PBD/ Δ KD using an α -GFP antibody (left panel of each section). Western blots were also probed with α -EF-1 α as a loading control.

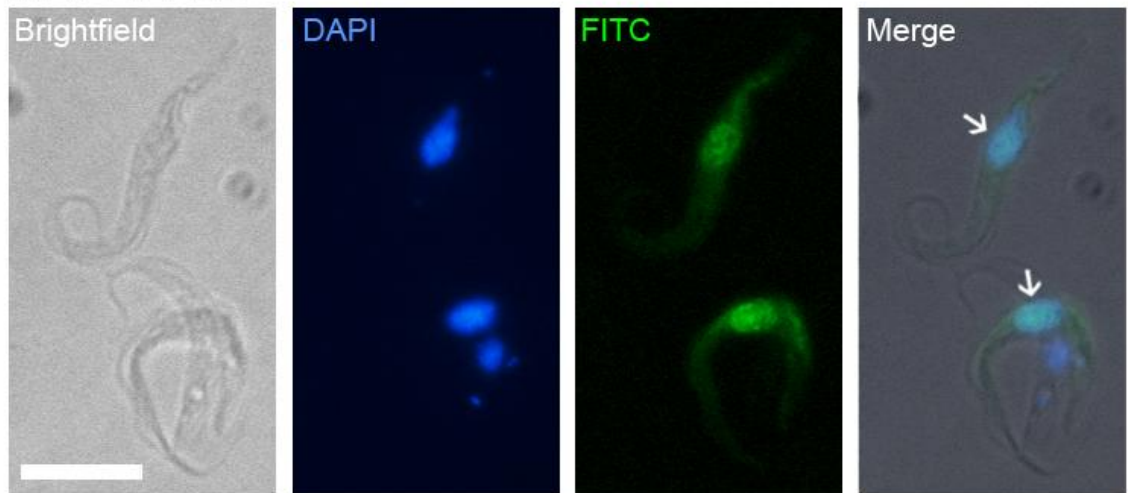
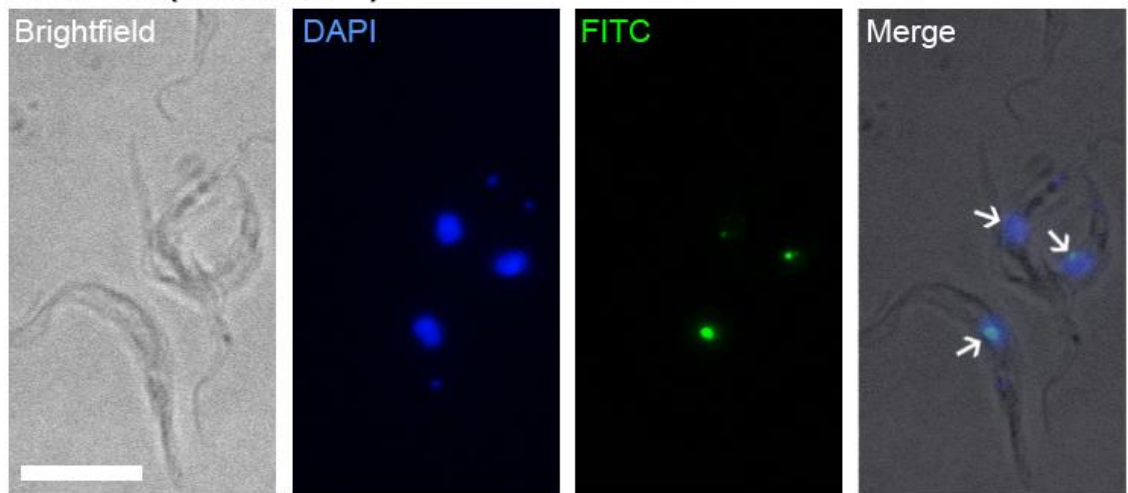
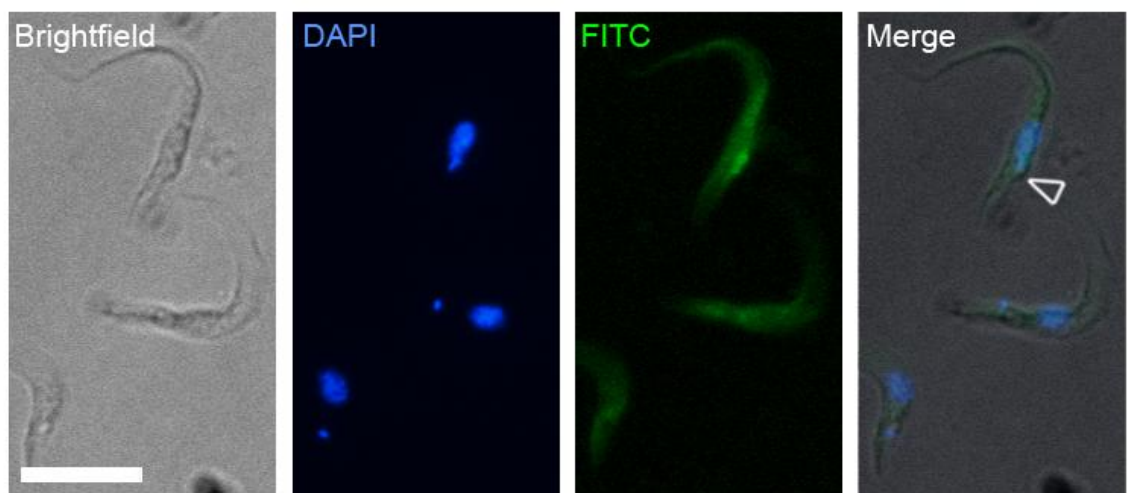
A YFP: Δ PBD⁴³¹**B** YFP: Δ (KD+PBD⁴³¹)**C** YFP: Δ KD

Figure 3-21 Localisation of YFP-tagged TbPLK truncations in PCF cells. Images show direct fluorescence of Δ PBD (A), Δ (KD+PBD⁴³¹) (B) and Δ KD (C) following 10 h induction with 1 μ g ml⁻¹ tetracycline (from left to right, Brightfield, DAPI and FITC channels) PCF *T. brucei* parasites. Arrows and open arrowheads indicate localisation of fusion proteins in the nucleus and in the bilobe area, respectively. Scale bar - 10 μ m.

All TbPLK RNAi phenotypes shown so far have been non-mitotic suggesting that TbPLK has no role in the nucleus (Hammarton et al. 2007). However, a function can never be thus ruled out as mRNA depletion via RNAi is never 100%. Here, a TbPLK fusion protein, which could possibly be active as a kinase, has been shown to exclusively localise to the nucleus and yet not induce any mitotic phenotypes. A key experiment in the future would be to show that this fusion protein is active as a kinase via *in vitro* kinase assays which would then provide further evidence indicating that TbPLK has no mitotic function.

Even more unusual is the localisation demonstrated by YFP: Δ KD+PBD⁴³¹. Again, this fusion protein localised within the nucleus but this time as discrete bright puncta which could coincide with specific nuclear structures (Figure 3-21B). The biological relevance of this observation is not clear at present and further investigations will need to be made. YFP: Δ KD, on the other hand, appears to localise in a cytosolic manner, sometimes with a particular bright staining in the bilobe area (Figure 3-21C), somewhat reminiscent of the localisation demonstrated by the full length TbPLK variants. Due to this more cytosolic nature of the localisation of YFP: Δ KD, it appears to contradict the notion that the PBD is the domain responsible for TbPLK localisation. This cannot be explained by higher expression levels, as it is expressed at levels equivalent to YFP:TbPLK (Figure 3-22). There could be issues with folding; however, this would need to be verified.

Coming back to the question of expression levels, surprisingly, the most highly expressed construct of all the TbPLK mutants expressed so far in PCF cells is YFP: Δ KD+PBD which is the region that was hypothesised to feature the destruction box. However, the addition of this region to KD (YFP: Δ PBD) does lower the expression level compared to KD on its own (YFP:KD; Figure 3-22). Similarly, the addition of this region (i.e. Δ KD+PBD) to PBD⁴³¹ (YFP: Δ KD) also lowers the expression level compared to PBD⁴³¹ on its own (YFP: PBD⁴³¹; Figure 3-22). The high levels of YFP: Δ KD+PBD could be explained by its inaccessibility to the degradation machinery when localised in the nucleus seen in Figure 3-21. However, this is yet to be directly proved.

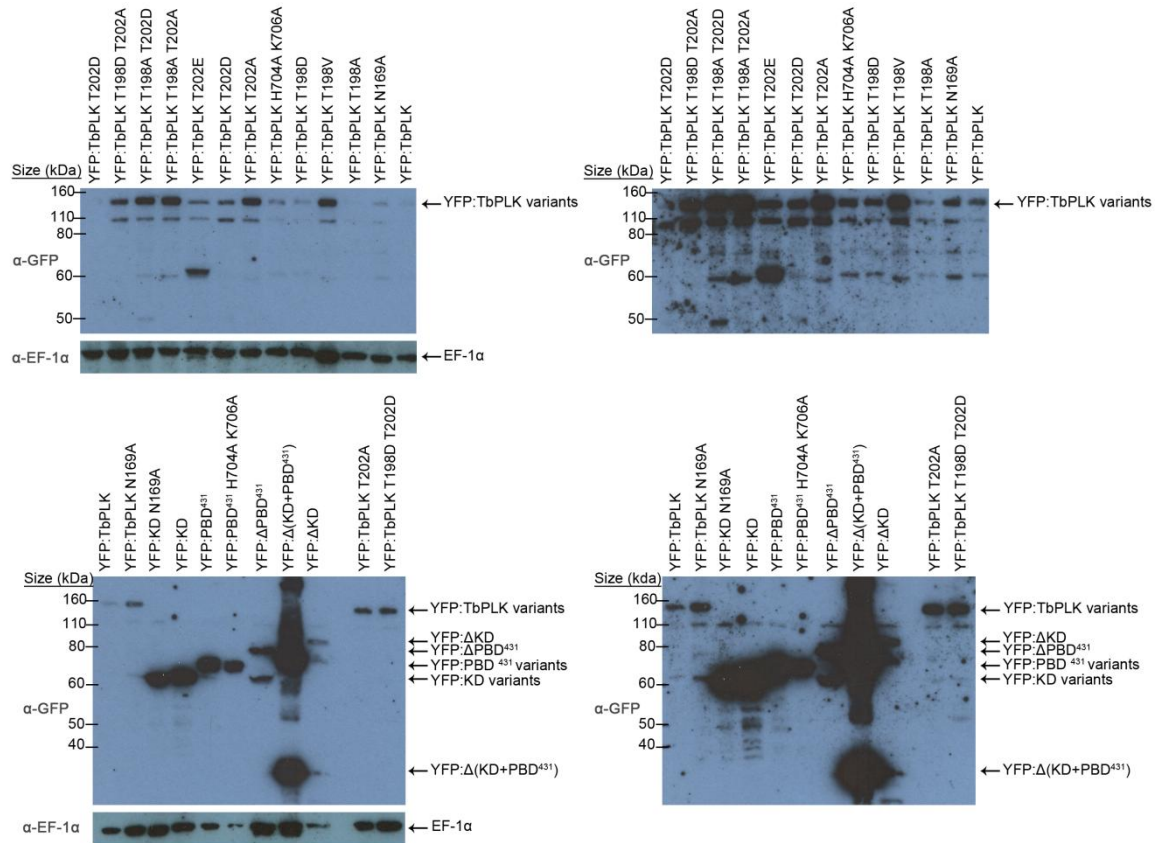


Figure 3-22 Western blots of all YFP:TbPLK fusion proteins. Whole cell extracts (1×10^6 cells/sample) of PCF cells induced with $1 \mu\text{g ml}^{-1}$ tetracycline to express N-terminal YFP-tagged TbPLK fusion proteins (as indicated) for 10 h were analysed simultaneously via Western blotting and probed with α -GFP to allow comparison of expression levels of YFP:TbPLK variants. Western blots were also probed with α -EF-1 α as a loading control. Right panels - α -GFP stained blot ~ 5 x longer exposed.

3.7 Discussion

The repeatable growth and cell cycle phenotypes that were generated following the expression of WT TbPLK and its kinase dead version (Hammarton et al. 2007; Yu et al. 2012) provided grounds by which the *in vivo* activity of TbPLK variants could be assayed in PCF cells, albeit indirectly. This has allowed pertinent questions to be asked addressing the regulatory mechanisms by which this essential cell cycle kinase's functions are controlled. The kinase domain of TbPLK is typical of any serine/threonine kinase domain, allowing the hypothesis that this domain is activated and inactivated in modes similar to its homologues. Indeed, the conserved threonine of the T-loop, T198 (T210 in human Plk1), was found to be essential for TbPLK kinase activity. Mutating this residue to alanine rendered the kinase inactive *in vitro* and *in vivo*. On the other hand, mutating it

to aspartic acid maintained the kinase active *in vivo* and *in vitro*, although the activity was not as strong as for WT TbPLK *in vitro*. The *in vivo* results here are in agreement with Yu et al (Yu et al. 2012). The difference in the extent of kinase activity between the WT and T198D mutant *in vitro* is in agreement with previous unpublished studies carried out in the Hammarton lab (May 2011) where similar experiments were performed. *In vivo*, no difference in the intensity of the expression phenotype is seen with the T198D mutation compared to WT protein and could be explained by the expressed WT kinase having reached the threshold of its kinase activity. An important experiment that needs to be done is testing the kinase activity of these (and all other TbPLK variants) expressed proteins via immuno-precipitation and subjecting the pulled down proteins to *in vitro* kinase assays. This would allow a direct comparison to be made between the activity levels of the different TbPLK variants.

Phosphorylation of T202 in TbPLK was shown to be just as essential as that of T198 for TbPLK activity in PCF parasites (Yu et al. 2012). Its corresponding residue in humans, T214, was found to be phosphorylated only at certain times during mitosis - it was found to be dephosphorylated after silencing of the spindle checkpoint in metaphase (Dulla et al. 2010). This suggested that this phosphorylation site may have functions other than regulating Plk1 activity which could also be conserved in *T. brucei*. Indeed, this threonine was found to be phosphorylated in other organisms too (Wind et al. 2002; Kelm et al. 2002; Dulla et al. 2010). Therefore, one of the aims of this study was to verify the essentiality of T202 for TbPLK activity and compare it with that of T198 phosphorylation.

Mutating T202 to alanine, aspartic acid or glutamic acid inactivated the kinase *in vivo* and *in vitro* in ways which could not be fully overcome by coupling these mutations with T198D. It is possible that, in this instance, the mutation to aspartic acid or glutamic acid failed to mimic phosphorylation, a phenomenon which has been reported elsewhere (Littlepage et al. 2002). The structural environment of this residue could prevent this mutation from mimicking phosphorylation. In humans, T214 is part of the P+1 loop which appears to be conserved, sequence-wise, in *T. brucei*. It has been reported that this residue in human Plk1 rotates outward in inactive kinases relative from the position of the corresponding residue in active kinase structures, preventing it from forming a

hydrogen bond with Lys178 from the catalytic loop, an interaction known to be conserved in the active states of Ser/Thr kinases (e.g., Thr201 and Lys168 in PKA) (Kothe et al. 2007; Krupa et al. 2004). Therefore, in TbPLK, mutating this residue could prevent this hydrogen bonding from taking place, thus preventing the kinase from being activated. This is, of course, assuming that the kinase domain of TbPLK assumes a structure similar to that of human Plk1. Additionally, T202 was not detected as a phosphosite in the only phosphoproteomic study in PCF parasites (Urbaniak et al. 2013). Further work needs to be done to settle the importance of T202 phosphorylation for TbPLK activity. It is possible that phosphoproteomic studies could miss important residues that are phosphorylated at specific stages of the cell. The phosphosites of pulled-down endogenous TbPLK in synchronised cells could be mapped, thus allowing the identification of important regulatory residues at various stages of the cell cycle, which could shed light on whether T202 really is an important phosphorylation site. Ultimately, a solved crystal structure of active TbPLK and TbPLK T198 and/or T202 mutants would provide clearer solutions to resolve this matter.

The PBD has been shown to be essential for the spatial regulation of PLK activities (section 3.3.5). Expressed YFP-tagged WT TbPLK in this study has been shown to display a localisation that is consistent with it being dynamic throughout the cell cycle, in agreement with the findings of de Graffenried's group (Ikeda & de Graffenried 2012; Lozano-Núñez et al. 2013). YFP-tagged WT TbPLK appeared to concentrate around the bilobe region (encompassing basal bodies, bilobe, FPC and FAZ; although further co-localisation studies would be required to confirm this). This was found to be the case in all full length TbPLK T198/T202 mutants, including the ones which inactivated the kinase, suggesting that TbPLK kinase activity by itself is unlikely to be essential for its localisation. Without a detailed analysis of the relationship between the localisations observed and cell cycle stages, it is difficult to identify the smaller details of localisation defects following TbPLK mutations. Therefore, it is possible that minor localisation defects following TbPLK kinase inactivation have gone unnoticed in this study. Such detailed studies enabled de Graffenried's group to observe that inhibited kinase failed to localise to the FAZ following karyokinesis (Lozano-Núñez et al. 2013). Also, the fact that these proteins are expressed could generate artefacts due to deregulated binding to substrates/binding

proteins or other proteins TbPLK wouldn't necessarily bind to. Even taking these caveats into consideration, the significant localisation defects observed upon expressing the various truncation mutants of TbPLK have still allowed to build a picture of how its domains mediate its localisation.

The putative His-Lys pincer does not seem to be important for TbPLK localisation. This study complements those done by Li's group (Yu et al. 2012) where the PBD of TbPLK was found to possess none of the other conserved residues found in other organisms - W414 and L490 in human Plk1. Indeed, the putative His and Lys residues of TbPLK were also not found to align well with the conserved His-Lys pincer in other organisms (Yu et al. 2012). These residues are essential for PBD binding to phospho-peptides (Elia, Rellos, et al. 2003; Elia, Cantley, et al. 2003; Yun et al. 2009). Could it be that TbPLK PBD does not bind phospho-peptides like PLK1 proteins do in yeast and metazoans? This could explain the non-mitotic, divergent function and localisation of TbPLK. The YFP:PBD⁴³¹ as a whole was, however, found to be required for TbPLK localisation. YFP:PBD⁴³¹ appeared to concentrate in the bilobe area and the flagellum similar to the full length proteins. YFP:KD, in the absence of the PBD, was unable to localise anywhere and remained cytoplasmic even though it was still able to function like the WT full length kinase, as evidenced by the similar expression phenotypes obtained.

Further truncation studies shed light on more intriguing aspects of TbPLK domain functions which includes a putative bi-partite NLS (Sun & Wang 2011) and a putative destruction box in the IDL region that is not included in the KD and PBD⁴³¹ constructs. Addition of this IDL region to the KD (Δ PBD) sequestered it into the nucleus. Expression of YFP: Δ PBD protein did not display a kinase active phenotype, suggesting the requirement for TbPLK localisation outside the nucleus (in the bilobe area and FAZ) to mediate its functions. The localisation of YFP: Δ PBD to the nucleus could be explained by the inclusion of the NLS in this truncated protein. This was supported by the fact that this IDL region (YFP: Δ KD+PBD) on its own also localised in the nucleus, albeit in discrete puncta, confirming work by Yu et al (Yu et al. 2012).

The power of the PBD in regulating TbPLK localisation can be found in the fact that addition of the PBD⁴³¹ to this IDL region (YFP: Δ KD) altered its nuclear

localisation to a cytoplasmic one, sometimes concentrating it to the bi-lobe region, although it did not completely restore the localisation observed for just YFP:PBD⁴³¹. The reason for the IDL region+PBD⁴³¹ (YFP:ΔKD) construct for not localising exactly like YFP:PBD⁴³¹ could be due to the tension between the competing localising effects of the IDL region (nucleus) and the PBD (bilobe region and FAZ). In all, it can be concluded that the PBD is required for TbPLK localisation. However, owing to the expressed PBD⁴³¹'s inability to prevent the endogenous TbPLK from accessing its substrates *in vivo*, it can also be considered that there is an additional need for an active kinase domain to allow TbPLK to specifically bind its substrates, which is in agreement with the observations made by Li's group (Yu et al. 2012). However, this conclusion cannot be conclusively drawn, as it cannot be assumed that the expressed YFP:TbPLK proteins are exclusively binding to their physiological substrates. Such joint importance of the kinase domain and the PBD in PLK substrate binding has been shown previously (Lin et al. 2000); the chemical and structural features of both the catalytic and C-terminal domains of Plk1 were required for binding to the substrate in question - GRASP65.

It is intriguing to note that a protein which so far has not shown to localise in the nucleus and have any nuclear functions should possess a functional NLS. TbPLK mutated to feature alanine, instead of the basic residues which characterises the NLS, was still able to rescue endogenous TbPLK depletion by RNAi (Yu et al. 2012). Expression of nuclear localised truncations (ΔPBD and ΔKD+PBD) in this study displayed no growth or cell cycle defects in PCF cells. Altogether, the studies done in this project indicate that the NLS plays no role in TbPLK function.

In this study, it has also been shown that the IDL region which possesses the putative destruction box, does play a role in TbPLK expression levels. This is in keeping with what is already known of PLK1 in other organisms and other cell cycle kinases (Lindon & Pines 2004; Archambault & Glover 2009; Liu et al. 2012). This, therefore, indicates that TbPLK proteins may be targeted for proteasomal degradation. Further experiments could be done to further confirm this hypothesis. The arginine and leucine residues of the destruction box could be mutated and then expressed from the endogenous locus and compared with the expression levels of WT proteins.

Future experiments that need to be done, to consolidate the findings described in this chapter, have been described in a number of places in the results section and above. In addition to these, a few more experiments are also required. It is possible that the phenotypes seen following the ectopic expression of proteins described here were due to their over-expression. Western blot analyses of lysates of WT and TbPLK variants expressing cell lines, using α -TbPLK antibodies, would be required to investigate if these proteins were expressed in levels above that of the endogenous protein. Also, unless otherwise mentioned, results obtained from only one clone have been described for the *in vivo* expression experiments. When conducting further experiments, second clones, which have already been generated, will also need to be analysed to demonstrate reproducibility.

TbPLK has been shown to be divergent in its functions but yet, in many ways, conserved in the means by which it is regulated. Future studies, characterising more of its substrates and how they come to interact with TbPLK would shed light on how this kinase mediates its functions in an environment so different from its homologues in yeast and metazoans.

4 Regulation of *T. brucei* Polo-like kinase in bloodstream form parasites

4.1 TbPLK in *T. brucei* BSF parasites

Previous work carried out by the Hammarton lab has shown that knockdown of TbPLK via RNAi in the BSF generates defects in cytokinesis (Hammarton, Kramer, Tetley, Boshart, & Mottram, 2007). A rise in 2N2K cells was noted, many of which were blocked midway in furrow ingression. No other studies on the role of TbPLK in BSF parasites have been published. This difference in phenotypes between PCF (section 3.4.1) and BSF parasites could be a result of the differences in cell cycle events between the two life cycle stages (section 1.3.2). In terms of understanding TbPLK regulation in BSF parasites, to date no studies have yet been conducted.

4.2 Project aims

The aims of this project were to characterise the regulation of TbPLK in BSF cells. The questions asked here are similar to those that were asked using PCF cells in Chapter 3. In this chapter, how the following domains regulated the activity of TbPLK was investigated:

- the Polo-box domain
- the residue T198 in the T-loop

4.3 Results

4.3.1 *TbPLK* expression

The first step was to investigate whether the expression of TbPLK in its kinase active (WT) and dead (TbPLK N169A) forms would generate differential cell cycle phenotypes compared to those observed with PCF parasites (section 3.6.1). In order to do this, the pLew100v5 (kind gift from George Cross;

http://tryps.rockefeller.edu/trypsru2_plasmids.html) plasmid, which allows tetracycline inducible expression of genes of interest from the rRNA spacer region, was modified to allow N-terminal tagging of the TbPLK proteins with a YFP epitope. First, *YFP* was sub-cloned from pHG329 (gift from Chris de Graffenried) as a HindIII-BamHI fragment into the same sites in pLew100v5 (section 2.3.2.6 and 2.3.2.7 for cloning details). Then a multiple cloning site was added at the 3' end of *YFP* to include ApalI, XhoI and HpaI restriction sites (section 2.3.2.8). *TbPLK* variants were then cloned as BamHI-XhoI fragments into this modified vector (now pHG399; section 2.3.2.7; Figure 4-1). These constructs were then linearised and transfected into BSF 427 pLew13 pLew90 (Hyg^r and Neo^r; Table 2-3) which expresses the TetR driven by a T7 promoter. The TetR binds to the operators (adjacent to the rRNA promoter which drives expression of the gene of interest) preventing the expression of the gene of interest until the addition of tetracycline.

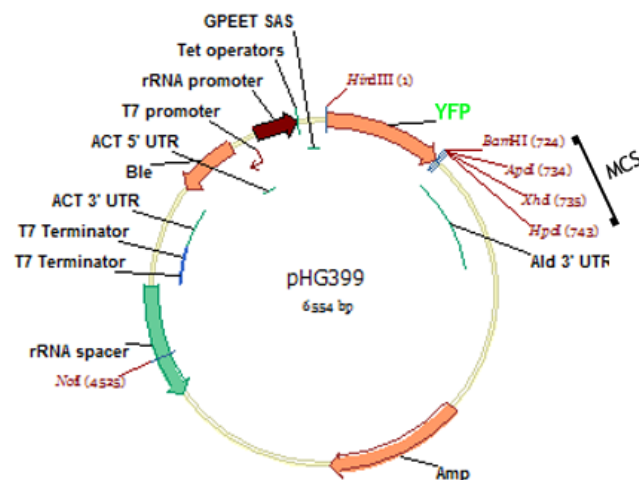
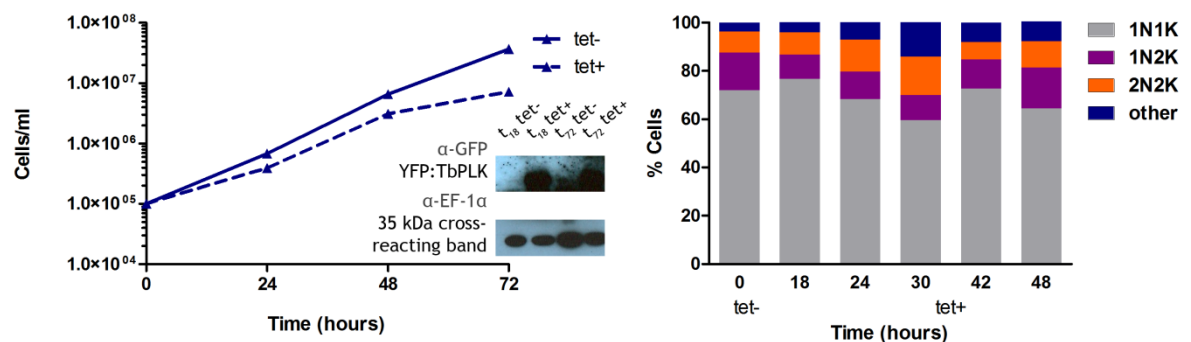


Figure 4-1 Plasmid map of pHG399. pHG316 (originally pLew100v5, see Table 2-5 for details; kind gift from George Cross, http://tryps.rockefeller.edu/trypsru2_plasmids.html) was modified to allow expression of N-terminal YFP-tagged proteins and to introduce a multiple cloning site (MCS) featuring the restriction sites ApalI, XhoI and HpaI. Amp - ampicillin resistance cassette. rRNA - ribosomal RNA spacer. Ble - Bleomycin resistance cassette. GPEET SAS - GPEET splice-acceptor site. ACT - Actin. Ald - Aldolase. For transfection, the constructs were linearised by digestion with with NotI (section 2.3.2.4).

Expression of YFP:TbPLK in BSF cells appears to give slight growth defects but without marked changes in cell cycle progression (Figure 4-2A). On the other hand, expression the kinase dead YFP:TbPLK N169A did not give strong phenotypic changes either in growth or cell cycle progression of BSF cells (Figure

4-2B). Western blotting confirmed that the proteins were expressed at detectable amounts as early as 18 h post-induction. For the loading control, a cross-reacting band which appeared at about 35 kDa was used instead of the one representing EF-1 α at about 50 kDa. This was because the size of EF-1 α was mistakenly thought to be 35 kDa during this experiment. After transfer during western blotting, the blotting membranes were often cut to allow separate incubation with different antibodies. In this experiment, the membrane was cut in such a way that proteins above 45 kDa in size, including EF-1 α , were excluded for incubation with EF-1 α primary antibody. Therefore, it was not possible to employ the EF-1 α as loading control here and will all need to be rectified in future repeat experiments.

A YFP:TbPLK



B YFP:TbPLK N169A

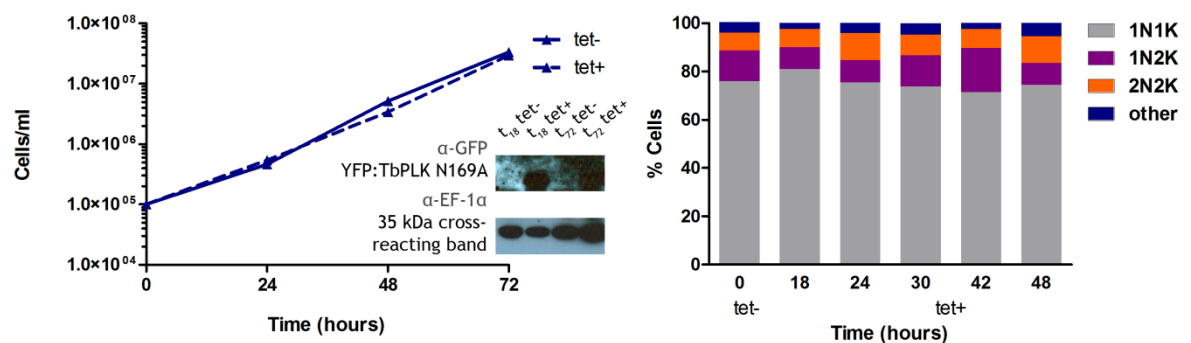


Figure 4-2 Expression of YFP-tagged TbPLK and TbPLK N169A in BSF cells. N-terminally YFP-tagged TbPLK (A) and TbPLK N169A (B) were expressed in BSF *T. brucei* cells by the addition of $1 \mu\text{g ml}^{-1}$ tetracycline (tet+) to the culture medium. Analyses of non-induced cells (tet-) have also been shown as controls. Cumulative growth curves (left panels of both sections) were generated and the numbers of nuclei (N) and kinetoplasts (K) in each cell ($n \geq 200$) following DAPI staining of samples (right panels of both sections) were recorded at the indicated time points post addition of tetracycline to the induced samples. Western blots (middle panels of both sections) were performed on whole cell extracts (1×10^6 cells/sample) taken at 18 and 72 hrs post-induction (t_{18} and t_{72} , respectively) to detect expression of YFP:TbPLK/YFP:TbPLK N169A using an

α -GFP antibody. Western blots were also probed with α -EF-1 α which generated a cross-reacting band at 35 kDa that has been used as the loading control.

A second independent clone of each of these cell lines was also analysed and gave the same results (data not shown). However, the difference in phenotypes between the two cell lines was not considered to be marked enough to be exploited for use in an expression assay as was done with PCF parasites (section 3.6.1). Efforts were then made to establish an RNAi complementation system instead as described below.

4.3.2 *TbPLK* RNAi complementation

The aim here was to determine how well the exogenous expression of *TbPLK* mutants was able to complement knockdown of endogenous *TbPLK* via RNAi. In order to knockdown endogenous *TbPLK* specifically without affecting expression of the exogenous *TbPLK* variants, the 3' UTR of endogenous *TbPLK* was targeted via RNAi. Since the *TbPLK* variants that were expressed using pHG399, used the *aldolase* 3' UTR, these exogenously expressed *TbPLK* variants were exempted from depletion via RNAi against the endogenous *TbPLK* 3' UTR. Also, since the stem loop generating RNAi vector, p2T7ti:GFP (LaCount, Bruse, Hill, & Donelson, 2000), was, like pHG399, bleomycin resistant, it was first modified to replace its bleomycin selective marker with a BSD resistance marker (see section 2.3.2.7 for cloning details) generating pHG456. This permitted transfection of the same cell line with both pHG456 and the modified expression vector pHG399 (section 4.3.1).

4.3.2.1 *TbPLK* knockdown via RNAi targeting its 3' UTR

The 549 bases, lying immediately downstream of the stop codon of the *TbPLK* gene, were cloned as a HindIII and BamHI fragment into pHG456 (section 2.3.2.7). This construct (pHG457) was then linearised with EcoRV and transfected into BSF 427 pLew13 pLew90 cells. *TbPLK* RNAi was induced with tetracycline for 24 hours in three independent clones before the cell lines were tested for *TbPLK* knockdown using an α -*TbPLK* antibody (kind gift from de Graffenried's lab; Ikeda & de Graffenried, 2012). In Figure 4-3 it can be seen

that all three clones showed good levels of TbPLK knockdown. Clone 1 was then selected for further analysis and used for the complementation assay.

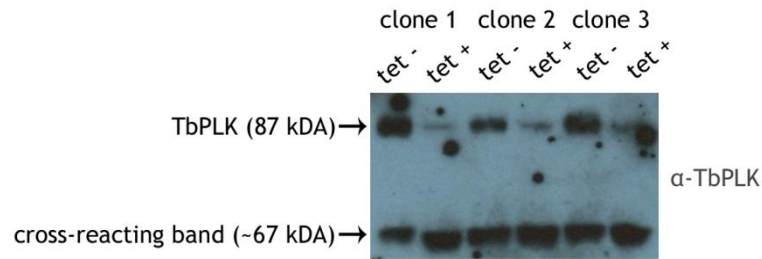


Figure 4-3 Western blot analysis of TbPLK knockdown via RNAi of its 3' UTR. The α -TbPLK antibody was used to probe Western blots of lysates of *TbPLK* 3' UTR RNAi clones following 24 hrs induction with $1 \mu\text{g ml}^{-1}$ tetracycline (tet⁺). Lysates of non-induced cells (tet⁻) have also been included as controls. The cross-reacting band verifies equal loading of lysates.

4.3.2.2 The RNAi complementation assay

Previously, in order to investigate the role of TbPLK in BSF cells, RNAi targeting the 5' end of endogenous *TbPLK* was used to knockdown the protein (Hammarton et al., 2007). Following RNAi induction, a rapid growth arrest was noted and a considerable increase in post-mitotic (2N2K) cells was observed. This accumulation of 2N2K cells suggested that cytokinesis was impaired by *TbPLK* RNAi. Further investigation of these 2N2K cells uncovered an increase in the proportion of furrowing 2N2K cells and concomitant decrease in the proportion of 2N2K cells which had completed furrow ingression but not abscission over time. Altogether, the data strongly suggested that furrow ingression is impaired when TbPLK is downregulated in bloodstream trypanosomes.

This TbPLK RNAi cell line (TbPLK RNAi; Hammarton et al., 2007) and the newly generated 3' UTR RNAi cell line (TbPLK 3' UTR RNAi; section 4.3.2.1) were then compared to determine whether the new cell line acted as expected. The cell lines were also induced with three different concentrations of tetracycline ($0.1 \mu\text{g ml}^{-1}$, $1 \mu\text{g ml}^{-1}$ and $10 \mu\text{g ml}^{-1}$; Figure 4-4) in order to test for differences in intensities of knockdown which could affect the efficiency of complementation by the exogenously expressed TbPLK variants. Reducing or increasing the tetracycline concentration generated very small changes, if any at all, in the growth phenotypes of the cell lines (Figure 4-4A and B, top panels). Overall, TbPLK 3' UTR RNAi did induce a cell death phenotype (Figure 4-4B). However,

the cells appear to grow, albeit at a slower rate, for the first 24 hours before their growth is arrested and the cell death phenotype becomes apparent (at 72 hours), which is in contrast to the original *TbPLK* RNAi cell line for which the cell death phenotype is apparent within the first 24 hours following RNAi induction (Figure 4-4A). Despite the milder growth phenotype, the cell cycle defects generated by *TbPLK* 3' UTR RNAi are comparable to those obtained with *TbPLK* RNAi (Figure 4-4A and B, bottom panels). Both cell lines demonstrate a rise in 2N2K cells by 6 hours post-induction with a subsequent rise in "other" aberrant cell types. Western blot analysis of these cell lines is vital at this point to confirm *TbPLK* knockdown. However, repeated attempts to visualise *TbPLK* staining with the α -*TbPLK* antibody (as seen in Figure 4-3) on Western blots of lysates from the two *TbPLK* RNAi cell lines were unsuccessful. Nevertheless, the *TbPLK* 3' UTR RNAi cell line was transfected with the vectors described in section 4.3.1 (for cloning details, see sections 2.3.2.6 and 2.3.2.7) to express YFP:*TbPLK* variants (this section, sections 4.3.2.3 and 4.3.2.4). In these doubly transfected cell lines, addition of tetracycline should induce *TbPLK* 3' UTR RNAi and the expression of YFP:*TbPLK* variants at the same time.

First, YFP:*TbPLK* and YFP:*TbPLK* N169A were expressed in a *TbPLK* 3' UTR RNAi background (Figure 4-4C and D, respectively). Expression of YFP:*TbPLK*, but not YFP:*TbPLK* N169A, was able to partially complement the growth defect induced by *TbPLK* knockdown. Analysis via Western blotting verified expression of these N-terminally YFP-tagged proteins. A slight, but not complete, alleviation of cell cycle defects was also observed with WT YFP:*TbPLK* expression (Figure 4-4C, middle panel) which was not the case with YFP:*TbPLK* N169A expression (Figure 4-4D, middle panel) suggesting that it is the kinase activity of *TbPLK* and not the protein in general that is responsible for the complementation. Varying the concentration of tetracycline did not vary the amount of recombinant protein expressed and, subsequently, no variations in growth phenotypes were observed (Figure 4-4C and D, top panels). These observable differences, in the ability of YFP:*TbPLK* and kinase dead YFP:*TbPLK* N169A to complement *TbPLK* 3' UTR RNAi, provided the basis by which the kinase activity of YFP:*TbPLK* variants could be tested.

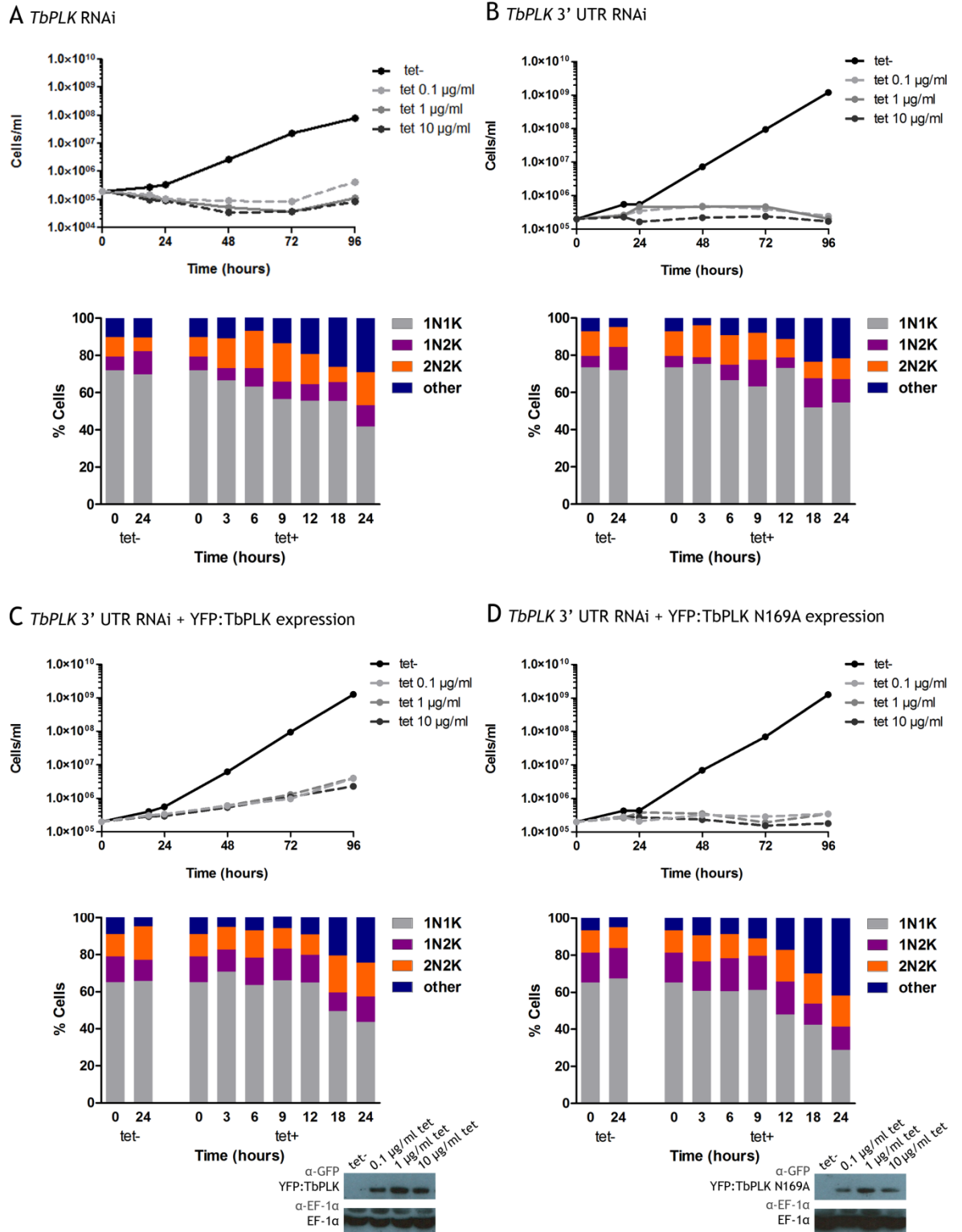


Figure 4-4 Controls for the RNAi complementation assay in BSF cells. *TbPLK* was knocked down in *T. brucei* BSF cells via RNAi either targeting its 5' end (A) or 3' UTR (B). N-terminally YFP-tagged *TbPLK* (C) and *TbPLK* N169A were also expressed in a *TbPLK* 3' UTR RNAi background. All cell lines were induced with three different concentrations of tetracycline (tet; 0.1 $\mu\text{g ml}^{-1}$, 1 $\mu\text{g ml}^{-1}$ and 10 $\mu\text{g ml}^{-1}$) which induced the RNAi and expression. Analyses of non-induced cells (tet-) are also shown as controls. Cumulative growth curves (top panel of each section) were generated for all cell lines and tetracycline concentrations. The numbers of nuclei (N) and kinetoplasts (K) in each cell ($n \geq 200$) following DAPI staining of samples were recorded at the indicated time

points post addition of $1 \mu\text{g ml}^{-1}$ tetracycline to the induced samples (bottom panels (A,B); middle panels (C,D)). Western blots were performed on whole cell extracts (1×10^6 cells/sample) taken at 18 h post addition of tetracycline to the induced samples for 3' UTR *TbPLK* RNAi + YFP:*TbPLK* expression (C, bottom panel) and 3' UTR *TbPLK* RNAi + YFP:*TbPLK* N196A expression (D, bottom panel).

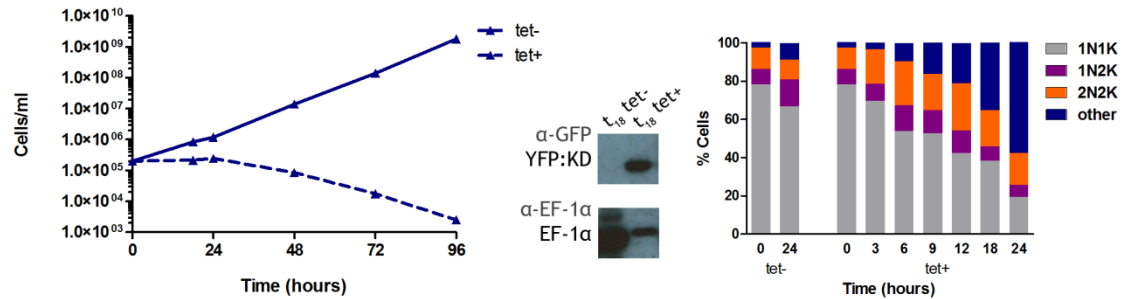
4.3.2.3 Role of the KD and PBD

In order to investigate the importance of the PBD for *TbPLK* activity, a few *TbPLK* truncations (same as those described in Chapter 3 - KD, KD N169A PBD⁴³¹, PBD⁴³¹ H704A K706A and *TbPLK* H704A K706A) were expressed using the pHG399 vector (section 4.3.1; for cloning details, see sections 2.3.2.6 and 2.3.2.7) in the *TbPLK* 3' UTR RNAi background (Figure 4-5). Expression of YFP:KD, which entirely lacked the PBD and the IDL region, compounded the cell death phenotype instead of alleviating it (compare Figure 4-5A with Figure 4-4C). This was accompanied by a rise in aberrant cell types, especially 2N1K cells (20% of total cells counted at t_{18} post-induction). Since the expression of the kinase dead version of KD, YFP:KD N169A, did not have any effect on the background *TbPLK* 3' UTR RNAi phenotypes (Figure 4-5B), this suggests that it is the kinase activity of KD rather than the protein itself that is responsible for the cell death phenotype. The dominant negative phenotype could possibly be attributed to unregulated kinase activity of the expressed YFP:KD, which would suggest that the PBD is required for the negative regulation of *TbPLK* kinase activity. The rise in 2N1K cells seen with YFP:KD expression in the *TbPLK* 3' UTR RNAi background is similar to what is seen with YFP:*TbPLK* expression in WT background PCF parasites (Hammarton et al., 2007 and Chapter 3). This suggests defects in kinetoplast segregation putatively linking *TbPLK* function to kinetoplast duplication in BSF cells.

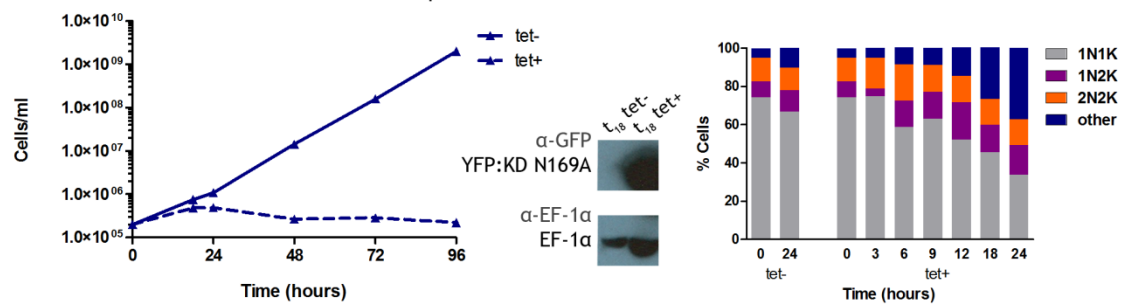
Expression of YFP:PBD⁴³¹ or YFP:PBD⁴³¹ H704A K706A, which lack the kinase domain were, unsurprisingly, unable to complement the *TbPLK* 3' UTR RNAi and did not compound the severity of the phenotype either (Figure 4-5C and D). When YFP:*TbPLK* H704A K706A was expressed in the *TbPLK* 3' UTR RNAi background, some alleviation of growth and cell cycle defects were seen although not to the same level as with YFP:*TbPLK* (Figures 4-5E and 4-4C). It is possible that the levels of YFP:*TbPLK* H704A K706A expression is lower than that

of YFP:TbPLK explaining the difference in phenotypes. A western blot allowing direct comparison of expression levels would help clarify this. If the two proteins are expressed at same levels, then these results suggest that the putative His-Lys pincer might play a role in regulating TbPLK activity in BSF cells.

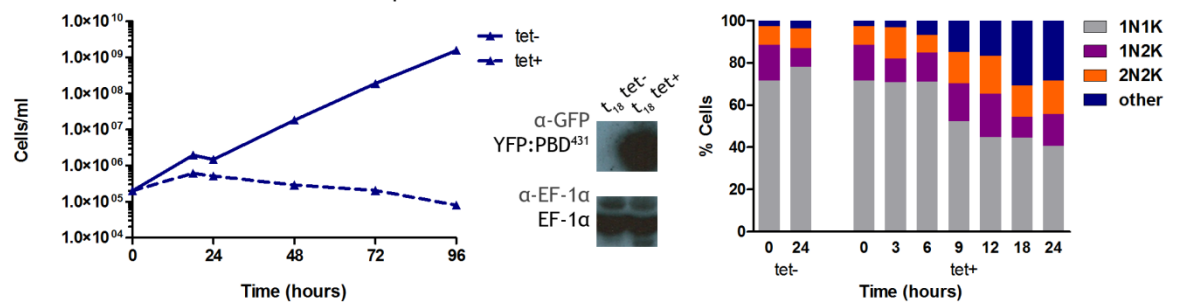
A *TbPLK* 3' UTR RNAi + YFP:KD expression



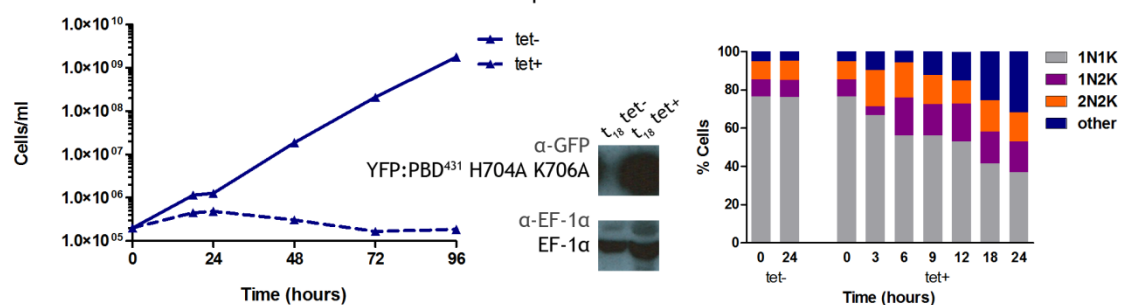
B *TbPLK* 3' UTR RNAi + YFP:KD N169A expression



C *TbPLK* 3' UTR RNAi + YFP:PBD⁴³¹ expression



D *TbPLK* 3' UTR RNAi + YFP:PBD⁴³¹ H704A K706A expression



E *TbPLK* 3' UTR RNAi + YFP:TbPLK H704A K706A expression

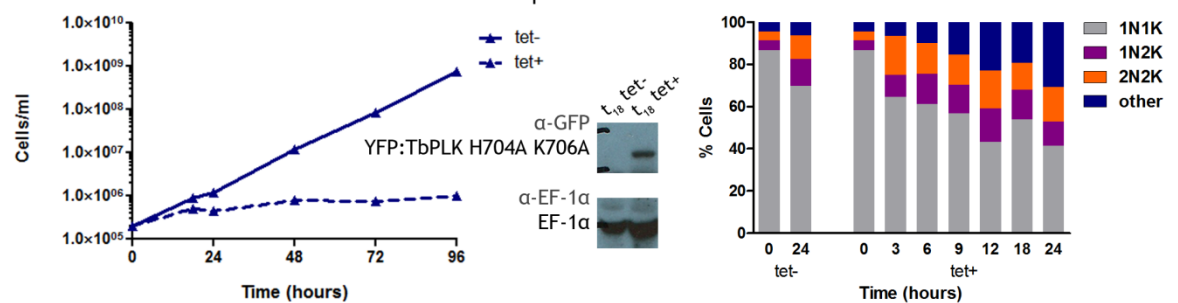


Figure 4-5 Analysis of the roles of the kinase domain and the PBD of TbPLK in BSF cells using an RNAi complementation assay. N-terminally YFP-tagged KD (A), KD N169A (B), PBD⁴³¹ (C), PBD⁴³¹ H704A K706A (D) and TbPLK H704A K706A (E) were expressed in BSF *T. brucei* cells, in a *TbPLK* 3' UTR RNAi background, with the addition of 1 $\mu\text{g ml}^{-1}$ tetracycline (tet+) to the culture medium. Analyses of non-induced cells (tet-) have also been shown as controls. Cumulative growth curves (left panel of each section) were generated and the numbers of nuclei (N) and kinetoplasts (K) in each cell ($n \geq 200$) following DAPI staining of samples (right panel of each section) were recorded at the indicated time points post addition of tetracycline to the induced samples. Western blots (middle panel of each section) were performed on whole cell extracts (1×10^6 cells/sample) taken at 18 h post addition of tetracycline to the induced samples (t_{18}) to detect expression of YFP:KD, YFP:KD N169A, YFP:PBD⁴³¹, YFP:PBD⁴³¹ H704A K706A and YFP:TbPLK H704A K706A using an α -GFP antibody. Western blots were also probed with α -EF-1 α as a loading control.

A second independent clone of all the cell lines mentioned in this section was also analysed and gave the same phenotypes (data not shown).

4.3.2.4 Role of T198

In order to investigate the role of T198 in regulating TbPLK activity, YFP:TbPLK with its T198 mutated to the non-phosphorylatable alanine/valine was expressed in a *TbPLK* 3' UTR RNAi background. Neither recombinant protein was able to alleviate the growth and cell cycle defects generated by the TbPLK RNAi (Figure 4-6). Second clones of these two cell lines were also analysed which also demonstrated similar phenotypes upon induction (data not shown). Altogether, the data suggest that phosphorylation at this residue is essential for activating TbPLK kinase activity. In order to provide further evidence for this conclusion, numerous attempts were made to generate cell lines expressing YFP:TbPLK T198D, but were unsuccessful. Mutating T198 to aspartic acid would have mimicked phosphorylation. If it was able to complement *TbPLK* 3' UTR RNAi at the levels of WT YFP:TbPLK, this could have revealed the importance of T198 phosphorylation for TbPLK activity.

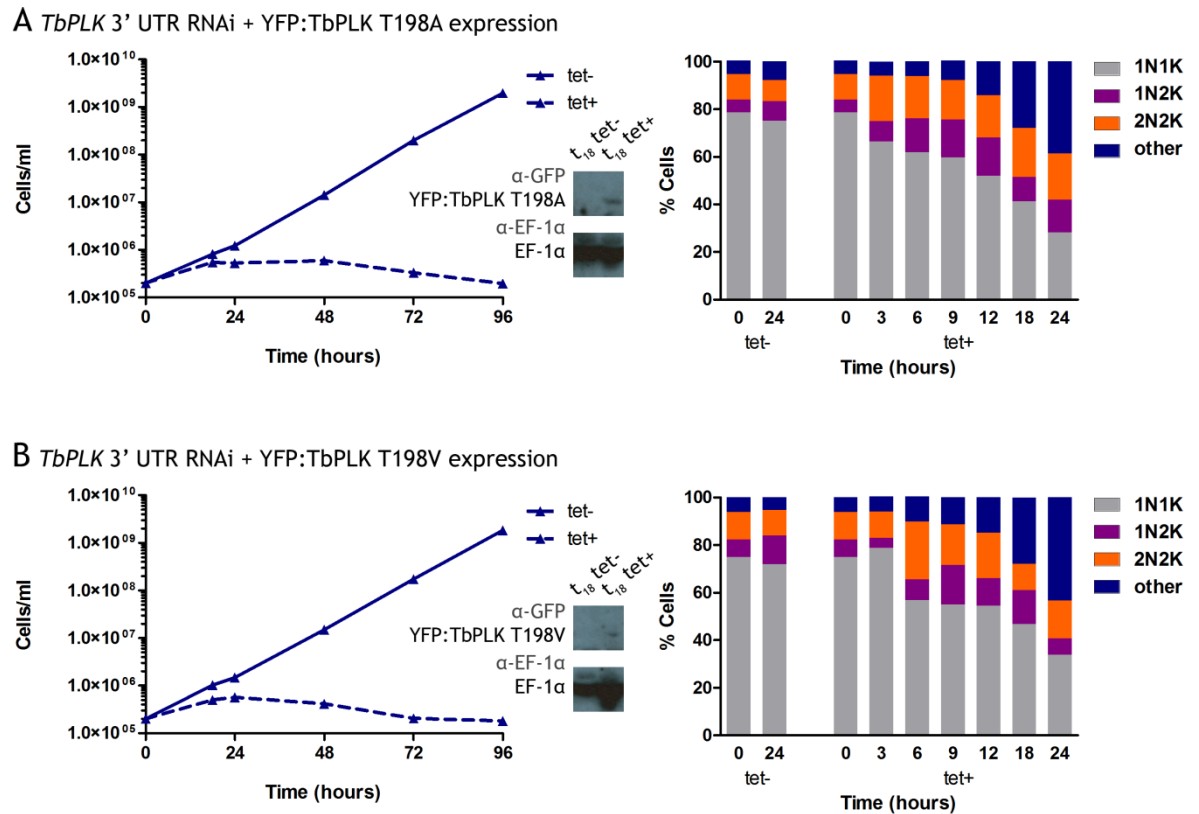


Figure 4-6 Analysis of the role of the TbPLK T198 residue in BSF cells using an RNAi complementation assay. N-terminally YFP-tagged TbPLK T198A and TbPLK T198V were expressed in BSF *T. brucei* cells, in a *TbPLK* 3' UTR RNAi background, with the addition of $1 \mu\text{g ml}^{-1}$ tetracycline (tet+) to the culture medium. Analyses of non-induced cells (tet-) have also been shown as controls. Cumulative growth curves were generated (left panels of both sections) and the numbers of nuclei (N) and kinetoplasts (K) in each cell ($n \geq 200$) following DAPI staining (right panels of both sections) of samples were recorded at the indicated time points post addition of tetracycline to the induced samples. Western blots (middle panels of both sections) were performed on whole cell extracts (1×10^6 cells/sample) taken at 18 h post addition of tetracycline to the induced samples (t_{18}) to detect expression of YFP:TbPLK T198A and YFP:TbPLK T198V using an α -GFP antibody. Western blots were also probed with α -EF-1 α as a loading control.

4.4 Discussion

The work described in this chapter sheds some light on how TbPLK activity is regulated in BSF trypanosomes. Expression of YFP:TbPLK did generate a small growth defect in BSF parasites however not to the extent observed in PCF cells (section 3.6.1; Hammarton et al., 2007; Yu, Liu, & Li, 2012). Since the expression of YFP:TbPLK was robust (Figure 4-2), this suggests differences in how TbPLK is regulated in addition to differences already observed in the functions of

TbPLK between the two life-cycle stages (Hammarton et al., 2007; Chapter 3). The smaller extent of phenotypic changes following expression of YFP:TbPLK could indicate that its activity is tightly regulated. On the other hand, it could also mean that the downstream pathways are not as responsive to extra TbPLK activity. Indeed, the toxicity of expressing just the kinase domain, even in a TbPLK RNAi background, suggests that the PBD and the IDL, which are not present in the KD protein described here, could be required to negatively regulate TbPLK activity. The rise in 2N1K cells when YFP:KD was expressed putatively links TbPLK function to kinetoplast duplication reflecting what is already known in PCF cells (Ikeda & de Graffenried, 2012). TbPLK knockdown is known to inhibit ingression of the furrow in BSF cells during cytokinesis (Hammarton et al., 2007). Altogether, there seems to be an indication that proper kinetoplast duplication is required for furrow ingression during cytokinesis.

The *TbPLK* RNAi cell line generated in this study, which targeted the 3' UTR of *TbPLK*, was confirmed to knockdown TbPLK and generated cell cycle defects which were comparable to that of *TbPLK* RNAi cell line which targeted the coding sequence (Hammarton et al., 2007), despite a milder growth phenotype. This suggested that targeting the 3' UTR of *TbPLK* is enough to silence the gene. However, expression of YFP:TbPLK in this RNAi background did not fully abrogate the growth and cell cycle phenotypes. The inability of YFP:TbPLK to fully complement *TbPLK* RNAi could be due to off-target effects or effects on the expression of genes immediately downstream of *TbPLK*. However, this strategy has previously been successfully used in PCF cells (Yu et al., 2012). The problem faced with implementing this strategy in BSF cells could be due to the differences in gene regulation between the two life-cycle stages. Nonetheless, the partial ability of YFP:TbPLK to complement *TbPLK* RNAi and the inability of YFP:TbPLK N169A to do the same, provided the basis by which the kinase activity of *TbPLK* mutants could be tested.

The inability of YFP:TbPLK H704A K706A to complement TbPLK RNAi as well as YFP:TbPLK does suggests that these residues are partially important for TbPLK activity. This is in contrast to conclusions drawn in PCF parasites (Chapter 3) again indicating differential regulation of TbPLK between the two life-cycle stages. Further work is essential to investigate this further. It is possible that the

expression levels of YFP:TbPLK H704A K706A is lower than that of YFP:TbPLK. In future experiments, the expression levels of these, and the rest of the proteins, in addition to endogenous TbPLK, will need to be verified. Imaging studies dissecting the localisation of YFP:TbPLK H704A K706A would help answer if this putative pincer is truly essential for TbPLK localisation and substrate binding.

T198 appears to play the same regulatory role as it does in PCF parasites and in other organisms (Chapter 3). Preventing phosphorylation at T198 of expressed YFP:TbPLK by mutating it to alanine or valine hinders the ability of the recombinant protein to reverse the effects of TbPLK RNAi. Additional studies with T198 mutated to aspartic acid which mimics phosphorylation would have been useful in confirming these conclusions. The inability in generating BSF cell lines which express YFP:TbPLK T198D could possibly be due to the toxicity of deregulated, hyperactive TbPLK. Despite tight regulation of these inducible expression vectors, perhaps the toxicity of YFP:TbPLK T198D could explain why attempts to generate these cell lines were unsuccessful.

5 RNAi-based Screening for Protein Kinases Involved in the *T. brucei* Cell Cycle

5.1 RNAi – discovery and mechanism

The discovery that double-stranded (ds) RNA was able to disrupt gene function in *C. elegans* (Fire et al., 1998) has revolutionized the way in which loss-of-function studies can be performed. This process, termed RNA interference (RNAi), involves dsRNA being cleaved to generate short interfering (si) RNAs, which then direct endonucleases towards the cognate mRNAs leading to their degradation and, consequently, gene silencing (Hammond, Bernstein, Beach, & Hannon, 2000; Zamore, Tuschl, Sharp, & Bartel, 2000). For organisms which possess the RNAi machinery, it is an essential part of post-transcriptional gene regulation and defence against viruses and mobile elements (Ding, Li, Lu, Li, & Li, 2004; Ghildiyal & Zamore, 2009; Schütz & Sarnow, 2006; Umbach & Cullen, 2009).

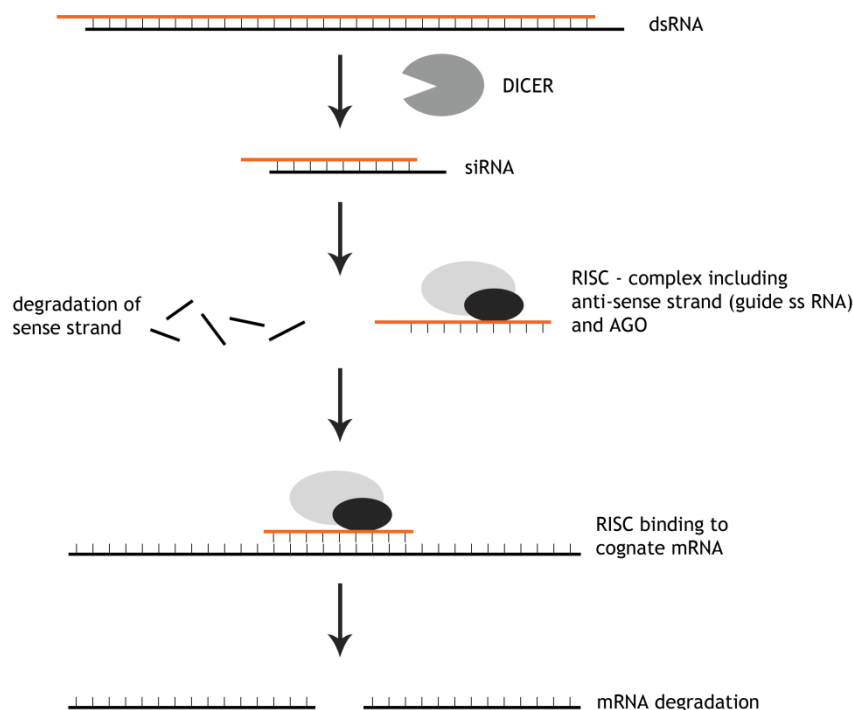


Figure 5-1 Schematic representing RNAi mechanism. Long dsRNA is cleaved into duplex siRNA by DICER endonuclease. The anti-sense strand of the siRNA (now known as guide RNA) along with AGO form the catalytic engine of the RISC complex which binds cognate mRNA and cleaves it.

The machinery responsible for driving RNA interference (RNAi) is now well defined (Figure 5-1). The common minimal machinery as understood from different model organisms includes: 1) a DICER endonuclease of the RNase III family which cleaves long dsRNAs into duplex siRNAs (Bernstein, Caudy, Hammond, & Hannon, 2001); 2) a DICER cofactor which enables siRNA biogenesis and loading of one of the strands of the siRNA duplex (now termed as the guide RNA; as opposed to passenger strand which is discarded) to 3) an Argonaute (AGO) “slicer” endonuclease (Meister, 2013). The AGO-siRNA complex forms the catalytic engine of the RNA-induced silencing complex (RISC; Hammond et al., 2000). Through complementary binding of the single-stranded (ss) guide siRNA, RISC cleaves the target mRNA thus silencing it (Elbashir, Lendeckel, & Tuschl, 2001; Elbashir, Martinez, Patkaniowska, Lendeckel, & Tuschl, 2001).

The discovery of RNAi has enabled gene function studies in a number of organisms and has significantly contributed towards the understanding of their biology. The relative ease by which RNAi can be induced has allowed the interrogation of gene functions at global scales (Kamath et al., 2003; Mohr, Bakal, & Perrimon, 2010). Genome-wide RNAi libraries which efficiently target almost every gene are now available for studying model cells and organisms such as *Drosophila*, *C. elegans* and humans. A variety of biological processes from cell-growth and viability (Boutros et al., 2004; Luo et al., 2008; Silva et al., 2008), signalling pathways (Bakal et al., 2008; Brown, 2005; Nybakken, Vokes, Lin, McMahon, & Perrimon, 2005; Z. Tu et al., 2009; Xu et al., 2007) to pathogen infections (Agaisse et al., 2005; Karlas et al., 2010; Krishnan et al., 2008; Sessions et al., 2009) have been focussed on, not to mention, the cell division cycle. High throughput RNAi studies which sought to screen for cell cycle regulators in *C. elegans*, *Drosophila* and human cells shall be reviewed in the next section.

5.2 RNAi-based cell cycle screens in other model organisms

The first ever large-scale study screening for cell cycle regulators demonstrated the huge amount of effort demanded by such projects. Initial studies restricted the screens to a specific cohort of genes reflecting the limitations of the RNAi technologies that were available then. Gönczy et al., screened about 96 % of predicted ORFs (2232 genes) on chromosome 3 of *C. elegans* to identify genes involved in cell cycle regulation (Gönczy et al., 2000). RNAi was induced by micro-injecting dsRNAs into wild-type hermaphrodites. The resulting embryos were then analysed via time-lapsed DIC assays and a progeny test. Due to decreasing potency of combining dsRNAs (when mixed with increasing volumes of different dsRNAs that were known to not cause any observable phenotypes), as first experimentally determined in the study, the genes could only be knocked down in pairs. This required about 1100 individual experiments, in addition to further analyses of “hits” (dsRNAs which gave a phenotype that was detectable via the DIC assay). 133 genes needed for the *C. elegans* cell cycle were thus identified, of which 122 genes had never been studied in the organism before, demonstrating the power of such studies. In another such study, the protein kinase (PK) gene family, was focussed on (Bettencourt-Dias et al., 2004). Again, RNAi was the tool of choice. Cell cycle progression determined via DNA content analysis using flow cytometry and the quantification of 20 other parameters were used to identify kinases required for cell cycle progression and/or mitosis in S2 *Drosophila* cells. Knockdown of a third of the kinome (80/228) was found to induce cell cycle defects such as an increase in the proportion of cells in G₁, a rise in aneuploid cells, an increase in the proportion of cells in G₂/M phase and a rise in polyploid cells, and the observation was made that compromising extracellular stress response pathways can have secondary effects on cell cycle progression. Later on, such studies were extended to a genome-wide level in *C. elegans* (Sönnichsen et al., 2005) and *Drosophila* (Björklund et al., 2006).

Other efforts in screening for regulators of cell cycle progression have concentrated on specific stages of the cell cycle. In one study, factors involved in the formation, maintenance and resolution of the *Drosophila* cytokinetic bridge were identified using an RNAi library targeting 7216 conserved genes. This

meant that the phenotypic analyses were less complex and more focussed than the previous studies described above, where a myriad of parameters were used to track a number of types of phenotypes, as many aspects of the cell cycle were investigated (Echard, Hickson, Foley, & O'Farrell, 2004). Eggert et al. combined genome-wide RNAi screening with that of a library of 51,000 small molecules, which included a mixture of commercial “drug-like” molecules, natural products and natural product-like libraries to look specifically for genes involved in *Drosophila* cytokinesis and small molecules which specifically inhibited them with tight temporal control (Eggert et al., 2004). This time, analyses were automated thus reducing the effort required for phenotypic analyses. Also, by performing such chemical genetic and genome-wide RNA interference screens in parallel, a richer dataset was obtained which allowed a systematic dissection of cytokinesis pathways aided by known small molecule inhibitors of them. 214 genes were found to be important for cytokinesis of which 25 had never been characterised before.

Automation, again, enabled phenotyping whilst conducting another genome-wide siRNA screen in humans (Mukherji et al., 2006). 24,373 predicted human genes and 500 “druggable” genes (predominantly enzymes and receptors) were targeted in the well-studied osteosarcoma U2OS cells. High-content automated single-cell fluorescence microscopy was used to acquire images of the complete surface of wells in which the cells were cultured, which were then segmented to define DAPI-stained nuclei. Fluorescence intensities, area, and the perimeter-to-area ratio (PAR), a geometric measure of nuclear shape, were calculated for all nuclei and eight descriptors were computed for each sample. 4.7 % genes (1,152 genes) of the genome were found to alter cell cycle progression, 57 of which had never been identified before. Another human genome-wide siRNA screen employed HeLa cells and a novel strategy for generating the siRNA library (Kittler et al., 2007). This time, endoribonuclease-prepared siRNAs (esiRNAs) were used. By enzymatically processing long dsRNAs, a heterogeneous pool of siRNAs was generated, which are purported to be more effective in knocking down mRNAs than single long dsRNAs (Buchholz, Kittler, Slabicki, & Theis, 2006). 17,828 genes were targeted and hundreds of genes were identified, which when knocked down, caused cell cycle arrest and/or cell division defects. High-throughput DNA content analysis was employed to initially detect cell cycle

arrest and altered ploidy phenotypes and hits were further analysed by fluorescence imaging, flow cytometry and time-lapse video microscopy. However, there was only 10 % overlap with the genes that were identified in the similar study done previously (Mukherji et al., 2006) highlighting the problem of the lack of reproducibility which has undermined the reliability of such screens. Here, esiRNAs were thought to reduce off-target effects 12-fold compared with chemically synthesised RNA suggesting that the data obtained by Mukherji et. al is marred by false-positives and false negatives. This poor overlap could also be due to poor comparability in the end-point analyses used. Problems with reproducibility also seemed to be the case for another genome-wide RNAi screen done in HeLa cells where mitotic phenotypes were exclusively searched for in order to identify candidate genes involved in key mitotic processes such as restructuring and segregation of mitotic chromosomes that were yet to be discovered (Neumann et al., 2010). Here, ~21,000 genes were targeted by multiple siRNAs in cells with fluorescently labelled chromosomes. A large dataset of ~190,000 time-lapse movies was generated, which was then subjected to computational image processing to quantify about 200 parameters in nuclear morphology and, subsequently, to classify phenotypes into 16 morphological classes thereby identifying 1,249 genes as potential mitotic hits. However, overlap of validated hits with other screens ranged from just 6-36 % which was attributed to poor comparability. This required following up the initial screen with a huge amount of further screens and analyses to eliminate false positives and negatives leaving only 572 genes that were confidently validated as mitotic genes.

Similar problems with false positives were also reported in the genome-wide RNAi screen performed in *S2 Drosophila* cells (Björklund et al., 2006) which initiated a much needed comparison study to investigate the reasons behind these problems (Guest et al., 2011). Here, results from the two screens done in *Drosophila* (Bettencourt-Dias et al., 2004; Björklund et al., 2006) were compared and only 24 genes were identified in both screens. An independent RNAi screen was then conducted targeting genes which were identified as potential cell cycle regulators with the aid of a virtual protein interaction network. The results confirmed many of the original phenotypes but also revealed many likely false positives and false negatives from the previous two screens making the case for

the use of such additional datasets in confirming true hits in the future. Another study made the case for supplementing screens with bioinformatics-based methods to help reduce off-target effects (Sigoillot et al., 2012).

Creative use of such genome-wide RNAi libraries has also been used to deliver answers regarding pathways regulating specific stages of the cell cycle (or any other cellular process of interest) such as centriole duplication and mitotic pericentriolar material recruitment (Dobbelaere et al., 2008), alternative splicing of mRNAs (Q. Wang & Silver, 2010), the DNA damage response network (Kondo & Perrimon, 2011), cell proliferation over time (Zhang et al., 2011) or promotion of developmentally programmed cell cycle quiescence (Roy et al., 2014). Altogether, these screens have hugely contributed towards the current understanding of cell cycle regulation. The power of high-throughput screens lies in the fact that many novel genes were assigned functions. This provides starting points by which, the current understanding of the complex interacting network, required for successfully promoting cell cycle progression, can be further enriched.

5.3 RNA interference in *T. brucei*

Around the same time when RNAi was discovered in *C. elegans* (Fire et al., 1998), Ngô and colleagues serendipitously discovered a similar phenomenon in *T. brucei*. *In vivo* expression of dsRNA of the α -tubulin mRNA 5' untranslated region led to rapid degradation of α -tubulin mRNA preventing the cells from undergoing cytokinesis (Ngô, Tschudi, Gull, & Ullu, 1998). *T. brucei*, *T. congolense* and *Leishmania braziliensis* are kinetoplastids for which functional RNAi pathways have been described so far (Kolev, Tschudi, & Ullu, 2011). With the publication of its genome (Berriman et al., 2005) and its amenability to genetic manipulation such as RNAi, *T. brucei* has taken centre stage in developing our understanding of kinetoplastid biology.

T. brucei features two DICER-like proteins (TbDCL1 and TbDCL2; Patrick et al., 2009; Huafang Shi, Tschudi, & Ullu, 2006), one AGO homologue (TbAGO1; Durand-Dubief & Bastin, 2003; Huafang Shi, Djikeng, Tschudi, & Ullu, 2004) and two RNAi interference factors (TbRIF4 and TbRIF5; Barnes, Shi, Kolev, Tschudi, &

Ullu, 2012). TbDCL1 is cytoplasmic (Huafang Shi et al., 2006) whilst TbDCL2 is nuclear (Patrick et al., 2009). Both proteins feature RNase III motifs, bind dsRNAs and contribute towards the generation of siRNAs; the latest model implicates TbDCL2 in fuelling the *T. brucei* nuclear RNAi pathway and TbDCL1 in patrolling the cytoplasm looking to silence harmful retrotransposons and repeats (Patrick et al., 2009). TbRIF4 is a 3'-5' exonuclease and is critical for the conversion of ds siRNAs to the ss form required for the generation of the *T. brucei* equivalent of the RISC complex. TbRIF5 is essential for cytoplasmic RNAi and acts as a TbDCL1 cofactor (Barnes et al., 2012). These RNAi components orchestrate *T. brucei* RNAi pathways in a canonical fashion. However, unlike in higher eukaryotes, *T. brucei* does not appear to possess an RNA-dependent RNA polymerase (RdRp) known to increase the impact of dsRNA gene silencing by amplifying dsRNAs (Kolev et al., 2011). This means that the RNAi effect of introduced dsRNA is transient and only lasts for one cell cycle (Ngô et al., 1998). To circumvent this, stable continuous expression of dsRNA was required which greatly influenced the ongoing development of a number of tetracycline-inducible expression systems in this parasite.

5.3.1 Development of inducible RNAi systems in *T. brucei*

The development of robust, tightly regulated, inducible transgene expression systems have been vital in developing RNAi systems for high-throughput screens in *T. brucei* as they were subsequently adapted to stably express dsRNA fragments for RNAi induction. The first generation systems developed for regulated transgene expression exploited the “strong” Pol1 promoter, *EP1* procyclin promoter, which was modified to include TetO sites (L. E. Wirtz & Clayton, 1995). This allowed the control of expression from these constructs when introduced into cells that constitutively expressed the TetR. However, the use of the *EP1* procyclin promoter limited the efficacy of these constructs in BSF parasites (Biebinger et al., 1996; Biebinger, Wirtz, Lorenz, & Clayton, 1997). These constructs faced further challenges, with reports of low expression of regulatory factors leading to high background expression of cassettes, which has since been attributed to the tandem arrangement of the dual promoters (one of them being the inducible *EP1* procyclin promoter driving expression of the gene of interest and the second promoter being a constitutive promoter, such as *VSG*

promoter or *rRNA* promoter, driving the expression of the selective marker; L. E. Wirtz, Leal, Ochatt, & Cross, 1999). Subsequent efforts to get round these problems led to the exploitation of the T7 phage polymerase system which has since been widely used in BSF & PCF parasites (E. Wirtz, Hoek, & Cross, 1998; L. E. Wirtz et al., 1999), where the constitutive expression of the TetR and the resistance marker were driven by T7 promoters and depended on their introduction into a T7 RNA polymerase background. Based on these constructs, RNAi systems were developed which either depended on the generation of stem-loop fragments or opposing promoter fragments (LaCount, Bruse, Hill, & Donelson, 2000; H. Shi et al., 2000; Z. Wang, Morris, Drew, & Englund, 2000). Stem loop systems were found to produce more rapid and efficient mRNA knockdown (Durand-Dubief, Kohl, & Bastin, 2003) compared to the opposing promoter system. These constructs are still widely used today and continue to remain important tools for *T. brucei* functional genomics. However, challenges in achieving high transfection efficiency and reducing inter-clonal variability remained, therefore, limiting the success of employing the RNAi systems described above to interrogate the *T. brucei* genome in larger-scale studies.

The variability between clones in the expression of transgenes has been largely blamed on the use of the rRNA spacers as loci for chromosomal integration. The intergenic regions of the rRNA loci are transcriptionally silent and, therefore, allow stable integration of regulated cassettes. However, *T. brucei* possesses nine rRNA spacers in a haploid genome (Berriman et al., 2005) with differing capacities for expression (Alsford, Kawahara, Glover, & Horn, 2005). To eliminate these positional effects, using cells with an improved TetR background (using the double-TetR system containing two TetR genes; Alibu, Storm, Haile, Clayton, & Horn, 2005), the rRNA spacers were screened for strong repression of regulated reporter cassettes with high inducible expression levels (Alsford et al., 2005). A desirable rRNA locus was thus selected and the reporter cassette was exchanged for an incomplete *HYG*-resistance marker cassette (now referred to as 2T1 cells). This would allow selection of cells that could stably integrate cassettes which possess an over-lapping and complementary *HYG* selectable marker/targeting fragment. Whilst achieving reliable, non-leaky, robust expression of transgenes, this strategy also resolved the problem of reported T7 RNA polymerase toxicity (Alsford et al., 2005) by returning to the use of

expression vectors driven by endogenous promoters such as the *EP1* procyclin promoter and the *rRNA* promoter. This provided the basis for a very reliable system for the generation of RNAi cell lines (Alsford & Horn, 2008; Alsford et al., 2005). A number of expression plasmids were then generated (Alsford & Horn, 2008) and the resulting pRPA^{ISL} stem loop RNAi constructs were used to generate the RNAi library employed in the study described in this chapter (Jones et al., 2014).

5.3.2 RNAi based screens in *T. brucei*

The success of implementing RNAi in *T. brucei* has led to a number of medium- to high-throughput systematic studies interrogating gene cohorts and even the whole genome to develop the current understanding of a variety of trypanosome cellular processes and pathways. A group of these studies utilised a gene-by-gene targeting approach with relative success. The first study (albeit not the first RNAi screen in *T. brucei*) of this kind saw a large collaborative effort where 210 predicted ORFs, mainly from chromosome 1, were individually knocked-down using constructs based on the p2T7 opposing promoter RNAi system (modified to allow direct cloning of PCR fragments; Alibu et al., 2005), in BSF parasites, and the resultant cell growth, viability, and/or cell cycle progression phenotypes were assessed (Subramaniam et al., 2006). A large proportion (45 genes; 23 %) of the investigated genes was found to be required for BSF *T. brucei* proliferation whilst 31 (16 %) of the genes were found to be required for normal cell cycle progression. A significant number of essential genes was conserved only amongst kinetoplastids which demonstrates the divergence of kinetoplastid biology compared to other model eukaryotic organisms and the huge potential to identify kinetoplastid-specific drug targets. Other gene-by-gene large scale RNAi screens include a study which focussed on proteins featuring the RNA Recognition Motif (RRM), where 25 genes (17 in BSF and seven in PCF) were found to be required for cell proliferation (Wurst et al., 2009) and another which sought to analyse a set of 31 PKs considered to be least studied (Mackey, Koupparis, Nishino, & McKerrow, 2011). Here, RNAi of five PKs were found to generate growth defects; CRK12, CRK8, CRK1, a CMGC/DYRK Tb927.7.4090 and the CMGC/MAPK, Tb927.10.5140 (called ERK8 in this publication; Mackey,

Koupparis, Nishino, & McKerrow, 2011), two of which, CRK12 and ERK8, were deemed essential for BSF cell proliferation.

The first study integrating RNAi in *T. brucei* (and in any other organism!) with a forward genetic approach on a global scale was in 2002 by the Englund lab in PCF parasites (Morris, Wang, Drew, & Englund, 2002). This was also the first time a high-throughput RNAi screen was ever carried out in *T. brucei*. Here, genomic DNA, sheared to an average size of 660 bp was cloned into the modified pZJM vector (opposing promoter system to generate dsRNA; Wang et al., 2000). This library of RNAi constructs was then transfected into PCF cells multiple times to ensure 5 X coverage of the RNAi library. Pools of cells were then screened for ConA binding to isolate genes responsible for EP procyclin expression, GPI biosynthesis, *N*-glycan biosynthesis or cell death. It was hypothesised that silencing such genes would cause the cells to become ConA resistant. Cells which did not bind ConA were then cloned out and target genes were identified via sequencing. A glycolytic enzyme, hexokinase, was thus identified, which upon further investigation was found to alter procyclin expression. RNAi of hexokinase was found to switch procyclin expression from glycosylated EP procyclins to unglycosylated GPEET procyclin expression. Modulation of procyclin expression was found to be linked to environmental glucose levels. The Englund lab pZJM library proved to be an important tool in conducting a number of such forward genetic screens in PCF cells. It was used to identify factors involved in maintaining the mitochondrial membrane potential by enriching pools of the RNAi library for cells featuring a decrease or disruption of mitochondrial membrane potential following RNAi induction (Verner, Paris, & Lukes, 2010). It was also used to understand the pathways responsible for the toxic activity of drugs of interest; e.g. tubercidin. In this study, pools of the RNAi cell line library were subjected to tubercidin treatment which led to the identification of a hexose transporter important for tubercidin susceptibility (Drew et al., 2003). Further analyses implicated the glycolytic pathway as the target of tubercidin in PCF cells (Drew et al., 2003).

Understanding drug mode of action is a subject of huge interest for the purposes of drug development. Another study saw the development of a brand new RNAi library of plasmids where the BSF stage-appropriate expression system was used to identify genes required for melarsoprol and eflornithine sensitivity which led

to the verification of the amino acid transporter 6 (AAT6) as an important player of eflornithine toxicity (Schumann Burkard, Jutzi, & Roditi, 2011). Such protocols which involve pools of cell lines that are subjected to a selection pressure and then cloned, vastly reduce the amount of work required to identify individual hits. However, examining RNAi effects in pools would not be appropriate for investigating other aspects of trypanosome biology where the relevant genes are essential for viability (as these clones would simply disappear from the pool) or the end-point analysis requires visual/microscopic phenotyping such as changes in cellular/organelle morphology or changes in localisation of proteins of interest. In such cases either the RNAi library of cell lines was cloned out and then subjected to screening or a gene-by-gene targeting approach was employed.

In one study conducted to identify genes required for kinetoplast integrity and maintenance, 1400 PCF cell lines were cloned out from the global pZJM library of pooled cell lines. They were then screened for kDNA size reduction/loss which led to the identification of p166, a molecular component of the TAC, as an important factor required for kDNA segregation (Zhao, Lindsay, Roy Chowdhury, Robinson, & Englund, 2008). In another study, a large scale screen of the Englund library was carried out to identify regulators of the PCF cell cycle (Monnerat, Clucas, Brown, Mottram, & Hammarton, 2009). Here, 200+ individual clones were selected via limiting dilution following transfection of PCF *T. brucei* cells with the Englund library of RNAi plasmids. DNA sequence analysis of clones excluded those that contained sequences of no interest (and those for which sequencing failed), following which only 76 clones were individually analysed to determine those which displayed a growth defect following RNAi induction. 16 cell lines were found to display growth defects following induction. Further analyses of these cell lines to identify genes required for PCF *T. brucei* cell cycle did not unambiguously yield novel cell cycle regulators. The fact that none of the CRKs or cyclins were identified and that the coverage of the screen was <1 % of protein-coding genes, undermined the robustness of the library. The outcomes of this study also magnified the limitations of the RNAi technology used, e.g., the relatively low transfection efficiency, and demonstrated the urgent need for effective high-throughput methods for the phenotypic analyses of such genome-wide libraries.

A solution to counter low transfection efficiency was found when the introduction of double strand breaks into the integration site of transfected plasmids (such as the rRNA spacer) was found to improve transfection efficiency (Glover & Horn, 2009). Capitalising on these findings, the Englund genome-wide RNAi library was transfected into BSF cells, that had been induced to feature a double strand break at the rRNA spacer of choice (selected to ensure high expression levels of transgenes with tight regulation of their expression as described in section 5.3.1) using the I-SceI meganuclease system (Baker, Alsford, & Horn, 2011). Transformation efficiency was found to have been increased by 250-fold. The resultant cell line library was then used to elucidate the pathways for nifurtimox and eflornithine toxicity in BSF cells by culturing pools in which RNAi had been induced in the presence or absence of the drugs. Genomic DNA was extracted from resistant populations and the RNAi fragments were recovered allowing the identification of target genes via next-generation sequencing. In agreement with previous studies, nitroreductase and AAT6 were found to be responsible for sensitivity to nifurtimox/benznidazole and eflornithine, respectively, thus validating this approach. This approach of identifying target genes heralded the paradigm shift in how RNAi libraries could be analysed. By integrating next-generation sequencing, a versatile new tool for genome-scale functional analysis had now been developed which was successfully employed to reveal global knockdown profiles with respect to trypanosome growth and development, thus linking thousands of previously uncharacterized and “hypothetical” genes to essential functions (Alsford et al., 2011). This new high-throughput phenotyping approach, termed RNAi target sequencing (RIT-seq) has already been successfully adapted to elucidate genes targeted by specific compounds such as CpdA (Gould et al., 2013) and current drugs used to treat HAT and AAT (Alsford et al., 2011) or pathways involved in differentiation induced by a cAMP analogue (Mony et al., 2014), and is a powerful new tool which should help advance current understanding of trypanosome biology.

5.4 *T. brucei* kinome-wide RNAi library

The kinome-wide RNAi library of individual *T. brucei* BSF cell lines is another tool that has newly been made available as a resource to perform large scale

functional analyses of specific gene families (Jones et al., 2014). The advantage here lies in the availability of individual cell lines which target specific PKs of interest to understand the roles they play in *T. brucei* biology. By capitalising on technologies available, such as the tagged-locus approach to ensure high expression levels and tight regulation (section 5.3.1; Alsford & Horn, 2008), to overcome the problems of low transformation efficiency and leaky expression faced by earlier attempts, a library of independent cell lines which successfully target the whole trypanosome kinome with robust, repeatable results was generated.

To set up the library, briefly, as a first step, a high-throughput system was established for the generation of the library of RNAi plasmids which individually target *T. brucei* PKs in a tetracycline inducible manner. To do this, the stem-loop RNAi vector which integrates at a single, tagged rRNA locus of a modified cell line (termed 2T1; Alsford & Horn, 2008), pRPa^{ISL}, was modified to allow integration of amplified gene fragments in a single recombinase reaction (Jones et al., 2014). RNAi constructs were made to target 190 PKs, each of which were individually transfected into BSF 2T1 parasites, following which two independent clones were recovered for analysis. Essential kinases were identified by employing a 72 hour cell viability Alamar Blue assay to assess loss of fitness of each induced cell line relative to their uninduced counterparts. In this study, cell lines which exhibited a loss of fitness following RNAi induction were then selected for further analysis to detect proliferation and cell cycle defects via growth curve generation and nuclear/kinetoplast configuration of DAPI-stained cells, respectively.

The loss of fitness phenotypes detected in this kinome-wide RNAi library were found to have excellent correlation with previous candidate-based gene studies (Jones et al., 2014). However, there was one notable discrepancy with published literature - PLK. The two clones thought to knockdown *PLK* mRNA in this library unexpectedly did not generate any loss of fitness phenotype. However, additional qPCR analysis demonstrated that there was no reduction in *PLK* mRNA upon RNAi induction (Jones et al., 2014), explaining the discrepancy. qPCR of another kinase, MKK1, known to be redundant in BSF parasites, also indicated inefficient knockdown (Jones et al., 2014), although this kinase is known to be non-essential (Jensen, Kifer, & Parsons, 2011). These instances do raise the

possibility of other false negative results, arising from inefficient mRNA knockdown, being present within the library analysis. Correlation with the genome-wide RITseq data (Baker et al., 2011) was also found to be good; however, 25 PKs that were 'hits' in this screen were not detected by Alsford and colleagues raising the possibility of off-target effects (Jones et al., 2014) or false negatives in the Alsford study. This could be explained by differences in the RNAi constructs used and the phenotypic analyses performed, but further validation of the library would be desirable.

The high correlation of phenotypes generated with published literature provided confidence in the effectiveness of this kinome-wide library and, subsequently, presented an excellent opportunity to interrogate the *T. brucei* kinome for the role it plays in regulating the *T. brucei* cell cycle. A popular method used to determine the cell cycle profile of a *T. brucei* cell line is microscopic determination of nuclear and kinetoplast configurations following DNA staining of cells using DAPI. Since, the nucleus and kinetoplast undergo discrete replication cycles in *T. brucei*, where the kinetoplast undergoes replication and segregation slightly ahead of the nucleus, the number of nuclei and kinetoplasts present in a cell can be used to determine its current cell cycle stage. A cell in G₁ phase would have 1 nucleus and 1 kinetoplast (1N1K cell) whilst a cell in G₂/M phase will have 1 nucleus and 2 kinetoplasts (1N2K) (Figure 5-2). A cell that has undergone mitosis but has not yet undergone cytokinesis will have 2 nuclei and 2 kinetoplasts (2N2K) (Figure 5-2). Any other NK configuration would be deemed aberrant and depending on how these cells deviate from normal configurations, the type of cell cycle defect can often be determined i.e., mitotic, defects in kinetoplast replication/segregation or cytokinetic. In the absence of automatic image processing, such phenotyping would be too onerous to be feasible for genome-wide high-throughput studies. However, focussing on screening kinases deemed essential/required for BSF cell proliferation, such an approach becomes possible. An automated microscopic system for conducting cell cycle analysis would have been useful, and a recently published study does seem to have successfully established such a system in *T. brucei* (Wheeler, Gull, & Gluenz, 2012). However, at the time when this project commenced, no such approach was available.

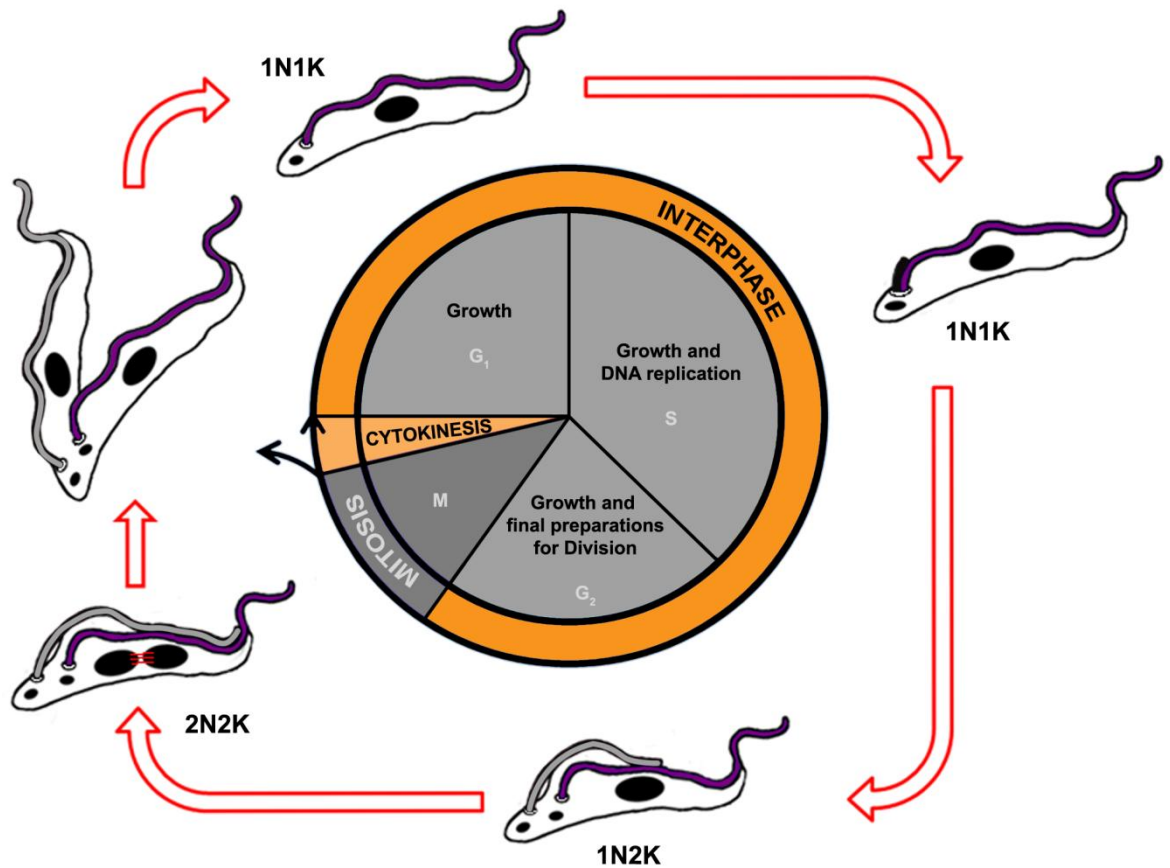


Figure 5-2 Schematic illustrating the cell division cycle of *T. brucei*. A cell in G₁ phase would have 1 nucleus and 1 kinetoplast (1N1K cell). A cell in G₂/M phase will have 1 nucleus and 2 kinetoplasts (1N2K). A cell that has undergone mitosis but has not yet undergone cytokinesis will have 2 nuclei and 2 kinetoplasts (2N2K). Adapted from Jones et al., 2014.

5.5 Project aim

The aim of this project was to utilise the kinome-wide RNAi library to identify regulators of the *T. brucei* cell cycle. Since cell cycle defects invariably affect the ability of cells to proliferate, cell lines which exhibited loss of fitness following RNAi induction were focussed on. Due to the divergent nature of the *T. brucei* cell cycle and its regulation, it was anticipated that regulators that had never been linked to the cell cycle in other organisms would be identified.

5.6 Results

5.6.1 Screening of RNAi cell lines for PKs involved in the *T. brucei* cell cycle

Following the determination of cell viability following RNAi induction via the Alamar Blue assay (performed by Nathaniel Jones, WTCMP), 50 cell lines showed loss of fitness phenotypes (>10 % reduction in Alamar Blue value in comparison with uninduced control values, i.e. Alamar Blue ratios of <0.90; Jones et al., 2014) and were selected for further analyses. These cell lines were individually cultured in flasks and RNAi was induced via the addition of tetracycline. Cumulative growth curves were obtained which were then used to determine optimal time-points for performing DAPI staining and flow cytometry analyses. This was to ensure that the cell cycle profiles were obtained just before, during and just after the appearance of the growth defect. During the early stages of this screen, generation of growth curves and microscopic slides for DAPI analysis were done in partnership with Manuel Saldivia (CSIC, Granada).

Based on just the growth phenotypes displayed following RNAi induction, the cell lines could be classified as showing no growth defect (Table 5-1A), slow growth (Table 5-1B), growth arrest (Table 5-1C) or cell death (Table 5-1D), with a strong correlation between Alamar Blue ratios and the growth phenotypes determined by growth curve (where lower Alamar blue ratios indicate stronger growth defects; Figures 5-3 to 5-12). This provided confidence in the Alamar Blue methodology that was used to identify PKs that are essential for BSF *T. brucei* growth (Jones et al., 2014).

(A) No growth defect						
Kinase family	Kinase name	Gene ID	Clone 1		Clone 2	
			S/R	AB ratio	S/R	AB ratio
CAMK	LDK	Tb927.11.8940	S	0.81	S	0.78
CAMK/CAMKL		Tb927.8.870	S	0.87	S	0.87
CK1/CK1	CK1	Tb927.3.1630	S	0.87	S	1.02
CMGC/DYRK		Tb927.10.9600	R	0.85	R	0.81
Other/NEK	NEK16	Tb927.10.14420	S	0.88	S	0.86

STE/STE11		Tb927.8.1100	S	0.84	S	0.83
pseudo Other/ULK		Tb927.11.8150	R	0.83	R	0.77
aPK-ABC1		Tb927.10.9900	R	0.70	S	0.88

(B) Slow growth						
Kinase family	Kinase name	Gene ID	Clone 1		Clone 2	
			S/R	AB ratio	S/R	AB ratio
AGC	PDK1	Tb927.9.4910	S	0.80	S	ND
AGC/NDR	PK53	Tb927.7.5770	S	0.84	S	1.00
AGC/PKA*	PKAC1	Tb927.9.11100	S	0.53	S	0.50
	PKAC2	Tb927.9.11030				
CAMK		Tb927.7.2750	S	0.83	S	0.75
CMGC		Tb927.11.5340		0.30		0.37
CMGC/CDK	CRK1	Tb927.10.1070	R	0.81	R	0.76
CMGC/CDK	CRK2	Tb927.7.7360	R	0.47	S	0.29
CMGC/CDK	CRK6	Tb927.11.1180	S	0.76	S	0.76
CMGC/MAPK	KFR1	Tb927.10.7780	R	0.42	S	0.55
Other/AUR	AUK3	Tb927.9.1670	S	0.35	R	0.46
Other/CAMKK		Tb927.10.15300	R	0.79	R	0.77
Other/WEE	WEE1	Tb927.4.3420	S	0.68	R	0.54
Pseudo-Orphan		Tb927.7.3210	S	0.89	R	0.75
aPK-PIKK/FRAP	TOR1	Tb927.10.8420	S	0.56	S	0.62
aPK-PIKK/FRAP	TOR4	Tb927.1.1930	S	0.71	S	0.92

(C) Growth arrest						
Kinase family	Kinase name	Gene ID	Clone 1		Clone 2	
			S/R	AB ratio	S/R	AB ratio
AGC/NDR	PK50	Tb927.10.4940	S	0.21	S	0.86
CAMK		Tb927.7.6220	S	0.77	S	0.84
CMGC/GSK	GSK3-short	Tb927.10.13780	S	0.46	R	0.61
CMGC/SRPK		Tb927.6.4970	S	0.68	R	0.78
Orphan	PK6	Tb927.9.10920	S	0.24	S	0.23
Other/CK2	CK2A1	Tb927.9.14430	S	0.63	S	0.65
Other/ULK		Tb927.11.4470	S	0.70	R	0.87
STE/STE11		Tb927.11.2040	S	0.20	R	0.20
STE/STE20	SLK1	Tb927.8.5730	R	0.46	S	0.21
STE/STE20	SLK2	Tb927.9.12880	R	0.32	R	0.78
pseudo Other/NAK		Tb927.9.6560	S	0.57	S	0.71
aPK-PIKK/ATR	ATR	Tb927.11.14680	S	0.43	S	0.82

aPK-RIO	RIO1	Tb927.3.5400	S	0.84	S	0.98
aPK-RIO	RIO2	Tb927.6.2840	R	0.72	R	0.70

(D) Cell death						
Kinase family	Kinase name	Gene ID	Clone 1		Clone 2	
			S/R	AB ratio	S/R	AB ratio
AGC		Tb927.3.2440	S	0.69	S	0.62
CK1/CK1*	CK1.1	Tb927.5.790	S	0.16	S	0.16
	CK1.2	Tb927.5.800				
CMGC/CDK	CRK3	Tb927.10.4990	S	0.32	S	0.27
CMGC/CDK	CRK9	Tb927.2.4510	S	0.17	S	0.18
CMGC/CDK	CRK12	Tb927.11.12310	S	0.20	S	0.20
CMGC/CLK	CLK1	Tb927.11.12410	S	0.21	S	0.26
CMGC/CLK	CLK2	Tb927.11.12420	R	0.18	S	0.19
CMGC/MAPK		Tb927.10.5140	S	0.21	S	0.22
CMGC/RCK		Tb927.3.690	R	0.23	R	0.18
Other/AUR	AUK1	Tb927.11.8220	S	0.19	R	0.19
NEK*	NEK12.1	Tb927.8.7110	S	0.19	S	ND
	NEK12.2 (RDK2)	Tb927.4.5310				
Other/TLK*	TLK1	Tb927.4.5180	S	0.21	R	0.22
	TLK2	Tb927.8.7220				
STE		Tb927.10.2040	S	0.32	S	0.26

Table 5-1 Summary of the characteristics of investigated RNAi cell lines. For each kinase knocked down, the puromycin sensitivity profile (S - sensitive; R - resistant) and Alamar Blue ratio (AB ratio) of each independent clone studied are shown. Cell proliferation analysis data for Clone 1 of each of the above cell lines are described in this chapter. The growth phenotypes displayed by these cell lines are the criteria by which they have been classified in this table - no growth defect (A), slow growth (B), growth arrest (C) or cell death (D). Asterisk denotes double knockdown cell lines.

Due to high levels of nucleotide sequence identity shared by some arrayed or paralogous PKs, some RNAi constructs were predicted to target more than one PK. For most of the cell lines this was already known upfront, such as PKAC1 & PKAC2, CK1.1 & CK1.2, NEK12.1 & NEK12.2, and TLK1 & TLK2, and the strategy was to generate individual RNAi cell lines if further characterisation was deemed to be of interest. As NEK12.1 and NEK12.2 had never been characterised before, and because they did generate growth defects upon RNAi induction (Figure 5-3B, bottom panels), efforts were made to individually target the two kinases (NEK12.1 and NEK12.2 RNAi cell lines were generated by Nathaniel Jones,

WTCMP; Jones et al., 2014). Two other cell lines that were assumed to knockdown CLK1 and CLK2 individually were found, following analyses of the RNAi constructs, to be double knockdown cell lines instead. The RNAi construct supposed to target CLK1 targeted CLK2 too and vice versa (see Figure 5-3B, top panels for the growth and cell cycle defects generated by one of the original double knockdown cell lines). This was because the two RNAi constructs were found to target different parts of the identical C-terminal kinase domains of CLK1 and CLK2 (Figure 5-3A). In order to address this, new RNAi constructs were made (see Jones et al., 2014 for details), this time targeting the non-identical N-terminal regions of CLK1 and CLK2, and the resulting cell lines were analysed for growth and cell cycle defects. CLK1 (not CLK2; as described later on) and NEK12.2 (not NEK12.1; as described later on) were found to be solely responsible for the growth and/or cell cycle defects demonstrated by the original double-RNAi cell lines (Figure 5-3B), the results of which (except from the NEK12.1 RNAi cell line) have been incorporated in the descriptions later on. In addition to these, the analyses of RDK1 and TOR2 RNAi cell lines, neither of which demonstrated loss of fitness upon RNAi induction in the initial Alamar Blue screen, have also been incorporated.

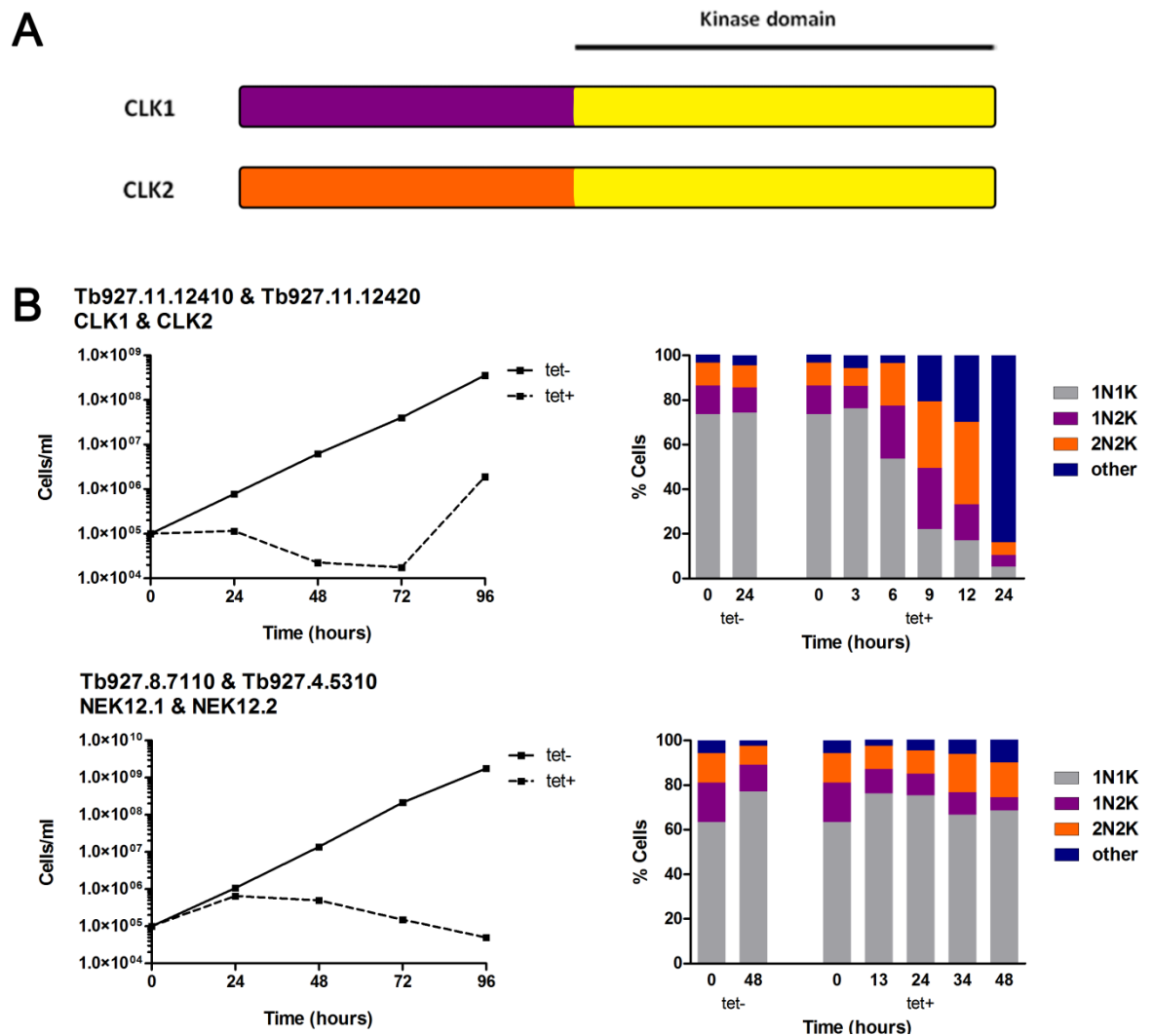


Figure 5-3 *In vitro* growth and cell cycle analysis of RNAi cell lines simultaneously knocking down two protein kinases. A: Schematic illustrating domain structure of CLK1 and CLK2 demonstrating that, sequentially, their N-termini are different whilst their C-terminal kinase domains are identical B: Cell proliferation and cell cycle phenotypes of CLK1/CLK2 (top panels) and NEK12.1/NEK12.2 (bottom panels) double knockdown cell lines. Cumulative growth curves were generated (left) and the numbers of nuclei (N) and kinetoplasts (K) in each cell ($n \geq 200$) following DAPI staining of samples were recorded at the indicated time points post addition of tetracycline to the induced samples (right). Analyses of non-induced cells (tet-) are also shown as controls.

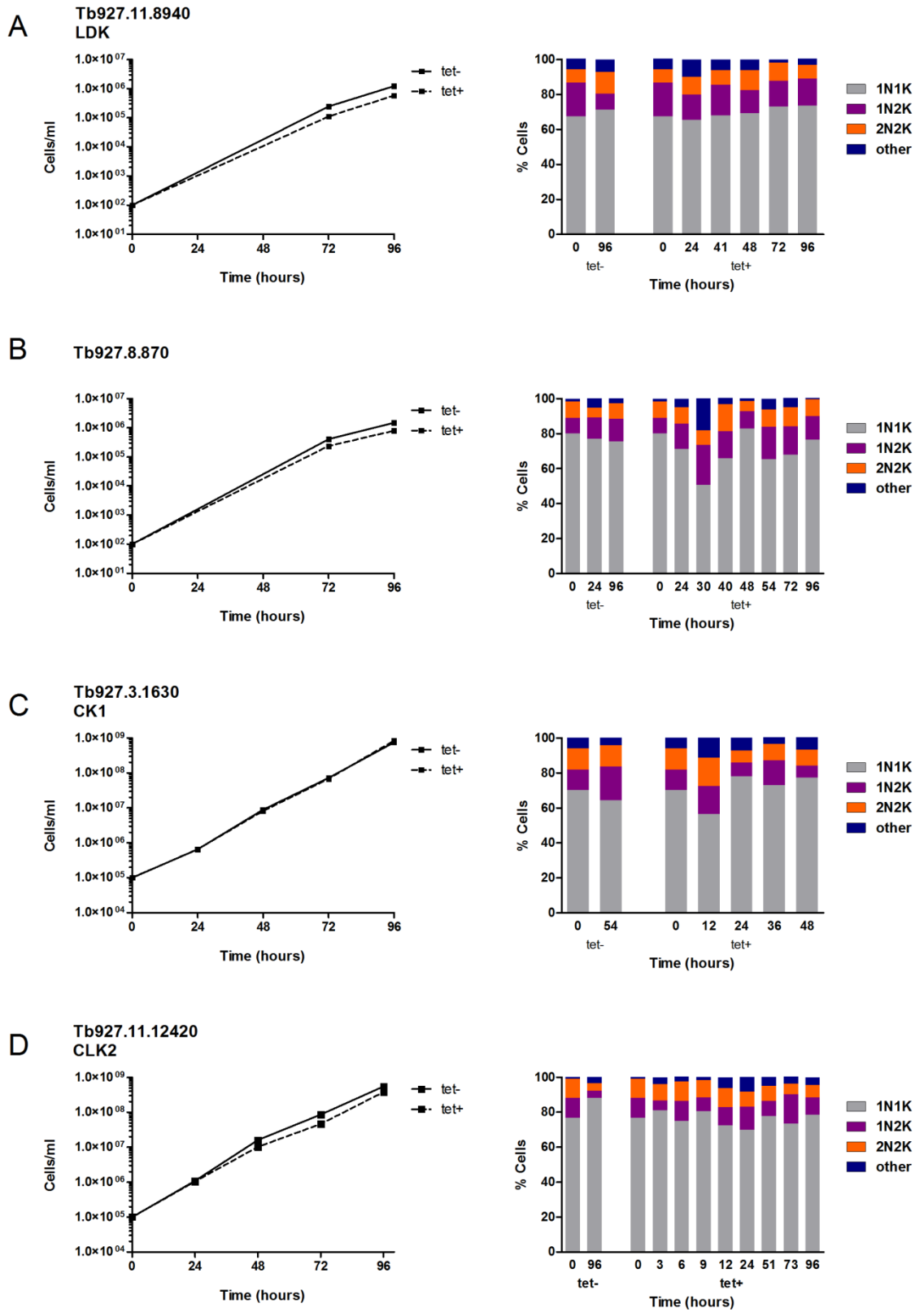
Once all these additional cell lines are taken into account, the growth and cell cycle analyses of the final cohort of 52 different cell lines representing 55 different kinases are described below. According to the proliferation and cell cycle phenotypes demonstrated following RNAi induction, these cell lines were classified as follows:

- No growth defects and no cell cycle defects - section 5.6.1.1

- Growth defects but no notable cell cycle defects - section 5.6.1.2
- G₁/S defects - section 5.6.1.3
- Mitosis defects - section 5.6.1.4
- Cytokinesis defects - section 5.6.1.5
- Kinetoplast duplication defects - section 5.6.1.6
- Mitosis and cytokinesis defects - section 5.6.1.7
- Kinetoplast duplication and cytokinesis defects - section 5.6.1.8
- Unclassified - section 5.6.1.9

5.6.1.1 Cell lines showing no growth defects and no cell cycle defects following RNAi induction

Nine cell lines (LDK (Figure 5-4A), Tb927.8.870 (Figure 5-4B), CK1 (Figure 5-4C), CLK2 (Figure 5-4D), Tb927.10.9600 (Figure 5-4E), NEK16 (Figure 5-4F), Tb927.8.1100 (Figure 5-4G), Tb927.11.8150 (Figure 5-4H) and Tb927.10.9900 (Figure 5-4I) displayed no growth or cell cycle defects following RNAi induction, which includes the 8 cell lines described in section A of Table 5-1 (no growth defect) and the newly generated CLK2 RNAi cell line as described earlier. This point towards the strong correlation which exist between aberrant cell cycle and growth defects, thus, demonstrating the appropriateness of choosing to limit the cell cycle screen to kinases that are required for the proliferation of BSF parasites.



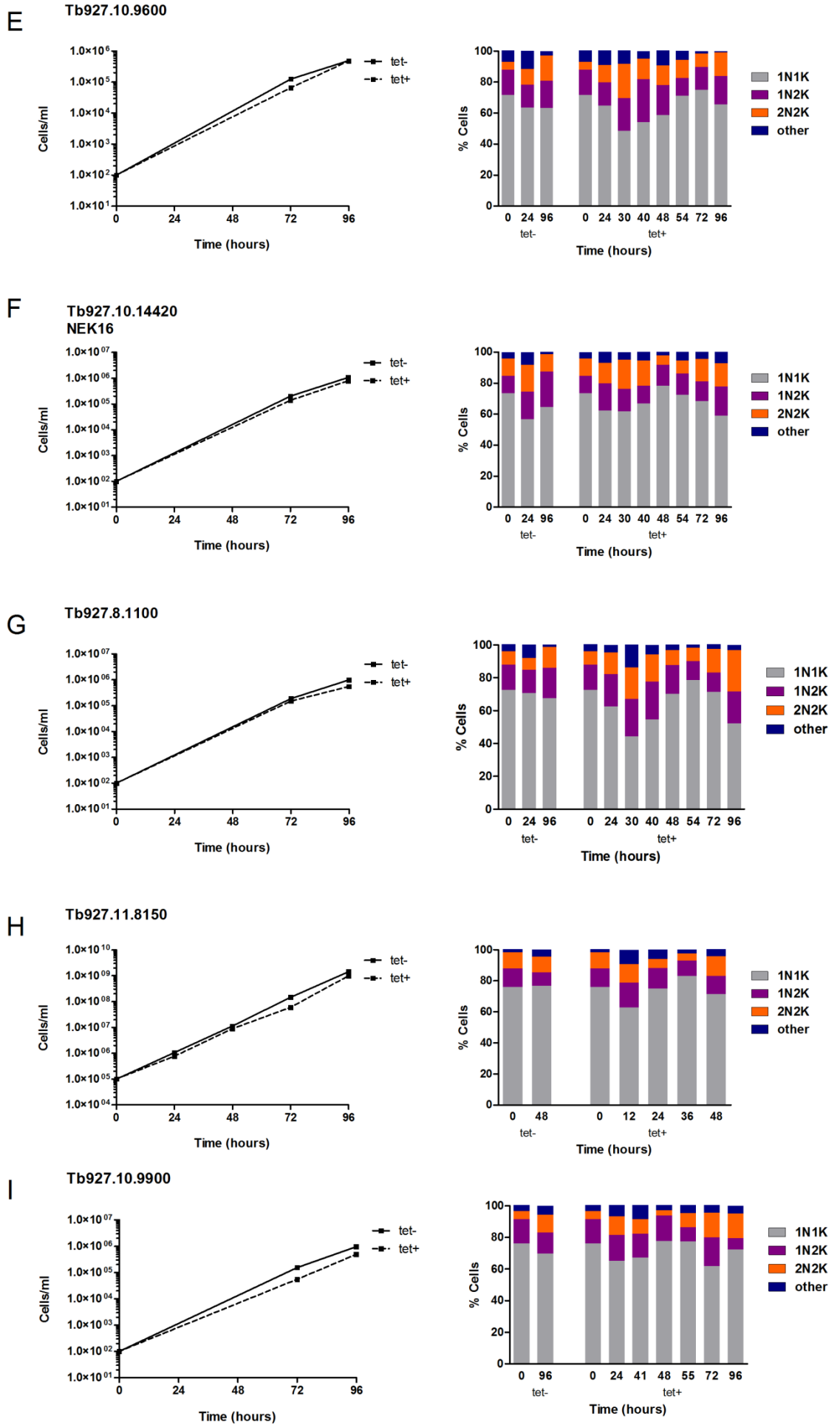


Figure 5-4 *In vitro* growth and cell cycle analysis for cell lines showing no growth or cell cycle defects following RNAi induction. A: LDK; B: Tb927.8.870; C: CK1; D: CLK2; E: Tb927.10.9600; F: NEK16; G: Tb927.8.1100; H: Tb927.11.8150; I: Tb927.10.9900. Cumulative growth curves were generated (left) and the numbers of nuclei (N) and kinetoplasts (K) in each cell ($n \geq 200$) following DAPI staining of samples were recorded at the indicated time points post addition of tetracycline to the induced samples (right). Analyses of non-induced cells (tet-) are also shown as controls.

5.6.1.2 Cell lines showing growth defects but no notable cell cycle defects following RNAi induction

The group of cell lines described in this section are those which displayed growth defects, to varying degrees, following RNAi induction which could not be attributed to cell cycle defects. Either no cell cycle defects were apparent or they emerged only after the appearance of growth defects. Altogether, 19 cell lines showed this type of phenotype indicating that the kinases knocked down in these cell lines likely play roles that are important but cell cycle-independent in BSF *T. brucei*.

This group includes two RNAi cell lines which were not hits in the initial Alamar Blue screen. One of these is the TOR2 RNAi cell line whose lack of loss of fitness upon RNAi induction (Alamar Blue values: Clone 1 - 1.00, clone 2 - 0.92; Jones et al., 2014) was found to be contrary to previous reports where incomplete knockdown of TOR2 was found to generate a growth defect (Barquilla, Crespo, & Navarro, 2008). Therefore, the TOR2 RNAi cell line was analysed via further growth curves and cell cycle analysis to reveal that the TOR2 knockdown via RNAi does indeed induce a phenotype. However, the phenotype generated was a cell death phenotype with no notable cell cycle defects (Figure 5-5A). The reason for this discrepancy between the results obtained from the Alamar Blue assay and the growth and cell cycle analyses could be due to probable changes in the metabolism preventing the loss of fitness being detected by the Alamar Blue assay; however, this possibility was not investigated. Also, the findings obtained following the growth and cell cycle analyses is in contrast to those of Barquilla and colleagues where TOR2 knockdown was found to induce a rise in cells at the G₂/M phase possibly due to defective cytokinesis although this was not further investigated (Barquilla et al., 2008). This discrepancy cannot be fully reconciled

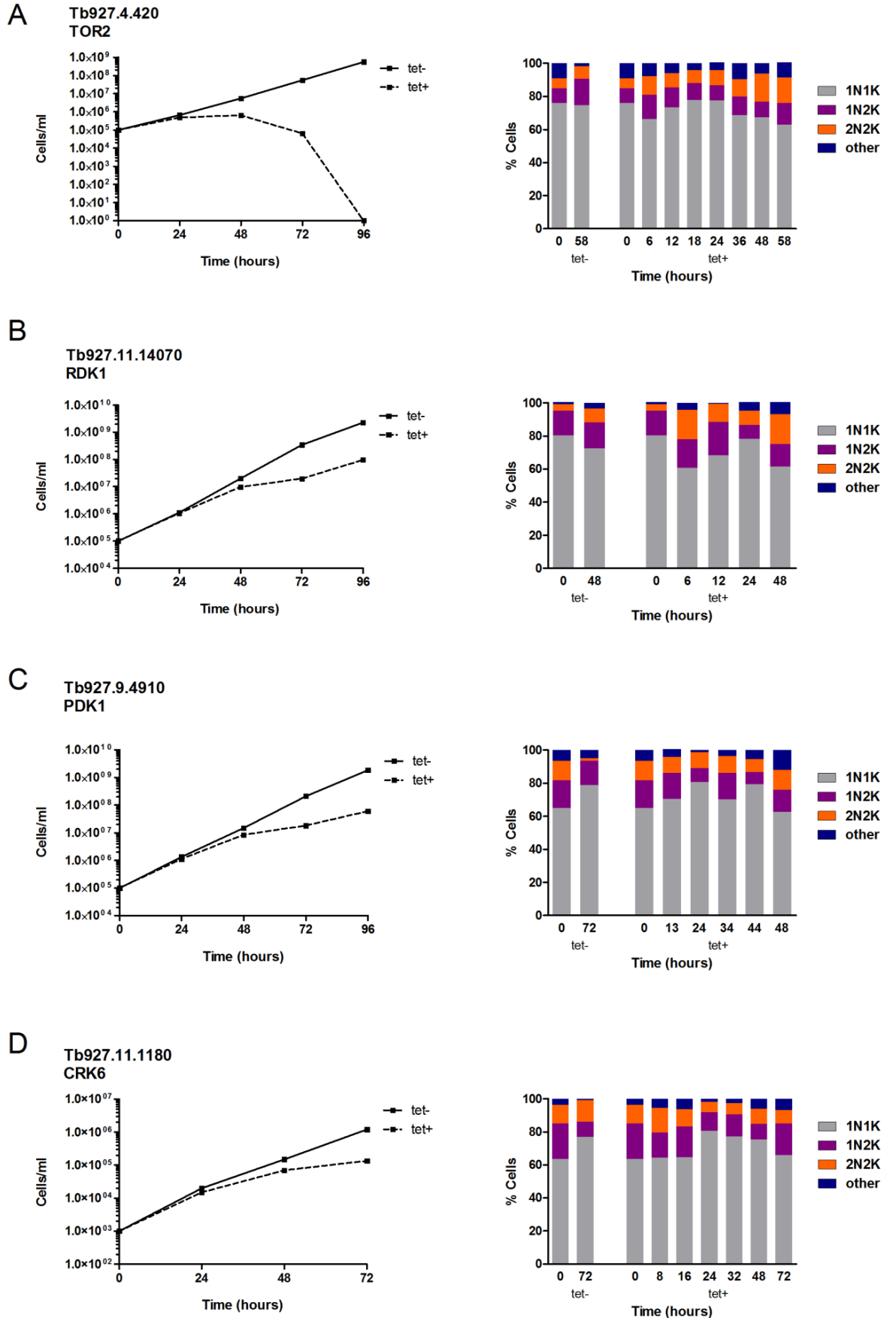
at present; however, differences in RNAi constructs used could be a possible explanation.

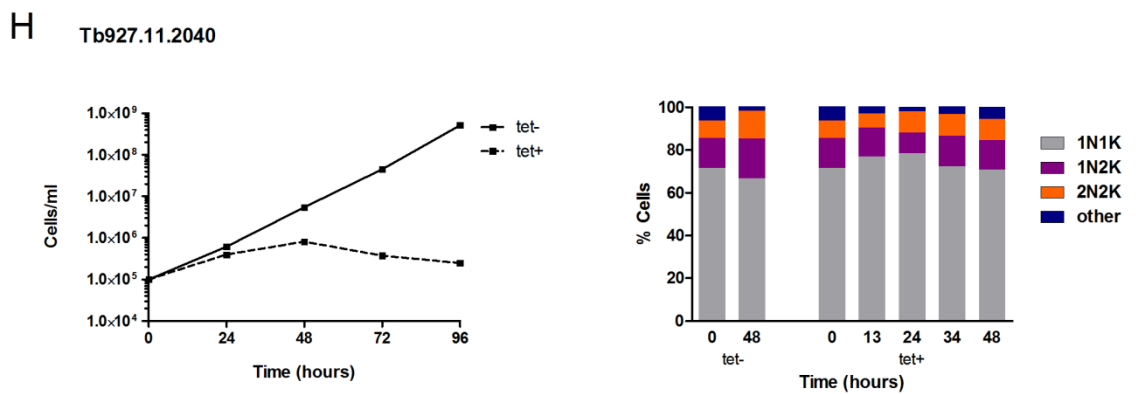
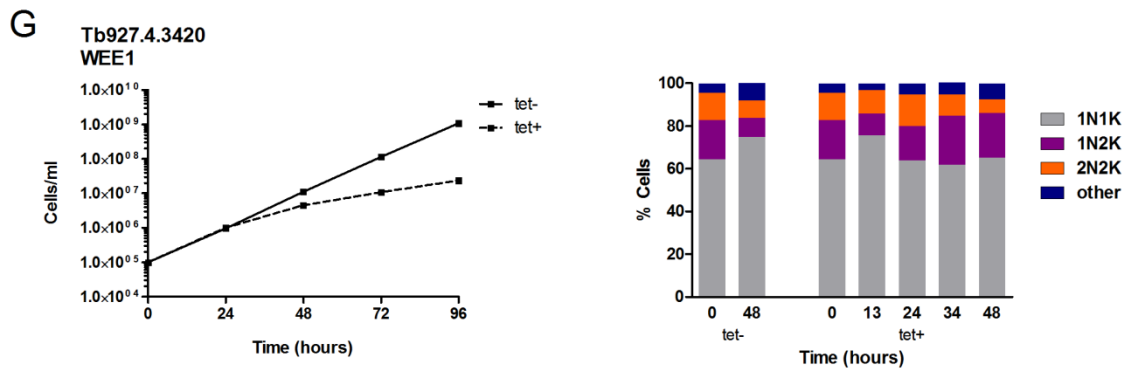
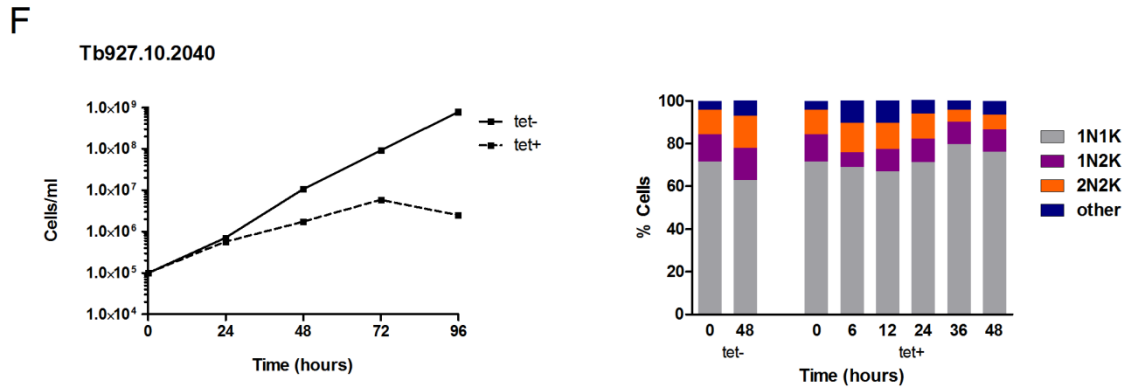
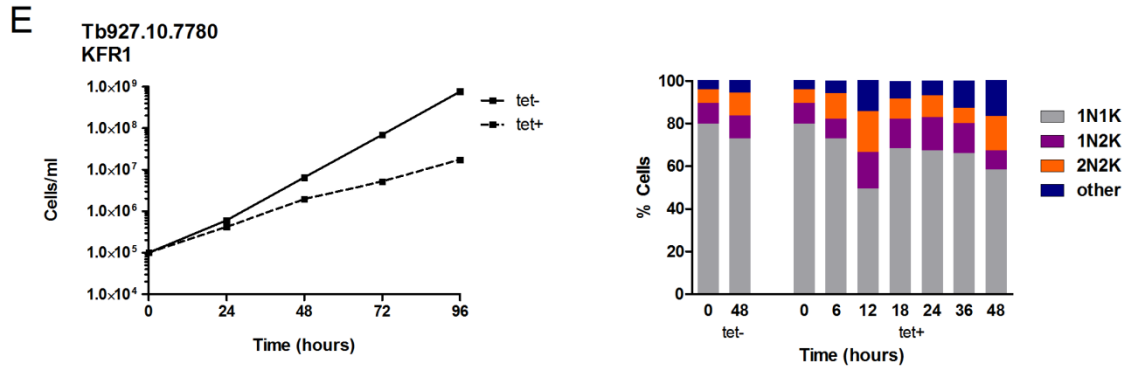
The second cell line which was not detected as a hit in the Alamar Blue screen was the RDK1 RNAi cell line. RDK1 was identified as a negative regulator of differentiation (Jones et al., 2014) and, therefore, qualified as a gene of interest to potentially play a role in the *T. brucei* cell cycle. Upon further investigation via growth curves and DAPI staining, whilst RDK1 RNAi did generate a mild growth defect, it did not cause any cell cycle defects (Figure 5-5B).

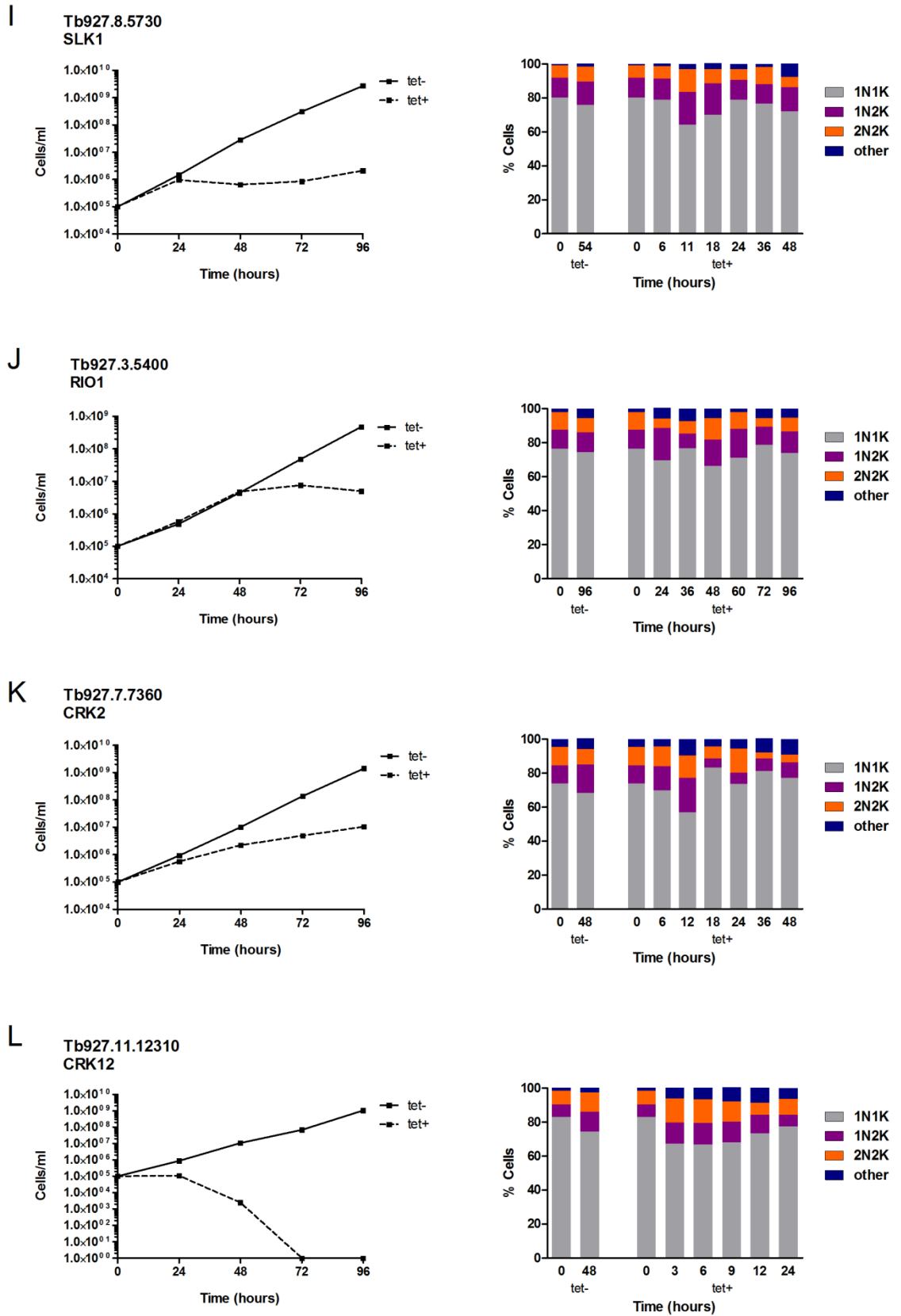
Eight of the 19 kinases within this group were shown for the first time to be essential for normal BSF cell proliferation: the newly identified negative regulator of differentiation kinase RDK1 (Figure 5-5B; Jones et al., 2014), PDK1 (a master AGC kinase in other eukaryotes (Pearce, Komander, & Alessi, 2010); Figure 5-5C), CRK6 (Figure 5-5D), the MAP kinase KFR1 (Figure 5-5E), the STE kinase, Tb927.10.2040 (Figure 5-5F), WEE1 (Figure 5-5G), whose homologues in other eukaryotes are required for the activation of the S-phase and G₂/M cell cycle checkpoints (Vriend, De Witt Hamer, Van Noorden, & Würdinger, 2013), the STE-11 type kinase Tb927.11.2040 (Figure 5-5H), SLK1 (Figure 5-5I) and RIO1 (Figure 5-5J).

CRK2 and CRK12 have already been individually characterised in the past. Knockdown of CRK2 was reported not to result in any growth defects in BSF cells (X. Tu & Wang, 2004) which is in contrast to the results obtained here (Figure 5-5K). CRK12 has been found to be essential for BSF proliferation which is in agreement (Figure 5-5L) with another study where the same clone was used (Monnerat et al., 2013). Previously, CRK12 RNAi was found to induce a growth defect in BSF parasites in the small protein kinase RNAi screen (Mackey et al., 2011), albeit not as strongly as in the clone described here. In another study, CRK12 was again found to be essential for BSF cell proliferation when a conditional null mutant approach was used (Merritt & Stuart, 2013); here the growth defect generated was as strong as the findings in this study (Figure 5-5L). CRK12 was also detected as being essential for BSF proliferation in the genome-wide RIT-seq RNAi study (Alsford et al., 2011) in addition to eight other kinases from this “growth defects but no cell cycle defects” group: TOR2 (Figure 5-5A), the CAMK, Tb927.7.2750 (Figure 5-5M), a serine arginine-rich protein kinase

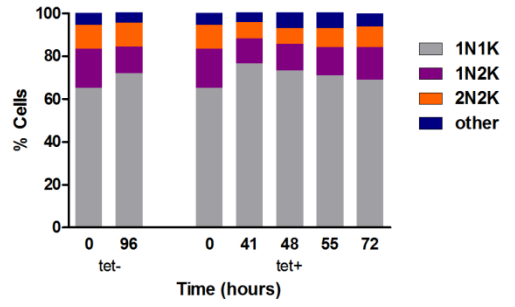
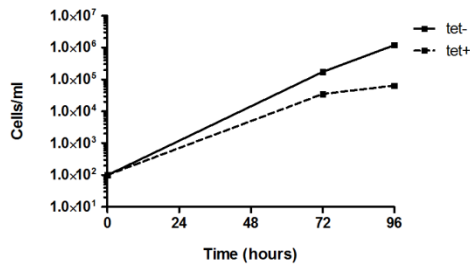
(SRPK), Tb927.6.4970 (Figure 5-5N), PK6 (Figure 5-5O), the CAMKK, Tb927.10.15300 (Figure 5-5P), SLK2 (Figure 5-5Q), the pseudokinase, Tb927.9.6560 (Figure 5-5R), and RIO2 (Figure 5-5S).



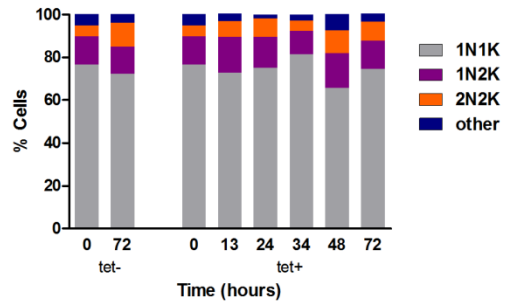
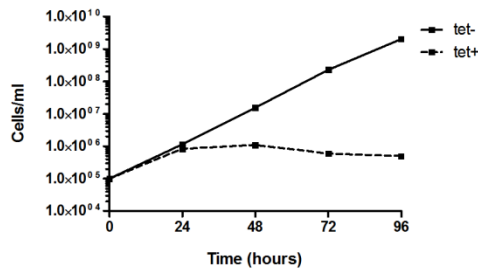




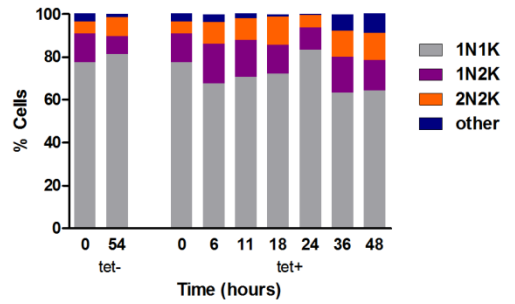
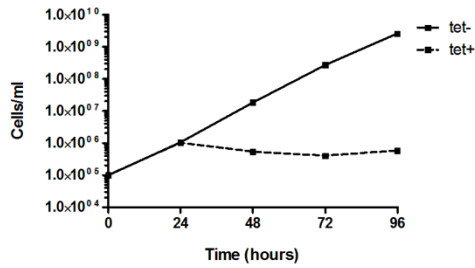
M Tb927.7.2750



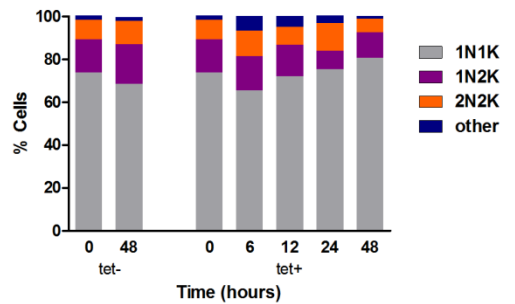
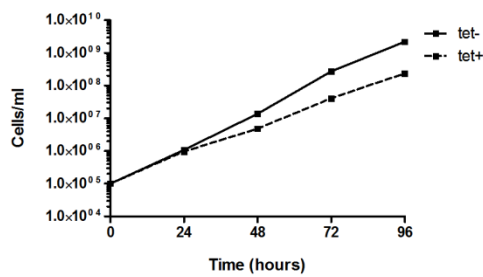
N Tb927.6.4970



O Tb927.9.10920
PK6



P Tb927.10.15300



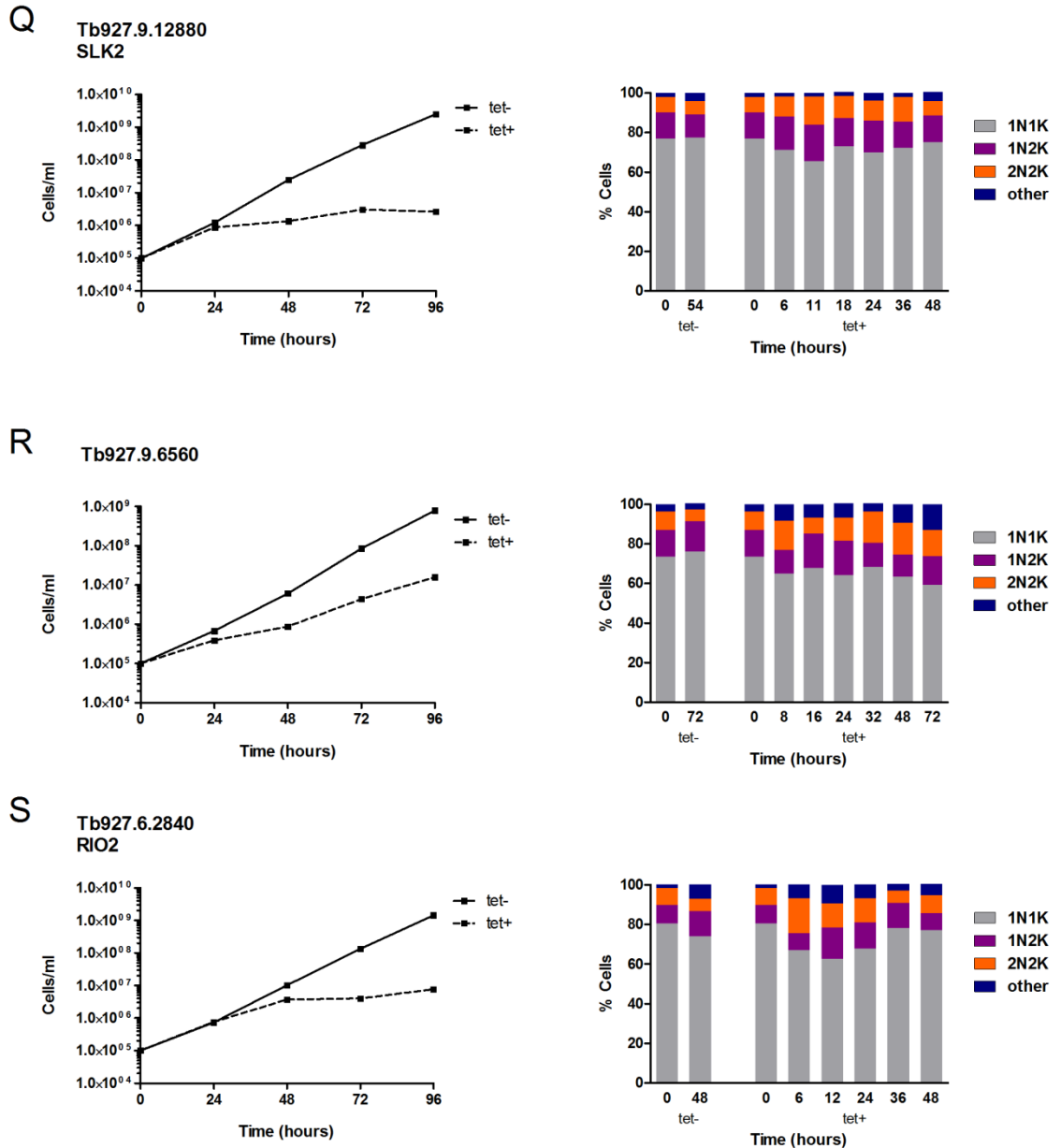


Figure 5-5 *In vitro* growth and cell cycle analysis for cell lines showing growth defects but no notable cell cycle defects following RNAi induction. A: TOR2; B: RDK1; C: PDK1; D: CRK6; E: KFR1; F: Tb927.10.2040; G: WEE1; H: Tb927.11.2040; I: SLK1; J: RIO1; K: CRK2; L: CRK12; M: Tb927.7.2750; N: Tb927.6.4970; O: PK6; P: Tb927.10.15300; Q: SLK2; R: Tb927.9.6560; S: RIO2. Cumulative growth curves were generated (left) and the numbers of nuclei (N) and kinetoplasts (K) in each cell ($n \geq 200$) following DAPI staining of samples were recorded at the indicated time points post addition of tetracycline to the induced samples (right). Analyses of non-induced cells (tet-) are also shown as controls.

5.6.1.3 Cell lines showing G₁/S defects following RNAi induction

Depletion of two kinases, CRK1 or TOR4, led to slight growth defects (more prominent following CRK1 depletion), accompanied by a rise in 1N1K cells

suggesting that knockdown of these kinases leads to the cells being blocked at G₁/S phase (Figure 5-6). These findings are in agreement with previous studies where CRK1 knockdown was shown to bring about a rise in G₁ phase and decrease in S phase cells (X. Tu & Wang, 2004) whilst TOR4 knockdown was found to cause an irreversible differentiation of the parasite to the quiescent stumpy form (Barquilla et al., 2012). Depletion of each of these kinases was previously shown to induce strong loss of fitness phenotypes (within 3 days) in the global RIT-seq study (Alsford et al., 2011).

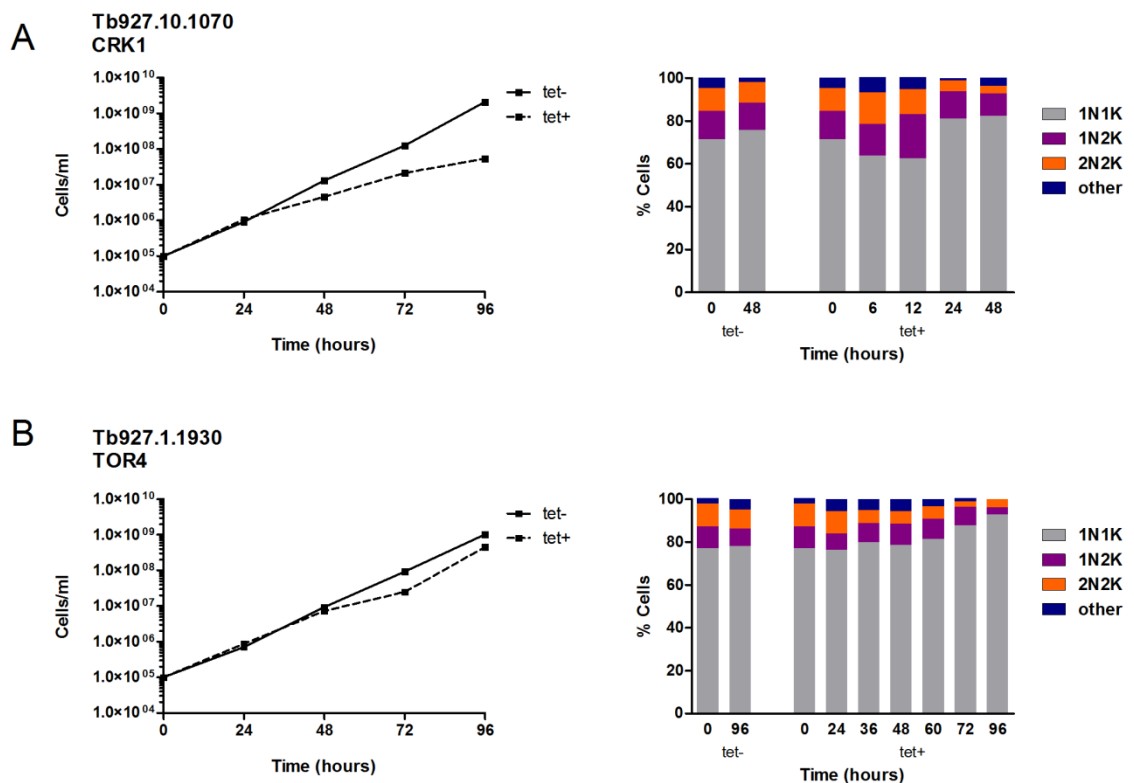


Figure 5-6 *In vitro* growth and cell cycle analysis for cell lines showing G₁/S defects following RNAi induction. A: CRK1; B: TOR4. Cumulative growth curves were generated (left) and the numbers of nuclei (N) and kinetoplasts (K) in each cell ($n \geq 200$) following DAPI staining of samples were recorded at the indicated time points post addition of tetracycline to the induced samples (right). Analyses of non-induced cells (tet-) are also shown as controls.

5.6.1.4 Cell lines showing mitosis defects following RNAi induction

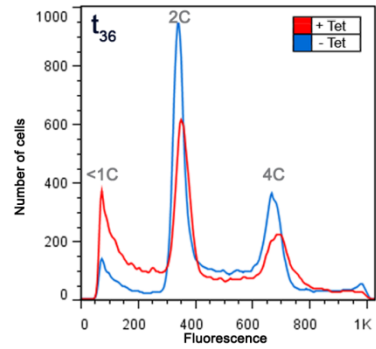
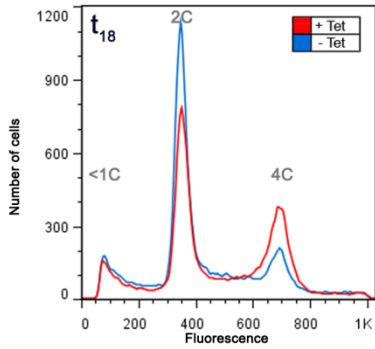
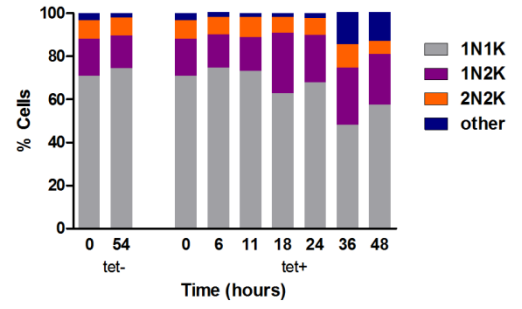
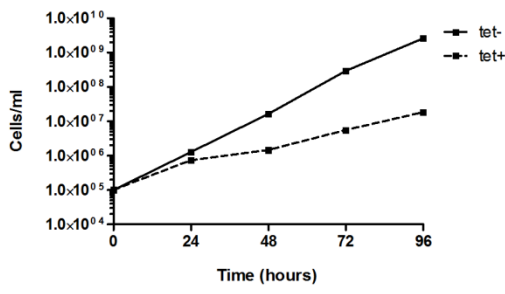
RNAi of four kinases (Tb927.11.5340, ATR, CRK3 and AUK1) led to defects in proliferation of BSF cells which appeared to be linked to a block in mitosis. These phenotypes were described for the first time for the CMGC kinase Tb927.11.5340 and ATR, a kinase which, in conjunction with ATM, orchestrates

the DNA damage response signalling pathway in other eukaryotes (Lovejoy & Cortez, 2009) (top panels of Figure 5-7A and B, respectively). RNAi of Tb927.11.5340 and ATR led to a rise in 1N2K cells and subsequent rise in 1N>2K cells (Table S1) with the phenotypes being more pronounced following ATR depletion (28 % and 6 % of total cell population, respectively, at 72 hours post-induction; Table S1). The appearance of 1N2K cells and 1N>2K cells could be explained by a delay or block in nuclear DNA replication and segregation whilst the progression of kDNA replication/segregation continues unimpeded. Flow cytometry analyses of propidium iodide (PI)-stained cells showed that Tb927.11.5340 and ATR RNAi induced cell lines had undergone DNA replication (bottom panels of Figure 5-7A and B) suggesting that it is the progression through mitosis, rather than DNA replication, that has been inhibited. In addition, a huge rise in cells with 4C DNA content is not seen, suggesting that mitosis is delayed rather than blocked in Tb927.11.5340 and ATR RNAi cells.

CRK3 and AUK1 displayed phenotypes that were consistent with published literature (Figure 5-7C and D, respectively). Previously, AUK1 was shown to play a role in spindle assembly (Li & Wang, 2006) in keeping with the roles played by its homologues in other eukaryotes (Goldenson & Crispino, 2014). Its knockdown was shown to generate severe growth defects and a block in mitosis demonstrated by the characteristic rise in 1N2K cells (Jetton et al., 2009; Li & Wang, 2006). CRK3, a homologue of the mitotic Cdk, Cdk1 (Hammarton, Clark, Douglas, Boshart, & Mottram, 2003), was previously shown to be essential for the promotion of the G₂/M transition (X. Tu & Wang, 2004). Also, knockdown of both kinases as part of the genome-wide RIT-seq data analysis (Alsford et al., 2011) generated loss of fitness phenotypes. Here, knockdown of CRK3 led to a rise in 1N2K cells which decreased over time (most likely due to the recovery of RNAi refractory cells; Figure 5-7C, right panel) whilst the knockdown of AUK1 led to a dramatic rise in 1N2K cells by 3 hours of RNAi induction (Figure 5-7D, right panel) further giving rise to 1N>2K cells at later time-points (60 % of 1N2K cells at 12 hours post-induction; 11 % of 1N>2K cells at 24 hours post-induction; Table S1). Both these results indicate a block in mitosis which is in agreement with previous findings.

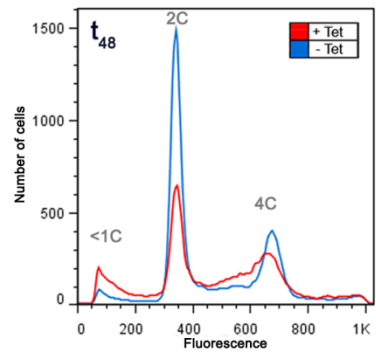
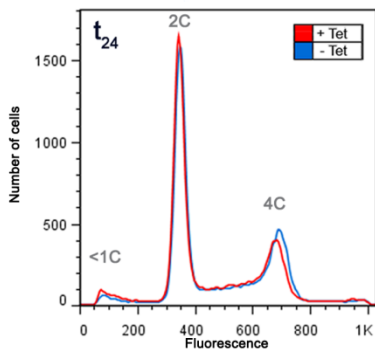
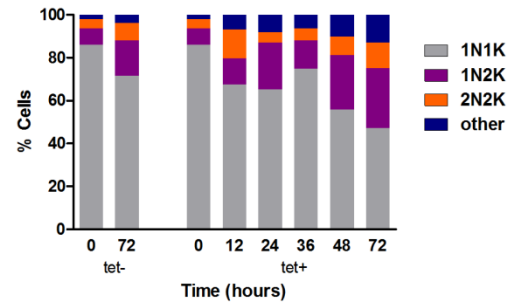
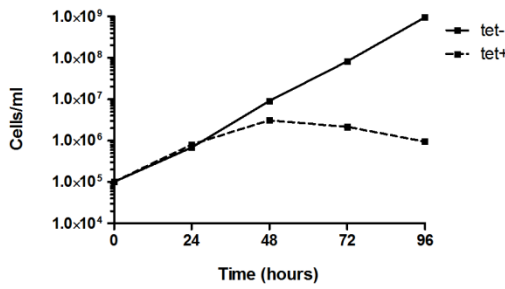
A

Tb927.11.5340



B

Tb927.11.14680
ATR



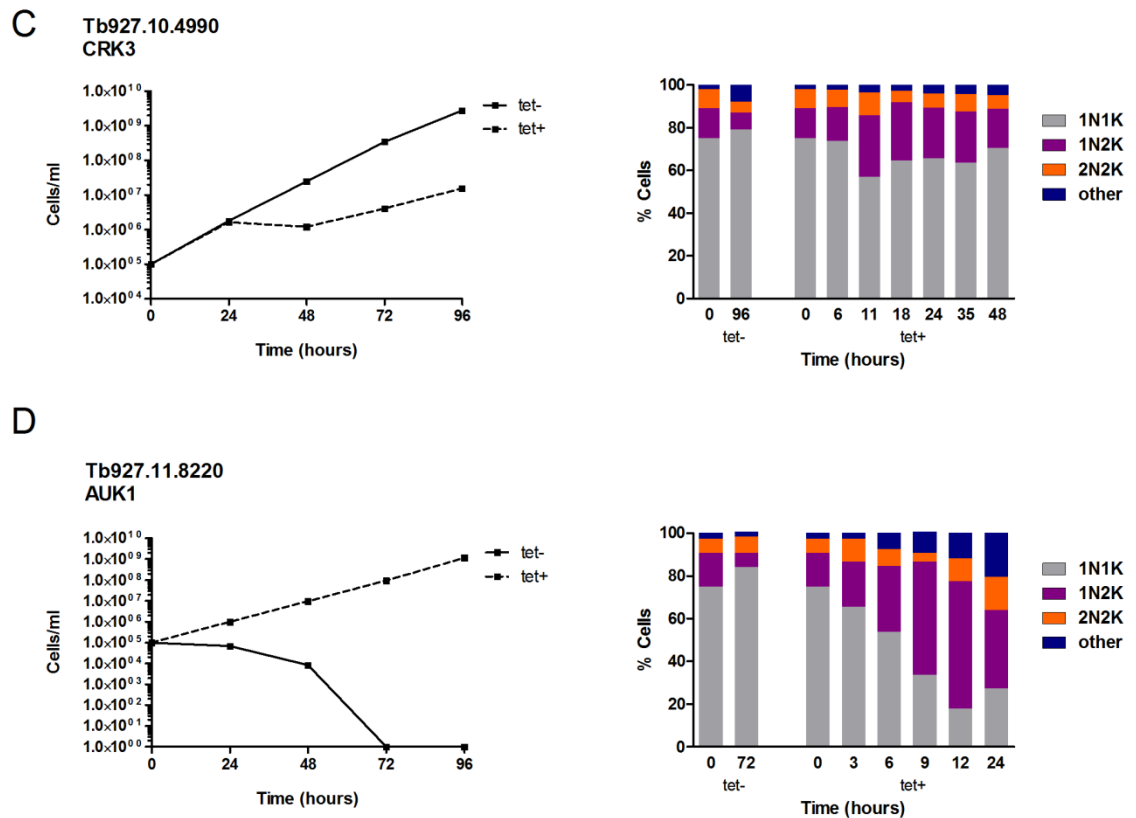


Figure 5-7 *In vitro* growth and cell cycle analysis for cell lines showing mitosis defects following RNAi induction. A: Tb927.11.5340; B: ATR; C: CRK3; D: AUK1. Cumulative growth curves were generated (left) and the numbers of nuclei (N) and kinetoplasts (K) in each cell ($n \geq 200$) following DAPI staining of samples were recorded at the indicated time points post addition of tetracycline to the induced samples (right). Analyses of non-induced cells (tet-) are also shown as controls. Flow cytometry profiles for 50,000 propidium iodide labelled cells at the indicated time-points were also obtained for Tb927.11.5340 (A - bottom panels) and ATR (B - bottom panels). The DNA content of each peak is indicated.

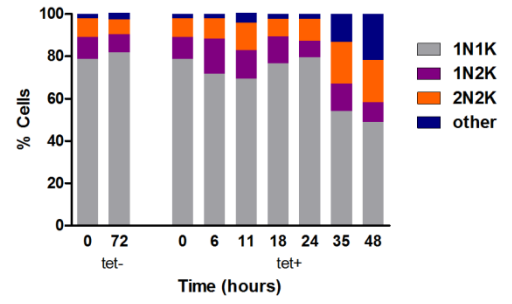
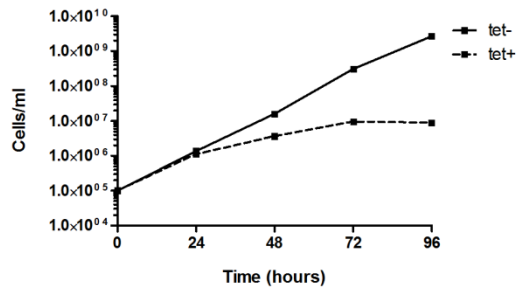
5.6.1.5 Cell lines showing cytokinesis defects following RNAi induction

Knockdown of seven kinases (Tb927.7.6220, Tb927.3.690, Tb927.3.2440, Tb927.10.5140, PKAC1 & PKAC2 and PK50) generated growth defects that could have been due to defects in cytokinesis. Among these, the essentiality of the CAMK, Tb927.7.6220, for BSF proliferation had never been described before (Figure 5-8A). The growth defect induced following RNAi of Tb927.7.6220 was found to coincide with a slight rise in 2N2K cells and was followed by a subsequent rise in >2N>2K cells (Figure 5-8A; Table S1), indicating that whilst the nucleus and kinetoplast are able to replicate and segregate, the cells are not able to divide to generate progeny. This phenotype was also observed following

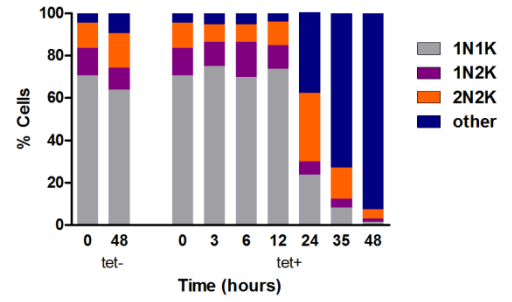
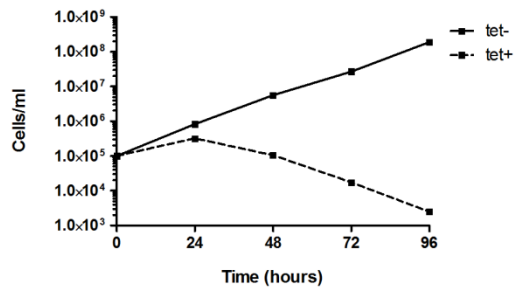
the knockdown of the rest of the kinases in this section thus indicating their putative roles in *T. brucei* BSF cytokinesis (Figure 5-8).

The CMGC/RCK kinase Tb927.3.690, the AGC kinase, Tb927.3.2440, the CMGC kinase, Tb927.10.5140 and PKAC1 & PKAC2 were already identified as being essential for BSF proliferation in the global RIT-seq screen (Alsford et al., 2011). Knockdown of Tb927.3.690 generated a spectacular rise in 2N2K cells within 24 hours (32 % of total cell population at 24 hours post-induction; Table S1) which was followed by a rise in cells featuring multiple nuclei and kinetoplasts (Figure 5-8B). This suggests that the cells that were unable to undergo cytokinesis in the first place, continued to replicate their nuclei and kinetoplasts leading to the subsequent rise in cells with multiple nuclei and kinetoplasts. Such a phenotype, therefore, firmly indicates the essential role of Tb927.3.690 in BSF cytokinesis. A similar phenotype was also observed following the depletion of Tb927.3.2440 albeit at a later time-point and with a less dramatic rise in 2N2K cells (Figure 5-8C; Table S1). In both cell lines, the majority of the cells were abnormal by 48 hours. Tb927.10.5140, which generated a similar rise in 2N2K cells and subsequent rise in cells with multiple nuclei and kinetoplasts (Figure 5-8D; Table S1) had already been identified as essential for BSF proliferation in the mini-RNAi screen conducted by Mackey and colleagues (Mackey et al., 2011) whilst PKAC1 & PKAC2 and PK50, also generating similar cell cycle defects (Figure 5-8E and F), have been individually studied elsewhere (Kramer, 2004; Ma et al., 2010).

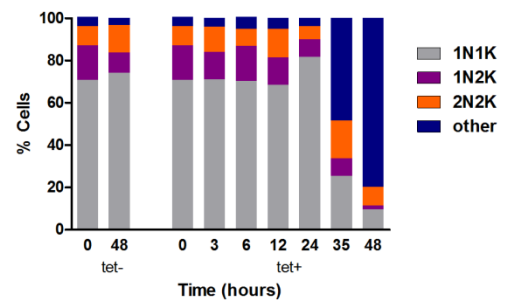
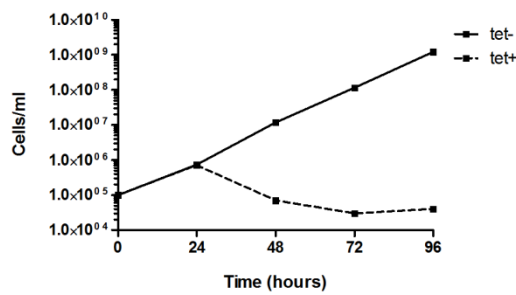
A Tb927.7.6220



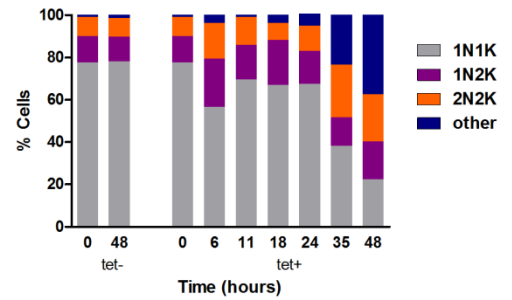
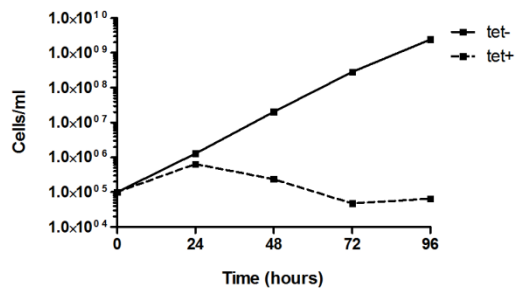
B Tb927.3.690



C Tb927.3.2440



D Tb927.10.5140



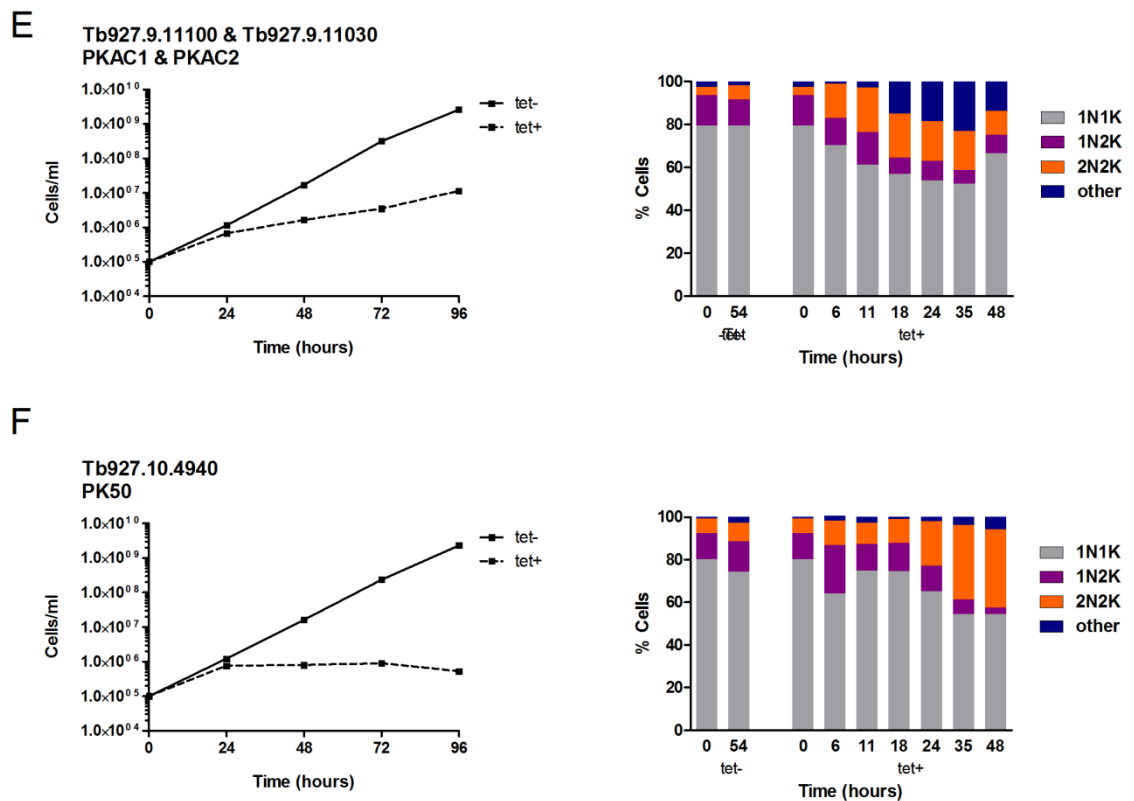


Figure 5-8 *In vitro* growth and cell cycle analysis for cell lines showing cytokinesis defects following RNAi induction. A: Tb927.7.6220; B: Tb927.3.690; C: Tb927.3.2440; D: Tb927.10.5140; E: PKAC1 & PKAC2; F: PK50. Cumulative growth curves were generated (left) and the numbers of nuclei (N) and kinetoplasts (K) in each cell ($n \geq 200$) following DAPI staining of samples were recorded at the indicated time points post addition of tetracycline to the induced samples (right). Analyses of non-induced cells (tet-) are also shown as controls.

5.6.1.6 Cell lines showing kinetoplast duplication defects following RNAi induction

Knockdown of CRK9 or CK2A1 (also known as CK2 α) led to growth defects that could be attributed to defective kinetoplast replication or segregation (Figure 5-9). Following knockdown of each kinase, a substantial rise in 2N1K cells was observed (13 % at 48 hours post-induction compared to 1 % before induction for CRK9; 19 % at 48 hours post-induction compared to 1 % before induction for CK2A1; Table S1) with no equivalent rise in 0N1K cells (or ‘zoids’). This indicates the completion of mitosis before the kinetoplasts have replicated/segregated. In both cases, no subsequent rise in >2N1K cells are observed, suggesting that there is a delay, rather than a block, in kinetoplast replication/segregation (Table S1). Both of these kinases were classified as essential for *T. brucei* BSF proliferation

in the global RIT-seq study published in 2011 (Alsford et al., 2011). They were also both previously studied on a candidate gene basis.

CRK9 was knocked down in two separate studies in the BSF stage. CRK9 knockdown was found to be lethal (Badjatia, Ambrósio, Lee, & Günzl, 2013) which was in contrast to an earlier report (Gourguechon & Wang, 2009) which could be explained by the different RNAi plasmids used (Badjatia et al., 2013). CRK9 was found to play important roles in the spliced leader trans-splicing process required for mRNA maturation in BSF parasites (Badjatia et al., 2013). Previous studies on CK2A1 localised it to the nucleolus and showed that it associated with NOPP44/46 (Park, Brekken, Randall, & Parsons, 2002), a nucleolar RNA-binding protein required for ribosome biogenesis (Jensen, Brekken, Randall, Kifer, & Parsons, 2005).

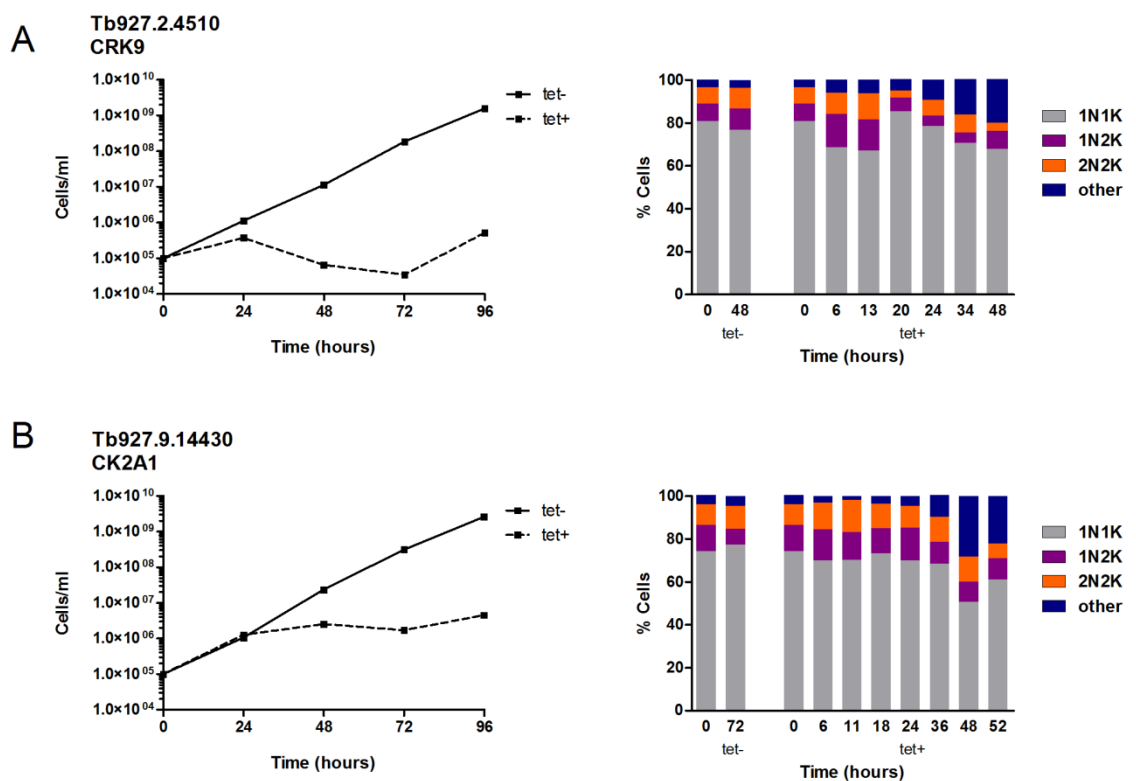


Figure 5-9 *In vitro* growth and cell cycle analysis for cell lines showing kinetoplast duplication defects following RNAi induction. A: CRK9; B: CK2A1. Cumulative growth curves were generated (left) and the numbers of nuclei (N) and kinetoplasts (K) in each cell ($n \geq 200$) following DAPI staining of samples were recorded at the indicated time points post addition of tetracycline to the induced samples (right). Analyses of non-induced cells (tet-) are also shown as controls.

5.6.1.7 Cell lines showing mitosis and cytokinesis defects following RNAi induction

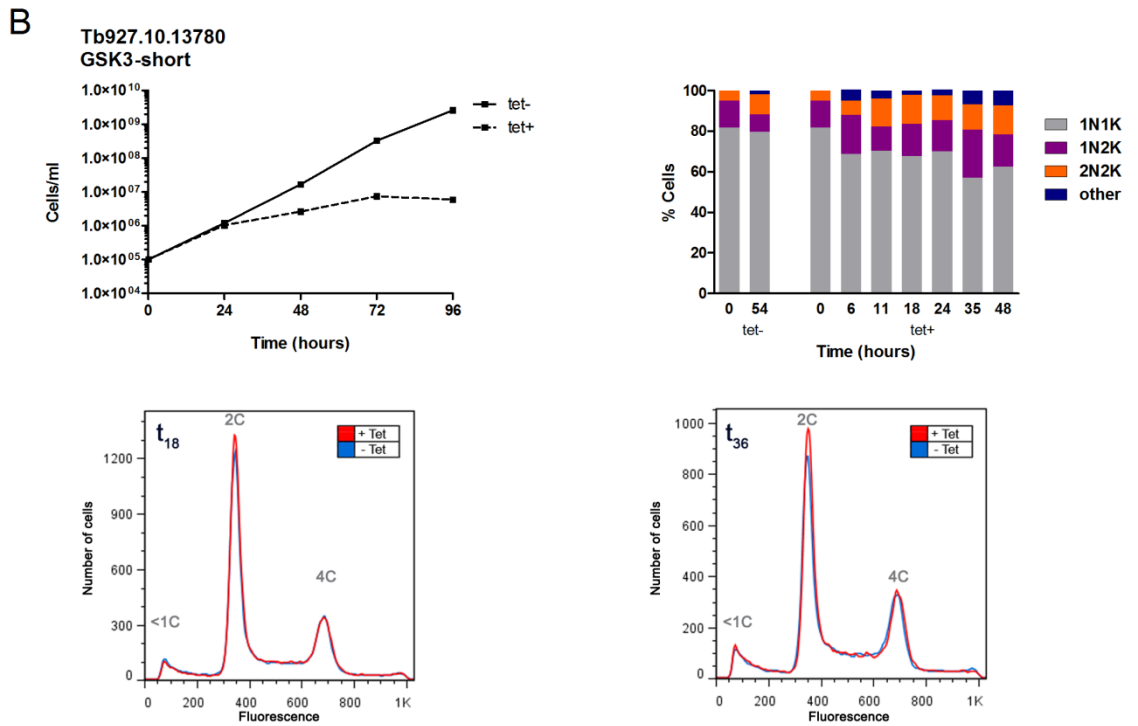
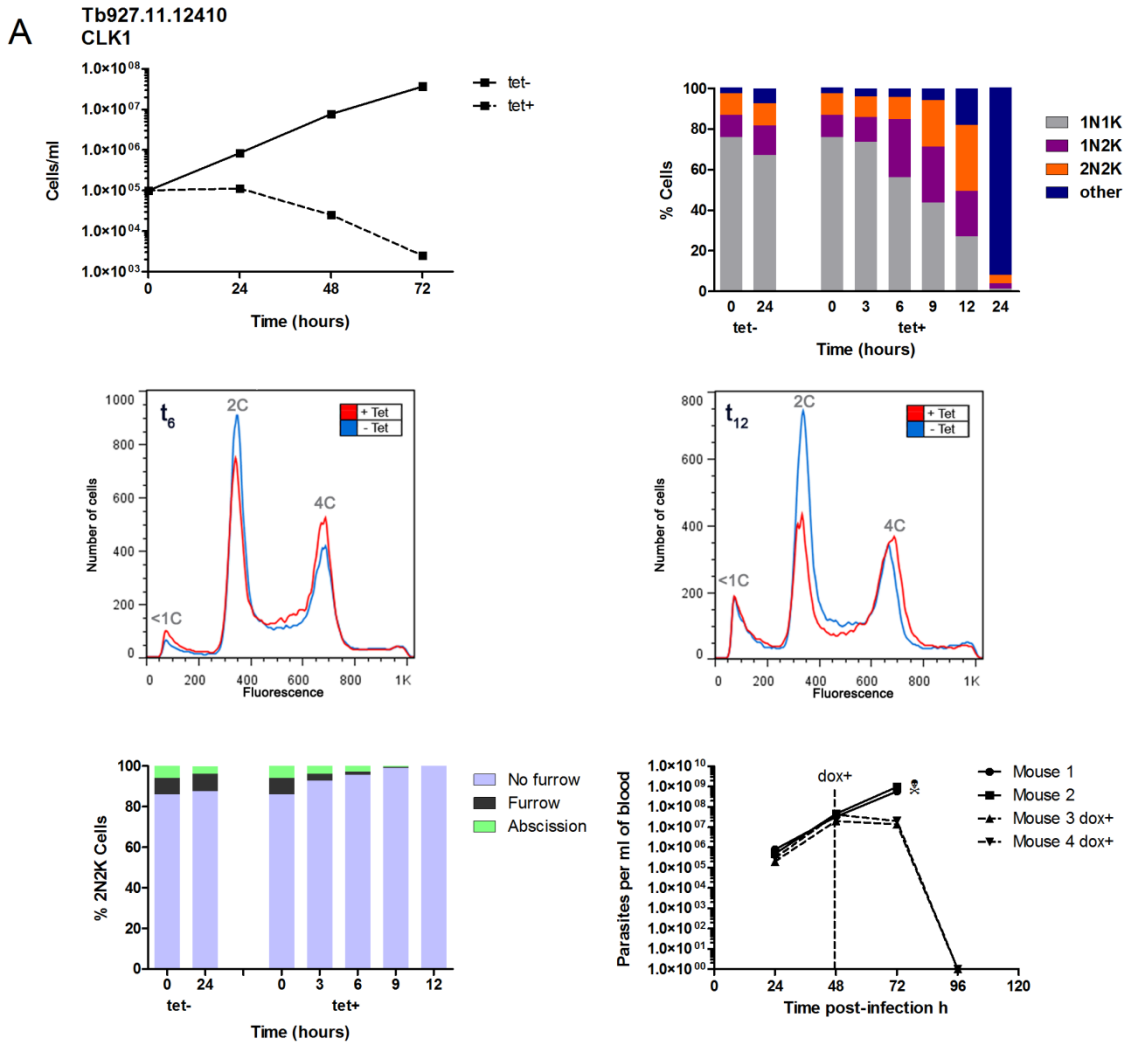
Three cell lines representing four kinases (CLK1, GSK3-short and TLK1 & TLK2) were found to give putative mitosis and cytokinesis defects upon RNAi induction. All of the kinases mentioned in this section were also shown to be essential for BSF cell proliferation in the genome-wide RIT-seq study (Alsford et al., 2011)

CLK1 has previously been found to be essential for BSF parasite proliferation and to be inhibited by the drug, hypothemycin previously known to target CDXG kinases in humans (Nishino et al., 2013). Here, depletion of CLK1 also resulted in a cell death phenotype and the characterisation of CLK1 was further extended in this screen. CLK1 depletion caused a dramatic rise in 1N2K and 2N2K cells by 6 hours post-induction (29 % and 11 %, respectively, compared to 11 % and 11 % before induction, respectively; Figure 5-10A, top right panel). By 12 hours, the majority of the “other” cells comprised 2N3K and 2N4K cells (8 % of total cell population; Table S1). These “other” cells at later timepoints proved difficult to classify due to difficulties in differentiating discrete kinetoplasts and nuclei (Table S1). The initial rise in 1N2K cells suggests defects in mitosis (see section 5.6.1.3), and when the appearance of cells with two nuclei at the same time is also taken into account, an indication is given that these defects could be causing delays in mitotic progression rather than its complete block. The initial rise in 2N2K cells and the subsequent rise of cells with multiple nuclei and kinetoplasts suggest a block in cytokinesis. Flow cytometry analysis revealed a decrease in the 2C peak and an increase in the 4C peak at 12 hours post-induction suggesting that the cells are able to replicate their DNA but either are unable to undergo karyokinesis and/or cytokinesis (Figure 5-10A, middle panels). In order to analyse the cytokinesis defects further, >200 2N2K cells were scored to determine their cytokinesis stage (Figure 5-10A, bottom left panel). A decline in the number of cells presenting visible cleavage furrows was observed suggesting that CLK1 plays an important role in the entry into cytokinesis or the early progression of furrow ingression during cytokinesis. CLK1 was also found to be essential for *T. brucei* BSF survival in a mouse model (experiment conducted by Ryan Ritchie, WTCMP), validating it as a potential drug target (Figure 5-10A, bottom right panel).

Depletion of GSK3-short also generated a cell death phenotype accompanied by a concomitant rise in 1N2K and 2N2K cells (24 % and 13 %, respectively at 35 hours post-induction compared to 13 % and 5 %, respectively before induction; Figure 5-10B, top panels) and flow cytometry analysis (Figure 5-10B, bottom panels) revealed that DNA replication proceeded normally. Similar to the reasons described for CLK1 above, the data indicates a delay, rather than a block in mitosis. However, unlike CLK1, depletion GSK3-short does not seem likely to block cytokinesis completely owing to the fact that a dramatic rise in aberrant cells was not seen to the extent seen following CLK1 knockdown. Previous studies had also established the essentiality of GSK3-short in BSF cell viability, in agreement with the findings here, in addition to its potential as a drug target (Ojo et al., 2008).

Whilst TLK2 has yet to be individually characterised in BSF parasites, RNAi based studies on TLK1 have shown it to interact with the components of the chromosomal-passenger complex (CPC), to play roles in mitotic spindle formation and chromosome segregation and, therefore, to be essential for BSF cell viability (Li, Umeyama, & Wang, 2008). In this study by the Wang lab, flow cytometry analysis of TLK1 knockdown cells saw a rise in the 4C peak and a decrease in the 2C peak, i.e. the cells were able to replicate their DNA but unable to undergo mitosis/cytokinesis. DAPI analysis shed further light on the mechanics of these cell cycle defects, where a rise in 1N2K cells indicated that the replicated nuclear DNA was not being segregated suggesting, at the very least, that delays occurred during mitosis. Here, the joint knockdown of TLK1 and TLK2 also led to a huge rise in 1N2K cells (Figure 5-10C, top right panel), which comprised 43 % of the total cell population at 36 hours post-induction (compared to 9 % before induction; Table S1). However, this was also accompanied by a concomitant rise in 0N1K (11 % and 13 % at 24 and 36 hours post induction, respectively, compared to none being found before induction; Table S1) and 1N>2K (9 % and 12 % at 36 and 48 hours post induction, respectively, compared to none being found before induction; Table S1) cells - phenotypes that were not reported in the Li et al. study (Li et al., 2008). These 0N1K and 1N>2K cells could have been generated from cells that were unable to undergo mitosis but completed cytokinesis nonetheless. These “extra” phenotypes suggest that the additional depletion of TLK2 brings about further

delays in mitosis, and promotes unchecked cytokinesis despite them. Flow cytometry analysis at 36 hours post-induction revealed a shift of the 4C peak to the right, indicating that many cells were polyploid and contained DNA that had been replicated repeatedly but had not been segregated appropriately (Figure 5-10D, bottom panels). Additionally, there was a rise in <1C peak, consistent with the increase in zoids observed by DAPI analysis. Altogether, the data suggest that TLK1 and TLK2 may play separate roles in promoting mitosis and TLK2 may also play an inhibitory role at the mitosis/cytokinesis checkpoint without which cytokinesis proceeds unchecked despite unsegregated nuclear DNA.



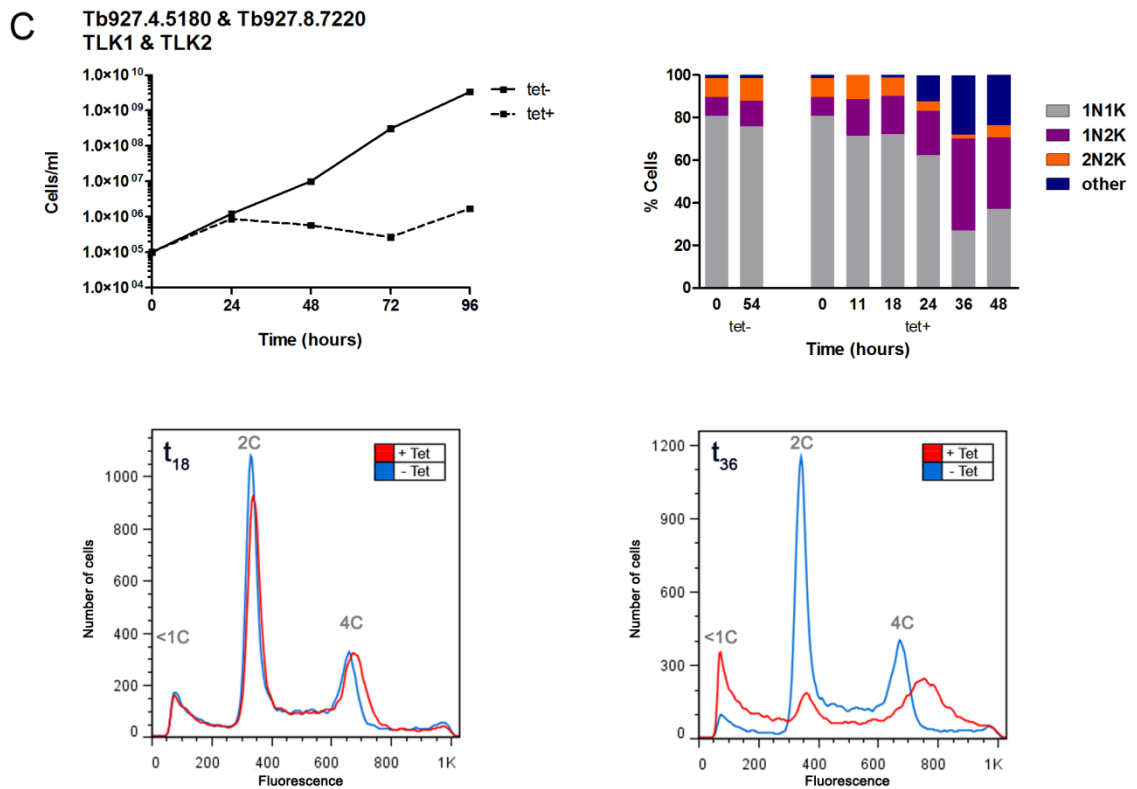


Figure 5-10 *In vitro* growth and cell cycle analysis for cell lines showing mitosis and cytokinesis defects following RNAi induction. A: CLK1; B: GSK-short; C: TLK1 & TLK2. Cumulative growth curves were generated (left) and the numbers of nuclei (N) and kinetoplasts (K) in each cell ($n \geq 200$) following DAPI staining of samples were recorded at the indicated time points post addition of tetracycline to the induced samples (right). Analyses of non-induced cells (tet-) are also shown as controls. Flow cytometry profiles for 50,000 propidium iodide labelled cells at the indicated time-points were also obtained for CLK1 (A - middle panels); GSK3-short (B - bottom panels) and TLK1 & TLK2 (C - bottom panels). The DNA content of each peak is indicated. For CLK1 (A), an analysis of the cytokinesis stage of 2N2K cells was also conducted ($n \geq 200$) (bottom left panel) in addition to analysing the proliferation of the CLK1 RNAi line in mice (bottom right panel). 1×10^5 trypanosomes were inoculated into 4 mice and RNAi was induced with doxycycline (dox, as indicated) in 2 mice 48 hours later. Uninduced mice were culled as indicated (☠) when their parasitaemias rose above 10^8 cells ml^{-1} (*in vivo* mouse experiments were conducted by Ryan Ritchie, WTCMP).

5.6.1.8 Cell lines showing kinetoplast duplication and cytokinesis defects following RNAi induction

Five cell lines representing six kinases (PK53, AUK3, CK1.1 & CK1.2, NEK12.2/RDK2 and Tb927.11.4470) presented growth defects following RNAi induction which may be attributed to joint defects in kinetoplast replication/segregation and cytokinesis. Three of these kinases have already

been studied on a candidate gene basis. Also, five kinases - CK1.1, CK1.2, AUK3, RDK2 and Tb927.11.4470, have all been shown to be essential for BSF cell proliferation in the genome-wide RIT-seq study (Alsford et al., 2011).

Knockdown of PK53 generated a slow growth phenotype (Figure 5-11A, left panel). Cell cycle analysis via DAPI staining following RNAi induction revealed a slight rise in 1N2K cells in addition to “other” cells, a lot of which were either 2N1K cells (9 % of total cell count at 48 hours post-induction) or “unclassified” cells (where discrete nuclei or kinetoplasts could not be clearly visualised) and small proportions of 0N1K, 1N0K and 2N0K (Figure 5-11A, right panel; Table S1). The rise in 2N1K cells, and the absence of equal number of zoids, indicates a delay in kinetoplast replication/segregation whilst the types of “other” cells generated suggest defects in cytokinesis. These findings do not exactly concur with what has already been published. PK53 RNAi was previously found to induce a stronger growth defect accompanied by a clear rise in 2N2K cells, many of which appeared to possess a visible cleavage furrow suggesting a block in progress to abscission (Ma et al., 2010). This difference in phenotypes could be due to differing levels of knockdown which has not been investigated during this study.

AUK3 RNAi (Figure 5-11B, right panel) resulted in the generation of large numbers of “other” cells by 18 hours post-induction, the majority of which were 0N1K, 1N0K and 2N1K cells (6 %, 2 % and 9 % of total cell count, respectively; Table S1). Later at 48 hours post-induction, the majority of the “other” cells were 1N0K and 2N1K cells (13 % and 11 % of total cell count, respectively; Table S1). Also prevalent were cells with multiple nuclei and kinetoplasts, i.e. >2N>2K cells, at the later time-points (Table S1). The initial appearance of 0N1K and 1N0K and 2N1K cells could be explained by inaccurate furrow ingression leading to the generation of these cells from 2N2K cells. On the other hand, the detection of 2N1K cells and the subsequent generation of >3N1K cells (2 % of total cell population at 35 hours post-induction; Table S1) suggest delays in kinetoplast division. The subsequent appearance of >2N>2K cells also suggests that the parasites were unable to undergo cytokinesis effectively. Altogether, these data suggest delays in kinetoplast division and/or cytokinesis or inaccurate furrow ingression which cannot be fully resolved without further investigations.

CK1.1 and CK1.2 have also been previously studied individually. Knockout of CK1.1 was found to have no effect on BSF parasites whilst CK1.2 RNAi was found to be lethal (Urbaniak, 2009). Here, the joint knockdown of CK1.1/CK1.2 supports these findings as they also generate a cell death phenotype (Figure 5-11C, left panel). DAPI analysis of induced cells revealed a huge rise in 2N2K cells (Figure 5-11B, right panel; 38 % and 23 % of the total cell population at 24 hours and 34 hours post-induction, respectively, compared to 12 % before induction; Table S1) with a concomitant rise in 2N1K cells (16 % and 14 % of the total cell population at 24 hours and 34 hours post-induction, respectively, compared to 1 % before induction; Table S1). When this is considered in combination with the fact that no substantial numbers of zoids or 1N>2K cells or cells with multiple nuclei and kinetoplasts were generated, the data, therefore, suggest delays in kinetoplast replication/segregation and cytokinesis rather than delayed mitosis or blocked cytokinesis. Similar phenotypes were also observed following knockdown of RDK2 or Tb927.11.4470 (Figure 5-11D and E, respectively), albeit on a smaller scale (for RDK2) or with a milder rise in 2N1K cells (for Tb927.11.4470; 9 % of total cell population at 48 hours post-induction compared to 1 % before induction; Table S1), which leads to the same conclusion being drawn for the roles of RDK2 and Tb927.11.4470 in the BSF parasite's cell cycle.

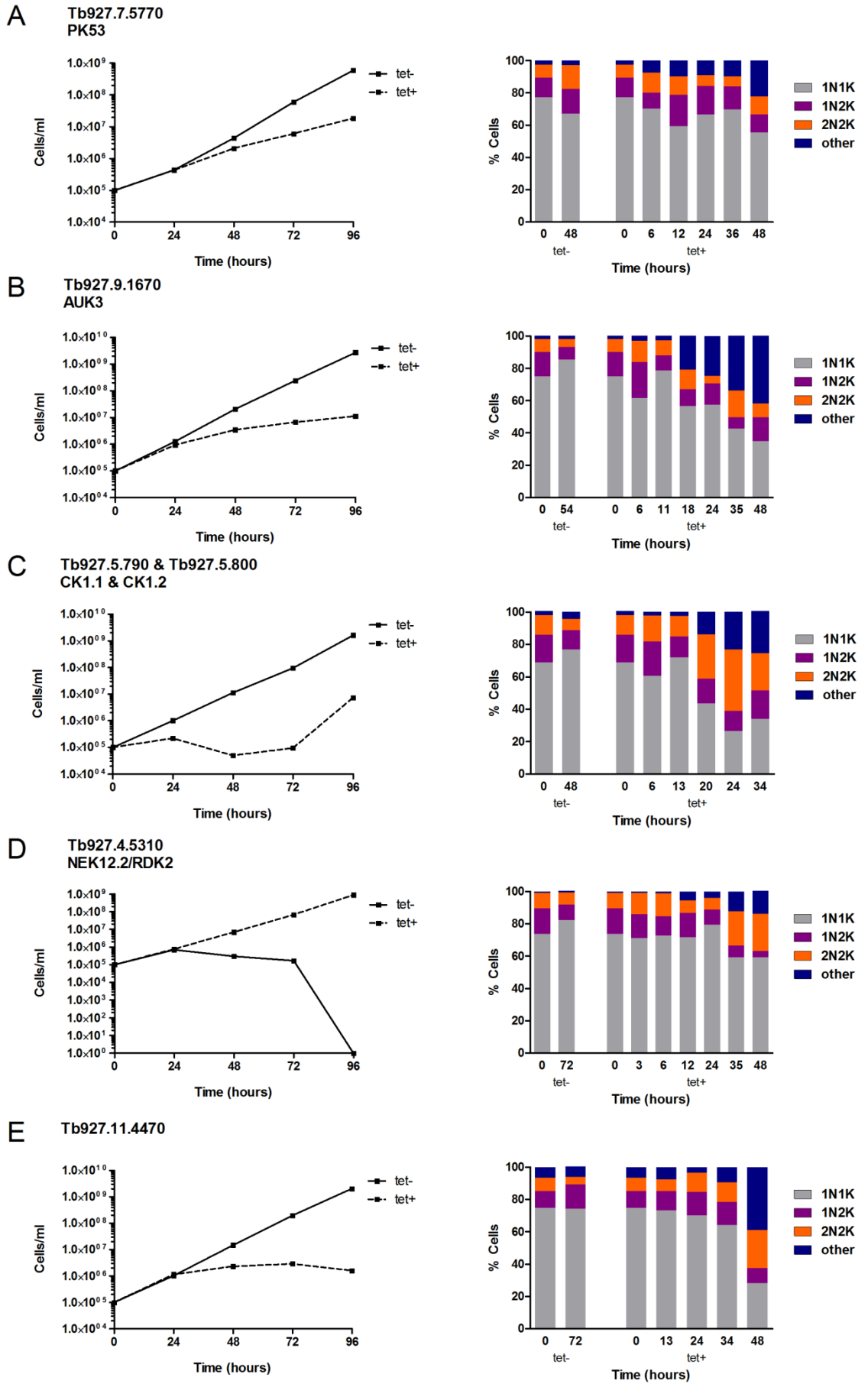


Figure 5-11 *In vitro* growth and cell cycle analysis for cell lines showing kinetoplast duplication and cytokinesis defects following RNAi induction. A: PK53; B: AUK3; C: CK1.1 & CK1.2; D: RDK2; E: Tb927.11.4470. Cumulative growth curves were generated (left) and the numbers of nuclei (N) and kinetoplasts (K) in each cell ($n \geq 200$) following DAPI staining of samples were recorded at the indicated time points post addition of tetracycline to the induced samples (right). Analyses of non-induced cells (tet-) are also shown as controls.

5.6.1.9 Cell lines showing growth defects and/or cell cycle defects that were unclassified following RNAi induction

The knockdown of two kinases generated ambiguous results which prevented them from being classified into a specific cell cycle phenotypic class. Knockdown of Tb927.7.3210 generated a slight growth defect (Figure 5-12A, left panel). At 30 hours post-induction of RNAi, a large proportion of the cell population comprised of aberrant cell types (Figure 5-12A, right panel). This generation of “other” cells, however, was not maintained at later time-points confounding unambiguous classification of this phenotype to a distinct cell cycle defect. Knockdown of TOR1 generated a stronger growth defect but was accompanied by a reversal in cell cycle defects (such as the rise in 1N2K and 2N2K cells seen at 12 post-induction of RNAi) similar to that seen following Tb927.7.3210 RNAi induction (Figure 5-12B, right panel). Both of these, Tb927.7.3210, which is a pseudo-orphan kinase, and TOR1, exhibited loss of fitness proliferation phenotypes in the global RIT-seq study (Alsford et al., 2011). A previous study investigating TOR1 function also found it to be essential for cell growth (Barquilla et al., 2008). It was thought to be part of TORC1 signalling which is required for proper RNA Pol I localisation, protein synthesis and maintenance of appropriate cell growth.

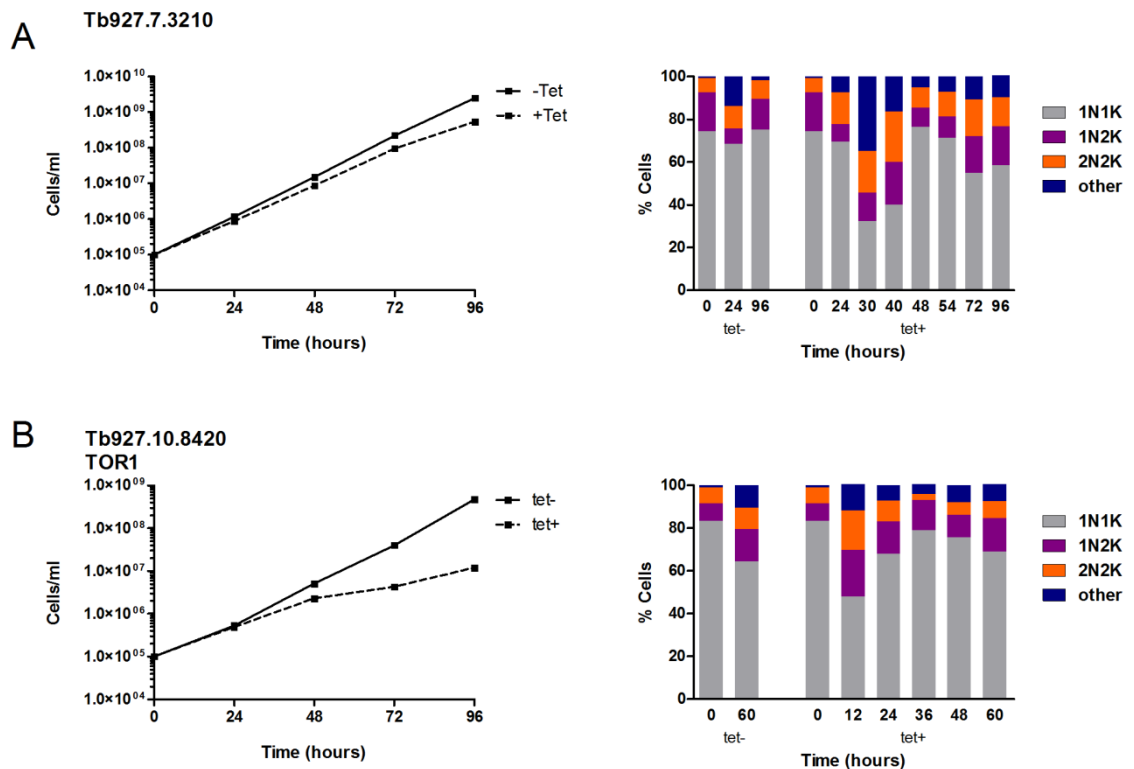


Figure 5-12 - *In vitro* growth and cell cycle analysis for cell lines showing growth and/or cell cycle defects that were unclassified following RNAi induction. A: Tb927.7.3210; B: TOR1. Cumulative growth curves were generated (left) and the numbers of nuclei (N) and kinetoplasts (K) in each cell ($n \geq 200$) following DAPI staining of samples were recorded at the indicated time points post addition of tetracycline to the induced samples (right). Analyses of non-induced cells (tet-) are also shown as controls.

5.7 Discussion

Compared to the outcomes of a previous cell cycle screen (Monnerat et al., 2009) which did not lead to the identification of any novel direct cell cycle regulators despite the use of a genome-wide RNAi library, the screening of the kinome-wide RNAi library of individual cell lines here has been a greater success. Thanks to the efficiency and robustness of the library, the majority of the previously known cell cycle kinases were detected and many novel cell cycle regulators were identified. 25 PKs were detected as potential *T. brucei* cell cycle kinases; this represents 13 % of the *T. brucei* kinome, demonstrating the importance of protein phosphorylation in *T. brucei* cell cycle regulation. At least 15 of these putative cell cycle kinases were detected for the first time - the CMGC kinase Tb927.11.5340, ATR, the AGC kinase, Tb927.3.2440, the CAMK, Tb927.7.6220, the CMGC, Tb927.10.5140, the CMGC/RCK kinase, Tb927.3.690,

CRK9, CK2A1, CLK1, GSK3-short, TLK2, CK1.1 & CK1.2, AUK3, RDK2 and Tb927.11.4470. Almost all of the rest of the kinases reproduced phenotypes, when knocked down, that are in agreement with published literature, thus raising the confidence level of the findings of this screen. Nevertheless, further analyses are required to confirm these phenotypes and further verify their functions. RNAi of a number of these putative cell cycle kinases induced rapid cell death signifying their potential as drug targets. These include the CMGC PKs CRK3, CRK9, CLK1, Tb927.10.5140, Tb927.3.690, the AGC kinase Tb927.3.2440, CK1.1, AUK1, RDK2 and TLK1/2 with CLK1 now being genetically validated as one in a mouse model.

Of the PKs implicated in cell cycle regulation, the majority were deemed to be involved in just cytokinesis or in combination with kinetoplast duplication or mitosis with surprisingly few in G_1/S (Figure 5-13). In other organisms, progression through G_1 phase and G_1/S transition is tightly regulated and involves multiple kinases required to induce the commitment point to enter the cell cycle (e.g. START in yeasts) and begin DNA replication (section 1.3.4.1). Here, the relatively short list of kinases thought to regulate G_1 progression and G_1/S transition suggests that G_1 progression and transition into S phase is less tightly regulated in *T. brucei*. On the other hand, it could be that these kinases are harder to detect via RNAi or that there is much greater redundancy of function between kinases involved in G_1 . The two putative G_1/S kinases identified in this study might represent two decisions the cell needs to make whilst at G_1 : 1) should the cell differentiate into the quiescent stumpy form stage; 2) should the cell commit to entering the cell cycle. Depletion of TOR4 was shown to cause irreversible differentiation of BSF cells to the G_0 stumpy form stage (Barquilla et al., 2012) which was reflected by the rise in 1N1K cells in this study (section 5.6.1.3). TOR4, therefore, would be part of the pathway which decides whether the cell should differentiate into the quiescent stumpy stage cells. Depletion of CRK1 also led to a rise in 1N1K cells. Previous studies showed a rise in G_1 cells and a decrease in S phase cells (X. Tu & Wang, 2004) suggesting that the 1N1K cells seen here are also in G_1 and have failed to progress through to S phase. Further studies monitoring early cell cycle events, such as basal body duplication, would help verify if the pathways involving CRK1 activities are

upstream of those which induce re-entry into the cell cycle and do indeed play a role in the START equivalent in *T. brucei*.

What is also remarkable is the relatively high number of kinases identified to be jointly involved in kinetoplast duplication and cytokinesis suggesting a link between the two events. This link could be explained by what has already been shown in PCF parasites where the replication of cytoskeletal structures such as basal bodies and flagellum are closely linked with cytokinesis (section 1.3.2; Ikeda & de Graffenried, 2012; Lozano-Núñez, Ikeda, Sauer, & de Graffenried, 2013; Wheeler, Scheumann, Wickstead, Gull, & Vaughan, 2013). The importance of the placement of the growing flagellum in establishing the furrow has already been shown (Wheeler et al., 2013). Indeed, when the types of aberrant cells generated following the RNAi of these PKs are closely looked at (section 5.6.1.8), misaligned furrows seem to be the cause of their generation giving credence to this hypothesis.

The PKs, CLK1 and GSK3-short, both of which upon RNAi induction generated a similar phenotype, i.e. concomitant rise in 1N2K and 2N2K cells, were thought to be involved in mitosis and cytokinesis simultaneously suggesting that these kinases are involved in pathways which link these two events. In the case of TLK1 & TLK2 dual knockdown, cytokinesis was found to progress inappropriately despite delayed mitosis. A possibility could be that, with CLK1 and GSK3-short on the one hand and TLK1/TLK2 on the other, represent the two sides of mitosis to cytokinesis transition as promoters and repressors, respectively.

The long list of kinases implicated in BSF *T. brucei* cytokinesis indicates a potentially highly complex regulatory network involved in orchestrating this event. The majority of these kinases do not have cell cycle related homologues in other organisms indicating the possibility of novel pathways being involved in BSF cytokinesis regulation which is not surprising considering the unique cell structure of this parasite compared to other eukaryotic model organisms (section 1.2.2). Furrow analysis, as was performed for CLK1 RNAi cells (Figure 5-10A), could be extended to the rest of the cell lines which presented with cytokinetic defects following knockdown in order to specify which stage of cytokinesis has been perturbed.

Further screens could be done in order to specify the cellular event at which these kinases function to promote cell cycle progression. In cell lines which present kinetoplast duplication defects, early events such as basal body duplication could be followed with the use of organelle specific markers such as anti-Centrin2 antibody (de Graffenried, Anrather, Von Raußendorf, & Warren, 2013) to identify regulators of basal body duplication. There lies a huge potential to extend this library of individual RNAi cell lines to a genome-wide scale. Such a study promises to deliver potential novel cell cycle regulators and enrich current understanding of the cell cycle regulatory network. Automation of end-point analyses of cell cycle screens in *T. brucei*, such as the methodology developed by Wheeler *et al.* (Wheeler *et al.*, 2012), would be essential before undertaking such a project. Automated microscopy would also present us with the opportunity to scrutinize various other aspects of the cell cycle, apart from the nucleus/kinetoplast configuration, such as the morphology of the nucleus or the kinetoplast etc. Other genome-wide approaches could involve employing the RIT-seq approach (Alsford *et al.*, 2011) on a pooled RNAi library following sorting based on DNA content which would identify genes which cause a block at various stages of the cell cycle. Whilst such a method could be successful in identifying regulators at the G₁/S or the G₂/M transitions, other more subtle phenotypes, such as those indicating defects in kinetoplast duplication or cytokinesis, would be missed and further screening would be required.

Whilst the findings of this screen build on our current understanding of the *T. brucei* cell cycle, limitations do exist. An absence of cell cycle phenotype upon RNAi induction does not necessarily eliminate cell cycle functions. Redundancy between PKs could mean that depletion of one would not have a detrimental effect on cells. Subtle effects on the cell cycle or insufficient knockdown could prevent a kinase from being detected. Transient knockdown would allow cells to recover and the potential cell cycle functions of kinases to remain undetected. The major challenge at present lies in placing confirmed *T. brucei* cell cycle regulators in signalling cascades and effector networks, the understanding of which still remains incredibly poor. Phosphoproteomic and chemical genetic approaches could enable the initial identification of potential substrates of these kinases. Such studies, however, would need to be followed up with individual characterisation of potential interactions. Shared phenotypes upon induction of

RNAi of some kinases, even those thought not to be directly involved in cell cycle regulation, could indicate that they are involved in the same pathway and be used as reference points to assemble signalling cascades. The fact that a high proportion of trypanosome PKs are differentially phosphorylated between the bloodstream and procyclic form (Nett et al., 2009; Urbaniak, Martin, & Ferguson, 2013) adds to the burden of work required to thoroughly dissect *T. brucei* cell cycle regulation. It cannot be assumed that what is true for one life-cycle stage would be true for the other.

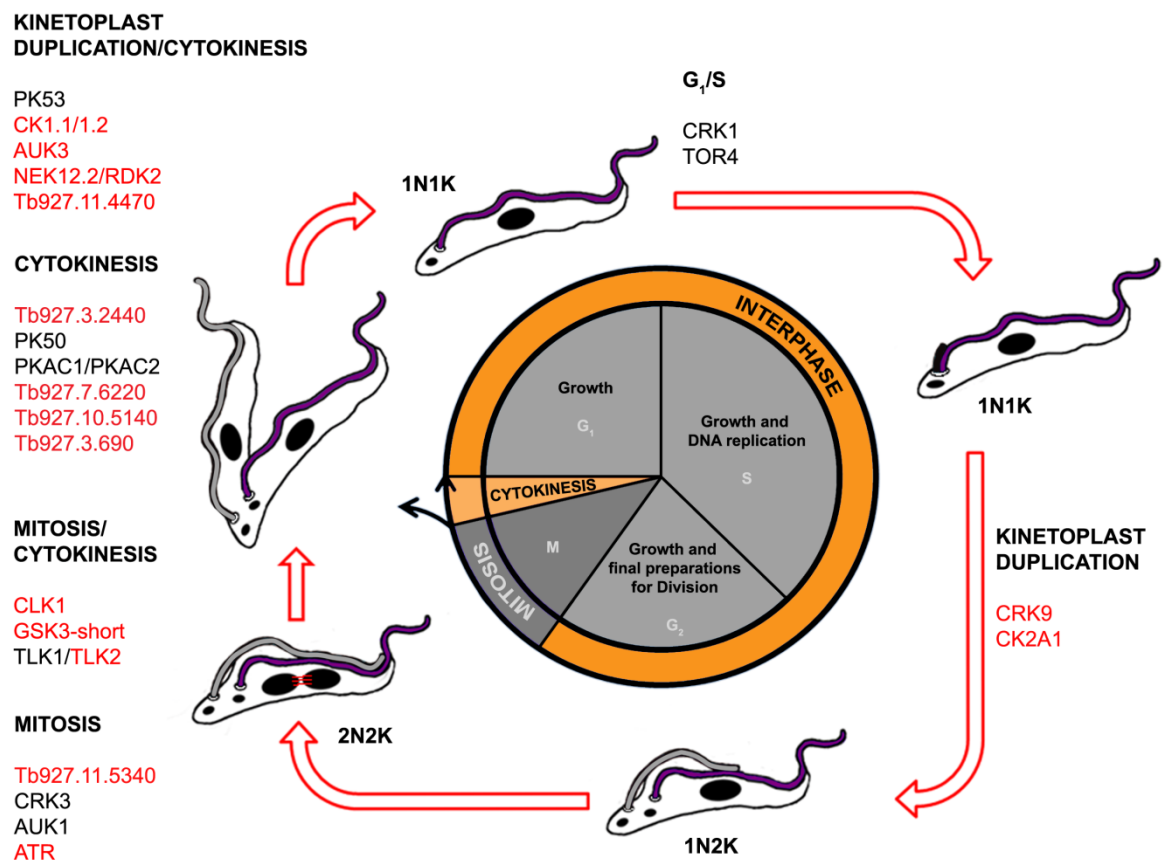


Figure 5-13 Schematic representation of BSF *T. brucei* cell cycle and protein kinases implicated in the regulation of indicated stages of the cell cycle. Protein kinases in red font - novel cell cycle functions identified in this study. Adapted from Jones et al., 2014.

6 General Discussion

Protein kinases (PKs) are an important group of enzymes that are vital participants of signalling cascades. They are required for the regulation of pathways by acting as signal processors, signal transducers and effectors. By post-translationally modifying other proteins, via phosphorylation, they alter the enzymatic activity (when relevant), localisation and binding ability/specificity of their substrates. It is not surprising that PKs play such an important role in a complex cellular process, such as the cell division cycle, which entails environmental sensing, requires strict regulation and involves dynamic structural changes.

The unusual features of *T. brucei* cellular architecture (e.g. the fixed longitudinal arrangement of its single copy organelles or the subpellicular corset of microtubules which define the parasite's shape) and cell cycle mechanisms (e.g. ingression of a cleavage furrow along the length of the cell for cytokinesis) implies divergent regulatory pathways compared to other well-studied eukaryotes, the majority of which are yet unknown. Whilst *T. brucei* homologues of conserved eukaryotic cell cycle regulators are useful starting points for studying the *T. brucei* cell cycle, such approaches are limited in their scope. The divergent nature of trypanosome cell biology has meant failure in detecting putative homologues with known cell cycle functions (e.g. CENP-A; Akiyoshi & Gull, 2013) and, conversely, structural conservation of proteins not equating with shared function (e.g. PLK in *T. brucei* is not known to have a mitotic role yet, unlike its homologues in other eukaryotes; Chapter 3 and 4). Nevertheless, the absence of a putative homologue does not necessarily mean it does not truly exist. It is possible the same role is performed by a protein/proteins with diverged sequences(s), which renders them undetectable by current homology search algorithms. It is also possible that other non-homologous/kinetoplastid specific proteins are fulfilling the same roles. This makes the case for the importance of conducting detailed characterisation of individual proteins, such as PLK (Chapter 3 and 4), and also for employing forward genetic approaches, such as the cell cycle screen described in this thesis (Chapter 5), in understanding the *T. brucei* cell cycle.

6.1 *T. brucei* PLK

PLKs in model eukaryotic organisms are one of the major regulators of the eukaryotic cell division cycle. Crucial roles of PLKs, especially members of the PLK1 subfamily, include progression through mitosis. *T. brucei* PLK (TbPLK) however, has yet to display mitotic localisation or function, demonstrating its divergent role in this protozoan organism. Nevertheless, it was able to complement temperature sensitive yeast knockout mutants confirming it as a functional homologue of the yeast PLK1 member, Cdc5. Divergence in function may simply be due to the differences in the cellular environment, although this needs to be investigated further. Detailed dissection of TbPLK function identified its role in the faithful segregation of the basal bodies, the bilobe, the Golgi and the FAZ, the impairment of which leads to defective kinetoplast duplication and flagellum inheritance in procyclic form (PCF) cells (de Graffenried et al., 2008; Hammarton et al., 2007a; Ikeda and de Graffenried, 2012; Lozano-Núñez et al., 2013). Studies investigating its role in bloodstream form (BSF) parasites indicated its role in kinetoplast division which could also be linked to defective basal body segregation, although this has not been looked into (Hammarton et al., 2007a). Knockdown of PLK in BSF cells also gave the additional phenotype of impaired ingression of the cleavage furrow thereby linking BSF kinetoplast duplication and cytokinesis together. Further investigations are needed to define this link.

The focus of part of the studies reported here have been to understand how TbPLK activity is regulated. Considering that TbPLK features largely conserved domains, i.e. N-terminal kinase domain and C-terminal polo-box domain, the working hypothesis was that the regulatory features of PLK1 members, as identified in other eukaryotes, have also been retained in *T. brucei*. Studies were conducted in both PCF and BSF parasites although the majority of the work focussed on the insect stage cells. This was due to the already established expression assay demonstrated in PCF cells (Hammarton et al., 2007a) that had not yet been attempted in BSF cells. Expression of wild-type (WT) TbPLK in PCF cells was found to generate growth and cell cycle defects whilst expression of the kinase dead version did not. This provided the basis by which the kinase activity of TbPLK variants could be assessed. Also, modification of the expression

vector, to add a YFP tag at the N-terminus, allowed localisation of the expressed proteins.

6.1.1 Procyclic stage

Overall, the experiments carried out in PCF parasites demonstrated that some aspects of PLK1 regulation are conserved in TbPLK. A conserved threonine residue, T198, in the regulatory T-loop of the kinase domain, was shown to require phosphorylation for the kinase activity of the protein. Another conserved threonine residue, T202, was also shown to be essential for TbPLK kinase activity; however, the question of whether phosphorylation of this residue is the means by which it regulates TbPLK activity could not be answered directly in these experiments. Indeed mutating this residue at all seemed to obliterate the activating capability of T198, suggesting T202's dominant role in maintaining TbPLK kinase activity. Since T202 is part of the highly conserved regulatory T-loop of the kinase domain, a closer look at the available structures of this region in other homologues could provide the answers needed.

Further experiments employing truncation of TbPLK demonstrated the joint importance of the kinase domain and PBD in the spatial regulation of TbPLK. The localising role of the PBD is conserved in PLKs studied so far. The additional requirement for an active kinase domain for appropriate localisation could be a structural issue. It also means that TbPLK, similar to its metazoan counterparts, is likely to phospho-prime its own substrates before binding to them and that this is a major mode of TbPLK spatial regulation. However, none of the residues required for phospho-peptide binding are conserved in TbPLK. Also, a putative His-Lys pincer required normally required for substrate binding by homologues does not appear to be essential for TbPLK kinase activity. This suggests a divergent mode of TbPLK PBD-substrate binding making a strong case for elucidating TbPLK's protein structure to provide the answers needed.

TbPLK was also found to possess a putative destruction box and experiments involving further truncations indicated that this domain is functional and that TbPLK might be subjected to proteosomal degradation as a means to temporally regulate its presence. This could be cell cycle dependent and further studies

would be needed to explore this possibility. The discovery of a functional NLS motif as a result of the truncation studies raises the question of whether TbPLK does localise in the nucleus in a manner yet to be detected and if this motif has a functional role at all.

A significant proportion of the questions addressed in these studies in PCF cells were covered in reports (Sun and Wang, 2011; Yu et al., 2012) published during the course of this research project undermining the impact of this study. Nonetheless, the majority of the findings of these reports have been corroborated here, despite differences in methodologies. However, some discrepancies do exist, notably in the questions regarding the importance of T202 phosphorylation in TbPLK. It is difficult to reconcile this at the moment and further studies are needed to do so.

6.1.2 Bloodstream form

Expression of TbPLK in BSF cells, both WT and kinase dead versions, had no effect on their growth or cell cycle. This meant that an expression assay could not be set up as was done in PCF parasites. Therefore, another approach was needed to ask how TbPLK is regulated in the bloodstream stage. To do this, attempts were made to set up an RNA interference (RNAi) complementation assay. Ectopic expression of WT TbPLK only partially rescued the debilitating growth and cell cycle defects generated by *TbPLK* RNAi. This limited the scope of the assay. Also, efforts to confirm knockdown of endogenous TbPLK in the cell lines featuring ectopic expression of TbPLK variants in *TbPLK* RNAi background, via Western blotting, were not successful and would need to be addressed in future studies. Nevertheless, assuming that knockdown of endogenous TbPLK was successful, some general observations could be made. The T198 residue is important for TbPLK activity in BSF parasites. However, without analysing the effects of T198D mutation (which mimics phosphorylation), it could not be directly verified if it is the phosphorylation state of this residue which modulates TbPLK activity. Evidence of differential regulation of TbPLK between the two life cycle stages was also seen. The putative His-Lys pincer seems to be required for TbPLK regulation in BSF cells but not in PCF parasites. Also, BSF cells seem to be more sensitive to deregulated TbPLK compared to PCF parasites. This could

be due to the differences in the roles cell cycle regulators, such as TbPLK, play in the two life cycle stages as a result of differences between their cell cycle mechanisms.

6.2 *T. brucei* cell cycle regulation by protein kinases

The advent of RNAi in trypanosomes, and the publication of *T. brucei* genome (Berriman et al., 2005), has enabled rapid discovery of potential cell cycle regulators and effectors, including PKs. The success of the screen conducted as part of this study (Chapter 5) in identifying known/novel cell cycle regulators reflects the huge improvements made in these RNAi systems to make them more robust, efficient and reliable. Modifying the existing pRPA^{ISL} for rapid recombineering to generate stem-loop RNAi constructs has enabled the production of a library of a couple of hundred RNAi plasmids individually targeting the whole complement of the *T. brucei* kinome (Jones et al., 2014). The pRPA^{ISL} system was designed for use in BSF cells that were adapted to ensure stable transfection of constructs into a single rRNA locus, thus enabling reliable knockdown of most of the targets (Alsford and Horn, 2008). The resulting kinome-wide RNAi library of BSF cell lines, therefore, promised to be a reliable resource for identifying cell cycle PK regulators at this clinically relevant life cycle stage. PKs that were considered to be important for BSF growth and replication, following an Alamar Blue screen of the library (Jones et al., 2014), were then analysed via growth curves and DAPI staining to identify PKs required for cell cycle progression. Many known regulators in BSF and a number of novel PKs were identified, satisfying the objectives of this screen. Closely following the types of aberrant cells (based on their nuclear and kinetoplast configurations) generated, has been greatly informative in identifying how these potential regulators are involved in enabling BSF *T. brucei* cell cycle progression.

25 PKs belonging to the AGC, CMGC, CK and 'Other' families were identified to be required for a number of cell cycle stages: G₁/S transition, kinetoplast duplication, mitosis and cytokinesis. A number of kinases were found to potentially have joint roles in mitosis and cytokinesis or kinetoplast duplication and cytokinesis thereby hinting at putative links between these processes. Individually characterising these kinases, with aims to uncover their interacting

partners, would shed light on how BSF *T. brucei* ensures the timing of its cell cycle events. Signalling pathways which promote *T. brucei* cell cycle progression are largely unknown and grouping proteins thought to be involved in similar cell cycle functions would be good starting points in uncovering such pathways. Efforts need to be made to go beyond identifying generalised putative cell cycle functions, to specify the mechanisms by which these PKs, and other proteins, impact the cell cycle. Conditional knockout systems can be a useful method for dissecting how individual PKs are themselves regulated and to characterise their interactions with other proteins (de Graffenried et al., 2013). Chemical genetics or the use of selective inhibitors can be used to dissect the temporal role of PKs as cell cycle regulators (Lozano-Núñez et al., 2013) and, in conjunction with phosphoproteomics, can be used to identify downstream substrates. Phosphosite-specific antibodies could be developed to systematically interrogate the kinome-wide RNAi library for PKs which phosphorylate a residue of interest. Technologies such as TAP-tagging (Monnerat et al., 2013) and BioID (Morriswood et al., 2013) are other effective tools that can be used to identify interacting partners.

The divergence and essentiality of many of these cell cycle regulators makes them attractive targets for novel drug development. Follow up work developing *in vitro* activity assays and determining protein structures is important to enable their progression through the drug development pipeline. The collective findings of candidate gene based studies so far have reported the functional differences of cell cycle regulators between the procyclic and bloodstream life cycle stages; e.g. TbPLK (Hammarton et al., 2007a), Wee1 (this study and Boynak et al., 2013) or CRK9 (Badjatia et al., 2013; Gourguechon and Wang, 2009). It is already known that differences in cell cycle mechanisms exist as evident by the fact that the dissociation between mitosis and cytokinesis seen in PCF cells is not found in BSF parasites. Therefore, extending the cell cycle screen performed here and carrying out follow up studies in the PCF stages would be hugely informative in understanding such differences.

References

- Agaisse, H., Burrack, L. S., Philips, J. A., Rubin, E. J., Perrimon, N., & Higgins, D. E. (2005). Genome-wide RNAi screen for host factors required for intracellular bacterial infection. *Science*, 309(5738), 1248-51.
- Akiyoshi, B., & Gull, K. (2013). Evolutionary cell biology of chromosome segregation: insights from trypanosomes. *Open Biology*, 3(5), 130023.
- Alibu, V. P., Storm, L., Haile, S., Clayton, C., & Horn, D. (2005). A doubly inducible system for RNA interference and rapid RNAi plasmid construction in *Trypanosoma brucei*. *Molecular and Biochemical Parasitology*, 139(1), 75-82.
- Alsford, S., Eckert, S., Baker, N., Glover, L., Sanchez-Flores, A., Leung, K.F., Turner, D.J., Field, M.C., Berriman, M. & Horn, D. (2012). High-throughput decoding of antitrypanosomal drug efficacy and resistance. *Nature*, 482(7384), 232-6.
- Alsford, S., Field, M. C., & Horn, D. (2013). Receptor-mediated endocytosis for drug delivery in African trypanosomes: fulfilling Paul Ehrlich's vision of chemotherapy. *Trends in Parasitology*, 29(5), 207-12.
- Alsford, S., & Horn, D. (2008). Single-locus targeting constructs for reliable regulated RNAi and transgene expression in *Trypanosoma brucei*. *Molecular and Biochemical Parasitology*, 161(1), 76-9.
- Alsford, S., Kawahara, T., Glover, L., & Horn, D. (2005). Tagging a *T. brucei* RRNA locus improves stable transfection efficiency and circumvents inducible expression position effects. *Molecular and Biochemical Parasitology*, 144(2), 142-8.
- Alsford, S., Turner, D.J., Obado, S.O., Sanchez-Flores, A., Glover, L., Berriman, M., Hertz-Fowler, C. & Horn, D. (2011). High-throughput phenotyping using parallel sequencing of RNA interference targets in the African trypanosome. *Genome Research*, 21(6), 915-24.
- Alvarez, B., Martínez-A, C., Burgering, B. M. T., Carrera, A. C., & Martinez, A. (2001). Forkhead transcription factors contribute to execution of the mitotic programme in mammals. *Nature*, 413(6857), 744-747.
- Ando, K., Ozaki, T., Yamamoto, H., Furuya, K., Hosoda, M., Hayashi, S., Fukuzawa, M. & Nakagawara, A. (2004). Polo-like kinase 1 (Plk1) inhibits p53 function by physical interaction and phosphorylation. *The Journal of Biological Chemistry*, 279(24), 25549-61.
- Andrysik, Z., Bernstein, W.Z., Deng, L., Myer, D.L., Li, Y.-Q., Tischfield, J.A., Stambrook, P.J. & Bahassi, E. M. (2010). The novel mouse Polo-like kinase 5 responds to DNA damage and localizes in the nucleolus. *Nucleic Acids Research*, 38(9), 2931-43.

- Archambault, V., D'Avino, P. P., Deery, M. J., Lilley, K. S., & Glover, D. M. (2008). Sequestration of Polo kinase to microtubules by phosphoprimer-independent binding to Map205 is relieved by phosphorylation at a CDK site in mitosis. *Genes & Development*, 22(19), 2707-20.
- Archambault, V., & Glover, D. M. (2009). Polo-like kinases: conservation and divergence in their functions and regulation. *Nature Reviews. Molecular Cell Biology*, 10(4), 265-275.
- Babokhov, P., Sanyaolu, A. O., Oyibo, W. A., Fagbenro-Beyioku, A. F., & Iriemenam, N. C. (2013). A current analysis of chemotherapy strategies for the treatment of human African trypanosomiasis. *Pathogens and Global Health*, 107(5), 242-52.
- Bader, J. R., Kasuboski, J. M., Winding, M., Vaughan, P. S., Hinchcliffe, E. H., & Vaughan, K. T. (2011). Polo-like kinase1 is required for recruitment of dynein to kinetochores during mitosis. *The Journal of Biological Chemistry*, 286(23), 20769-77.
- Badjatia, N., Ambrósio, D. L., Lee, J. H., & Günzl, A. (2013). Trypanosome cdc2-related kinase 9 controls spliced leader RNA cap4 methylation and phosphorylation of RNA polymerase II subunit RPB1. *Molecular and Cellular Biology*, 33(10), 1965-75.
- Bahassi, E. M. (2011). Polo-like kinases and DNA damage checkpoint: beyond the traditional mitotic functions. *Experimental Biology and Medicine*, 236(6), 648-57.
- Bähler, J., Steever, A. B., Wheatley, S., Wang, Y. I., Pringle, J. R., Gould, K. L., & McCollum, D. (1998). Role of polo kinase and Mid1p in determining the site of cell division in fission yeast. *The Journal of Cell Biology*, 143(6), 1603-16.
- Bakal, C., Linding, R., Llense, F., Heffern, E., Martin-Blanco, E., Pawson, T., & Perrimon, N. (2008). Phosphorylation networks regulating JNK activity in diverse genetic backgrounds. *Science*, 322(5900), 453-6.
- Baker, N., Alsford, S., & Horn, D. (2011). Genome-wide RNAi screens in African trypanosomes identify the nifurtimox activator NTR and the eflornithine transporter AAT6. *Molecular and Biochemical Parasitology*, 176(1), 55-7.
- Baker, N., de Koning, H. P., Mäser, P., & Horn, D. (2013). Drug resistance in African trypanosomiasis: the melarsoprol and pentamidine story. *Trends in Parasitology*, 29(3), 110-8.
- Balasegaram, M., Young, H., Chappuis, F. F., Priotto, G., Raguenaud, M.-E. E., & Checchi, F. (2009). Effectiveness of melarsoprol and eflornithine as first-line regimens for gambiense sleeping sickness in nine Medecins Sans Frontieres programmes. *Transactions of the Royal Society of Tropical Medicine and Hygiene*, 103(3), 280-290.

- Balasubramanian, M. K., Bi, E., & Glotzer, M. (2004). Comparative analysis of cytokinesis in budding yeast, fission yeast and animal cells. *Current Biology*, 14(18), R806-R818.
- Bandeiras, T.M., Hillig, R.C., Matias, P.M., Eberspaecher, U., Fanghänel, J., Thomaz, M., Miranda, S., Crusius, K., Pütter, V., Amstutz, P., Gulotti-Georgieva, M., Binz, H.K., Holz, C., Schmitz, A. a P., Lang, C., Donner, P., Egner, U., Carrondo, M. A., & Müller-Tiemann, B. (2008). Structure of wild-type Plk-1 kinase domain in complex with a selective DARPIn. *Acta Crystallographica. Section D, Biological Crystallography*, 64(Pt 4), 339-53.
- Barnes, R. L., Shi, H., Kolev, N. G., Tschudi, C., & Ullu, E. (2012). Comparative genomics reveals two novel RNAi factors in *Trypanosoma brucei* and provides insight into the core machinery. *PLoS Pathogens*, 8(5), e1002678.
- Barquilla, A., Crespo, J. L., & Navarro, M. (2008). Rapamycin inhibits trypanosome cell growth by preventing TOR complex 2 formation. *Proceedings of the National Academy of Sciences of the United States of America*, 105(38), 14579-84.
- Barquilla, A., Saldivia, M., Diaz, R., Bart, J.-M., Vidal, I., Calvo, E., Hall, M.N., & Navarro, M. (2012). Third target of rapamycin complex negatively regulates development of quiescence in *Trypanosoma brucei*. *Proceedings of the National Academy of Sciences of the United States of America*, 109(36), 14399-404.
- Barr, F. A., & Gruneberg, U. (2007). Cytokinesis: Placing and Making the Final Cut. *Cell*, 131(5), 847-860.
- Barr, F. A., Sillje, H. H. W., Nigg, E. A., & Silljé, H. H. W. (2004). Polo-like kinases and the orchestration of cell division. *Nature Reviews. Molecular Cell Biology*, 5(6), 429-441.
- Barrett, M. P., Boykin, D. W., Brun, R., & Tidwell, R. R. (2007). Human African trypanosomiasis: pharmacological re-engagement with a neglected disease. *British Journal of Pharmacology*, 152(8), 1155-1171.
- Barrientes, S., Cooke, C., & Goodrich, D. W. (2000). Glutamic acid mutagenesis of retinoblastoma protein phosphorylation sites has diverse effects on function. *Oncogene*, 19(4), 562-70.
- Barth, P. (1989). A new method for the isolation of the trypanocidal factor from normal human serum. *Acta Tropica*, 46(1), 71-3.
- Bastin, P., Bagherzadeh, A., Matthews, K. R., Gull, K., & Bagherzadeh, Z. (1996). A novel epitope tag system to study protein targeting and organelle biogenesis in *Trypanosoma brucei*. *Molecular and Biochemical Parasitology*, 77(2), 235-9.
- Bastin, P., Pullen, T. J., Moreira-Leite, F. F., & Gull, K. (2000). Inside and outside of the trypanosome flagellum: a multifunctional organelle. *Microbes and Infection / Institut Pasteur*, 2(15), 1865-74.

- Beach, D., Durkacz, B., & Nurse, P. (1982). Functionally homologous cell cycle control genes in budding and fission yeast. *Nature*, 300(5894), 706-9.
- Bernstein, E., Caudy, A. A., Hammond, S. M., & Hannon, G. J. (2001). Role for a bidentate ribonuclease in the initiation step of RNA interference. *Nature*, 409(6818), 363-6.
- Beroza, P., Villar, H. O., Wick, M. M., & Martin, G. R. (2002). Chemoproteomics as a basis for post-genomic drug discovery. *Drug Discovery Today*, 7(15), 807-814.
- Berriman, M., Ghedin, E., Hertz-Fowler, C., Blandin, G., Lennard, N.J., Bartholomeu, D.C., Renault, H.J., Caler, E., Hamlin, N.E., Haas, B., Harris, B.R., Hannick, L., Barrell, B.G., Donelson, J.E., Hall, N., Fraser, C.M., Melville, S.E., El Sayed, N.M., Bohme, U.C., Shallom, J., Aslett, M.A., Hou, L., Atkin, B., Barron, A.J., Bringaud, F., Brooks, K., Cherevach, I., Chillingworth, T.J., Churcher, C., Clark, L.N., Corton, C.H., Cronin, A., Davies, R.M., Doggett, J., Djikeng, A., Feldblyum, T., Fraser, A., Goodhead, I., Hance, Z., Harper, A.D., Hauser, H., Hostetler, J., Jagels, K., Johnson, D., Johnson, J., Jones, C., Kerhornou, A.X., Koo, H., Larke, N., Larkin, C., Leech, V., Line, A., MacLeod, A., Mooney, P.J., Moule, S., Mungall, K., Norbertczak, H., Ormond, D., Pai, G., Peterson, J., Quail, M.A., Rajandream, M.A., Reitter, C., Sanders, M., Schobel, S., Sharp, S., Simmonds, M., Simpson, A.J., Tallon, L., Turner, C.M.M., Tait, A., Tivey, A.R., Van Aken, S., Walker, D., Wanless, D., White, B., White, O., Whitehead, S., Wortman, J., Barry, J.D.D., Fairlamb, A.H., Field, M.C., Gull, K., Landfear, S., Marcello, L., Martin, D.M.A., Opperdoes, F., Ullu, E., Whickstead, B., Alsmark, C., Arrowsmith, C., Carrington, M., Embley, T.M.M., Ivens, A., Lord, A., Morgan, G.M.W., Peacock, C.S., Rabinowitsch, E., Salzberg, S.L., Wang, S., Woodward, J., Adams, M.D., Böhme, U., Wickstead, B., Alsmark, U.C., Atkin, R.J., Harper, D., & Jones, K. (2005). The genome of the African trypanosome, *Trypanosoma brucei*. *Science*, 309(5733), 416-422.
- Bessat, M., & Ersfeld, K. (2009). Functional characterization of cohesin SMC3 and separase and their roles in the segregation of large and minichromosomes in *Trypanosoma brucei*. *Molecular Microbiology*, 71(6), 1371-85.
- Bettencourt-Dias, M., Giet, R., Sinka, R., Mazumdar, A., Lock, W.G., Balloux, F., Zafiropoulos, P.J., Yamaguchi, S., Winter, S., Carthew, R.W., Cooper, M., Jones, D., Frenz, L. & Glover, D. M. (2004). Genome-wide survey of protein kinases required for cell cycle progression. *Nature*, 432(7020), 980-7.
- Bettencourt-Dias, M., Rodrigues-Martins, A., Carpenter, L., Riparbelli, M., Lehmann, L., Gatt, M.K., Carmo, N., Balloux, F., Callaini, G. & Glover, D. M. (2005). SAK/PLK4 is required for centriole duplication and flagella development. *Current Biology: CB*, 15(24), 2199-207.
- Biebinger, S., Rettenmaier, S., Flaspohler, J., Hartmann, C., Pena-Diaz, J., Wirtz, L. E. & Peña-Diaz, J. (1996). The PARP promoter of *Trypanosoma brucei* is developmentally regulated in a chromosomal context. *Nucleic Acids Res*, 24(0305-1048 (Print)), 1202-1211.

- Biebinger, S., Wirtz, L. E., Lorenz, P., & Clayton, C. (1997). Vectors for inducible expression of toxic gene products in bloodstream and procyclic *Trypanosoma brucei*. *Molecular and Biochemical Parasitology*, 85(0166-6851 (Print)), 99-112.
- Bitton, R.J., Figg, W.D., Venzon, D.J., Dalakas, M.C., Bowden, C., Headlee, D., Reed, E., Myers, C.E., D. & Cooper, M. R. (1995). Pharmacologic variables associated with the development of neurologic toxicity in patients treated with suramin. *Journal of Clinical Oncology: Official Journal of the American Society of Clinical Oncology*, 13(9), 2223-9.
- Björklund, M., Taipale, M., Varjosalo, M., Saharinen, J., Lahdenperä, J., & Taipale, J. (2006). Identification of pathways regulating cell size and cell-cycle progression by RNAi. *Nature*, 439(7079), 1009-13.
- Bonhivers, M., Nowacki, S., Landrein, N., & Robinson, D. R. (2008). Biogenesis of the trypanosome endo-exocytotic organelle is cytoskeleton mediated. *PLoS Biology*, 6(5), e105.
- Booher, R. N., Holman, P. S., & Fattaey, A. (1997). Human Myt1 is a cell cycle-regulated kinase that inhibits cdc2 but not Cdk2 activity. *Journal of Biological Chemistry*, 272(35), 22300-22306.
- Boucher, N., Dacheux, D., Giroud, C., & Baltz, T. (2007). An essential cell cycle-regulated nucleolar protein relocates to the mitotic spindle where it is involved in mitotic progression in *Trypanosoma brucei*. *The Journal of Biological Chemistry*, 282(18), 13780-90.
- Boutros, M., Kiger, A. A., Armknecht, S., Kerr, K., Hild, M., Koch, B. & Perrimon, N. (2004). Genome-wide RNAi analysis of growth and viability in *Drosophila* cells. *Science*, 303(5659), 832-5.
- Boynak, N. Y., Rojas, F., D'Alessio, C., Vilchez Larrea, S. C., Rodriguez, V., Ghiringhelli, P. D., & Téllez-Iñón, M. T. (2013). Identification of a Wee1-like kinase gene essential for procyclic *Trypanosoma brucei* survival. *PloS One*, 8(11), e79364.
- Bräuninger, A., Strebhardt, K., & Rübsamen-Waigmann, H. (1995). Identification and functional characterization of the human and murine polo-like kinase (Plk) promoter. *Oncogene*, 11(9), 1793-800.
- Brennan, I. M., Peters, U., Kapoor, T. M., & Straight, A. F. (2007). Polo-like kinase controls vertebrate spindle elongation and cytokinesis. *PLoS ONE*, 2(5), e409.
- Briggs, L. J., McKean, P. G., Baines, A., Moreira-Leite, F., Davidge, J., Vaughan, S., & Gull, K. (2004). The flagella connector of *Trypanosoma brucei*: an unusual mobile transmembrane junction. *Journal of Cell Science*, 117(9), 1641-1651.
- Brown, A. M. C. (2005). Canonical Wnt signaling: high-throughput RNAi widens the path. *Genome Biology*, 6(9), 231.

- Bruinsma, W., Macurek, L., Freire, R., Lindqvist, A., & Medema, R. H. (2014). Bora and Aurora-A continue to activate Plk1 in mitosis. *Journal of Cell Science*, 127(Pt 4), 801-11.
- Brun, R., Schonenberger, & Schönenberger. (1979). Cultivation and in vitro cloning or procyclic culture forms of *Trypanosoma brucei* in a semi-defined medium. Short communication. *Acta Tropica*, 36(3), 289-92.
- Buchholz, F., Kittler, R., Slabicki, M., & Theis, M. (2006). Enzymatically prepared RNAi libraries. *Nature Methods*, 3(9), 696-700.
- Bülow, R., Nonnengässer, C., & Overath, P. (1989). Release of the variant surface glycoprotein during differentiation of bloodstream to procyclic forms of *Trypanosoma brucei*. *Molecular and Biochemical Parasitology*, 32(1), 85-92.
- Burkard, M. E., Randall, C. L., Larochelle, S., Zhang, C., Shokat, K. M., Fisher, R. P., & Jallepalli, P. V. (2007). Chemical genetics reveals the requirement for Polo-like kinase 1 activity in positioning RhoA and triggering cytokinesis in human cells. *Proceedings of the National Academy of Sciences*, 104(11), 4383-4388.
- Burri, C. (2010). Chemotherapy against human African trypanosomiasis: Is there a road to success? *Parasitology*, 137(Special Issue 14), 1987-1994.
- Capewell, P., Veitch, N. J., Turner, C. M. R., Raper, J., Berriman, M., Hajduk, S. L., & MacLeod, A. (2011). Differences between *Trypanosoma brucei gambiense* groups 1 and 2 in their resistance to killing by trypanolytic factor 1. *PLoS Neglected Tropical Diseases*, 5(9), e1287.
- Carmena, M., Wheelock, M., Funabiki, H., & Earnshaw, W. C. (2012). The chromosomal passenger complex (CPC): from easy rider to the godfather of mitosis. *Nature Reviews. Molecular Cell Biology*, 13(12), 789-803.
- Casenghi, M., Barr, F. A., & Nigg, E. A. (2005). Phosphorylation of Nlp by Plk1 negatively regulates its dynein-dynactin-dependent targeting to the centrosome. *Journal of Cell Science*, 118(21), 5101-5108.
- Casenghi, M., Meraldi, P., Weinhart, U., Duncan, P. I., Körner, R., & Nigg, E. A. (2003). Polo-like kinase 1 regulates Nlp, a centrosome protein involved in microtubule nucleation. *Developmental Cell*, 5(1), 113-125.
- Chan, K. Y., & Ersfeld, K. (2010). The role of the Kinesin-13 family protein TbKif13-2 in flagellar length control of *Trypanosoma brucei*. *Molecular and Biochemical Parasitology*, 174(2), 137-40.
- Chase, D., Golden, A., Heidecker, G., & Ferris, D. K. (2000). *Caenorhabditis elegans* contains a third polo-like kinase gene. *DNA Sequence: The Journal of DNA Sequencing and Mapping*, 11(3-4), 327-34.
- Chase, D., Serafinas, C., Ashcroft, N., Kosinski, M., Longo, D., Ferris, D. K., & Golden, A. (2000). The polo-like kinase PLK-1 is required for nuclear

envelope breakdown and the completion of meiosis in *Caenorhabditis elegans*. *Genesis*, 26(1), 26-41.

Cheng, K.-Y., Lowe, E. D., Sinclair, J., Nigg, E. A., & Johnson, L. N. (2003). The crystal structure of the human polo-like kinase-1 polo box domain and its phospho-peptide complex. *The EMBO Journal*, 22(21), 5757-68.

Clay, F. J., McEwen, S. J., Bertoncetto, I., Wilks, A. F., & Dunn, A. R. (1993). Identification and cloning of a protein kinase-encoding mouse gene, Plk, related to the polo gene of *Drosophila*. *Proceedings of the National Academy of Sciences of the United States of America*, 90(11), 4882-4886.

Coley, A. F., Dodson, H. C., Morris, M. T., & Morris, J. C. (2011). Glycolysis in the african trypanosome: targeting enzymes and their subcellular compartments for therapeutic development. *Molecular Biology International*, 2011, 123702.

Cooke, C. A., Heck, M. M., & Earnshaw, W. C. (1987). The inner centromere protein (INCENP) antigens: movement from inner centromere to midbody during mitosis. *The Journal of Cell Biology*, 105(5), 2053-67.

Courtin, D., Berthier, D., Thevenon, S., Dayo, G.-K., Garcia, A., & Bucheton, B. (2008). Host genetics in African trypanosomiasis. *Infection, Genetics and Evolution: Journal of Molecular Epidemiology and Evolutionary Genetics in Infectious Diseases*, 8(3), 229-38.

Coverley, D., Pelizon, C., Trewick, S., & Laskey, R. A. (2000). Chromatin-bound Cdc6 persists in S and G2 phases in human cells, while soluble Cdc6 is destroyed in a cyclin A-cdk2 dependent process. *Journal of Cell Science*, 113(Pt 1), 1929-38.

De Cárcer, G., Escobar, B., Higuero, A.M., García, L., Ansóñ, A., Pérez, G., Mollejo, M., Manning, G., Meléndez, B., Abad-Rodríguez, J. & Malumbres, M. (2011). Plk5, a polo box domain-only protein with specific roles in neuron differentiation and glioblastoma suppression. *Molecular and Cellular Biology*, 31(6), 1225-39.

De Cárcer, G., Manning, G., & Malumbres, M. (2011). From Plk1 to Plk5: functional evolution of polo-like kinases. *Cell Cycle*, 10(14), 2255-62.

De Graffenried, C. L., Anrather, D., Von Raußendorf, F., & Warren, G. (2013). Polo-like kinase phosphorylation of bilobe-resident TbCentrin2 facilitates flagellar inheritance in *Trypanosoma brucei*. *Molecular Biology of the Cell*, 24(12), 1947-63.

De Graffenried, C. L., Ho, H. H., & Warren, G. (2008). Polo-like kinase is required for Golgi and bilobe biogenesis in *Trypanosoma brucei*. *The Journal of Cell Biology*, 181(3), 431-438.

De Greef, C., Imberechts, H., Matthyssens, G., Van Meirvenne, N., & Hamers, R. (1989). A gene expressed only in serum-resistant variants of *Trypanosoma brucei rhodesiense*. *Molecular and Biochemical Parasitology*, 36(2), 169-76.

- De Koning, H. P. (2001). Uptake of pentamidine in *Trypanosoma brucei brucei* is mediated by three distinct transporters: implications for cross-resistance with arsenicals. *Molecular Pharmacology*, 59(3), 586-92.
- De Koning, H. P., & Jarvis, S. M. (2001). Uptake of pentamidine in *Trypanosoma brucei brucei* is mediated by the P2 adenosine transporter and at least one novel, unrelated transporter. *Acta Tropica*, 80(3), 245-50.
- Denise, H., & Barrett, M. P. (2001). Uptake and mode of action of drugs used against sleeping sickness. *Biochemical Pharmacology*, 61(1), 1-5.
- Descombes, P., & Nigg, E. A. (1998). The polo-like kinase Plx1 is required for M phase exit and destruction of mitotic regulators in *Xenopus* egg extracts. *EMBO J*, 17(5), 1328-1335.
- Ding, S.-W., Li, H., Lu, R., Li, F., & Li, W.-X. (2004). RNA silencing: a conserved antiviral immunity of plants and animals. *Virus Research*, 102(1), 109-15.
- Do Carmo Avides, M., & Glover, D. M. (1999). Abnormal spindle protein, Asp, and the integrity of mitotic centrosomal microtubule organizing centers. *Science*, 283(5408), 1733-5.
- Dobbelaere, J., Josué, F., Suijkerbuijk, S., Baum, B., Tapon, N., & Raff, J. (2008). A genome-wide RNAi screen to dissect centriole duplication and centrosome maturation in *Drosophila*. *PLoS Biology*, 6(9), e224.
- Domenicali-Pfister, D., Burkard, G., Morand, S., Renggli, C. K., Roditi, I., & Vassella, E. (2006). A mitogen-activated protein kinase controls differentiation of bloodstream forms of *Trypanosoma brucei*. *Eukaryotic Cell*, 5(7), 1126-35.
- Donaldson, M. M., Tavares, A. A., Ohkura, H., Deak, P., & Glover, D. M. (2001). Metaphase arrest with centromere separation in polo mutants of *Drosophila*. *The Journal of Cell Biology*, 153(4), 663-76.
- Donohue, P. J., Alberts, G. F., Guo, Y., & Winkles, J. A. (1995). Identification by targeted differential display of an immediate early gene encoding a putative serine/threonine kinase. *The Journal of Biological Chemistry*, 270(17), 10351-7.
- Doua, F., & Yapo, F. B. (1993). Human trypanosomiasis in the Ivory Coast: therapy and problems. *Acta Tropica*, 54(3-4), 163-8.
- Drew, M. E., Morris, J. C., Wang, Z., Wells, L., Sanchez, M., Landfear, S. M., & Englund, P. T. (2003). The adenosine analog tubercidin inhibits glycolysis in *Trypanosoma brucei* as revealed by an RNA interference library. *The Journal of Biological Chemistry*, 278(47), 46596-600.
- Dulla, K., Daub, H., Hornberger, R., Nigg, E. A., & Körner, R. (2010). Quantitative site-specific phosphorylation dynamics of human protein kinases during mitotic progression. *Molecular & Cellular Proteomics : MCP*, 9(6), 1167-81.

- Duncan, P. I., Pollet, N., Niehrs, C., & Nigg, E. A. (2001). Cloning and characterization of Plx2 and Plx3, two additional polo-like kinases from *Xenopus laevis*. *Experimental Cell Research*, 270(1), 78-87.
- Dunphy, W. G. (1994). The decision to enter mitosis. *Trends in Cell Biology*, 4(6), 202-7.
- Durand-Dubief, M., & Bastin, P. (2003). TbAGO1, an argonaute protein required for RNA interference, is involved in mitosis and chromosome segregation in *Trypanosoma brucei*. *BMC Biology*, 1, 2.
- Durand-Dubief, M., Kohl, L., & Bastin, P. (2003). Efficiency and specificity of RNA interference generated by intra- and intermolecular double stranded RNA in *Trypanosoma brucei*. *Molecular and Biochemical Parasitology*, 129(1), 11-21.
- Dyson, N. (1998). The regulation of E2F by pRB-family proteins. *Genes & Development*, 12(15), 2245-62.
- Earnshaw, W. C., & Cooke, C. A. (1991). Analysis of the distribution of the INCENPs throughout mitosis reveals the existence of a pathway of structural changes in the chromosomes during metaphase and early events in cleavage furrow formation. *Journal of Cell Science*, 98(Pt 4), 443-61.
- Echard, A., Hickson, G. R. X., Foley, E., & O'Farrell, P. H. (2004). Terminal cytokinesis events uncovered after an RNAi screen. *Current Biology: CB*, 14(18), 1685-93.
- Eckerdt, F., Yamamoto, T. M., Lewellyn, A. L., & Maller, J. L. (2011). Identification of a polo-like kinase 4-dependent pathway for de novo centriole formation. *Current Biology: CB*, 21(5), 428-32.
- Eggert, U. S., Kiger, A. A., Richter, C., Perlman, Z. E., Perrimon, N., Mitchison, T. J., & Field, C. M. (2004). Parallel chemical genetic and genome-wide RNAi screens identify cytokinesis inhibitors and targets. *PLoS Biology*, 2(12), e379.
- Elbashir, S. M., Lendeckel, W., & Tuschl, T. (2001). RNA interference is mediated by 21- and 22-nucleotide RNAs. *Genes & Development*, 15(2), 188-200.
- Elbashir, S. M., Martinez, J., Patkaniowska, A., Lendeckel, W., & Tuschl, T. (2001). Functional anatomy of siRNAs for mediating efficient RNAi in *Drosophila melanogaster* embryo lysate. *The EMBO Journal*, 20(23), 6877-88.
- Elia, A. E. H., Cantley, L. C., & Yaffe, M. B. (2003). Proteomic screen finds pSer/pThr-binding domain localizing Plk1 to mitotic substrates. *Science*, 299(5610), 1228-31.
- Elia, A.E.H., Rellos, P., Haire, L.F., Chao, J.W., Ivins, F.J., Hoepker, K., Mohammad, D., Cantley, L.C., Smerdon, S.J. & Yaffe, M. B. (2003). The

molecular basis for phosphodependent substrate targeting and regulation of Plks by the polo-box domain. *Cell*, 115(1), 83-95.

- Elowe, S., Hümmer, S., Uldschmid, A., Li, X., & Nigg, E. A. (2007). Tension-sensitive Plk1 phosphorylation on BubR1 regulates the stability of kinetochore microtubule interactions. *Genes & Development*, 21(17), 2205-19.
- Engstler, M., & Boshart, M. (2004). Cold shock and regulation of surface protein trafficking convey sensitization to inducers of stage differentiation in *Trypanosoma brucei*. *Genes & Development*, 18(22), 2798-2811.
- Engstler, M., Thilo, L., Weise, F., Grunfelder, C. G., Schwarz, H., Boshart, M., & Overath, P. (2004). Kinetics of endocytosis and recycling of the GPI-anchored variant surface glycoprotein in *Trypanosoma brucei*. *Journal of Cell Science*, 117(7), 1105-1115.
- Farr, H., & Gull, K. (2012). Cytokinesis in trypanosomes. *Cytoskeleton*, 69(11), 931-41.
- Ferris, D. K., Maloid, S. C., & Li, C. C. (1998). Ubiquitination and proteasome mediated degradation of polo-like kinase. *Biochemical and Biophysical Research Communications*, 252(2), 340-344.
- Fèvre, E. M., Coleman, P. G., Odiit, M., Magona, J. W., Welburn, S. C., & Woolhouse, M. E. (2001). The origins of a new *Trypanosoma brucei rhodesiense* sleeping sickness outbreak in eastern Uganda. *Lancet*, 358(9282), 625-8.
- Fèvre, E. M., Wissmann, B. V, Welburn, S. C., & Lutumba, P. (2008). The burden of human African trypanosomiasis. *PLoS Negl Trop Dis*, 2(12), e333.
- Field, M. C., & Carrington, M. (2009). The trypanosome flagellar pocket. *Nature Reviews. Microbiology*, 7(11), 775-86.
- Fire, A., Xu, S., Montgomery, M. K., Kostas, S. A., Driver, S. E., & Mello, C. C. (1998). Potent and specific genetic interference by double-stranded RNA in *Caenorhabditis elegans*. *Nature*, 391(6669), 806-11.
- Fode, C., Motro, B., Yousefi, S., Heffernan, M., & Dennis, J. W. (1994). Sak, a murine protein-serine/threonine kinase that is related to the *Drosophila* polo kinase and involved in cell proliferation. *Proceedings of the National Academy of Sciences of the United States of America*, 91(14), 6388-6392.
- Galanti, N., Galindo, M., Sabaj, V., Espinoza, I., & Toro, G. C. (1998). Histone genes in trypanosomatids. *Parasitology Today (Personal Ed.)*, 14(2), 64-70.
- García-Alvarez, B., de Cárcer, G., Ibañez, S., Bragado-Nilsson, E., & Montoya, G. (2007). Molecular and structural basis of polo-like kinase 1 substrate recognition: Implications in centrosomal localization. *Proceedings of the National Academy of Sciences of the United States of America*, 104(9), 3107-12.

- Genovese, G., Friedman, D.J., Ross, M.D., Lecordier, L., Uzureau, P., Freedman, B.I., Bowden, D.W., Langefeld, C.D., Oleksyk, T.K., Uscinski Knob, A.L., Bernhardt, A.J., Hicks, P.J., Nelson, G.W., Vanhollebeke, B., Winkler, C.A., Kopp, J.B., Pays, E. & Pollak, M. R. (2010). Association of trypanolytic ApoL1 variants with kidney disease in African Americans. *Science*, 329(5993), 841-5.
- Ghildiyal, M., & Zamore, P. D. (2009). Small silencing RNAs: an expanding universe. *Nature Reviews. Genetics*, 10(2), 94-108.
- Ginger, M. L., Blundell, P. A., Lewis, A. M., Browitt, A., Günzl, A., & Barry, J. D. (2002). Ex vivo and in vitro identification of a consensus promoter for VSG genes expressed by metacyclic-stage trypanosomes in the tsetse fly. *Eukaryotic Cell*, 1(6), 1000-9.
- Glover, L., & Horn, D. (2009). Site-specific DNA double-strand breaks greatly increase stable transformation efficiency in *Trypanosoma brucei*. *Molecular and Biochemical Parasitology*, 166(2), 194-197.
- Gluenz, E., Povelones, M. L., Englund, P. T., & Gull, K. (2011). The kinetoplast duplication cycle in *Trypanosoma brucei* is orchestrated by cytoskeleton-mediated cell morphogenesis. *Molecular and Cellular Biology*, 31(5), 1012-1021.
- Gluenz, E., Sharma, R., Carrington, M., & Gull, K. (2008). Functional characterization of cohesin subunit SCC1 in *Trypanosoma brucei* and dissection of mutant phenotypes in two life cycle stages. *Molecular Microbiology*, 69(3), 666-80.
- Goldenson, B., & Crispino, J. D. (2014). The aurora kinases in cell cycle and leukemia. *Oncogene*.
- Golsteyn, R. M., Mundt, K. E., Fry, A. M., & Nigg, E. A. (1995). Cell cycle regulation of the activity and subcellular localization of Plk1, a human protein kinase implicated in mitotic spindle function. *The Journal of Cell Biology*, 129(6), 1617-1628.
- Gönczy, P., Echeverri, C., Oegema, K., Coulson, A., Jones, S.J., Copley, R.R., Duperon, J., Oegema, J., Brehm, M., Cassin, E., Hannak, E., Kirkham, M., Pichler, S., Flohrs, K., Goessen, A., Leidel, S., Alleaume, A.M., Martin, C., Ozlü, N., Bork, P. & Hyman, A. A. (2000). Functional genomic analysis of cell division in *C. elegans* using RNAi of genes on chromosome III. *Nature*, 408(6810), 331-6.
- Gould, M.K., Bachmaier, S., Ali, J.A.M., Alsford, S., Tagoe, D.N.A., Munday, J.C., Schnauffer, A.C., Horn, D., Boshart, M., J. C. & de Koning, H. P. (2013). Cyclic AMP effectors in African trypanosomes revealed by genome-scale RNA interference library screening for resistance to the phosphodiesterase inhibitor CpdA. *Antimicrobial Agents and Chemotherapy*, 57(10), 4882-93.

- Gourguechon, S., Savich, J. M., & Wang, C. C. (2007). The multiple roles of cyclin E1 in controlling cell cycle progression and cellular morphology of *Trypanosoma brucei*. *J Mol Biol*, 368(4), 939-950.
- Gourguechon, S., & Wang, C. C. (2009). CRK9 contributes to regulation of mitosis and cytokinesis in the procyclic form of *Trypanosoma brucei*. *BMC Cell Biology*, 10(1), 68.
- Graham, T. M., Tait, A., & Hide, G. (1998). Characterisation of a polo-like protein kinase gene homologue from an evolutionary divergent eukaryote, *Trypanosoma brucei*. *Gene*, 207(1), 71-77.
- Guest, S. T., Yu, J., Liu, D., Hines, J. A., Kashat, M. A., & Finley, R. L. (2011). A protein network-guided screen for cell cycle regulators in *Drosophila*. *BMC Systems Biology*, 5, 65.
- Guizetti, J., & Gerlich, D. W. (2010). Cytokinetic abscission in animal cells. *Seminars in Cell & Developmental Biology*, 21(9), 909-916.
- Gull, K. (1999). The cytoskeleton of trypanosomatid parasites. *Annual Review of Microbiology*, 53(1), 629-55.
- Hajduk, S. L., Moore, D. R., Vasudevacharya, J., Siqueira, H., Torri, A. F., Tytler, E. M., & Esko, J. D. (1989). Lysis of *Trypanosoma brucei* by a toxic subspecies of human high density lipoprotein. *The Journal of Biological Chemistry*, 264(9), 5210-7.
- Hall, J. P. J., Wang, H., & Barry, J. D. (2013). Mosaic VSGs and the scale of *Trypanosoma brucei* antigenic variation. *PLoS Pathogens*, 9(7), e1003502.
- Hamanaka, R., Maloid, S., Smith, M. R., O'Connell, C. D., Longo, D. L., & Ferris, D. K. (1994). Cloning and characterization of human and murine homologues of the *Drosophila* polo serine-threonine kinase. *Cell growth & differentiation: the molecular biology journal of the American Association for Cancer Research*, 5(3), 249-57.
- Hamanaka, R., Smith, M.R., O'Connor, P.M., Maloid, S., Mihalic, K., Spivak, J.L., Longo, D.L., & Ferris, D. K. (1995). Polo-like Kinase Is a Cell Cycle-regulated Kinase Activated during Mitosis. *Journal of Biological Chemistry*, 270(36), 21086-21091.
- Hammarton, T. C. (2007). Cell cycle regulation in *Trypanosoma brucei*. *Molecular and Biochemical Parasitology*, 153(1), 1-8.
- Hammarton, T. C., Clark, J., Douglas, F., Boshart, M., & Mottram, J. C. (2003). Stage-specific differences in cell cycle control in *Trypanosoma brucei* revealed by RNA interference of a mitotic cyclin. *The Journal of Biological Chemistry*, 278(25), 22877-86.
- Hammarton, T. C., Engstler, M., & Mottram, J. C. (2004). The *Trypanosoma brucei* cyclin, CYC2, is required for cell cycle progression through G1 phase and for maintenance of procyclic form cell morphology. *The Journal of Biological Chemistry*, 279(23), 24757-64.

- Hammarton, T. C., Kramer, S., Tetley, L., Boshart, M., & Mottram, J. C. (2007). *Trypanosoma brucei* Polo-like kinase is essential for basal body duplication, kDNA segregation and cytokinesis. *Molecular Microbiology*, 65(5), 1229-48.
- Hammarton, T. C., Lillico, S. G., Welburn, S. C., & Mottram, J. C. (2005). *Trypanosoma brucei* MOB1 is required for accurate and efficient cytokinesis but not for exit from mitosis. *Mol Microbiol*, 56, 104-116.
- Hammarton, T. C., Monnerat, S. S., & Mottram, J. C. (2007). Cytokinesis in trypanosomatids. *Current Opinion in Microbiology*, 10(6), 520-527.
- Hammond, S. M., Bernstein, E., Beach, D., & Hannon, G. J. (2000). An RNA-directed nuclease mediates post-transcriptional gene silencing in *Drosophila* cells. *Nature*, 404(6775), 293-6.
- Hanisch, A., Wehner, A., Nigg, E. A., & Silljé, H. H. W. (2006). Different Plk1 functions show distinct dependencies on polo-box domain-mediated targeting. *Molecular Biology of the Cell*, 17(1), 448-59.
- Hansen, D. V., Loktev, A. V, Ban, K. H., & Jackson, P. K. (2004). Plk1 Regulates activation of the anaphase promoting complex by phosphorylating and triggering SCF^{BTrCP}-dependent destruction of the APC inhibitor Emi1. *Molecular Biology of the Cell*, 15(12), 5623-5634.
- Hauf, S., Roitinger, E., Koch, B., Dittrich, C. M., Mechtler, K., & Peters, J. M. (2005). Dissociation of cohesin from chromosome arms and loss of arm cohesion during early mitosis depends on phosphorylation of SA2. *PLoS Biol*, 3(3), e69.
- He, C.Y., Ho, H.H., Malsam, J., Chalouni, C., West, C.M., Ullu, E., Toomre, D., & Warren, G. (2004). Golgi duplication in *Trypanosoma brucei*. *The Journal of Cell Biology*, 165(3), 313-321.
- He, C. Y., Pypaert, M., & Warren, G. (2005). Golgi duplication in *Trypanosoma brucei* requires Centrin2. *Science*, 310(5751), 1196-1198.
- Higgins, M. K., Tkachenko, O., Brown, A., Reed, J., Raper, J., & Carrington, M. (2013). Structure of the trypanosome haptoglobin-hemoglobin receptor and implications for nutrient uptake and innate immunity. *Proceedings of the National Academy of Sciences of the United States of America*, 110(5), 1905-10.
- Hirano, T. (2000). Chromosome cohesion, condensation, and separation. *Annual Review of Biochemistry*, 69(1), 115-44.
- Hirumi, H., & Hirumi, K. (1989). Continuous cultivation of *Trypanosoma brucei* blood stream forms in a medium containing a low concentration of serum protein without feeder cell layers. *J Parasitol*, 75(0022-3395 (Print)), 985-989.
- Hood, E. A., Kettenbach, A. N., Gerber, S. A., & Compton, D. A. (2012). Plk1 regulates the kinesin-13 protein Kif2b to promote faithful chromosome

segregation. *Molecular Biology of the Cell*, 23(12), 2264-74.
doi:10.1091/mbc.E11-12-1013

- Hughes, L. C., Ralston, K. S., Hill, K. L., & Zhou, Z. H. (2012). Three-dimensional structure of the trypanosome flagellum suggests that the paraflagellar rod functions as a biomechanical spring. *PLoS One*, 7(1), e25700.
- Hughes, L., Towers, K., Starborg, T., Gull, K., & Vaughan, S. (2013). A cell-body groove housing the new flagellum tip suggests an adaptation of cellular morphogenesis for parasitism in the bloodstream form of *Trypanosoma brucei*. *Journal of Cell Science*, 126(Pt 24), 5748-57.
- Ikeda, K. N., & de Graffenried, C. L. (2012). Polo-like kinase is necessary for flagellum inheritance in *Trypanosoma brucei*. *Journal of Cell Science*, 125(Pt 13), 3173-84.
- Inoue, D., & Sagata, N. (2005). The Polo-like kinase Plx1 interacts with and inhibits Myt1 after fertilization of *Xenopus* eggs. *EMBO J*, 24(5), 1057-1067.
- Iten, M., Matovu, E., Brun, R., & Kaminsky, R. (1995). Innate lack of susceptibility of Ugandan *Trypanosoma brucei rhodesiense* to DL-alpha-difluoromethylornithine (DFMO). *Tropical Medicine and Parasitology : Official Organ of Deutsche Tropenmedizinische Gesellschaft and of Deutsche Gesellschaft Für Technische Zusammenarbeit (GTZ)*, 46(3), 190-4.
- Iten, M., Mett, H., Evans, A., Enyaru, J. C., Brun, R., & Kaminsky, R. (1997). Alterations in ornithine decarboxylase characteristics account for tolerance of *Trypanosoma brucei rhodesiense* to D,L-alpha-difluoromethylornithine. *Antimicrobial Agents and Chemotherapy*, 41(9), 1922-5.
- Jackson, M.W., Agarwal, M.K., Yang, J., Bruss, P., Uchiumi, T., Agarwal, M.L., Stark, G.R., & Taylor, W. R. (2005). p130/p107/p105Rb-dependent transcriptional repression during DNA-damage-induced cell-cycle exit at G2. *Journal of Cell Science*, 118(Pt 9), 1821-32.
- Jacobs, R.T., Nare, B., Wring, S.A., Orr, M.D., Chen, D., Sligar, J.M., Jenks, M.X., Noe, R.A., Bowling, T.S., Mercer, L.T., Rewerts, C., Gaukel, E., Owens, J., Parham, R., Randolph, R., Beaudet, B., Bacchi, C.J., Yarlett, N., Plattner, J.J., Freund, Y., Ding, C., Akama, T., Zhang, Y.-K., Brun, R., Kaiser, M., Scandale, I., & Don, R. (2011). SCYX-7158, an orally-active benzoxaborole for the treatment of stage 2 human African trypanosomiasis. *PLoS Neglected Tropical Diseases*, 5(6), e1151.
- Jana, S. C., Bazan, J. F., Bettencourt-Dias, M., & Bettencourt Dias, M. (2012). Polo boxes come out of the crypt: a new view of PLK function and evolution. *Structure*, 20(11), 1801-4.
- Jang, Y. J., Lin, C. Y., Ma, S., & Erikson, R. L. (2002). Functional studies on the role of the C-terminal domain of mammalian polo-like kinase. *Proceedings of the National Academy of Sciences of the United States of America*, 99(4), 1984-1989.

- Jang, Y. J., Ma, S., Terada, Y., & Erikson, R. L. (2002). Phosphorylation of threonine 210 and the role of serine 137 in the regulation of mammalian polo-like kinase. *Journal of Biological Chemistry*, 277(46), 44115-44120.
- Jensen, B. C., Brekken, D. L., Randall, A. C., Kifer, C. T., & Parsons, M. (2005). Species specificity in ribosome biogenesis: a nonconserved phosphoprotein is required for formation of the large ribosomal subunit in *Trypanosoma brucei*. *Eukaryotic Cell*, 4(1), 30-5.
- Jensen, B. C., Kifer, C. T., & Parsons, M. (2011). *Trypanosoma brucei*: two mitogen activated protein kinase kinases are dispensable for growth and virulence of the bloodstream form. *Experimental Parasitology*, 128(3), 250-5.
- Jetton, N., Rothberg, K. G., Hubbard, J. G., Wise, J., Li, Y., Ball, H. L., & Ruben, L. (2009). The cell cycle as a therapeutic target against *Trypanosoma brucei*: Hesperadin inhibits Aurora kinase-1 and blocks mitotic progression in bloodstream forms. *Molecular Microbiology*, 72(2), 442-58.
- Johnson, T. M., Antrobus, R., & Johnson, L. N. (2008). Plk1 activation by ste20-like Kinase (Slk) phosphorylation and polo-box phosphopeptide binding assayed with the substrate translationally controlled tumor protein (TCTP). *Biochemistry*, 47(12), 3688-3696.
- Jones, N. G., Thomas, E. B., Brown, E., Dickens, N. J., Hammarton, T. C., & Mottram, J. C. (2014). Regulators of *Trypanosoma brucei* cell cycle progression and differentiation identified using a kinome-wide RNAi screen. *PLoS Pathogens*, 10(1), e1003886.
- Kamath, R.S., Fraser, A.G., Dong, Y., Poulin, G., Durbin, R., Gotta, M., Kanapin, A., Le Bot, N., Moreno, S., Sohrmann, M., Welchman, D.P., Zipperlen, P., & Ahringer, J. (2003). Systematic functional analysis of the *Caenorhabditis elegans* genome using RNAi. *Nature*, 421(6920), 231-7.
- Kang, Y.H., Park, J.-E., Yu, L.-R., Soung, N.-K., Yun, S.-M., Bang, J.K., Seong, Y.-S., Yu, H., Garfield, S., Veenstra, T.D., & Lee, K. S. (2006). Self-regulated Plk1 recruitment to kinetochores by the Plk1-PBIP1 interaction is critical for proper chromosome segregation. *Molecular Cell*, 24(3), 409-22.
- Karlas, A., Machuy, N., Shin, Y., Pleissner, K.-P., Artarini, A., Heuer, D., Becker, D., Khalil, H., Ogilvie, L.A., Hess, S., Mäurer, A.P., Müller, E., Wolff, T., Rudel, T., & Meyer, T. F. (2010). Genome-wide RNAi screen identifies human host factors crucial for influenza virus replication. *Nature*, 463(7282), 818-22.
- Kaur, M., Reed, E., Sartor, O., Dahut, W., & Figg, W. D. (2002). Suramin's development: what did we learn? *Investigational New Drugs*, 20(2), 209-19.
- Kelm, O., Wind, M., Lehmann, W. D., & Nigg, E. A. (2002). Cell cycle-regulated phosphorylation of the *Xenopus* polo-like kinase Plx1. *The Journal of Biological Chemistry*, 277(28), 25247-56.

- Kennedy, P. G. E. (2004). Human African trypanosomiasis of the CNS: current issues and challenges. *The Journal of Clinical Investigation*, 113(4), 496-504.
- Kieft, R., Capewell, P., Turner, C. M. R., Veitch, N. J., MacLeod, A., & Hajduk, S. (2010). Mechanism of *Trypanosoma brucei gambiense* (group 1) resistance to human trypanosome lytic factor. *Proceedings of the National Academy of Sciences of the United States of America*, 107(37), 16137-41.
- Kitada, K., Johnson, A. L., Johnston, L. H., & Sugino, A. (1993). A multicopy suppressor gene of the *Saccharomyces cerevisiae* G1 cell cycle mutant gene *dbf4* encodes a protein kinase and is identified as CDC5. *Molecular and Cellular Biology*, 13(7), 4445-57.
- Kittler, R., Pelletier, L., Heninger, A.-K., Slabicki, M., Theis, M., Miroslaw, L., Poser, I., Lawo, S., Grabner, H., Kozak, K., Wagner, J., Surendranath, V., Richter, C., Bowen, W., Jackson, A.L., Habermann, B., Hyman, A., & Buchholz, F. (2007). Genome-scale RNAi profiling of cell division in human tissue culture cells. *Nature Cell Biology*, 9(12), 1401-12.
- Klingbeil, M. M., & Englund, P. T. (2004). Closing the gaps in kinetoplast DNA network replication. *Proceedings of the National Academy of Sciences of the United States of America*, 101(13), 4333-4334.
- Knüsel, S., & Roditi, I. (2013). Insights into the regulation of GPEET procyclin during differentiation from early to late procyclic forms of *Trypanosoma brucei*. *Molecular and Biochemical Parasitology*, 191(2), 66-74.
- Kohl, L., Robinson, D., & Bastin, P. (2003). Novel roles for the flagellum in cell morphogenesis and cytokinesis of trypanosomes. *The EMBO Journal*, 22(20), 5336-46.
- Kolev, N. G., Ramey-Butler, K., Cross, G. A. M., Ullu, E., & Tschudi, C. (2012). Developmental progression to infectivity in *Trypanosoma brucei* triggered by an RNA-binding protein. *Science*, 338(6112), 1352-3.
- Kolev, N. G., Tschudi, C., & Ullu, E. (2011). RNA interference in protozoan parasites: achievements and challenges. *Eukaryotic Cell*, 10(9), 1156-63.
- Kondo, S., & Perrimon, N. (2011). A genome-wide RNAi screen identifies core components of the G₂-M DNA damage checkpoint. *Science Signaling*, 4(154), rs1.
- Kops, G. J. P. L., & Shah, J. V. (2012). Connecting up and clearing out: how kinetochore attachment silences the spindle assembly checkpoint. *Chromosoma*, 121(5), 509-25.
- Kothe, M., Kohls, D., Low, S., Coli, R., Cheng, A.C., Jacques, S.L., Johnson, T.L., Lewis, C., Loh, C., Nonomiya, J., Sheils, A.L., Verdries, K.A., Wynn, T.A., Kuhn, C., & Ding, Y.-H. (2007). Structure of the catalytic domain of human polo-like kinase 1. *Biochemistry*, 46(20), 5960-71.

- Kramer, S. (2004). *Characterisation of a PKA-like kinase from Trypanosoma brucei*. Ludwig-Maximilians-Universitat. Munchen.
- Krishnan, M.N., Ng, A., Sukumaran, B., Gilfoy, F.D., Uchil, P.D., Sultana, H., Brass, A.L., Adametz, R., Tsui, M., Qian, F., Montgomery, R.R., Lev, S., Mason, P.W., Koski, R.A., Elledge, S.J., Xavier, R.J., Agaisse, H., & Fikrig, E. (2008). RNA interference screen for human genes associated with West Nile virus infection. *Nature*, 455(7210), 242-5.
- Krupa, A., Preethi, G., & Srinivasan, N. (2004). Structural modes of stabilization of permissive phosphorylation sites in protein kinases: distinct strategies in Ser/Thr and Tyr kinases. *Journal of Molecular Biology*, 339(5), 1025-39.
- Kuepfer, I., Schmid, C., Allan, M., Edielu, A., Haary, E.P., Kakembo, A., Kibona, S., Blum, & Burri, C. (2012). Safety and efficacy of the 10-day melarsoprol schedule for the treatment of second stage Rhodesiense sleeping sickness. *PLoS Neglected Tropical Diseases*, 6(8), e1695.
- Kumagai, A., & Dunphy, W. G. (1991). The cdc25 protein controls tyrosine dephosphorylation of the cdc2 protein in a cell-free system. *Cell*, 64(5), 903-14.
- Kumagai, A., & Dunphy, W. G. (1996). Purification and molecular cloning of Plx1, a Cdc25-regulatory kinase from *Xenopus* egg extracts. *Science*, 273(5280), 1377-80.
- Kumar, P., & Wang, C. C. (2005). Depletion of anaphase-promoting complex or cyclosome (APC/C) subunit homolog APC1 or CDC27 of *Trypanosoma brucei* arrests the procyclic form in metaphase but the bloodstream form in anaphase. *The Journal of Biological Chemistry*, 280(36), 31783-91.
- Kumar, P., & Wang, C. C. (2006). Dissociation of cytokinesis initiation from mitotic control in a eukaryote. *Eukaryotic Cell*, 5(1), 92-102.
- La Greca, F., & Magez, S. (2011). Vaccination against trypanosomiasis: can it be done or is the trypanosome truly the ultimate immune destroyer and escape artist? *Human Vaccines*, 7(11), 1225-33.
- Lacomble, S., Vaughan, S., Gadelha, C., Morphew, M. K., Shaw, M. K., McIntosh, J. R., & Gull, K. (2010). Basal body movements orchestrate membrane organelle division and cell morphogenesis in *Trypanosoma brucei*. *Journal of Cell Science*, 123(17), 2884-2891.
- Lacomble, S., Vaughan, S., Gadelha, C., Morphew, M. K., Shaw, M. K., McIntosh, J. R. R., & Gull, K. (2009). Three-dimensional cellular architecture of the flagellar pocket and associated cytoskeleton in trypanosomes revealed by electron microscope tomography. *Journal of Cell Science*, 122(8), 1081-1090.
- LaCount, D. J., Bruse, S., Hill, K. L., & Donelson, J. E. (2000). Double-stranded RNA interference in *Trypanosoma brucei* using head-to-head promoters. *Molecular and Biochemical Parasitology*, 111(1), 67-76.

- Lane, H. A., & Nigg, E. A. (1996). Antibody microinjection reveals an essential role for human polo-like kinase 1 (Plk1) in the functional maturation of mitotic centrosomes. *The Journal of Cell Biology*, 135(6 Pt 2), 1701-13.
- Langousis, G., & Hill, K. L. (2014). Motility and more: the flagellum of *Trypanosoma brucei*. *Nature Reviews. Microbiology*, 12(7), 505-18.
- Laveran, A. (1902). De l'action du sérum humain sur le trypanosome de Nagana (*T. brucei*). *Comptes Rendus de l'Académie Des Sciences*, (134), 735-739.
- Laxman, S., Riechers, A., Sadilek, M., Schwede, F., & Beavo, J. A. (2006). Hydrolysis products of cAMP analogs cause transformation of *Trypanosoma brucei* from slender to stumpy-like forms. *Proceedings of the National Academy of Sciences of the United States of America*, 103(50), 19194-9.
- Lee, K. S., Grenfell, T. Z., Yarm, F. R., & Erikson, R. L. (1998). Mutation of the polo-box disrupts localization and mitotic functions of the mammalian polo kinase Plk. *Proceedings of the National Academy of Sciences of the United States of America*, 95(16), 9301-9306.
- Lee, K. S., Park, J. E., Asano, S., & Park, C. J. (2005). Yeast polo-like kinases: functionally conserved multitask mitotic regulators. *Oncogene*, 24(2), 217-229.
- Lee, K. S., Song, S., & Erikson, R. L. (1999). The polo-box-dependent induction of ectopic septal structures by a mammalian polo kinase, plk, in *Saccharomyces cerevisiae*. *Proceedings of the National Academy of Sciences of the United States of America*, 96(25), 14360-5.
- Lee, K. S., Yuan, Y. L., Kuriyama, R., & Erikson, R. L. (1995). Plk is an M-phase-specific protein kinase and interacts with a kinesin-like protein, CHO1/MKLP-1. *Molecular and Cellular Biology*, 15(12), 7143-51.
- Leung, G. C., Hudson, J. W., Kozarova, A., Davidson, A., Dennis, J. W., & Sicheri, F. (2002). The Sak polo-box comprises a structural domain sufficient for mitotic subcellular localization. *Nature Structural Biology*, 9(10), 719-24.
- Li, B., Ouyang, B., Pan, H., Reissmann, P.T., Slamon, D.J., Arceci, R., Lu, L., & Dai, W. (1996). Prk, a cytokine-inducible human protein serine/threonine kinase whose expression appears to be down-regulated in lung carcinomas. *The Journal of Biological Chemistry*, 271(32), 19402-8.
- Li, H., Liu, X. S., Yang, X., Wang, Y., Wang, Y., Turner, J. R., & Liu, X. (2010). Phosphorylation of CLIP-170 by Plk1 and CK2 promotes timely formation of kinetochore-microtubule attachments. *The EMBO Journal*, 29(17), 2953-65.
- Li, Z. (2012). Regulation of the cell division cycle in *Trypanosoma brucei*. *Eukaryotic Cell*, 11(10), 1180-90.
- Li, Z., Gourguechon, S., & Wang, C. C. (2007). Tousled-like kinase in a microbial eukaryote regulates spindle assembly and S-phase progression by interacting

with Aurora kinase and chromatin assembly factors. *Journal of Cell Science*, 120(Pt 21), 3883-94.

- Li, Z., Lee, J. H., Chu, F., Burlingame, A. L., Günzl, A., & Wang, C. C. (2008). Identification of a novel chromosomal passenger complex and its unique localization during cytokinesis in *Trypanosoma brucei*. *PloS One*, 3(6), e2354.
- Li, Z., Umeyama, T., & Wang, C. C. (2008). The chromosomal passenger complex and a mitotic kinesin interact with the Tousled-like kinase in trypanosomes to regulate mitosis and cytokinesis. *PloS One*, 3(11), e3814.
- Li, Z., & Wang, C. C. (2003). A PHO80-like cyclin and a B-type cyclin control the cell cycle of the procyclic form of *Trypanosoma brucei*. *The Journal of Biological Chemistry*, 278(23), 20652-8.
- Li, Z., & Wang, C. C. (2006). Changing roles of aurora-B kinase in two life cycle stages of *Trypanosoma brucei*. *Eukaryotic Cell*, 5(7), 1026-35.
- Liao, S., Wang, T., Fan, K., & Tu, X. (2010). The small ubiquitin-like modifier (SUMO) is essential in cell cycle regulation in *Trypanosoma brucei*. *Experimental Cell Research*, 316(5), 704-15.
- Lim, S., & Kaldis, P. (2013). Cdks, cyclins and CKIs: roles beyond cell cycle regulation. *Development (Cambridge, England)*, 140(15), 3079-93.
- Lin, C. Y., Madsen, M. L., Yarm, F. R., Jang, Y. J., Liu, X., & Erikson, R. L. (2000). Peripheral Golgi protein GRASP65 is a target of mitotic polo-like kinase (Plk) and Cdc2. *Proceedings of the National Academy of Sciences of the United States of America*, 97(23), 12589-94.
- Lin, Y.-C., Chen, Y.-N., Lin, K.-F., Wang, F.-F., Chou, T.-Y., & Chen, M.-Y. (2014). Association of p21 with NF-YA suppresses the expression of polo-like kinase 1 and prevents mitotic death in response to DNA damage. *Cell Death & Disease*, 5, e987.
- Lindon, C., & Pines, J. (2004). Ordered proteolysis in anaphase inactivates Plk1 to contribute to proper mitotic exit in human cells. *The Journal of Cell Biology*, 164(2), 233-241.
- Littlepage, L. E., Wu, H., Andresson, T., Deanehan, J. K., Amundadottir, L. T., & Ruderman, J. V. (2002). Identification of phosphorylated residues that affect the activity of the mitotic kinase Aurora-A. *Proceedings of the National Academy of Sciences of the United States of America*, 99(24), 15440-5.
- Liu, J., Lewellyn, A. L., Chen, L. G., & Maller, J. L. (2004). The polo box is required for multiple functions of Plx1 in mitosis. *The Journal of Biological Chemistry*, 279(20), 21367-73.
- Liu, Y., Hu, H., & Li, Z. (2013). The cooperative roles of PHO80-like cyclins in regulating the G1/S transition and posterior cytoskeletal morphogenesis in *Trypanosoma brucei*. *Molecular Microbiology*, 90(1), 130-46.

- Liu, Z., Yuan, F., Ren, J., Cao, J., Zhou, Y., Yang, Q., & Xue, Y. (2012). GPS-ARM: computational analysis of the APC/C recognition motif by predicting D-boxes and KEN-boxes. *PloS One*, 7(3), e34370.
- Llamazares, S., Moreira, A., Tavares, A., Girdham, C., Spruce, B.A., Gonzalez, C., Karess, R.E., Glover, D.M., C., & Sunkel, C. E. (1991). polo encodes a protein kinase homolog required for mitosis in *Drosophila*. *Genes & Development*, 5(12a), 2153-2165.
- Lovejoy, C. A., & Cortez, D. (2009). Common mechanisms of PIKK regulation. *DNA Repair*, 8(9), 1004-8.
- Lowery, D. M., Lim, D., & Yaffe, M. B. (2005). Structure and function of Polo-like kinases. *Oncogene*, 24(2), 248-259.
- Lozano-Núñez, A., Ikeda, K. N., Sauer, T., & de Graffenried, C. L. (2013). An analogue-sensitive approach identifies basal body rotation and flagellum attachment zone elongation as key functions of PLK in *Trypanosoma brucei*. *Molecular Biology of the Cell*, 24(9), 1321-33.
- Luo, B., Cheung, H.W., Subramanian, A., Sharifnia, T., Okamoto, M., Yang, X., Hinkle, G., Boehm, J.S., Beroukhim, R., Weir, B.A., Mermel, C., Barbie, D.A., Awad, T., Zhou, X., Nguyen, T., Piquani, B., Li, C., Golub, T.R., Meyerson, M., Hacohen, N., Hahn, W.C., Lander, E.S., Sabatini, D.M., Root, & D. E. (2008). Highly parallel identification of essential genes in cancer cells. *Proceedings of the National Academy of Sciences of the United States of America*, 105(51), 20380-5.
- Lythgoe, K. A., Morrison, L. J., Read, A. F., & Barry, J. D. (2007). Parasite-intrinsic factors can explain ordered progression of trypanosome antigenic variation. *Proceedings of the National Academy of Sciences of the United States of America*, 104(19), 8095-100.
- Ma, J., Benz, C., Grimaldi, R., Stockdale, C., Wyatt, P., Frearson, J., & Hammarton, T. C. (2010). Nuclear DBF-2-related kinases are essential regulators of cytokinesis in bloodstream stage *Trypanosoma brucei*. *The Journal of Biological Chemistry*, 285(20), 15356-68.
- MacGregor, P., & Matthews, K. (2010). New discoveries in the transmission biology of sleeping sickness parasites: applying the basics. *Journal of Molecular Medicine*, 88(9), 865-871.
- MacGregor, P., Szöör, B., Savill, N. J., & Matthews, K. R. (2012). Trypanosomal immune evasion, chronicity and transmission: an elegant balancing act. *Nature Reviews. Microbiology*, 10(6), 431-8.
- Maciejewski, P. M., Peterson, F. C., Anderson, P. J., & Brooks, C. L. (1995). Mutation of serine 90 to glutamic acid mimics phosphorylation of bovine prolactin. *The Journal of Biological Chemistry*, 270(46), 27661-5.
- Mackey, Z. B., Koupparis, K., Nishino, M., & McKerrow, J. H. (2011). High-throughput analysis of an RNAi library identifies novel kinase targets in *Trypanosoma brucei*. *Chemical Biology & Drug Design*, 78(3), 454-63.

- Macurek, L., Lindqvist, A., Lim, D., Lampson, M.A., Klompaker, R., Freire, R., Clouin, C., Taylor, S.S., Yaffe, M.B., & Medema, R. H. (2008). Polo-like kinase-1 is activated by aurora A to promote checkpoint recovery. *Nature*, 455(7209), 119-123.
- Maekawa, H., Priest, C., Lechner, J., Pereira, G., & Schiebel, E. (2007). The yeast centrosome translates the positional information of the anaphase spindle into a cell cycle signal. *The Journal of Cell Biology*, 179(3), 423-36.
- Maia, A.R.R., Garcia, Z., Kabeche, L., Barisic, M., Maffini, S., Macedo-Ribeiro, S., Cheeseman, I.M., Compton, D.A., Kaverina, I., S., & Maiato, H. (2012). Cdk1 and Plk1 mediate a CLASP2 phospho-switch that stabilizes kinetochore-microtubule attachments. *The Journal of Cell Biology*, 199(2), 285-301.
- Malumbres, M., & Barbacid, M. (2005). Mammalian cyclin-dependent kinases. *Trends in Biochemical Sciences*, 30(11), 630-641.
- Malumbres, M., & Barbacid, M. (2009). Cell cycle, CDKs and cancer: a changing paradigm. *Nat Rev Cancer*, 9(3), 153-166.
- Marcello, L., & Barry, J. D. (2007). Analysis of the VSG gene silent archive in *Trypanosoma brucei* reveals that mosaic gene expression is prominent in antigenic variation and is favored by archive substructure. *Genome Research*, 17(9), 1344-52.
- Mardin, B. R., & Schiebel, E. (2012). Breaking the ties that bind: new advances in centrosome biology. *The Journal of Cell Biology*, 197(1), 11-8.
- Martin, B. T., & Strebhardt, K. (2006). Polo-like kinase 1: target and regulator of transcriptional control. *Cell Cycle (Georgetown, Tex.)*, 5(24), 2881-5.
- Massagué, J. (2004). G1 cell-cycle control and cancer. *Nature*, 432(7015), 298-306.
- Matthews, K. R. (2005). The developmental cell biology of *Trypanosoma brucei*. *Journal of Cell Science*, 118(Pt 2), 283-90.
- Maudlin, I. (2006). African trypanosomiasis. *Annals of Tropical Medicine and Parasitology*, 100(8), 679-701.
- Maurice, J. (2013). New WHO plan targets the demise of sleeping sickness. *The Lancet*, 381(9860), 13-14.
- May, S. F. (2010). *Research on regulation of cytokinesis in Trypanosoma brucei*.
- May, S. F., Peacock, L., Almeida Costa, C. I. C., Gibson, W. C., Tetley, L., Robinson, D. R., & Hammarton, T. C. (2012). The *Trypanosoma brucei* AIR9-like protein is cytoskeleton-associated and is required for nucleus positioning and accurate cleavage furrow placement. *Molecular Microbiology*, 84(1), 77-92.

- McIntosh, J. R., & O'Toole, E. T. (1999). Life cycles of yeast spindle pole bodies: getting microtubules into a closed nucleus. *Biology of the Cell / under the Auspices of the European Cell Biology Organization*, 91(4-5), 305-12.
- McLatchie, A.P., Burrell-Saward, H., Myburgh, E., Lewis, M.D., Ward, T.H., Mottram, J.C., Croft, S.L., Kelly, J.M., & Taylor, M. C. (2013). Highly sensitive in vivo imaging of *Trypanosoma brucei* expressing “red-shifted” luciferase. *PLoS Neglected Tropical Diseases*, 7(11), e2571.
- Medina-Acosta, E., & Cross, G. A. (1993). Rapid isolation of DNA from trypanosomatid protozoa using a simple “mini-prep” procedure. *Molecular and Biochemical Parasitology*, 59(2), 327-9.
- Meister, G. (2013). Argonaute proteins: functional insights and emerging roles. *Nature Reviews. Genetics*, 14(7), 447-59.
- Merritt, C., & Stuart, K. (2013). Identification of essential and non-essential protein kinases by a fusion PCR method for efficient production of transgenic *Trypanosoma brucei*. *Molecular and Biochemical Parasitology*, 190(1), 44-9.
- Meunier, S., & Vernos, I. (2012). Microtubule assembly during mitosis - from distinct origins to distinct functions? *Journal of Cell Science*, 125(Pt 12), 2805-14.
- Moellering, R. E., & Cravatt, B. F. (2012). How chemoproteomics can enable drug discovery and development. *Chemistry & Biology*, 19(1), 11-22.
- Mohr, S., Bakal, C., & Perrimon, N. (2010). Genomic screening with RNAi: results and challenges. *Annual Review of Biochemistry*, 79, 37-64.
- Monnerat, S., Almeida Costa, C.I., Forkert, A.C., Benz, C., Hamilton, A., Tetley, L., Burchmore, R., Novo, C., Mottram, J.C., & Hammarton, T. C. (2013). identification and functional characterisation of CRK12:CYC9, a novel cyclin-dependent kinase (CDK)-cyclin complex in *Trypanosoma brucei*. *PloS One*, 8(6), e67327.
- Monnerat, S., Clucas, C., Brown, E., Mottram, J. C., & Hammarton, T. C. (2009). Searching for novel cell cycle regulators in *Trypanosoma brucei* with an RNA interference screen. *BMC Research Notes*, 2, 46.
- Mony, B. M., MacGregor, P., Ivens, A., Rojas, F., Cowton, A., Young, J., & Matthews, K. (2014). Genome-wide dissection of the quorum sensing signalling pathway in *Trypanosoma brucei*. *Nature*, 505(7485), 681-5.
- Moore, A., & Wordeman, L. (2004). The mechanism, function and regulation of depolymerizing kinesins during mitosis. *Trends in Cell Biology*, 14(10), 537-46.
- Morand, S., Renggli, C. K., Roditi, I., & Vassella, E. (2012). MAP kinase kinase 1 (MKK1) is essential for transmission of *Trypanosoma brucei* by *Glossina morsitans*. *Molecular and Biochemical Parasitology*, 186(1), 73-6.

- Morris, J. C., Wang, Z., Drew, M. E., & Englund, P. T. (2002). Glycolysis modulates trypanosome glycoprotein expression as revealed by an RNAi library. *The EMBO Journal*, 21(17), 4429-38.
- Morrison, L. J. (2011). Parasite-driven pathogenesis in *Trypanosoma brucei* infections. *Parasite Immunology*, 33(8), 448-55.
- Morrison, L. J., Marcello, L., & McCulloch, R. (2009). Antigenic variation in the African trypanosome: molecular mechanisms and phenotypic complexity. *Cellular Microbiology*, 11(12), 1724-1734.
- Morriswood, B., Havlicek, K., Demmel, L., Yavuz, S., Sealey-Cardona, M., Vidilaseris, K., Anrather, D., Kostan, J., Djinovic-Carugo, K., Roux, K.J., & Warren, G. (2013). Novel bilobe components in *Trypanosoma brucei* identified using proximity-dependent biotinylation. *Eukaryotic Cell*, 12(2), 356-67.
- Moshe, Y., Boulaire, J., Pagano, M., & Hershko, A. (2004). Role of Polo-like kinase in the degradation of early mitotic inhibitor 1, a regulator of the anaphase promoting complex/cyclosome. *Proceedings of the National Academy of Sciences of the United States of America*, 101(21), 7937-7942.
- Mukherji, M., Bell, R., Supekova, L., Wang, Y., Orth, A.P., Batalov, S., Miraglia, L., Huesken, D., Lange, J., Martin, C., Sahasrabudhe, S., Reinhardt, M., Natt, F., Hall, J., Mickanin, C., Labow, M., Chanda, S.K., Cho, C.Y., & Schultz, P. G. (2006). Genome-wide functional analysis of human cell-cycle regulators. *Proceedings of the National Academy of Sciences of the United States of America*, 103(40), 14819-24.
- Munday, J.C., Eze, A.A., Baker, N., Glover, L., Clucas, C., Aguinaga Andrés, D., Natto, M.J., Teka, I.A., McDonald, J., Lee, R.S., Graf, F.E., Ludin, P., Burchmore, R.J.S., Turner, C.M.R., Tait, A., Macleod, A., Mäser, P., Barrett, M.P., Horn, D., & De Koning, H.P. (2014). *Trypanosoma brucei* aquaglyceroporin 2 is a high-affinity transporter for pentamidine and melaminophenyl arsenic drugs and the main genetic determinant of resistance to these drugs. *The Journal of Antimicrobial Chemotherapy*, 69(3), 651-63.
- Mundt, K. E., Golsteyn, R. M., Lane, H. A., & Nigg, E. A. (1997). On the regulation and function of human polo-like kinase 1 (PLK1): Effects of Overexpression on Cell Cycle Progression. *Biochemical and Biophysical Research Communications*, 239(2), 377-385.
- Murakami, H., Aiba, H., Nakanishi, M., & Murakami-Tonami, Y. (2010). Regulation of yeast forkhead transcription factors and FoxM1 by cyclin-dependent and polo-like kinases. *Cell Cycle*, 9(16), 3233-42.
- Murray, M., Morrison, W. I., & Whitelaw, D. D. (1982). Host susceptibility to African trypanosomiasis: trypanotolerance. *Advances in Parasitology*, 21, 1-68.
- Myburgh, E., Coles, J.A., Ritchie, R., Kennedy, P.G.E., McLatchie, A.P., Rodgers, J., Taylor, M.C., Barrett, M.P., Brewer, J.M., & Mottram, J. C. (2013). In

vivo imaging of trypanosome-brain interactions and development of a rapid screening test for drugs against CNS stage trypanosomiasis. *PLoS Neglected Tropical Diseases*, 7(8), e2384. doi:10.1371/journal.pntd.0002384

- Naessens, J., Leak, S. G. A., Kennedy, D. J., Kemp, S. J., & Teale, A. J. (2003). Responses of bovine chimaeras combining trypanosomosis resistant and susceptible genotypes to experimental infection with *Trypanosoma congolense*. *Veterinary Parasitology*, 111(2-3), 125-142.
- Nare, B., Wring, S., Bacchi, C., Beaudet, B., Bowling, T., Brun, R., Chen, D., Ding, C., Freund, Y., Gaukel, E., Hussain, A., Jarnagin, K., Jenks, M., Kaiser, M., Mercer, L., Mejia, E., Noe, A., Orr, M., Parham, R., Plattner, J., Randolph, R., Rattendi, D., Rewerts, C., Sligar, J., Yarlett, N., Don, R., & Jacobs, R. (2010). Discovery of novel orally bioavailable oxaborole 6-carboxamides that demonstrate cure in a murine model of late-stage central nervous system African Trypanosomiasis. *Antimicrobial Agents and Chemotherapy*, 54(10), 4379-4388.
- Natesan, S. K. A., Peacock, L., Matthews, K., Gibson, W., & Field, M. C. (2007). Activation of endocytosis as an adaptation to the mammalian host by trypanosomes. *Eukaryotic Cell*, 6(11), 2029-37.
- Neef, R., Gruneberg, U., Kopajtich, R., Li, X., Nigg, E. A., Sillje, H., & Barr, F. A. (2007). Choice of Plk1 docking partners during mitosis and cytokinesis is controlled by the activation state of Cdk1. *Nature Cell Biology*, 9(4), 436-44.
- Nett, I. R. E., Martin, D. M. a, Miranda-Saavedra, D., Lamont, D., Barber, J. D., Mehlert, A., & Ferguson, M. a J. (2009). The phosphoproteome of bloodstream form *Trypanosoma brucei*, causative agent of African sleeping sickness. *Molecular & Cellular Proteomics*, 8(7), 1527-38.
- Neumann, B., Walter, T., Hériché, J.-K., Bulkescher, J., Erfle, H., Conrad, C., Rogers, P., Poser, I., Held, M., Liebel, U., Cetin, C., Sieckmann, F., Pau, G., Kabbe, R., Wünsche, A., Satagopam, V., Schmitz, M.H.A., Chapuis, C., Gerlich, D.W., Schneider, R., Eils, R., Huber, W., Peters, J.-M., Hyman, A.A., Durbin, R., Pepperkok, R., & Ellenberg, J. (2010). Phenotypic profiling of the human genome by time-lapse microscopy reveals cell division genes. *Nature*, 464(7289), 721-7.
- Ngô, H., Tschudi, C., Gull, K., & Ullu, E. (1998). Double-stranded RNA induces mRNA degradation in *Trypanosoma brucei*. *Proceedings of the National Academy of Sciences of the United States of America*, 95(25), 14687-92.
- Nishino, M., Choy, J.W., Gushwa, N.N., Osés-Prieto, J.A., Koupparis, K., Burlingame, A.L., Renslo, A.R., McKerrow, J.H., Taunton, J. (2013). Hypothemycin, a fungal natural product, identifies therapeutic targets in *Trypanosoma brucei*. *eLife*, 2, e00712.
- Nybakken, K., Vokes, S. A., Lin, T.-Y., McMahon, A. P., & Perrimon, N. (2005). A genome-wide RNA interference screen in *Drosophila melanogaster* cells for new components of the Hh signaling pathway. *Nature Genetics*, 37(12), 1323-32.

- O'Connell, K. F., Caron, C., Kopish, K. R., Hurd, D. D., Kempfues, K. J., Li, Y., & White, J. G. (2001). The *C. elegans* zyg-1 gene encodes a regulator of centrosome duplication with distinct maternal and paternal roles in the embryo. *Cell*, *105*(4), 547-58.
- Oberholzer, M., Langousis, G., Nguyen, H.T., Saada, E.A., Shimogawa, M.M., Jonsson, Z.O., Nguyen, S.M., Wohlschlegel, J.A., & Hill, K. L. (2011). Independent analysis of the flagellum surface and matrix proteomes provides insight into flagellum signaling in mammalian-infectious *Trypanosoma brucei*. *Molecular & Cellular Proteomics*, *10*(10), M111.010538
- Oberle, M., Balmer, O., Brun, R., & Roditi, I. (2010). Bottlenecks and the maintenance of minor genotypes during the life cycle of *Trypanosoma brucei*. *PLoS Pathogens*, *6*(7), e1001023.
- Odiit, M., Coleman, P.G., Liu, W.-C.C., McDermott, J.J., Fèvre, E.M., Welburn, S.C., Woolhouse, M.E.J., & Fèvre, E. M. (2005). Quantifying the level of under-detection of *Trypanosoma brucei rhodesiense* sleeping sickness cases. *Tropical Medicine & International Health*, *10*(9), 840-849.
- Ogbadoyi, E., Ersfeld, K., Robinson, D., Sherwin, T., & Gull, K. (2000). Architecture of the *Trypanosoma brucei* nucleus during interphase and mitosis. *Chromosoma*, *108*(8), 501-13.
- Ogbadoyi, E. O., Robinson, D. R., & Gull, K. (2003). A high-order trans-membrane structural linkage is responsible for mitochondrial genome positioning and segregation by flagellar basal bodies in trypanosomes. *Molecular Biology of the Cell*, *14*(5), 1769-79.
- Ohkura, H., Hagan, I. M., & Glover, D. M. (1995). The conserved *Schizosaccharomyces pombe* kinase plo1, required to form a bipolar spindle, the actin ring, and septum, can drive septum formation in G1 and G2 cells. *Genes & Development*, *9*(9), 1059-1073.
- Ojo, K.K., Gillespie, J.R., Riechers, A.J., Napuli, A.J., Verlinde, C.L.M.J., Buckner, F.S., Gelb, M.H., Domostoj, M.M., Wells, S.J., Scheer, A., Wells, T.N.C., & Van Voorhis, W. C. (2008). Glycogen synthase kinase 3 is a potential drug target for African trypanosomiasis therapy. *Antimicrobial Agents and Chemotherapy*, *52*(10), 3710-7.
- Ooi, C.-P., & Bastin, P. (2013). More than meets the eye: understanding *Trypanosoma brucei* morphology in the tsetse. *Frontiers in Cellular and Infection Microbiology*, *3*, 71.
- Oshimori, N., Ohsugi, M., & Yamamoto, T. (2006). The Plk1 target Kizuna stabilizes mitotic centrosomes to ensure spindle bipolarity. *Nat Cell Biol*, *8*(10), 1095-1101.
- Ouyang, B., Wang, Y., & Wei, D. (1999). *Caenorhabditis elegans* contains structural homologs of human prk and plk. *DNA Sequence : The Journal of DNA Sequencing and Mapping*, *10*(2), 109-13.

- Overath, P., Czichos, J., Stock, U., & Nonnengaesser, C. (1983). Repression of glycoprotein synthesis and release of surface coat during transformation of *Trypanosoma brucei*. *The EMBO Journal*, 2(10), 1721-8.
- Paine, M.F., Wang, M.Z., Generaux, C.N., Boykin, D.W., Wilson, W.D., De Koning, H.P., Olson, C.A., Pohlig, G., Burri, C., Brun, R., Murilla, G.A., Thuita, J.K., Barrett, M.P., & Tidwell, R. R. (2010). Diamidines for human African trypanosomiasis. *Current Opinion in Investigational Drugs (London, England : 2000)*, 11(8), 876-83.
- Park, C. J., Song, S., Lee, P. R., Shou, W., Deshaies, R. J., & Lee, K. S. (2003). Loss of CDC5 function in *Saccharomyces cerevisiae* leads to defects in Swe1p regulation and Bfa1p/Bub2p-independent cytokinesis. *Genetics*, 163(1), 21-33.
- Park, J.-E., Soung, N.-K., Johmura, Y., Kang, Y.H., Liao, C., Lee, K.H., Park, C.H., Nicklaus, M.C., & Lee, K. S. (2010). Polo-box domain: a versatile mediator of polo-like kinase function. *Cellular and Molecular Life Sciences : CMLS*, 67(12), 1957-70.
- Park, J.-H. H., Brekken, D. L., Randall, A. C., & Parsons, M. (2002). Molecular cloning of *Trypanosoma brucei* CK2 catalytic subunits: the alpha isoform is nucleolar and phosphorylates the nucleolar protein Nopp44/46. *Mol Biochem Parasitol*, 119(1), 97-106.
- Patrick, K. L., Shi, H., Kolev, N. G., Ersfeld, K., Tschudi, C., & Ullu, E. (2009). Distinct and overlapping roles for two Dicer-like proteins in the RNA interference pathways of the ancient eukaryote *Trypanosoma brucei*. *Proceedings of the National Academy of Sciences of the United States of America*, 106(42), 17933-8.
- Pays, E., Vanhollebeke, B., Vanhamme, L., Paturiaux-Hanocq, F., Nolan, D. P., & Pérez-Morga, D. (2006). The trypanolytic factor of human serum. *Nature Reviews. Microbiology*, 4(6), 477-86.
- Pearce, L. R., Komander, D., & Alessi, D. R. (2010). The nuts and bolts of AGC protein kinases. *Nature Reviews. Molecular Cell Biology*, 11(1), 9-22. doi:10.1038/nrm2822
- Pérez-Morga, D., Vanhollebeke, B., Paturiaux-Hanocq, F., Nolan, D.P., Lins, L., Homblé, F., Vanhamme, L., Tebabi, P., Pays, A., Poelvoorde, P., Jacquet, A., Brasseur, R., & Pays, E. (2005). Apolipoprotein L-I promotes trypanosome lysis by forming pores in lysosomal membranes. *Science*, 309(5733), 469-72.
- Petersen, B. O., Lukas, J., Sørensen, C. S., Bartek, J., & Helin, K. (1999). Phosphorylation of mammalian CDC6 by cyclin A/CDK2 regulates its subcellular localization. *The EMBO Journal*, 18(2), 396-410.
- Petronczki, M., Glotzer, M., Kraut, N., & Peters, J.-M. M. (2007). Polo-like Kinase 1 triggers the initiation of cytokinesis in human cells by promoting recruitment of the RhoGEF Ect2 to the central spindle. *Developmental Cell*, 12(5), 713-725.

- Petronczki, M., Lénárt, P., & Peters, J.M. (2008). Polo on the rise - from mitotic entry to cytokinesis with Plk1. *Developmental Cell*, 14(5), 646-659.
- Pollard, T. D. (2010). Mechanics of cytokinesis in eukaryotes. *Current Opinion in Cell Biology*, 22(1), 50-56.
- Portman, N., & Gull, K. (2010). The paraflagellar rod of kinetoplastid parasites: from structure to components and function. *International Journal for Parasitology*, 40(2), 135-48.
- Portman, N., Lacomble, S., Thomas, B., McKean, P. G., & Gull, K. (2009). Combining RNA interference mutants and comparative proteomics to identify protein components and dependences in a eukaryotic flagellum. *The Journal of Biological Chemistry*, 284(9), 5610-9.
- Priotto, G., Fogg, C., Balasegaram, M., Erphas, O., Louga, A., Checchi, F., Ghabri, S., & Piola, P. (2006). Three drug combinations for late-stage *Trypanosoma brucei gambiense* sleeping sickness: a randomized clinical trial in Uganda. *PLoS Clinical Trials*, 1, e39.
- Priotto, G., Kasparian, S., Ngouama, D., Ghorashian, S., Arnold, U., Ghabri, S., & Karunakara, U. (2007). Nifurtimox-Eflornithine Combination Therapy for Second-Stage *Trypanosoma brucei gambiense* Sleeping Sickness: A Randomized Clinical Trial in Congo. *Clinical Infectious Diseases*, 45(11), 1435-1442.
- Pullen, T. J., Ginger, M. L., Gaskell, S. J., & Gull, K. (2004). Protein targeting of an unusual, evolutionarily conserved adenylate kinase to a eukaryotic flagellum. *Molecular Biology of the Cell*, 15(7), 3257-65.
- Qi, W., Tang, Z., & Yu, H. (2006). Phosphorylation- and polo-box-dependent binding of Plk1 to Bub1 is required for the kinetochore localization of Plk1. *Molecular Biology of the Cell*, 17(8), 3705-16.
- Raper, J., Fung, R., Ghiso, J., Nussenzweig, V., & Tomlinson, S. (1999). Characterization of a novel trypanosome lytic factor from human serum. *Infection and Immunity*, 67(4), 1910-6.
- Raper, J., Nussenzweig, V., & Tomlinson, S. (1996). The main lytic factor of *Trypanosoma brucei brucei* in normal human serum is not high density lipoprotein. *The Journal of Experimental Medicine*, 183(3), 1023-9.
- Reynolds, N., & Ohkura, H. (2003). Polo boxes form a single functional domain that mediates interactions with multiple proteins in fission yeast polo kinase. *Journal of Cell Science*, 116(Pt 7), 1377-87.
- Rico, E., Rojas, F., Mony, B. M., Szoor, B., Macgregor, P., & Matthews, K. R. (2013). Bloodstream form pre-adaptation to the tsetse fly in *Trypanosoma brucei*. *Frontiers in Cellular and Infection Microbiology*, 3, 78.
- Robinson, D. R., & Gull, K. (1991). Basal body movements as a mechanism for mitochondrial genome segregation in the trypanosome cell cycle. *Nature*, 352(6337), 731-3.

- Robinson, D. R., Sherwin, T., Ploubidou, A., Byard, E. H., & Gull, K. (1995). Microtubule polarity and dynamics in the control of organelle positioning, segregation, and cytokinesis in the trypanosome cell cycle. *The Journal of Cell Biology*, 128(6), 1163-1172.
- Rodgers, J., Jones, A., Gibaud, S., Bradley, B., McCabe, C., Barrett, M.P., Gettinby, G., & Kennedy, P. G. E. (2011). Melarsoprol cyclodextrin inclusion complexes as promising oral candidates for the treatment of human African trypanosomiasis. *PLoS Neglected Tropical Diseases*, 5(9), e1308.
- Roditi, I., Carrington, M., & Turner, M. (1987). Expression of a polypeptide containing a dipeptide repeat is confined to the insect stage of *Trypanosoma brucei*. *Nature*, 325(6101), 272-4.
- Roditi, I., & Clayton, C. (1999). An unambiguous nomenclature for the major surface glycoproteins of the procyclic form of *Trypanosoma brucei*. *Molecular and Biochemical Parasitology*, 103(1), 99-100.
- Rothberg, K. G., Burdette, D. L., Pfannstiel, J., Jetton, N., Singh, R., & Ruben, L. (2006). The RACK1 homologue from *Trypanosoma brucei* is required for the onset and progression of cytokinesis. *The Journal of Biological Chemistry*, 281(14), 9781-90.
- Rotureau, B., Subota, I., Buisson, J., & Bastin, P. (2012). A new asymmetric division contributes to the continuous production of infective trypanosomes in the tsetse fly. *Development*, 139(10), 1842-50.
- Rotureau, B., & Van Den Abbeele, J. (2013). Through the dark continent: African trypanosome development in the tsetse fly. *Frontiers in Cellular and Infection Microbiology*, 3, 53.
- Roy, S.H., Tobin, D. V., Memar, N., Beltz, E., Holmen, J., Clayton, J.E., Chiu, D.J., Young, L.D., Green, T.H., Lubin, I., Liu, Y., Conradt, B., & Saito, R. M. (2014). A complex regulatory network coordinating cell cycles during *C. elegans* development is revealed by a genome-wide RNAi screen. *G3*, 4(5), 795-804.
- Sands, M., Kron, M. A., & Brown, R. B. (1985). Pentamidine: a review. *Reviews of Infectious Diseases*, 7(5), 625-34.
- Santamaria, A., Neef, R., Eberspacher, U., Eis, K., Husemann, M., Mumberg, D., Prechtel, S., Schulze, V., Siemeister, G., Wortmann, L., Barr, F.A., & Nigg, E. A. (2007). Use of the novel plk1 inhibitor ZK-Thiazolidinone to elucidate functions of Plk1 in early and late stages of mitosis. *Molecular Biology of the Cell*, 18(10), 4024-4036.
- Satyanarayana, A., & Kaldis, P. (2009). Mammalian cell-cycle regulation: several Cdk, numerous cyclins and diverse compensatory mechanisms. *Oncogene*, 28(33), 2925-39.
- Schumann Burkard, G., Jutzi, P., & Roditi, I. (2011). Genome-wide RNAi screens in bloodstream form trypanosomes identify drug transporters. *Molecular and Biochemical Parasitology*, 175(1), 91-4.

- Schütz, S., & Sarnow, P. (2006). Interaction of viruses with the mammalian RNA interference pathway. *Virology*, 344(1), 151-7.
- Seki, A., Coppinger, J. a, Jang, C.-Y. Y., Yates, J. R., & Fang, G. (2008). Bora and the kinase Aurora A cooperatively activate the kinase Plk1 and control mitotic entry. *Science*, 320(5883), 1655-1658.
- Selvapandiyan, A., Kumar, P., Morris, J. C., Salisbury, J. L., Wang, C. C., & Nakhasi, H. L. (2007). Centrin1 Is Required for organelle segregation and cytokinesis in *Trypanosoma brucei*. *Molecular Biology of the Cell*, 18(9), 3290-3301.
- Sessions, O.M., Barrows, N.J., Souza-Neto, J.A., Robinson, T.J., Hershey, C.L., Rodgers, M.A., Ramirez, J.L., Dimopoulos, G., Yang, P.L., Pearson, J.L., & Garcia-Blanco, M. A. (2009). Discovery of insect and human dengue virus host factors. *Nature*, 458(7241), 1047-50.
- Sherr, C. J., & Roberts, J. M. (1999). CDK inhibitors: positive and negative regulators of G1-phase progression. *Genes Dev*, 13(12), 1501-1512.
- Sherr, C. J., & Roberts, J. M. (2004). Living with or without cyclins and cyclin-dependent kinases. *Genes & Development*, 18(22), 2699-711.
- Sherwin, T., & Gull, K. (1989). The cell division cycle of *Trypanosoma brucei brucei*: timing of event markers and cytoskeletal modulations. *Philosophical Transactions of the Royal Society of London. Series B, Biological Sciences*, 323(1218), 573-88.
- Shi, H., Djikeng, A., Mark, T., Wirtz, E., Tschudi, C., & Ullu, E. (2000). Genetic interference in *Trypanosoma brucei* by heritable and inducible double-stranded RNA. *RNA*, 6(7), 1069-76.
- Shi, H., Djikeng, A., Tschudi, C., & Ullu, E. (2004). Argonaute protein in the early divergent eukaryote *Trypanosoma brucei*: control of small interfering RNA accumulation and retroposon transcript abundance. *Molecular and Cellular Biology*, 24(1), 420-7.
- Shi, H., Tschudi, C., & Ullu, E. (2006). An unusual Dicer-like1 protein fuels the RNA interference pathway in *Trypanosoma brucei*. *RNA*, 12(12), 2063-72.
- Sigoillot, F. D., Lyman, S., Huckins, J. F., Adamson, B., Chung, E., Quattrochi, B., & King, R. W. (2012). A bioinformatics method identifies prominent off-targeted transcripts in RNAi screens. *Nature Methods*, 9(4), 363-6.
- Silljé, H. H., Takahashi, K., Tanaka, K., Van Houwe, G., & Nigg, E. A. (1999). Mammalian homologues of the plant Tousled gene code for cell-cycle-regulated kinases with maximal activities linked to ongoing DNA replication. *The EMBO Journal*, 18(20), 5691-702.
- Silva, J.M., Marran, K., Parker, J.S., Silva, J., Golding, M., Schlabach, M.R., Elledge, S.J., Hannon, & G.J., Chang, K. (2008). Profiling essential genes in human mammary cells by multiplex RNAi screening. *Science*, 319(5863), 617-20.

- Simarro, P. P., Diarra, A., Ruiz Postigo, J. A., Franco, J. R., & Jannin, J. G. (2011). The human African trypanosomiasis control and surveillance programme of the World Health Organization 2000-2009: the way forward. *PLoS Neglected Tropical Diseases*, 5(2), e1007.
- Simmons, D. L., Neel, B. G., Stevens, R., Evett, G., & Erikson, R. L. (1992). Identification of an early-growth-response gene encoding a novel putative protein kinase. *Molecular and Cellular Biology*, 12(9), 4164-4169.
- Smith, A. B., Esko, J. D., & Hajduk, S. L. (1995). Killing of trypanosomes by the human haptoglobin-related protein. *Science*, 268(5208), 284-6.
- Snead, J.L., Sullivan, M., Lowery, D.M., Cohen, M.S., Zhang, C., Randle, D.H., Taunton, J., Yaffe, M.B., Morgan, & Shokat, K. M. (2007). A coupled chemical-genetic and bioinformatic approach to Polo-like kinase pathway exploration. *Chemistry & Biology*, 14(11), 1261-72.
- Song, S., Grenfell, T. Z., Garfield, S., Erikson, R. L., & Lee, K. S. (2000). Essential function of the polo box of Cdc5 in subcellular localization and induction of cytokinetic structures. *Molecular and Cellular Biology*, 20(1), 286-98.
- Sönnichsen, B., Koski, L.B., Walsh, A., Marschall, P., Neumann, B., Brehm, M., Alleaume, A.-M., Artelt, J., Bettencourt, P., Cassin, E., Hewitson, M., Holz, C., Khan, M., Lazik, S., Martin, C., Nitzsche, B., Ruer, M., Stamford, J., Winzi, M., Heinkel, R., Röder, M., Finell, J., Häntsch, H., Jones, S.J.M., Jones, M., Piano, F., Gunsalus, K.C., Oegema, K., Gönczy, P., Coulson, A., Hyman, A.A., & Echeverri, C. J. (2005). Full-genome RNAi profiling of early embryogenesis in *Caenorhabditis elegans*. *Nature*, 434(7032), 462-9.
- Stephens, N. A., & Hajduk, S. L. (2011). Endosomal localization of the serum resistance-associated protein in African trypanosomes confers human infectivity. *Eukaryotic Cell*, 10(8), 1023-33.
- Sternberg, J. M., & Maclean, L. (2010). A spectrum of disease in human African trypanosomiasis: the host and parasite genetics of virulence. *Parasitology*, 137(14), 2007-15.
- Steverding, D. (2008). The history of African trypanosomiasis. *Parasites & Vectors*, 1(1), 3.
- Steverding, D. (2010). The development of drugs for treatment of sleeping sickness: a historical review. *Parasites & Vectors*, 3(1), 15.
- Stijlemans, B., Caljon, G., Natesan, S.K.A., Saerens, D., Conrath, K., Pérez-Morga, D., Skepper, J.N., Nikolaou, A., Brys, L., Pays, E., Magez, S., Field, M.C., De Baetselier, & Muyldermans, S. (2011). High affinity nanobodies against the Trypanosome brucei VSG are potent trypanolytic agents that block endocytosis. *PLoS Pathogens*, 7(6), e1002072.
- Stockdale, C., Swiderski, M. R., Barry, J. D., & McCulloch, R. (2008). Antigenic Variation in *Trypanosoma brucei*: Joining the DOTs. *PLoS Biol*, 6(7), e185.

- Strebhardt, K., & Ullrich, A. (2006). Targeting polo-like kinase 1 for cancer therapy. *Nature Reviews. Cancer*, 6(4), 321-30.
- Subota, I., Rotureau, B., Blisnick, T., Ngwabyt, S., Durand-Dubief, M., Engstler, M., & Bastin, P. (2011). ALBA proteins are stage regulated during trypanosome development in the tsetse fly and participate in differentiation. *Molecular Biology of the Cell*, 22(22), 4205-19.
- Subramaniam, C., Veazey, P., Redmond, S., Hayes-Sinclair, J., Chambers, E., Carrington, M., Gull, K., Matthews, K., Horn, D., & Field, M. C. (2006). Chromosome-wide analysis of gene function by RNA interference in the african trypanosome. *Eukaryotic Cell*, 5(9), 1539-49.
- Sumara, I., Vorlaufer, E., Stukenberg, P. T., Kelm, O., Redemann, N., Nigg, E. A., & Peters, J. M. (2002). The Dissociation of Cohesin from Chromosomes in Prophase Is Regulated by Polo-like Kinase. *Molecular Cell*, 9(3), 515-525.
- Sun, L., & Wang, C. C. (2011). The structural basis of localizing polo-like kinase to the flagellum attachment zone in *Trypanosoma brucei*. *PloS One*, 6(11), e27303.
- Sunkel, C. E., & Glover, D. M. (1988). polo, a mitotic mutant of *Drosophila* displaying abnormal spindle poles. *Journal of Cell Science*, 89(1), 25-38.
- Symula, R.E., Beadell, J.S., Sstrom, M., Agbebakun, K., Balmer, O., Gibson, W., Aksoy, S., & Caccone, A. (2012). *Trypanosoma brucei gambiense* group 1 is distinguished by a unique amino acid substitution in the HpHb receptor implicated in human serum resistance. *PLoS Neglected Tropical Diseases*, 6(7), e1728.
- Szöör, B., Ruberto, I., Burchmore, R., & Matthews, K. R. (2010). A novel phosphatase cascade regulates differentiation in *Trypanosoma brucei* via a glycosomal signaling pathway. *Genes & Development*, 24(12), 1306-16.
- Szöör, B., Wilson, J., McElhinney, H., Taberner, L., & Matthews, K. R. (2006). Protein tyrosine phosphatase TbPTP1: A molecular switch controlling life cycle differentiation in trypanosomes. *The Journal of Cell Biology*, 175(2), 293-303.
- Takaki, T., Trenz, K., Costanzo, V., & Petronczki, M. (2008). Polo-like kinase 1 reaches beyond mitosis-cytokinesis, DNA damage response, and development. *Current Opinion in Cell Biology*, 20(6), 650-660.
- Takizawa, C. G., & Morgan, D. O. (2000). Control of mitosis by changes in the subcellular location of cyclin-B1-Cdk1 and Cdc25C. *Current Opinion in Cell Biology*, 12(6), 658-665.
- Tanaka, K., Petersen, J., Maclver, F., Mulvihill, D. P., Glover, D. M., & Hagan, I. M. (2001). The role of Plo1 kinase in mitotic commitment and septation in *Schizosaccharomyces pombe*. *The EMBO Journal*, 20(6), 1259-70.
- Tarral, A., Blesson, S., Mordt, O.V., Torreele, E., Sassella, D., Bray, M.A., Hovsepian, L., Evène, E., Gualano, V., Felices, M., & Strub-Wourgaft, N.

- (2014). Determination of an Optimal Dosing Regimen for Fexinidazole, a Novel Oral Drug for the Treatment of Human African Trypanosomiasis: First-in-Human Studies. *Clinical Pharmacokinetics*.
- Taylor, J. E., & Rudenko, G. (2006). Switching trypanosome coats: what's in the wardrobe? *Trends in Genetics*, 22(11), 614-620.
- Tetley, L., Turner, C. M., Barry, J. D., Crowe, J. S., & Vickerman, K. (1987). Onset of expression of the variant surface glycoproteins of *Trypanosoma brucei* in the tsetse fly studied using immunoelectron microscopy. *Journal of Cell Science*, 87 (Pt 2), 363-72.
- Tetley, L., & Vickerman, K. (1985). Differentiation in *Trypanosoma brucei*: host-parasite cell junctions and their persistence during acquisition of the variable antigen coat. *Journal of Cell Science*, 74, 1-19.
- Tomlinson, S., Muranjan, M., Nussenzweig, V., & Raper, J. (1997). Haptoglobin-related protein and apolipoprotein AI are components of the two trypanolytic factors in human serum. *Molecular and Biochemical Parasitology*, 86(1), 117-120.
- Torreele, E., Bourdin Trunz, B., Tweats, D., Kaiser, M., Brun, R., Mazué, G., Bray, M.A., & Pécoul, B. (2010). Fexinidazole--a new oral nitroimidazole drug candidate entering clinical development for the treatment of sleeping sickness. *PLoS Neglected Tropical Diseases*, 4(12), e923.
- Tu, X., Kumar, P., Li, Z., & Wang, C. C. (2006). An aurora kinase homologue is involved in regulating both mitosis and cytokinesis in *Trypanosoma brucei*. *The Journal of Biological Chemistry*, 281(14), 9677-87.
- Tu, X., & Wang, C. C. (2004). The involvement of two cdc2-related kinases (CRKs) in *Trypanosoma brucei* cell cycle regulation and the distinctive stage-specific phenotypes caused by CRK3 depletion. *J Biol Chem*, 279(19), 20519-20528.
- Tu, X., & Wang, C. C. (2005). Pairwise knockdowns of cdc2-related kinases (CRKs) in *Trypanosoma brucei* identified the CRKs for G1/S and G2/M transitions and demonstrated distinctive cytokinetic regulations between two developmental stages of the organism. *Molecular Biology of the Cell*, 16(1), 97-105.
- Tu, Z., Argmann, C., Wong, K.K., Mitnaul, L.J., Edwards, S., Sach, I.C., Zhu, J., & Schadt, E. E. (2009). Integrating siRNA and protein-protein interaction data to identify an expanded insulin signaling network. *Genome Research*, 19(6), 1057-67.
- Tweats, D., Bourdin Trunz, B., & Torreele, E. (2012). Genotoxicity profile of fexinidazole--a drug candidate in clinical development for human African trypanomiasis (sleeping sickness). *Mutagenesis*, 27(5), 523-32.
- Tyler, K. M., Matthews, K. R., & Gull, K. (2001). Anisomorphic Cell Division by African Trypanosomes. *Protist*, 152(4), 367-378.

- Uchiumi, T., Longo, D. L., & Ferris, D. K. (1997). Cell Cycle Regulation of the Human Polo-like Kinase (PLK) Promoter. *Journal of Biological Chemistry*, 272(14), 9166-9174.
- Umbach, J. L., & Cullen, B. R. (2009). The role of RNAi and microRNAs in animal virus replication and antiviral immunity. *Genes & Development*, 23(10), 1151-64.
- Umeyama, T., & Wang, C. C. (2008). Polo-Like Kinase Is expressed in S/G2/M phase and associated with the flagellum attachment zone in both procyclic and bloodstream forms of *Trypanosoma brucei*. *Eukaryotic Cell*, 7(9), 1582-1590.
- Urbaniak, M. D. (2009). Casein kinase 1 isoform 2 is essential for bloodstream form *Trypanosoma brucei*. *Molecular and Biochemical Parasitology*, 166(2), 183-5.
- Urbaniak, M. D., Martin, D. M. A., & Ferguson, M. A. J. (2013). Global quantitative SILAC phosphoproteomics reveals differential phosphorylation is widespread between the procyclic and bloodstream form lifecycle stages of *Trypanosoma brucei*. *Journal of Proteome Research*, 12(5), 2233-44.
- Urwyler, S., Studer, E., Renggli, C. K., & Roditi, I. (2007). A family of stage-specific alanine-rich proteins on the surface of epimastigote forms of *Trypanosoma brucei*. *Molecular Microbiology*, 63(1), 218-28.
- Van de Weerd, B. C. M., Littler, D. R., Klompmaker, R., Huseinovic, A., Fish, A., Perrakis, A., & Medema, R. H. R. H. (2008). Polo-box domains confer target specificity to the Polo-like kinase family. *Biochimica et Biophysica Acta*, 1783(6), 1015-1022.
- Van de Weerd, B. C. M., & Medema, R. H. R. H. (2006). Polo-like kinases: a team in control of the division. *Cell Cycle*, 5(8), 853-64.
- Van Den Abbeele, J., Claes, Y., van Bockstaele, D., Le Ray, D., & Coosemans, M. (1999). *Trypanosoma brucei* spp. development in the tsetse fly: characterization of the post-mesocyclic stages in the foregut and proboscis. *Parasitology*, 118 (Pt 5), 469-78.
- Van Hellemond, J.J., Neuville, P., Schwarz, R.T., Matthews, K.R., & Mottram, J.C. (2000). Isolation of *Trypanosoma brucei* CYC2 and CYC3 Cyclin Genes by Rescue of a Yeast G1 Cyclin Mutant. *Journal of Biological Chemistry*, 275(12), 8315-8323.
- Van Vugt, M. A., Smits, V. A., Klompmaker, R., & Medema, R. H. (2001). Inhibition of Polo-like kinase-1 by DNA damage occurs in an ATM- or ATR-dependent fashion. *The Journal of Biological Chemistry*, 276(45), 41656-60.
- Van Vugt, M. A. T. M., & Medema, R. H. R. H. (2005). Getting in and out of mitosis with Polo-like kinase-1. *Oncogene*, 24(17), 2844-2859.
- Vanhamme, L., Paturiaux-Hanocq, F., Poelvoorde, P., Nolan, D.P., Lins, L., Van Den Abbeele, J., Pays, A., Tebabi, P., Van Xong, H., Jacquet, A.,

- Moguilevsky, N., Dieu, M., Kane, J.P., De Baetselier, P., Brasseur, R., & Pays, E. (2003). Apolipoprotein L-I is the trypanosome lytic factor of human serum. *Nature*, 422(6927), 83-7.
- Vanhollebeke, B., De Muylder, G., Nielsen, M.J., Pays, A., Tebabi, P., Dieu, M., Raes, M., Moestrup, S.K., & Pays, E. (2008). A haptoglobin-hemoglobin receptor conveys innate immunity to *Trypanosoma brucei* in humans. *Science*, 320(5876), 677-81.
- Vanhollebeke, B., & Pays, E. (2010). The trypanolytic factor of human serum: many ways to enter the parasite, a single way to kill. *Molecular Microbiology*, 76(4), 806-14.
- Vansterkenburg, E. L., Coppens, I., Wilting, J., Bos, O. J., Fischer, M. J., Janssen, L. H., & Opperdoes, F. R. (1993). The uptake of the trypanocidal drug suramin in combination with low-density lipoproteins by *Trypanosoma brucei* and its possible mode of action. *Acta Tropica*, 54(3-4), 237-50.
- Vassella, E., Krämer, R., Turner, C. M., Wankell, M., Modes, C., van den Bogaard, M., & Boshart, M. (2001). Deletion of a novel protein kinase with PX and FYVE-related domains increases the rate of differentiation of *Trypanosoma brucei*. *Molecular Microbiology*, 41(1), 33-46.
- Vassella, E., Reuner, B., Yutzy, B., & Boshart, M. (1997). Differentiation of African trypanosomes is controlled by a density sensing mechanism which signals cell cycle arrest via the cAMP pathway. *Journal of Cell Science*, 110 (Pt 2), 2661-71.
- Vaughan, S., & Gull, K. (2008). The structural mechanics of cell division in *Trypanosoma brucei*. In *Biochemical Society Transactions* 36, 421-424.
- Verner, Z., Paris, Z., & Lukes, J. (2010). Mitochondrial membrane potential-based genome-wide RNAi screen of *Trypanosoma brucei*. *Parasitology Research*, 106(5), 1241-4.
- Vickerman, K. (1985). Developmental cycles and biology of pathogenic trypanosomes. *British Medical Bulletin*, 41(2), 105-114.
- Vickerman, K., Tetley, L., Hendry, K. A. K., & Turner, C. M. (1988). Biology of African trypanosomes in the tsetse fly. *Biology of the Cell*, 64(2), 109-119.
- Vriend, L. E. M., De Witt Hamer, P. C., Van Noorden, C. J. F., & Würdinger, T. (2013). WEE1 inhibition and genomic instability in cancer. *Biochimica et Biophysica Acta*, 1836(2), 227-35.
- Waitzman, J. S., & Rice, S. E. (2014). Mechanism and regulation of kinesin-5, an essential motor for the mitotic spindle. *Biology of the Cell / under the Auspices of the European Cell Biology Organization*, 106(1), 1-12.
- Walczak, C. E., & Heald, R. (2008). Mechanisms of mitotic spindle assembly and function. *International Review of Cytology*, 265, 111-58.

- Wang, Q., & Silver, P. A. (2010). Genome-wide RNAi screen discovers functional coupling of alternative splicing and cell cycle control to apoptosis regulation. *Cell Cycle*, 9(22), 4419-21.
- Wang, Z., Morris, J. C., Drew, M. E., & Englund, P. T. (2000). Inhibition of *Trypanosoma brucei* gene expression by RNA interference using an integratable vector with opposing T7 promoters. *The Journal of Biological Chemistry*, 275(51), 40174-9.
- Watanabe, N. N., Arai, H., Nishihara, Y., Taniguchi, M., Hunter, T., & Osada, H. (2004). M-phase kinases induce phospho-dependent ubiquitination of somatic Wee1 by SCFB-TrCP. *Proceedings of the National Academy of Sciences of the United States of America*, 101(13), 4419-4424.
- Weinberg, R. A. (1995). The retinoblastoma protein and cell cycle control. *Cell*, 81(3), 323-30.
- Wenzler, T., Boykin, D. W., Ismail, M. A., Hall, J. E., Tidwell, R. R., & Brun, R. (2009). New treatment option for second-stage African sleeping sickness: in vitro and in vivo efficacy of aza analogs of DB289. *Antimicrobial Agents and Chemotherapy*, 53(10), 4185-92.
- Wenzler, T., Yang, S., Braissant, O., Boykin, D. W., Brun, R., & Wang, M. Z. (2013). Pharmacokinetics, *Trypanosoma brucei gambiense* efficacy, and time of drug action of DB289, a preclinical candidate for treatment of second-stage human African trypanosomiasis. *Antimicrobial Agents and Chemotherapy*, 57(11), 5330-43.
- Wheeler, R. J., Gull, K., & Gluenz, E. (2012). Detailed interrogation of trypanosome cell biology via differential organelle staining and automated image analysis. *BMC Biology*, 10, 1.
- Wheeler, R. J., Scheumann, N., Wickstead, B., Gull, K., & Vaughan, S. (2013). Cytokinesis in *Trypanosoma brucei* differs between bloodstream and tsetse trypomastigote forms: implications for microtubule-based morphogenesis and mutant analysis. *Molecular Microbiology*, 90(6), 1339-55.
- WHO/TDR. (2012). *Research Priorities for Chagas Disease, Human African Trypanosomiasis and Leishmaniasis* (p. 116).
- Widener, J., Nielsen, M. J., Shiflett, A., Moestrup, S. K., & Hajduk, S. (2007). Hemoglobin is a co-factor of human trypanosome lytic factor. *PLoS Pathogens*, 3(9), 1250-61.
- Wind, M., Kelm, O., Nigg, E. A., & Lehmann, W. D. (2002). Identification of phosphorylation sites in the polo-like kinases Plx1 and Plk1 by a novel strategy based on element and electrospray high resolution mass spectrometry. *Proteomics*, 2(11), 1516-23.
- Winkles, J. A., & Alberts, G. F. (2005). Differential regulation of polo-like kinase 1, 2, 3, and 4 gene expression in mammalian cells and tissues. *Oncogene*, 24(2), 260-266.

- Wirtz, E., Hoek, M., & Cross, G. A. (1998). Regulated processive transcription of chromatin by T7 RNA polymerase in *Trypanosoma brucei*. *Nucleic Acids Research*, 26(20), 4626-34.
- Wirtz, L. E., & Clayton, C. (1995). Inducible gene expression in trypanosomes mediated by a prokaryotic repressor. *Science*, 268(0036-8075 (Print)), 1179-1183.
- Wirtz, L. E., Leal, S., Ochatt, C., & Cross, G. A. (1999). A tightly regulated inducible expression system for conditional gene knock-outs and dominant-negative genetics in *Trypanosoma brucei*. *Mol Biochem Parasitol*, 99(0166-6851 (Print)), 89-101.
- Woodward, R., & Gull, K. (1990). Timing of nuclear and kinetoplast DNA replication and early morphological events in the cell cycle of *Trypanosoma brucei*. *Journal of Cell Science*, 95(Pt 1), 49-57.
- Wurst, M., Robles, A., Po, J., Luu, V.-D., Brems, S., Marentije, M., Stoitsova, S., Quijada, L., Hoheisel, J., Stewart, M., Hartmann, & C., Clayton, C. (2009). An RNAi screen of the RRM-domain proteins of *Trypanosoma brucei*. *Molecular and Biochemical Parasitology*, 163(1), 61-5.
- Xu, J., Shen, C., Wang, T., & Quan, J. (2013). Structural basis for the inhibition of Polo-like kinase 1. *Nature Structural & Molecular Biology*, 20(9), 1047-53.
- Xu, L., Yao, X., Chen, X., Lu, P., Zhang, B., & Ip, Y. T. (2007). Msk is required for nuclear import of TGF- β /BMP-activated Smads. *The Journal of Cell Biology*, 178(6), 981-94.
- Yeh, C.-H., Yang, H.-J., Lee, I.-J., & Wu, Y.-C. (2010). *Caenorhabditis elegans* TLK-1 controls cytokinesis by localizing AIR-2/Aurora B to midzone microtubules. *Biochemical and Biophysical Research Communications*, 400(2), 187-93.
- Yu, Z., Liu, Y., & Li, Z. (2012). Structure-function relationship of the Polo-like kinase in *Trypanosoma brucei*. *Journal of Cell Science*, 125(Pt 6), 1519-30.
- Yun, S.-M., Moulaei, T., Lim, D., Bang, J.K., Park, J.-E., Shenoy, S.R., Liu, F., Kang, Y.H., Liao, C., Soung, N.-K., Lee, S., Yoon, D.-Y., Lim, Y., Lee, D.-H., Otaka, A., Appella, E., McMahon, J.B., Nicklaus, M.C., Burke, T.R., Yaffe, M.B., Wlodawer, A., & Lee, K. S. (2009). Structural and functional analyses of minimal phosphopeptides targeting the polo-box domain of polo-like kinase 1. *Nature Structural & Molecular Biology*, 16(8), 876-82.
- Zamore, P. D., Tuschl, T., Sharp, P. A., & Bartel, D. P. (2000). RNAi: double-stranded RNA directs the ATP-dependent cleavage of mRNA at 21 to 23 nucleotide intervals. *Cell*, 101(1), 25-33.
- Zhang, J.D., Koerner, C., Bechtel, S., Bender, C., Keklikoglou, I., Schmidt, C., Irsigler, A., Ernst, U., Sahin, O., Wiemann, S., & Tschulena, U. (2011). Time-resolved human kinome RNAi screen identifies a network regulating mitotic-events as early regulators of cell proliferation. *PloS One*, 6(7), e22176.

- Zhang, L., Shao, H., Huang, Y., Yan, F., Chu, Y., Hou, H., Zhu, M., Fu, C., Aikhionbare, F., Fang, G., Ding, X., & Yao, X. (2011). PLK1 phosphorylates mitotic centromere-associated kinesin and promotes its depolymerase activity. *The Journal of Biological Chemistry*, 286(4), 3033-46.
- Zhang, N., Panigrahi, A. K., Mao, Q., & Pati, D. (2011). Interaction of Sororin protein with polo-like kinase 1 mediates resolution of chromosomal arm cohesion. *The Journal of Biological Chemistry*, 286(48), 41826-37.
- Zhao, Z., Lindsay, M. E., Roy Chowdhury, A., Robinson, D. R., & Englund, P. T. (2008). p166, a link between the trypanosome mitochondrial DNA and flagellum, mediates genome segregation. *The EMBO Journal*, 27(1), 143-54.
- Zhu, H., Chang, B., Uchiumi, T., & Roninson, I. (2002). Identification of Promoter Elements Responsible for Transcriptional Inhibition of Polo-like Kinase 1 and Topoisomerase IIa Genes by p21WAF1/CIP1/SDI1. *Cell Cycle*, 1(1), 55-63.
- Zitouni, S., Nabais, C., Jana, S. C., Guerrero, A., & Bettencourt-Dias, M. (2014). Polo-like kinases: structural variations lead to multiple functions. *Nature Reviews. Molecular Cell Biology*, 15(7), 433-52.